1 of 1

RTD-TDR-63-4131

256-P #21.00

SUMMARY OF THE SEVENTH REFRACTORY COMPOSITES WORKING GROUP MEETING

Volume I

TECHNICAL DOCUMENTARY REPORT NO. RTD-TDR-63-4131
November 1963

Air Force Materials Laboratory
Research and Technology Division
Air Force Systems Command
Wright-Patterson Air Force Base, Ohio

Project No. 7381, Task No. 738103

(Prepared by Mr. L. N. Hjelm, Lt. Darrell R. James, and Capt. C. S. Lee, Materials Engineering Branch, Materials Applications Division, Air Force Materials Laboratory)

NOTICES

When Government drawings, specifications, or other data are used for any purpose other than in connection with a definitely related Government procurement operation, the United States Government thereby incurs no responsibility nor any obligation whatsoever; and the fact that the Government may have formulated, furnished, or in any way supplied the said drawings, specifications, or other data, is not to be regarded by implication or otherwise as in any manner licensing the holder or any other person or corporation, or conveying any rights or permission to manufacture, use, or sell any patented invention that may in any way be related thereto.

Qualified requesters may obtain copies of this report from the Defense Documentation Center (DDC), (formerly ASTIA), Cameron Station, Building 5, 5010 Duke Street, Alexandria 4, Virginia.

Copies of this report should not be returned to the Research and Technology Division, unless return is required by security considerations, contractual obligations, or notice on a specific document.

CLEARINGHOUSE FOR FEDERAL SCIENTIFIC AND TECHNICAL INFORMATION CFSTI
DOCUMENT MANAGEMENT BRANCH 410.11

LIMITATIONS IN REPRODUCTION QUALITY

ACCESSION # AD 601 264

☒ 1. WE REGRET THAT LEGIBILITY OF THIS DOCUMENT IS IN PART UNSATISFACTORY. REPRODUCTION HAS BEEN MADE FROM BEST AVAILABLE COPY.

☒ 2. A PORTION OF THE ORIGINAL DOCUMENT CONTAINS FINE DETAIL WHICH MAY MAKE READING OF PHOTOCOPY DIFFICULT.

☐ 3. THE ORIGINAL DOCUMENT CONTAINS COLOR, BUT DISTRIBUTION COPIES ARE AVAILABLE IN BLACK-AND-WHITE REPRODUCTION ONLY.

☐ 4. THE INITIAL DISTRIBUTION COPIES CONTAIN COLOR WHICH WILL BE SHOWN IN BLACK-AND-WHITE WHEN IT IS NECESSARY TO REPRINT.

☒ 5. LIMITED SUPPLY ON HAND: WHEN EXHAUSTED, DOCUMENT WILL BE AVAILABLE IN MICROFICHE ONLY.

☐ 6. LIMITED SUPPLY ON HAND: WHEN EXHAUSTED DOCUMENT WILL NOT BE AVAILABLE.

☐ 7. DOCUMENT IS AVAILABLE IN MICROFICHE ONLY.

☐ 8. DOCUMENT AVAILABLE ON LOAN FROM CFSTI (TT DOCUMENTS ONLY).

☐ 9.

NBS 9/64

PROCESSOR: GL

RTD-TDR-63-4131

SUMMARY OF THE SEVENTH REFRACTORY COMPOSITES WORKING GROUP MEETING

Volume I

TECHNICAL DOCUMENTARY REPORT NO. RTD-TDR-63-4131
November 1963

Air Force Materials Laboratory
Research and Technology Division
Air Force Systems Command
Wright-Patterson Air Force Base, Ohio

Project No. 7381, Task No. 738103

(Prepared by Mr. L. N. Hjelm, Lt. Darrell R. James, and Capt. C. S. Lee, Materials Engineering Branch, Materials Applications Division, Air Force Materials Laboratory)

ABSTRACT

This three-volume report is a compilation of 49 papers describing most of the information discussed at the Seventh Refractory Composites Working Group Meeting held at the Lockheed Missiles and Space Company, Palo Alto, California, on 12-14 March 1963. The representatives of approximately 40 organizations presented informal discussions of their current activities in fields of development, evaluation, and application of inorganic refractory composites for use in high-temperature environments.

This technical documentary report has been reviewed and is approved.

W. P. Conrardy
Chief Materials Engineering Branch
Materials Physics Division
Air Force Materials Laboratory

FOREWORD

This three-volume report consists of a series of papers presented at the Seventh Refractory Composites Working Group Meeting held in Palo Alto, California, on 12, 13, and 14 March 1963.

The meeting was co-chairmaned by J. J. Gangler of NASA and L. N. Hjelm of ASD, with the Lockheed Missiles and Space Company acting as host.

The assistance given by the Lockheed Missiles and Space Company and its personnel in acting as host are deeply appreciated. The assistance of the personnel of the University of Dayton Research Institute in preparation of this report is gratefully acknowledged.

In all listing of papers, the speaker's name appears first, followed by any persons collaborating in the effort.

TABLE OF CONTENTS

Volume I

TABLE OF CONTENTS (Cont'd)

TABLE OF CONTENTS (Cont'd)

TABLE OF CONTENTS (Cont'd)

TABLE OF CONTENTS (Cont'd)

TABLE OF CONTENTS (Cont'd)

LIST OF ATTENDEES

REFRACTORY COATING WORKING GROUP

March 12, 13, 14, 1963

Accountius, O. E.
Rocketdyne Div., NAA

Alvares, W. J.
U. S. Naval Radiological
Defense Labs.

Anthony, F. M.
Bell Aerosystems Co.

Aves, W. L.
Chance Vought Corp.

Beckley, D. A.
Aerojet-General Corp.

Bliton, J. L.
Armour Research Foundation

Bradshaw, W. G.
Lockheed Missiles & Space Co.

Bradstreet, S. W.
Electro Refractories & Abrasives Corp.

Bramer, S. A.
Aerojet-General Corp.

Breidenbach, L. J.
Lockheed Missiles & Space Co.

Browning, M. E.
Am. Mach. & Foundry Co.

Bruce, E.
Lockheed Missiles & Space Co.

Burroughs, J. E.
General Dynamics/Fort Worth

Chao, P. J.
Pfaudler Co.

Cherniack, G. B.
Lockheed Missiles & Space Co.

Cherry, J. A.
University of Dayton
Research Institute

Commanday, M. R.
Chromizing Corp.

Coons, W. C.
Lockheed Missiles & Space Co.

Culp, J. D.
McDonnell Aircraft Corp.

Davis, L. W.
Harvey Aluminum Corp.

DiMartino, B.
North American Aviation, L. A. D.

Eisenlohr, A.
Arde, Inc.

Elliott, A. G.
Lockheed Missiles & Space Co.

Epner, M.
Chromalloy Corp.

Gangler, J. J.
NASA

Gibeaut, W. A.
Battelle Memorial Institute

Gilligan, J. E.
Lockheed Missiles & Space Co.

Goetzel, C. G.
Lockheed Missiles & Space Co.

Graham, J. W.
Astro Met Associates, Inc.

Greening, T. A.
Lockheed Missiles & Space Co.

Grisaffe, S. J.
NASA

Hahn, H.
Curtis-Wright Corp.

Hallse, R. L.
General Dynamics Corp.

Harris, G. M.
Avco Corp.

Headman, M.
Western Gear Corp.

Hjelm, L. N.
Aeronautical Systems Div.

Ingham, H. S., Jr.
Metco, Inc.

Ingram, MSgt. J. C., Jr.
Aeronautical Systems Div.

Jacobsen, W. E.
Lockheed Missiles & Space Co.

Johnson, R. R.
Lockheed Missiles & Space Co.

Johnson, W. P.
Aeronautical Systems Div.

Jurevic, W. G.
Lockheed Missiles & Space Co.

Kushner, M.
The Boeing Co.

Lavendel, H. W.
Lockheed Missiles & Space Co.

Lee, Capt. C. S.
Aeronautical Systems Div.

Leeds, D. H.
Aerospace Corp.

Levy, N.
U. S. Army Materials Res. Agency

Lisagor, W. B.
NASA

Long, R. A.
Narmco Res. & Development

Lorimer, D. M.
Lockheed Missiles & Space Co.

Lushra, G. H.
Norton Co.

Merlet, C. F.
Lockheed Missiles & Space Co.

Moore, D.
National Bureau of Standards

Neiman, A. S.
Lockheed Missiles & Space Co.

Ogden, H. R.
Battelle Memorial Institute

Olcott, E.
Atlantic Research Corp.

Palsulich, J. M.
Western Gear Corp.

Payne, S. S.
Pfaudler Company

Pearl, H. A.
Republic Aviation Corp.

Perkins, R. A.
Lockheed Missiles & Space Co.

Pincus, A. G.
University of California

Price, W. L.
Lockheed Missiles & Space Co.

Rausch, J. J.
Armour Research Foundation

Rovin, S.
Lockheed Missiles & Space Co.

Rynders, J. F.
Lawrence Radiation Lab.

Sama, L.
General Telephone & Electronics

Schwartz, M. A.
United Technologies Corp.

Shannon, W. E.
Lockheed Missiles & Space Co.

Siebert, M. E.
Lockheed Missiles & Space Co.

Simpson, F A.
The Boeing Co.

Singleton, R. H.
Allison Div., GM

Sklarew, S.
The Marquardt Corp.

Sleinberg, M. A.
Lockheed Missiles & Space Co.

Stetson, A. R.
Solar Research

Strauss, E. L.
Martin Company

Sutton, W. H.
General Electric Co.

Tietz, T. E.
Lockheed Missiles & Space Co.

Tiner, N. A.
Astropower, Inc.

Unger, R.
Plasmadyne Corp.

VanHouton, R.
General Electric Co. -NMPO

Wells, R. L.
Martin Company

Woerner, P. F.
Texas Instruments, Inc.

Wright, E. S.
Stanford Research Institute

Wurst, J. C.
University of Dayton
Research Institute

HEADQUARTERS

Aeronautical Systems Division

AIR FORCE SYSTEMS COMMAND

UNITED STATES AIR FORCE

WRIGHT-PATTERSON AIR FORCE BASE, OHIO

REPLY TO ATTN. OF: ASRCEE-1 (L. N. Hjelm) 18 January 1963

SUBJECT: Refractory Composites Working Group

TO:

1. The seventh meeting of the Refractory Composites Working Group is planned for 12 thru 14 March 1963 at Lockheed Missiles and Space Company Research Laboratories, Palo Alto, California.

2. The Refractory Composites Working Group is an informal organization of individuals who are actively engaged in the development, evaluation, and application of high temperature inorganic composites. The Group is unique and significant in that meetings are organized and Co-Chairmaned by J. J. Gangler of NASA and L. N. Hjelm of ASD every nine months, for the purpose of presenting and discussing each attendee's current activities in this important field. The reports of activities are up to date and complete, with little restriction because of supposed proprietary information. Presentations are informal and discussions are free and constructive. The Group has performed the significant function of keeping its members up to date with the bulk of the current activities in this field.

3. You, or a designated representative of your organization, are invited to participate in this meeting. Attendance is limited to one individual who is cognizant of your organization activities in the field of refractory composites, able and willing to discuss them in detail, and willing to discuss and comment on activities of others in similar areas.

4. Each attendee will be required to prepare a paper covering his organization's activities, including pertinent details, data, etc., and to present a brief 5 to 10 minute informal oral summary of these activities. One, typed on bond, reproducible copy of the detailed paper is required for preparation of an ASD technical report summarizing the meeting. Eighty preprint copies of this report are required for prior distribution to the attendees. These reports should be forwarded to the undersigned prior to 25 February 1963.

5. Lockheed's Materials Science Laboratory is acting as host for this meeting. A block of rooms is being held at Rickeys Studio Inn for the attendees and the attached reservation card should be marked "Refractory Composites Working Group". These reservations should be made prior to

28 February 1963. They would like us to share rooms where possible. Lockheed will provide bus transportation to their plant and back to the motel leaving Rickeys at 8:30 AM each day. Arrangements have been made for lunch in Lockheed's cafeteria.

6. The sub-committee of the Working Group that has been active in the area of testing techniques will meet on 11 March at 9:00 AM in Marsten Hall at Rickeys. This group will discuss the current and future activities in high temperature testing of interest to the Working Group. The results of the meeting will be summarized to the Working Group during the regular meeting so that only the active interested members of the sub-committee need attend this meeting.

7. Report preprints and correspondence concerning the meeting should be forwarded to:

L. N. Hjelm, Co-Chairman
Refractory Composites Working Group
ASD (ASRCEE-1)
Wright Patterson AFB, Ohio

The telephone numbers CL-3-7111 (Dayton, Ohio) extension 21208.

8. Please indicate who will represent your organization along with his function, title, and mailing address so that preprints and meeting information will be properly routed.

9. It is suggested that security clearances be established with Lockheed's Security Officer, 3251 Hanover St., Palo Alto, California, to avoid difficulties and to allow for possible separate classified discussions and possible plant tours.

Lawrence N. Hjelm

LAWRENCE N. HJELM, Co-Chairman
Refractory Composites Working Group

1 Atch
Reservation Card

IMPROVED PROCESSING TECHNIQUES PROVIDE APPLICATION VERSATILITY FOR VOUGHT'S HIGH TEMPERATURE OXIDATION RESISTANT COATING SYSTEMS

W. L. AVES, JR.

Chance Vought Corporation

Dallas, Texas

IMPROVED PROCESSING TECHNIQUES PROVIDE APPLICATION VERSATILITY FOR VOUGHT'S HIGH TEMPERATURE OXIDATION RESISTANT COATING SYSTEMS

ABSTRACT

A brief outline of the current application techniques employed by Vought Aeronautics to improve coating continuity, applicability, and system reliability is provided. Processing techniques designated "slip-pack," and "segregated-pack" are described. The application of tailored high temperature oxidation resistant coating systems to refractory metal substrates by use of pyrophoric or thermit heat sources are presented for discussion.

The processing techniques and coating systems described in this paper, improved modifications of which are currently under evaluation, were conceived to provide Vought with a capability for coating large and/or highly configurated components or fabrications (i.e., cross-flow heat exchangers, weldments, convergent-divergent nuclear ram-jet nozzles, I.D. and O.D. of configurated lengths of instrumentation tubing, buckets, heat shields, large leading edge panels, etc.). The systems revealed are versatile and highly adaptable to scale-up use.

INTRODUCTION

The merits and limitations of conventional pack cementation processes are fairly well known in industry varying but little from processor to processor. In summary, however, the pack

cementation process appears to be the most promising for depositing tailored, diffusion bonded high temperature oxidation resistant coatings on the refractory metal substrates. It is realized that such other processing techniques as vapor screaming, slurry plus diffusion, fluidized bed, hot dipping, electro-deposition plus diffusion and/or pressure sintering and flame spraying plus impregnation do have their applications and merits, many of which are to deposit high temperature coating systems.

As a result of current and pending applications for high temperature oxidation resistant coatings for the protection of instrumentation tubing, large skin assemblies, brazed or diffusion bonded honeycomb panels, heat shields, nozzles, fasteners, etc., it became necessary to develop new improved coating techniques which are now under evaluation by Vought Aeronautics. These techniques are designed to incorporate the processing merits of pack cementation and, at the same time, offset its limitations.

Those factors which influence both the processing technique employed and the coating system composition used are as follows:

1. Overall Design - To include basic material composition and all mating material compositions.
2. Joining Techniques - Welded, fasteners (types and locations), brazing (braze alloy compositions), etc.
3. Tolerances - Coating thickness, straightness, growth, etc.

4. Operative Parameters - Environment, loading, time, temperatures, medium flow, etc.

5. Component Design - Configuration, type (i.e., tube, foil, etc.)

6. Fabrication Requirements - Post coating formability, strength.

7. Emissivity Requirements

The above is not to be considered a breakdown of all factors which are taken into consideration when employing a process or specific coating system, however, they are the principle ones to be considered.

DISCUSSION

For the purpose of this presentation, the application techniques shall be discussed in brief under the following specific headings: (1) Slip-pack, (2) Segregated-Pack, and (3) Exothermic Heat Deposition.

1. Slip-Pack is the processing term provided to designate that coating technique whereby the substrate is first provided with a slip of the pack composition required to deposit a coating of the desired analysis, followed by packing or suitably racking in a retort. The advantages of this technique over conventional pack cementation as employed by Vought are as follows:

a. Allows for reliably coating the I.D. of long configurated tubes and sheathes.

b. Allows for coating constrictions and I.D. of cell walls in long tubes, heat exchangers, truss core, open face or end honeycomb panels, etc.

c. Allows for closer tolerance control on coating thickness and coating build-up.

d. Ideally suited for reliably coating components and assemblies of large size irrespectible of weight, design or configuration.

e. Allows for coating assemblies fabricated from dissimilar alloys with few restrictions.

f. Allows for selective coating on one component or assembly. Stop-off is simplified.

g. Readily adaptable for the application of touch-up coatings to components or assemblies.

h. Processing material costs are substantially reduced providing for a more economical system.

i. Allows for a much more rapid overall process cycle which includes packing, thermal processing, and post process cleaning.

Base alloys of tantalum, molybdenum, and columbium are currently being processed by this technique for evaluation in the following manner:

(1) Pre-cleaning is being accomplished by vapor degreasing, followed by one or more of the following techniques by vapor blasting, abrasive flow cleaning or acid etching.

(2) Slip coating with a silicon bearing pack compound in slurry form the percent solids being determined by the substrate configuration and size. For example, foil gauge materials and small diameter (.030") deep holes require a thin (approximately .10") slip coat thickness, whereas for additional coating thickness on a sheet or plate for longer operative life a heavier (.025 to .100") slip thickness is desirable. Where thick coatings are desirable, slip thickness build-up may be accomplished by re-dipping after drying between each application.

(3) Dry the applied slip between 205 and 212°F for 30 minutes to two hours as required to completely remove the moisture from the slip, the time to dry the slip being dependent upon slip thickness, part size and mass, and oven recovery time after insertion.

(4) Pack or suitably rack in a conventional retort.

(5) The processing time depends upon the thermal conductivity of the mass or atmosphere surrounding the slip coated part, the size of the retort, the temperature employed, desired coating thickness, and the ability of the processing furnace to recover after insertion of the retort.

(6) Remove retort from furnace still on fixture and cool, and unload or unrack the part or parts.

(7) Dry bristle brush or air blast cleaning is simplified by the ease with which the spent slip parts from the coated substrate as a result of a non-adherent inert material layer which forms during processing in the slip adjacent to the coated substrate.

(8) Where a Vought IV (Si, Cr, B) coating system is desired, repeat steps 2 through 7 using a Cr-B pack slip compound.

Representative coatings applied to refractory metal substrates by this technique are similar to those applied by normal pack cementation (Figures 1 through 6). The most noticeable difference between the coatings applied by conventional pack cementation and the slip-pack process is not a structural difference but rather is one of appearance, since the slip-pack applied coatings are on the average more uniform in overall coating thickness.

Three variations in the application technique using the slip-pack process have been employed for applying coatings to small 1"x1" and 1/2" x 2" foil (.005) and sheet (.016 and .020") refractory metal specimens of both the pure metal and such alloys as TZM, C-103, Ta 10%W, D-36, Cb 1%Zr, D-31, FS 82 and Mo 50%Re. At this time, only the first two variations have been employed for processing configurated molybdenum tubes. The variations listed in order of their chronological evaluation are as follows:

(1) Pack medium for the slip coated parts consisted of conventional pack cementation compound.

(2) Pack medium for the slip coated parts consisted of inert material.

(3) Pack medium for the slip coated parts consists of a gaseous medium (parts are racked for support).

Conventional Vought oxidation resistant coatings were applied by use of the above three modifications and in each case surpassed the requirements of the oxidation resistant feasibility tests to which they were subjected. The tests consisted of introducing the specimens to 16 hours at 2,000°F 4 hours at 1500°F, and 8 hours static cyclic oxidation at 2500°F. A new set of specimens was employed for the tests at 2500°F. As a result of these tests on an average of eight specimens of each metal and alloy tested, excellent feasibility and processing reliability was demonstrated by the absence of any coating failures.

The slip coating has been applied by dipping, brushing, and troweling-on procedures, however, the slurry composition is applicable for applying by spraying and flow-coating techniques to large surfaces which are for the most part accessible. A large cellular structure, such as a heat exchanger, radiator, honeycomb, etc., would possibly necessitate repeated vacuum impregnation of the thinned slurry followed by draining to assure complete internal coverage by the slip. Tubular components are reliably covered internally by flowing the slurry through the tube, followed by immersing the tube in the slurry to which a wetting agent has been added.

The third variation offers the greatest promise of success for processing large refractory metal skin structures measured in terms of 100 square feet of surface area and up, as well as nozzle structures 5 feet and up in diameter. The rate of process heat-up and resulting time for heat uniformity is considerably more rapid in this variation. The I.D. of the molybdenum tubes coated by the slip-pack technique were in essence processed by this variation since pack compound was not introduced to the slip-coated inner surface. The coating applied was continuous, uniform and no defects were evidenced upon exposure to the 2500°F feasibility test.

2. Segregated-Pack is the processing term employed by Vought to designate that pack modification whereby the halide salt employed is segregated from the coating material which is adjacent to the substrate being coated. This technique has been developed and evaluated by Vought Aeronautics as a means of assuring coating continuity on large surface areas. Metallographic evaluation of occassional pin-hole type defects on the surfaces of large molybdenum skins processed both by Vought using the (Si, Cr, Al) system and another processor using pack cementation techniques revealed the presence of uncoated pool type indentations in the substrate at the base of the pin hole. After performing verification tests whereby large halide particles were used in compounding the pack, it was concluded that either oversize particles or agglomerates of the halides in contact with the substrate during processing resulted in

both pin hole type defect in the coating as well as the indentation in the substrate. It was further discovered that even though a fine halide powder was employed, agglomerates did have a tendency to form during mixing as a result of cohesive forces. These agglomerates were large enough to cause the pin hole type defects when they were in contact with the substrate during processing.

As a result of the findings, Vought evaluated and is now employing two process modifications. Boron has been introduced in a quantity large enough to provide the coating with exceptional self-healing properties without noticeably having an influence on the peak use temperature of the coating system. A halide separation technique is also being employed which assures the absence of pin hole and like defects.

The extent of separation of the halide from the surface to be coated (Figure 7) has not been determined; however, since the carrier gas completely fills the retort chamber, it is believed that distances amounting to many feet can be realized between the halide salt and the substrate without impairing the coating process or the quality of the resultant coating system. Molybdenum tubes 1 foot in length by 1/4 inch in I.D. have been efficiently coated overall by this technique which tends to verify the mobility of the carrier gas in the system since the tubes were packed in the horizontal position, and the halide salt was in one thin layer over three inches from the lower O.D. of the tube. A highly permeable pack is employed. Where many skins are processed together in a

attacked position, however, small patch layers of the halide salt employed are positioned in various segregated areas of the pack to allow for more uniform decomposition of the salt.

Vought coatings applied by this modification are identical in composition to those formed during conventional pack cementation. The elimination of post process pin hole and edge defects has substantially enhanced the merits of this process variation. The total absence of contamination in the coating from such metals as sodium, potassium, calcium, etc., when such metal salts are employed in the pack also enhances the use of the segregated-pack technique.

Although this processing technique is being employed on only molybdenum and columbium base alloy skins at present, it should be equally as suitable for use in applying coatings to tantalum and tungsten substrates. Effort is still being conducted by Vought Aeronautics to verify the merits and determine the limitations of this process variation.

A modification of this technique whereby C-103 columbium alloy sheet specimens were encapsulated with 1/4 inch of pack material less halide, and the halide salt layer was over two inches away buried in the inert material around the thin pack, was used in a normal Vought IV coating system (Figure 8). Such modifications require little costly pack material and are therefore much more economical than conventional techniques.

The advantages of this technique over conventional pack cementation techniques as employed are as follows:

a. Has markedly increased coating reliability through the elimination of post-coating pin hole type defects or surface imperfections.

b. Allows for closer tolerance control on coating thickness and build-up.

c. Facilitates unloading and post-cleaning of the specimen.

d. Processing material costs can be reduced by encapsulation instead of total packing the specimen in the pack compound.

3. Exothermic Heat Deposition is the term used to designate those oxidation resistant coating systems deposited by employing pyrophoric or thermit reactions as the processing heat source. A requirement for a very high processing temperature (3,000°F and up), short time (5 seconds to 5 minutes) cycle necessitated the evaluation of a new heat source by the Vought Aeronautics and Missiles Division. Although induction, plasma arc, oxy-acetylene heated zirconia pot furnace and 5,000°F inert gas carbon tube furnaces were available for use, desired versatility was lacking and numerous problems were foreseen by their use. As a result, both pyrophoric and thermit heat sources were studied and employed for depositing a new family of high temperature oxidation resistant coatings to refractory metal and carbonaceous substrates. This family of coating systems while deposited insitu forms an adequately bonded structure which is diffusion bonded to the substrates.

As a result of the evaluations at this time, the merits of coating deposition by employing an exothermic heat source both controlled and partially controlled are considerable. The merits as revealed by use of feasibility and analytical tests are disclosed as follows:

a. Allows for a high degree of reliability for applying touch-up coatings to defective coating areas both in the field and at home.

b. Allows for the deposition of predetermined coating compositions.

c. Allows for the deposition of high temperature oxidation resistant coatings to graphite and other carbonaceous bodies.

d. Allows for selective coating (stop-off is simple, if desired).

e. Provides a heat source for the coating of large components and assemblies at a high processing temperature (3,000-5,000°F) which is unavailable in the larger existant processing furnaces.

f. Provides a heat source adaptable for the internal fusion of impregnated porous coatings, as well as the formation of a diffusion type bond with the substrate.

g. Provides a heat source suitable for sintering slip type coating systems.

h. Short processing cycle (5 seconds to 5 minutes).

i. High temperature short time cycle allows for coating application without resulting in substrate melting or recrystallization.

j. Far more economical than pack cementation for processing large fabrications, primarily because of furnace requirements for conventional pack cementation coated assemblies.

Coating applications by use of exothermic heat sources are, for the purpose of this report, divided into three classifications. These classifications consist of (1) controlled pyrophoric, (2) pyrophoric, and (3) thermit. A brief description and summary evaluation of each processing technique and resultant high temperature coating follows:

1. A Controlled Pyrophoric reaction was obtained by controlled metering of oxygen gas to the pyrophoric compound. A schematic set-up of a typical laboratory type installation is shown in Figure 9. Refractory metal substrates were processed in the following manner:

   a. Cleaning was accomplished by use of low pressure (10 to 20 pounds) vapor blasting with an alumina slurry, followed by rinsing and drying.

   b. The specimens were next slip coated with the desired coating slip (i.e., a Si plus SiC slip for a tungsten substrate), Figure 10.

   c. After drying the slip, a pyrophoric slurry (i.e., a fine metal powder or combination of powders of metals such as zirconium, titanium, aluminum, etc.) is applied overall to the slip coated specimen normally between 1/8 and 3/8 inches thick, dependent upon such factors as desired time and temperature of the reaction, as well as the fuel employed, coating composition desired for deposition, and substrate alloy or material.

d. Dry the slurry thoroughly between 200 and 212°F and position the slip-slurry coated parts on graphite or zirconia supports in a conventional sand sealed vapor blanket retort.

e. Purge the retort of air with an inert gas such as helium, and introduce the retort to a furnace chamber pre-heated to between 1500 and 2000°F (Figure 9).

f. Hold at temperature for from five to ten minutes for retorts containing from 100 to 400 cubic inches, respectively, or longer for larger capacity retorts, with a helium flow of about three cfh continuing ever since the purge.

g. At this point, introduce a slow controlled oxygen flow along with the helium. A pyrophoric reaction is initiated when the oxygen vapors contact the powdered metal slurry, the temperature and time of reaction now being dependent upon the rate of oxygen flow. The heat produced by the exothermic reaction has (dependent upon the slip composition employed and coating system desired), produced coatings which have (1) impregnated a porous substrate (Figures 11 and 12), (2) deposited as a diffusion bonded coating system (Figure 13), and (3) deposited as an adherent bonded composite (Figure 14). By use of multi-process deposition, high temperature oxidation resistant coating systems similar to

those deposited by conventional pack-cementation systems are being realized. The time of reaction varies from a few seconds to five minutes.

h. The retort is then removed from the furnace and allowed to air cool prior to removal of the retort lid and parts from the retort.

i. Cleaning of the residual oxidized slurry and spent slip from the coated substrate can normally be accomplished by brushing, or by use of a shop air blast or water flow.

Feasibility for employing this coating process has been established by the application of oxidation resistant coating systems such as (Si, Cr, B), (Si, Cr, Al), (Si, SiC), (ZrB_2, $MoSi_2$, BN), and (Si, Cr, Fe, B) to all four refractory metals and in some cases a carbonaceous substrate. Additional evaluation effort is being conducted to extend the control of this application technique to provide a maximum degree of reproducibility and reliability to the coating system.

2. Straight Pyrophoric reactions are being [illegible] provide a high temperature heat source for [illegible] coatings (i.e., pre-coated defective areas where touch-up is required), as well as encapsulating coating systems to refractory metal substrates. A typical application for this technique is described as follows:

a. The substrate to be coated is suitably cleaned.

b. A slip of the desired coating composition is applied.

c. A pyrophoric, slurry or pack application is applied to the pre-slip coated and dried substrate.

d. Ignition is initiated by use of a secondary heat source such as an electric spark, torch, or insertion to a pre-heated furnace chamber.

e. Cleaning is readily accomplished by brushing, air blasting, and washing.

Uniformity of coating thickness by this technique has not been realized at this time; however, the coating continuity is good (Figures 15 and 16). Additional work is in progress to markedly improve coating thickness uniformity.

A modification of this technique whereby the coating ingredients are incorporated in the slurry has proven unpractical; however, partial success warrants additional study.

3. Thermit heating used as a heat source to provide high temperature coating systems for refractory metals and superalloys has proven to be very feasible, and success in applying tailored coating systems has been effectively realized (Figure 17). The fuels evaluated consist as the term implies of mixtures of metal oxide powders and metal powders theoretically compounded so as to provide a desired high temperature (up to 5,000°F) for a short period of time. The coating analysis is dependent upon the pre-applied slip composition and the substrate alloy.

thick coatings (.004 inch) can be realized by this technique by employing repeated application.

Oxidation resistant coatings are being applied by this technique in a manner similar to that used for applying coatings by use of a straight pyrophoric heat source. An initial advantage of this processing technique over that employing a straight pyrophoric heat source is the improved coating thickness uniformity realized.

The application of high temperature ceramic coatings to refractory metal and carbonaceous substrates has proven to be feasible when employing suitable oxide formers and binders in the thermit composition instead of a pre-applied slip.

Where a slip coating of the desired composition is pre-applied to a defective area in a coating and a thermit slurry applied over it and ignited, a reliable, reproducible touch-up coating similar or identical to the adjoining coating may be obtained. Such coatings may be applied in the shop or at a launch site. Considerable versatility is provided for deposition of a desired coating composition on refractory metal or superalloy substrates by this technique.

Although a high degree of success has been initially realized by use of exothermic heat sources, their full potential is still not known, and additional effort is required and being conducted to further evaluate their merits and limitations. It is believed that a high degree of success will soon be realized for applying very high temperature (3500-5000°F)

oxidation resistant coating compositions on refractory base alloys and carbonaceous substrates, by use of exothermic reactions.

SUMMARY

By use of such modified processing techniques as those described in this paper, new improved high temperature coating systems of good integrity will be realized. By use of the described processing techniques, coatings of similar properties to those deposited by conventional pack cementation processes are obtained. However, these modified processes lend themselves more readily to the application of oxidation resistant coatings to large scaled-up structures and components.

One of the greatest future potentials for the presented modified exothermic processing techniques, however, is their proven ability to deposit a coating of a pre-determined composition and structure, as an oxidation resistant system. This property will prove highly advantageous for use in the development of coating systems for the protection of substrates from oxidation at temperatures above 2,000°F.

The adaption of the pack compound in the form of a slip coating procedure adds considerable versatility to the coating application tool. By applying the pack composition in this manner, the following advantages have been realized as follows.

1. Ease of reliable application of oxidation resistant coatings to deep small I.D. holes and constrictions.

2. Ease of reliable application of a coating system to small cellular structures.
3. Ease of application of a protective coating system to large assemblies and components.
4. Ease of applying a specific thickness coating to very thin (.001 to .002 inch) foil cell walls.
5. Ease of application of a protective coating to deep narrow recesses and crevices.
6. Ease of controlling coating thickness within reasonably close tolerances.
7. Considerable economic savings are realized in the use of the relatively small amounts of pack material employed.
8. Selective coating of specific areas of a fabrication or component is readily obtainable.
9. Touch-up coatings of equal quality to that originally applied are obtainable.
10. Ease of application to highly configurated structures and components.
11. Ease of post removal of spent slip material and post-cleaning.

FIGURE 1.

SLIP-PACK (Si-Cr-B) COATED
6 MIL Ta FOIL.

150X

FIGURE 2.

SLIP-PACK (Si-Cr-Fe-B) COATED
6 MIL TZM FOIL.

250X

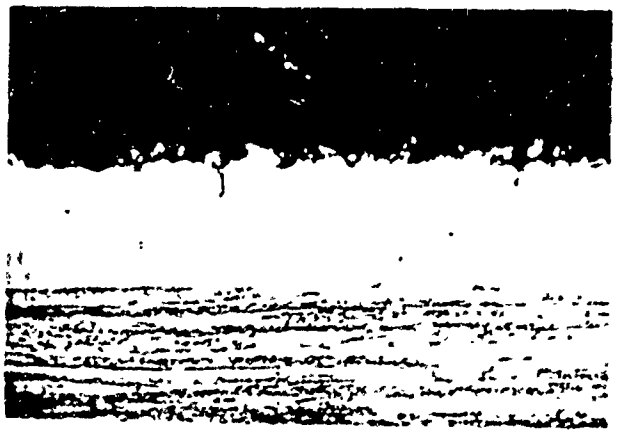

FIGURE 3.

SLIP-PACK (Si-Cr-Al) COATED
MOLY-.5% Ti, .030" SHEET.

250X

FIGURE 4.

SLIP-PACK (Si-Cr-B) COATED Cb-1%Zr, .060" SHEET.

250X

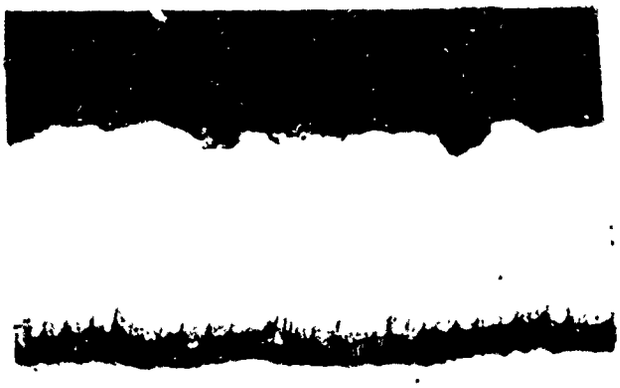

FIGURE 5.

SLIP-PACK (Si-B-N) COATED W, .060" SHEET.

250X

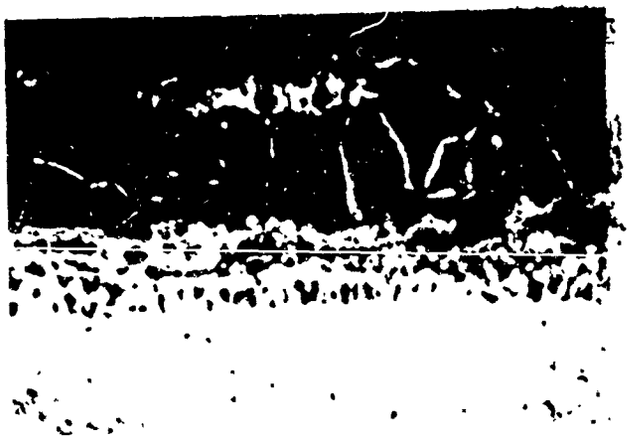

FIGURE 6.

SLIP-PACK (Al-Cr) COATED RENE' 41 AT 19 HOUR TEST AT 2100°F IN FLOWING AIR.

250X

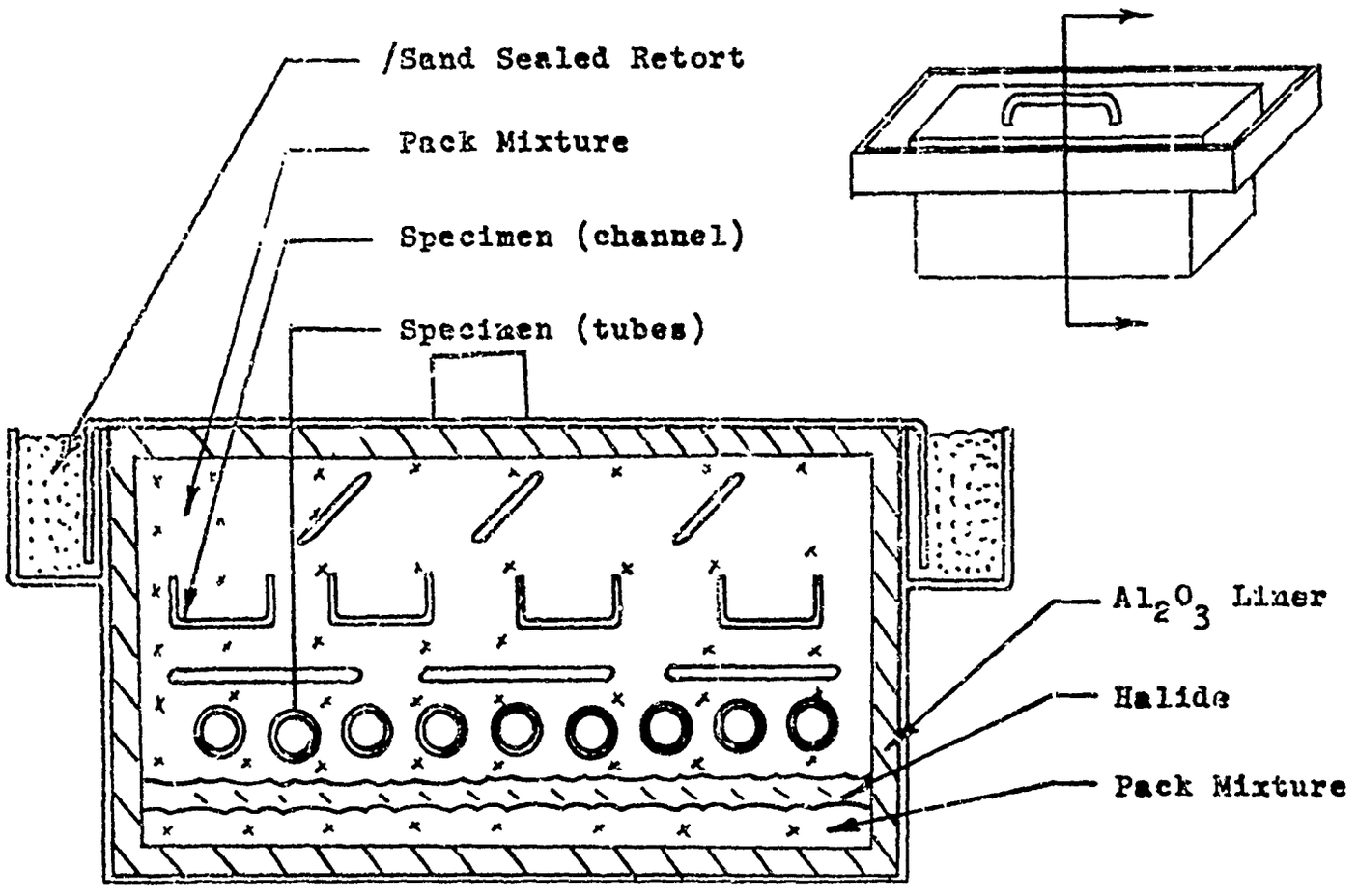

FIGURE 7. SEGREGATED HALIDE PROCESSING PROCEDURE

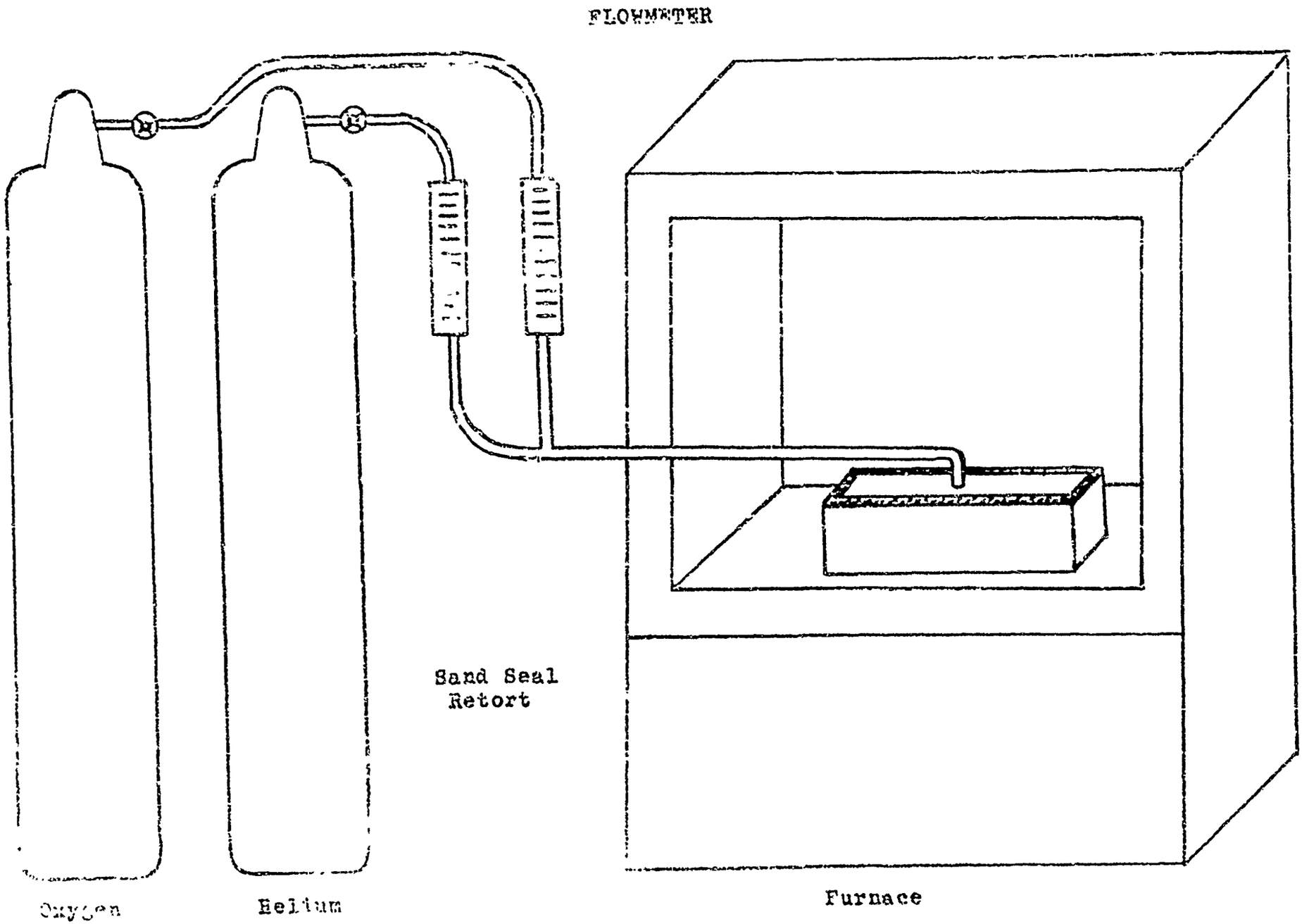

FIGURE 9

SCHEMATIC OF PYROLYTIC REACTION PROCESS

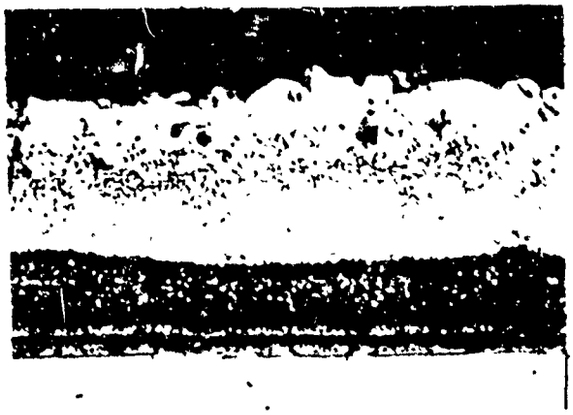

FIGURE 8.

SEGREGATED-PACK (Si-Cr-B) VOUGHT IV COATED C-103 COLUMBIUM SHEET.

250X

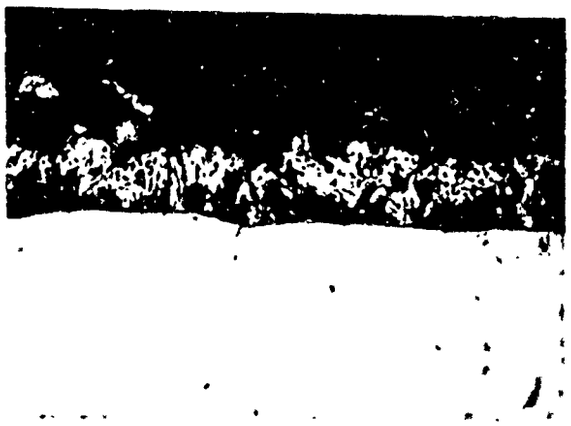

FIGURE 10.

A (Si-SiC) COATING APPLIED TO .030" W SHEET BY USE OF A CONTROLLED PYROPHORIC REACTION.

250X

FIGURE 11.

A (Si-SiC) COATING APPLIED TO A POROUS GRAPHITIC SUBSTRATE BY USE OF A CONTROLLED PYROPHORIC REACTION.

100X

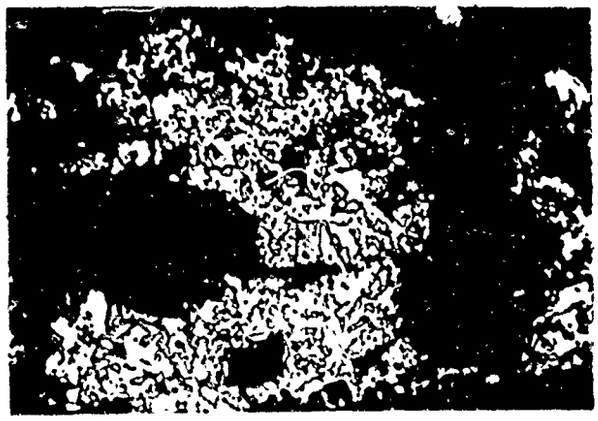

FIGURE 12.

A (Si-SiC) IMPREGNATED VOID IN THE POROUS GRAPHITIC SUBSTRATE SHOWN IN FIGURE 11.

750X

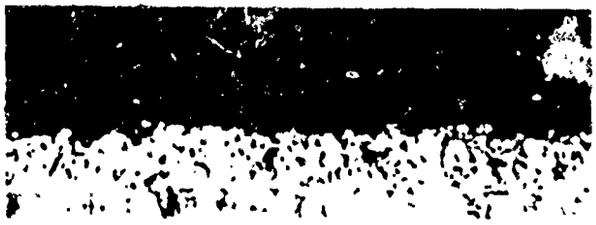

FIGURE 13.

A (Si-Cr-Ti) COATING ON A .020" D-31 SHEET APPLIED BY USE OF A CONTROLLED PYROPHORIC REACTION.

250X

FIGURE 14.

A (Si-SiC) COATING ON Ta-10% W APPLIED BY USE OF A CONTROLLED PYROPHORIC REACTION.

250X

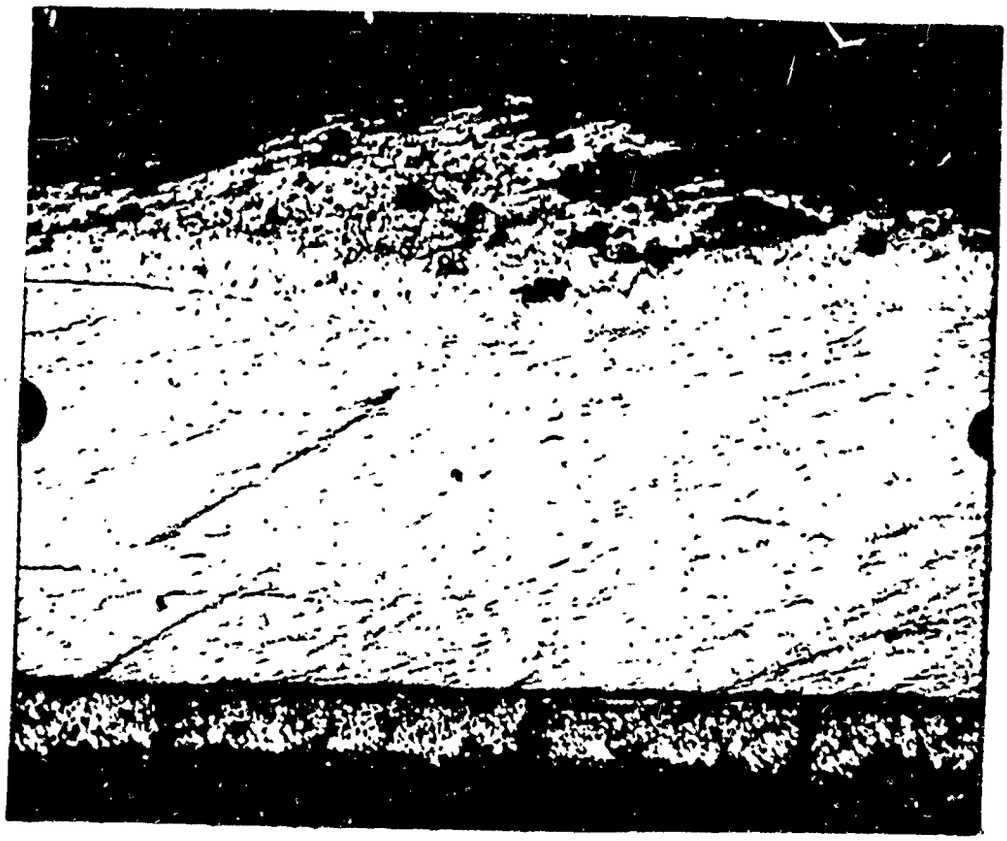

FIGURE 15. A (Si-SiC) COATING ON Ta-10% W APPLIED BY USE OF AN UNCONTROLLED PYROPHORIC REACTION. 250X

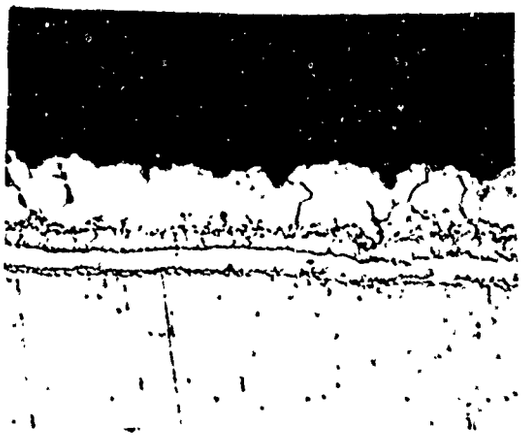

FIGURE 16.

A (Si-SiC-B) **COATING ON** Cb-1% Zr APPLIED BY USE OF AN UNCONTROLLED PYROPHORIC REACTION.

250X

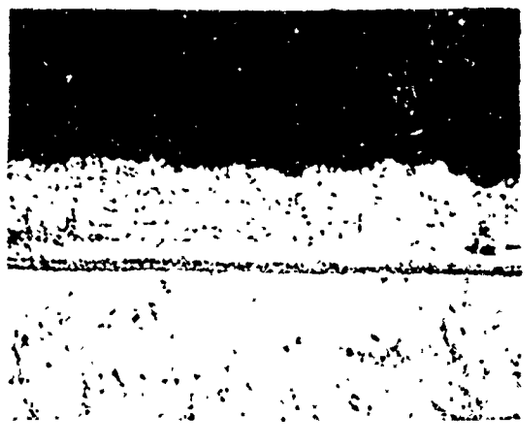

FIGURE 17.

A (Si-SiC) COATING ON FS 82 APPLIED BY USE OF A THERMIT REACTION.

250X

ACTIVITIES OF CHROMALLOY DIVISION IN THE DEVELOPMENT OF COATINGS FOR REFRACTORY METALS

MARTIN EPNER

Chromalloy Corporation

West Nyack, New York

INTRODUCTION

Since the last meeting of this group, the Chromalloy Division has been active in two areas concerned with the protection of refractory alloys from oxidation. The first, with interest initiated by a paper presented before this group last summer is the effect of low pressures on the oxidation protection of silicide coatings on molybdenum. The second area is in the semi-production coating of various molybdenum components, which may be of interest to this group.

Low Pressure Oxidation Testing

After the almost catastrophic effects on the protectiveness of various coatings on molybdenum, as reported to this group last summer, we set about to study the phenomena on the W-3 coating, which had not been tested before.

We designed and built a test furnace. A schematic diagram of the test chamber is shown in Figure I. The equipment is made up primarily of a vacuum chamber, with precision valve, vacuum gauge, a pump and electrical circuit capable of heating by direct resistance our specimens which are in this case .025" diameter wire filaments.

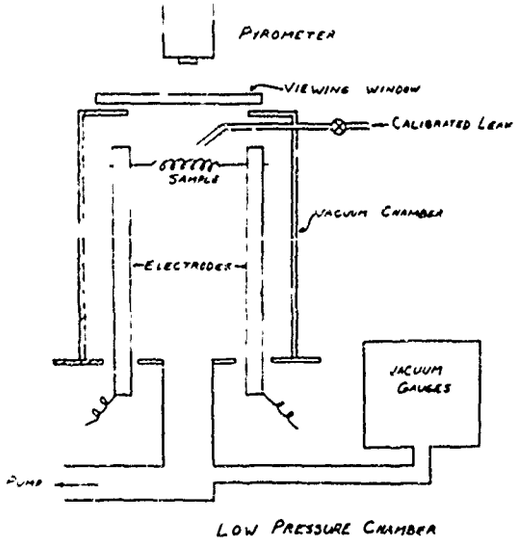

Figure I- Schematic Arrangement of Low Pressure Test Chamber

Our test procedure was to bring our chamber down to a vacuum of 10 microns or less, then by adjustment of the valve produce the low pressure-leak desired, in air or other gas. The specimen was then heated to the desired temperature.

The temperature was measured with an optical pyrometer (no adjus ment w. s made for emmitance prope ties of the specimen). Under the above conditions a steady state was maintained until specimen failure. Figure II presents the low pressure ' otherms determined on W-3 coated molybdenum specimens, both powder metallurgy and arc cast stock. Method of consolidation of the substrate seemed to play no part in its behavior, at least for these resistance heated specimens. Figure III shows the isobars plotted from the test data.

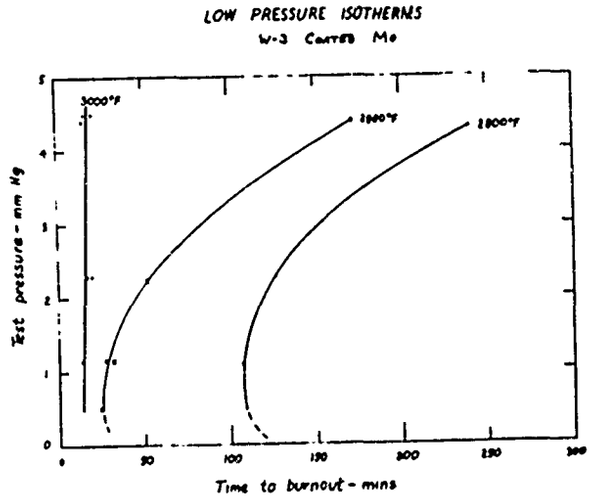

Figure II- Low Pressure Oxidation of W-3 (Isotherms)

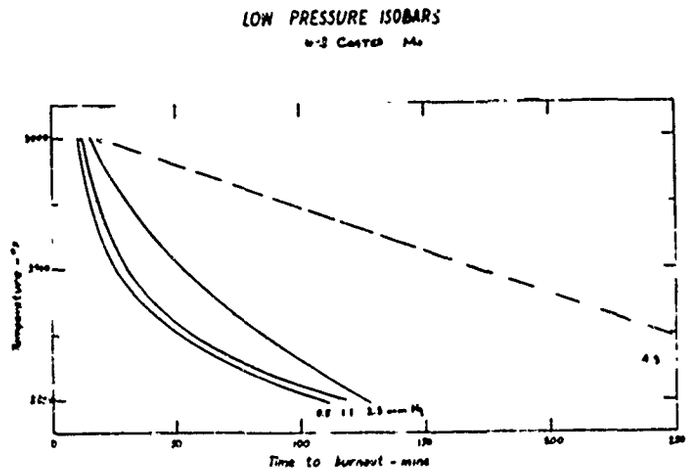

Figure III- Low Pressure Oxidation of W-3 (Isobars)

There is no doubt that the oxidation protection of W-3 on molybdenum is reduced at low pressure. These curves show this quite clearly since at atmospheric pressure the average life for W-5 coated specimens at 3000° F is about three hours and 2700° F it is in excess of 200 hours.

The prime concern at present however is will such coatings withstand orbital and sub-orbital missions planned for them in the near future. For this purpose, at least for the immediate future, they seem to exhibit sufficient protection.

Semi-Production Coatings

In the past six months, Chromalloy has coated some molybdenum hardware which I believe would be of interest to this audience. For the Republic Aviation Corporation, a series of various types of hardware made of molybdenum have been coated.

As the first part of the series, test specimens such as tensile, oxidation, rivet, shear, etc. were prepared and coated. These have been tested and I believe the results may be presented in a later paper. Next in the series were three small corrugation type specimens in which various rivet types and distributions were evaluated. These panels and rivets were coated first as components, then assembled and finally recoated. The as-coated parts can be seen in Figure IV. These panels were evaluated upon return to Republic and oxidation tested. Figure V shows the same panels after oxidation. Notice should be taken of the fact that two small oxidation failures occurred, one on the skin, the other on a rivet.

After these panels were prepared and tested, still another larger panel, approximately 12" x 14" was prepared and coated. One view of this panel can be seen in Figure VI.

CHROMALLOY W-3

AS COATED

Mo-½ Ti CORRUGATED

Figure IV- Molybdenum Alloy Test Specimen W-3 As-coated

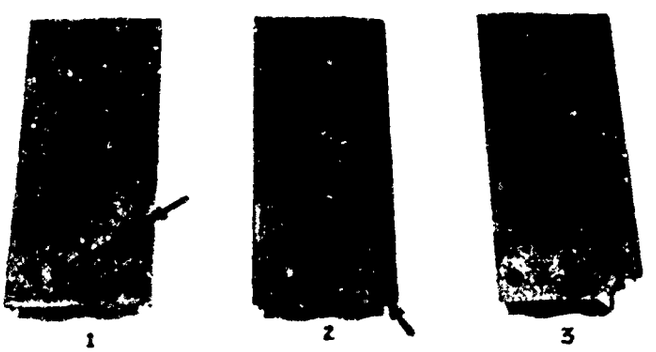

Figure V- Molybdenum Alloy Test Specimen W-3 After Oxidation Test (Arrows denote points of failure)

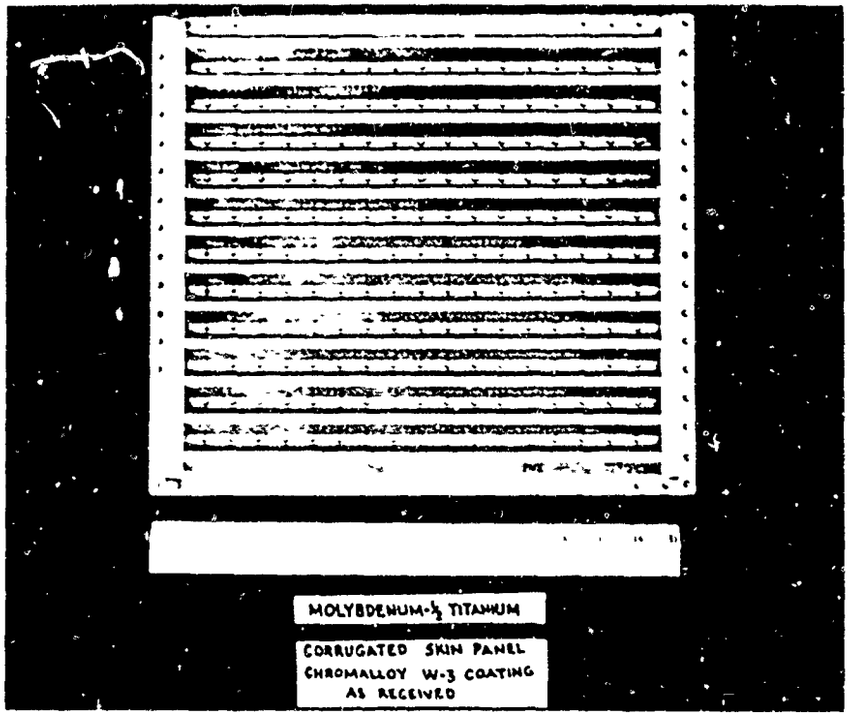

Figure VI- Sample Molybdenum Skin Panel
W-3 Coated

Oxidation test of this panel was 3 one hour cycles at 2500° F. A few small edge failures were noticed.

Of further interest is the fact that a crack was noticed prior to the final coating, but due to its location, rework was not carried out and Figure VII shows this crack after the three hours of oxidation testing. No failure was noticed by eye, or with the aid of X-ray.

Before going on, and to answer questions as to what sort and size of retorts we used for some of these parts, I felt the photographs of retorts in Figures VIII and IX might be of interest. These are the retorts which have been used in coating some of the hardware shown here. Still larger retorts are available for which the processing parameters are established and are presently in use for less exotic materials.

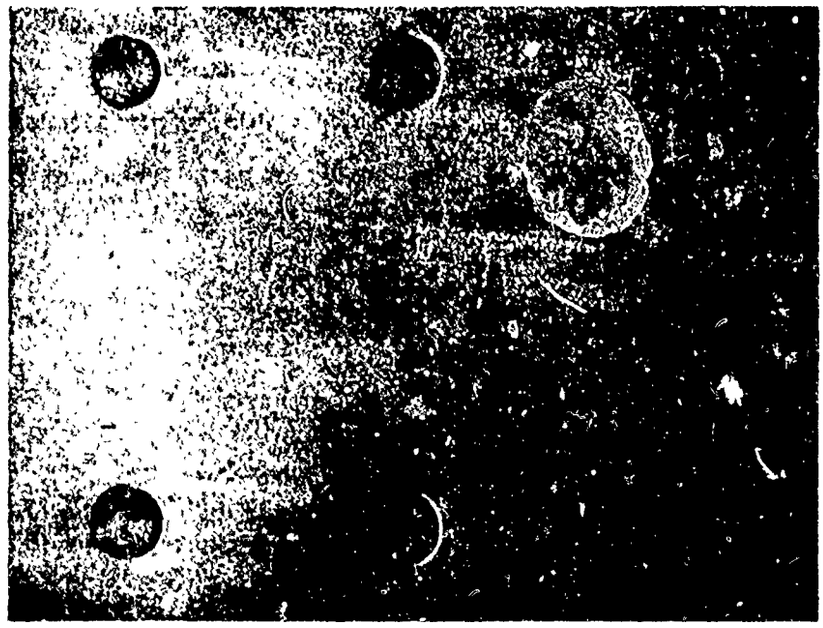

Figure VII- Pre-Test Crack in Skin Panel After Oxidation Testing. Note: No failure Visible.

Figure VIII- Retort Used in Coating Molybdenum Panels and Parts

Figure IX- Retort Used to Coat Parts Shown in Figure X.

We only await larger molybdenum parts to put these to use. I might also say here that a retort like the one in Figure IX was first used to coat a molybdenum ram jet tailpipe for the Marquardt Corporation in December, 1958.

Among the parts which have been recently W-3 coated, are those shown in Figure X. The parts seen here are samples of various components necessary to complete one entire assembly. Excluding the bolts, over 70 rods of various size and shape go into this assembly, which is a prototype of a piece of ground support equipment being designed and built for the Department of Defense by the Curtiss Wright Corporation. The parts shown are all made of alloy molybdenum and over 750 pounds of this material is required for one assembly.

Prior to building the entire assembly a few full scale parts were prepared, coated and tested at temperatures in excess of 3100° F in gas streams of supersonic velocity.

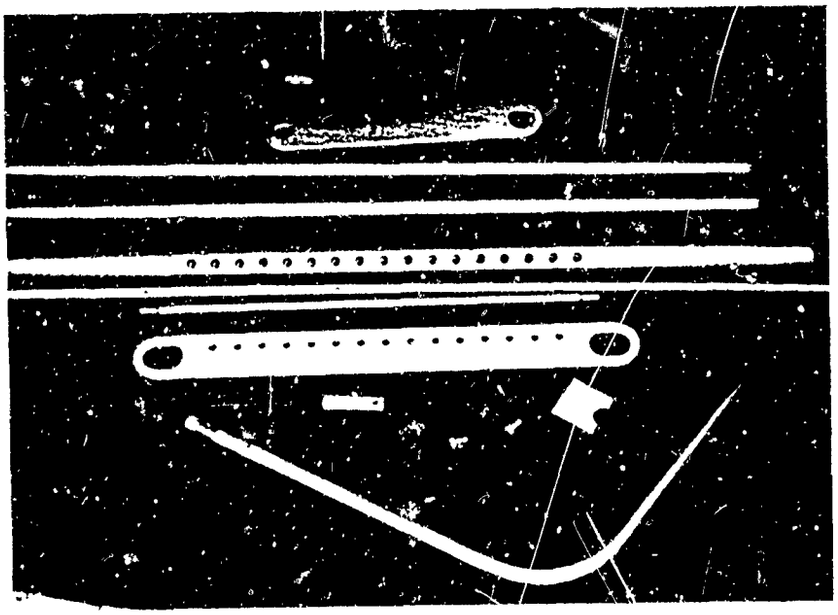

Figure X- Selected Molybdenum Alloy Parts from the Group Coated for the Curtiss Wright Corporation

In these tests no catastrophic failures were seen. Two pinhole failures were noticed in the first few minutes, but neither of these progressed beyond the size first noticed, for the remainder of the test. A total of over 25 thermal cycles from test temperature to ambient totalling just over one hour at the high temperature comprised the test.

It was on one such bar that a purposely induced defect (a 1/8" drilled hole) was "field" repaired prior to test. The repair was applied under what may be considered field conditions with the only source of heat being an oxy-acetylene torch. No retort was used. No failure was noticed on the repaired area.

The one coating project which has been taking more time and energy than any of the others recently is our work on "ASSET". Figure XI is a artist's representation of this vehicle in flight. The nose skirt and six underside panels are molybdenum which is being W-3 coated. Figures XII to XVIII show various components of this vehicle which are being W-3 coated. More information on this project will be presented in a later paper.

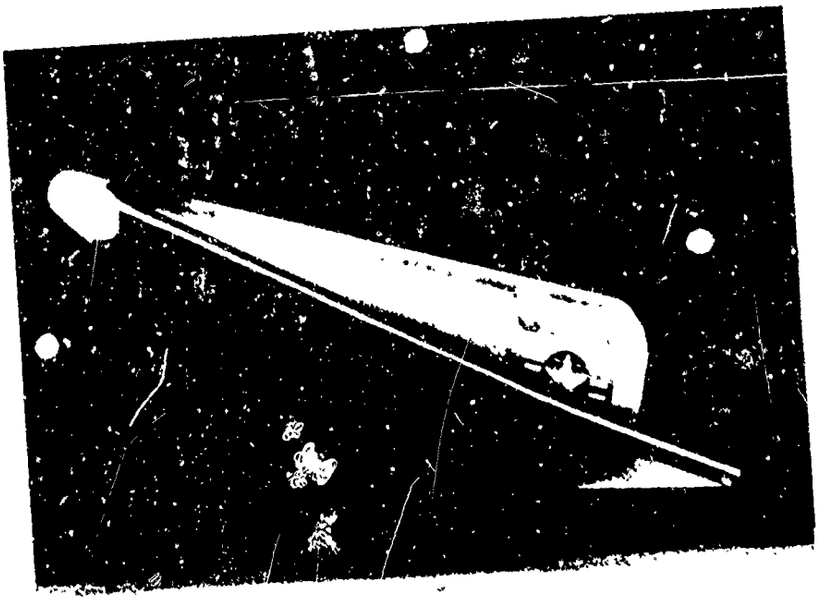

Figure XI- Artist's Conception of ASSET in Flight

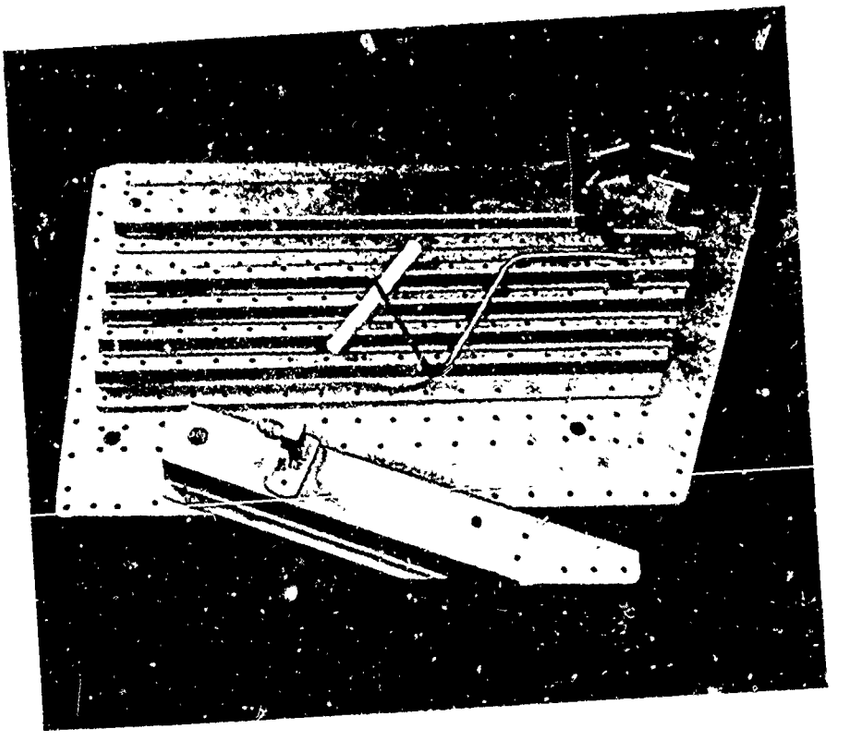

Figure XII- Selected ASSET Components Prior to Coating or Assembly

Figure XIII- Rear View of ASSET Nose Skirt

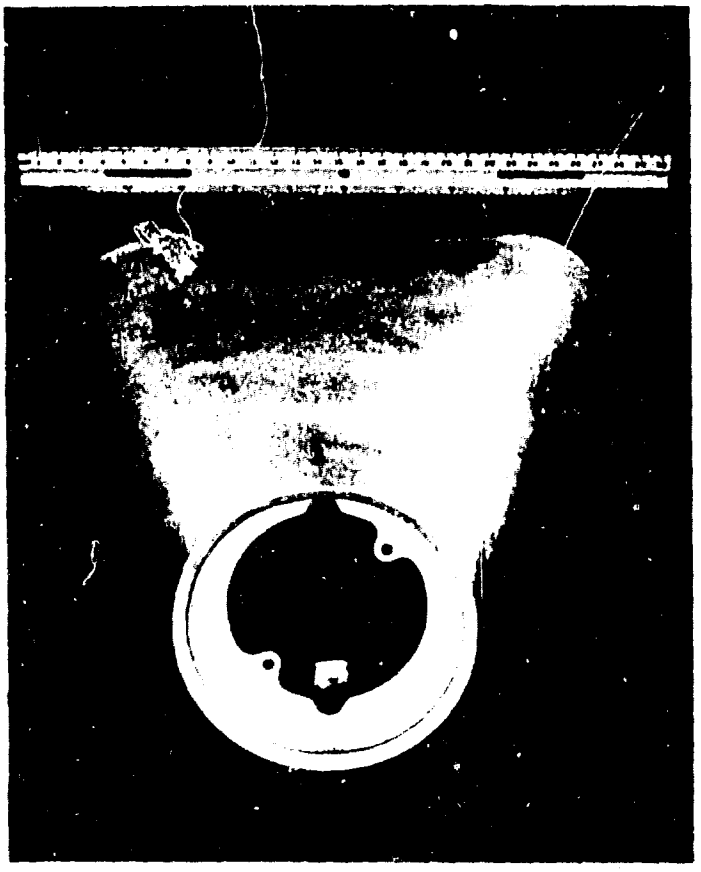

Figure XIV- Front View of ASSET Nose Skirt

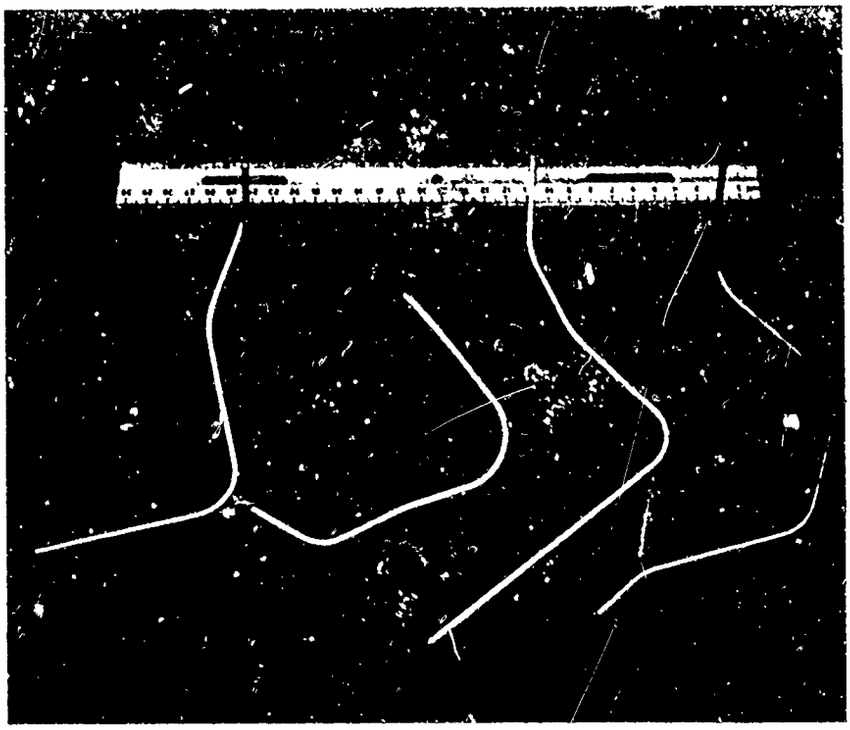

Figure XV- Selected Molybdenum Sheathed Thermocouples as W-3 Coated

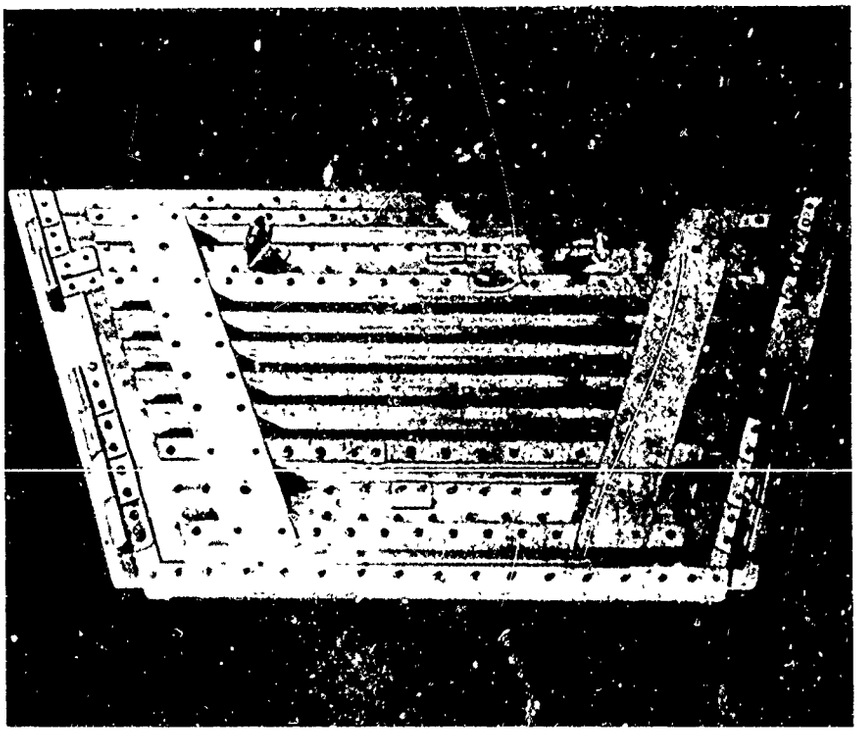

Figure XVI- Rear View of Typical ASSET Panel (As-coated)

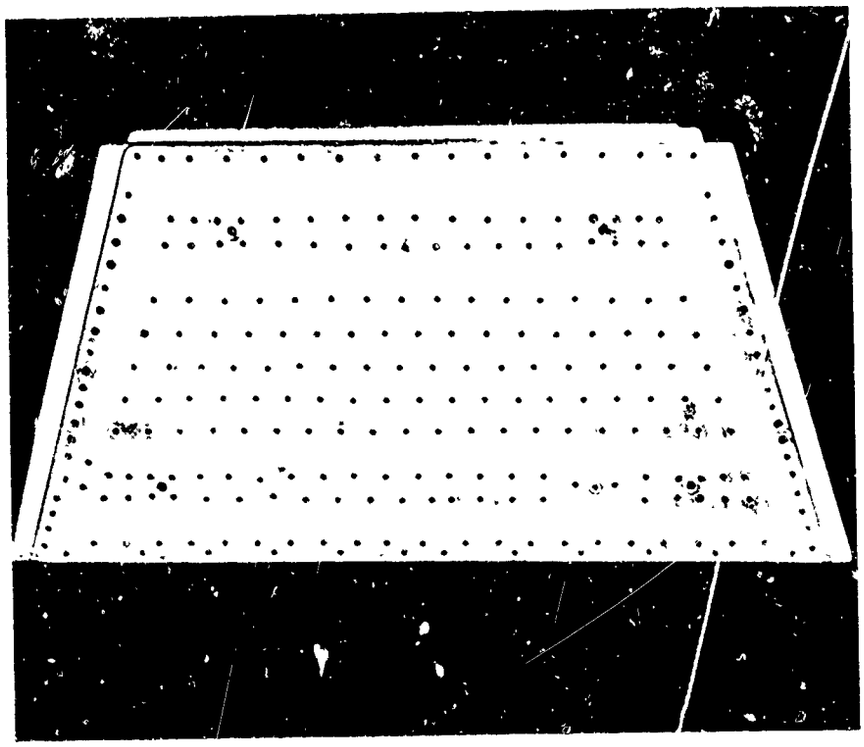

Figure XVII- Skin Side of Typical ASSET Panel
(As-coated)

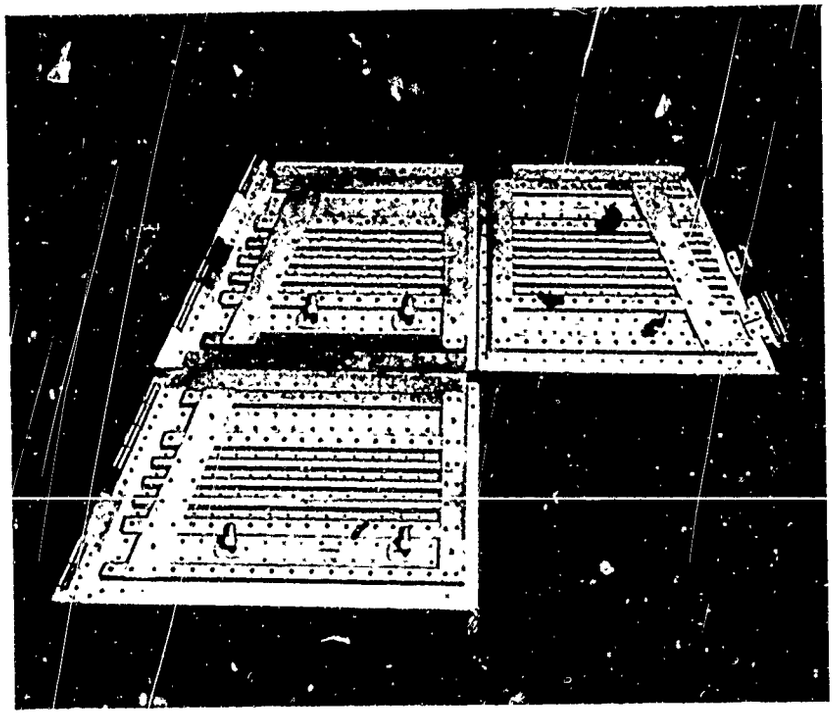

Figure XVIII- Three ASSET Panels Showing Assembly Arrangement

I want to take this oppottunity to thank the Republic Aviation Corporation, The Curtiss Wright Corporation and McDonnell Aircraft for photographs and permission to use them.

SILICIDE COATINGS FOR TANTALUM-BASE ALLOYS

H. R. OGDEN

J. B. HALLOWELL

D. J. MAYKUTH

Battelle Memorial Institute

Columbus, Ohio

INTRODUCTION

This paper describes the results of the second of 2 years of work sponsored by ASD and aimed at the development of silicide coatings for the oxidation protection of tantalum-base alloys. The first year's work, which has been reported at the 5th and 6th meetings of the Refractory Composite Working Group, showed that good protection was achieved with modified silicide coatings applied by pack-cementation methods. The protectiveness of the silicide-base coating was attributed to the formation of glassy oxidation products at temperatures above 2200 F. The vitrification of the silicate scale was promoted by modifying additions with low-melting oxides.

The objective of the second year's work was to optimize modified silicide coatings for tantalum-base alloys, using the more promising modifiers from the previous work, namely Al, B, and Mn, and three alloy substrates of greatest current interest, specifically Ta-10W, Ta-30Cb-7.5V, and Ta-8W-2Hf. Also included in this program was a study of the effects of substrate alloying additions on the behavior of straight silicide coatings, and a survey of other modifiers which held promise for aiding vitrification of the silicate scales. As the program progressed, results of all three phases indicated the importance of vanadium as a silicide modifier, and therefore vanadium-modified silicides were included in additional studies.

METHODS

Coatings were applied by a two-cycle, pack-cementation method with the modifier, where used, deposited in the first cycle and silicon deposited in the second cycle. Based on previous work, a coating thickness of 3 to 5 mils per side was chosen as a target value. These thicknesses correspond, respectively, to total weight gains of 17 to 28 mg/cm^2. Thus, in order to explore wide ranges of composition for each of the silicide modifiers, coating times and/or temperatures were adjusted to meet these weight-gain values. Modifying elements were deposited at temperatures of 1800 to 2400 F and with coating times ranging from 1 to 14 hours. Second-cycle siliciding was done at 2000 to 2400 F in 4 to 24 hours. Pack compositions consisted of 15 to 40 wt% coating element, 1/2 to 3-1/2 wt% halide carrier, and the balance -100 + 140-mesh Al_2O_3. The alloys used as substrates were 40-mil-thick sheet, except for the Ta-8W-2Hf alloy, which was 20 mils thick.

RESULTS

For the study of the effects of substrate alloying additions, straight silicide coatings were applied to tantalum-base alloys containing binary or ternary combinations of Mo, W, V, or Hf. Evaluation of these materials included cyclic oxidation tests at 1800 and 2700 F and electron-beam microprobe analyses of selected coatings. The 1800 F exposures were used because earlier work had shown that this temperature was at the middle of a range in which accelerated oxidation failures occurred in unmodified silicide coatings.

The principal conclusions from this work were:

(1) Alloying additions in the substrates appeared in the silicide coatings in the same proportions as in the substrates.
(2) The results of cyclic oxidation tests at 2700 F ranked substrate additions in order of decreasing benefit as V, Mo, W, and Hf.
(3) Only alloys containing V survived 100 hours' exposure at 1800 F.

The program for optimizing the modified silicides for the three major substrates was started by first screening a relatively large number of coating variations in which the amount as well as the type of modifier, i.e., Al, B, Mn, or V, was varied. Coating performance was rated on (1) 2700 F cyclic oxidation life, (2) oxidation weight-gain behavior, (3) glass-forming tendencies, and (4) microstructure. After this initial survey, six coating-substrate combinations were subjected to more detailed evaluation. This advanced screening included (1) verification of prior 2700 F cyclic oxidation lives, (2) evaluation of self-healing characteristics at 2700 F, (3) determination of 2700 F static oxidation behavior, (4) measurement of 1800 F cyclic oxidation resistance (to gage resistance of the coating system to accelerated failure), and (5) measurement of the effects of the coating process on substrate bend ductility. The results of these tests, summarized in Table 1, serve to illustrate representative performance of the better coatings as well as some of the problems encountered in this work.

TABLE 1. SUMMARY OF PERFORMANCE OF MODIFIED SILICIDE COATINGS ON TANTALUM-BASE ALLOYS

Alloy Substrate	Coating Composition, atomic %	Coating Thickness, mils/side	Average[a] 2700 F Cyclic Oxidation Lives, hours		1800 F Cyclic Oxidation Lives, hours	Room-Temperature Bend Properties of Substrate After Coating
			Undefected Samples	Defected Samples[b]		
Ta-30Cb-7.5V	100 Si	4-5	6-1/2 (8)	<1 (2)	>100	0T
Ta-30Cb-7.5V	Si-50B	3-5	16 (5)	<1 (2)	>100	>20T
Ta-10W	Si-V	4-5	5-1/2 (8)	<1 (2)	75-100	>20T
Ta-10W	Si-20Mn[c]	6-7[d]	10 (2)	<1 (2)	1-3	0T
Ta-8W-2Hf	100 Si	4-5	2-1/2 (4)	<1 (2)	3-25	0T
Ta-8W-2Hf	Si-30Mn[c]	6-8[d]	2 (5)	>7 (2)	3-8	0T

(a) Number of samples tested is given in parentheses.
(b) 0.040-inch-diameter hole drilled through one side of sample.
(c) Rough estimates due only to weight losses from poor edges in as-coated condition.
(d) Coating thickness, discounting edges and corners.

The performance of the straight silicide coating on the Ta-30Cb-7.5V alloy was markedly superior to straight silicides on the Ta-10W and Ta-8W-2Hf. This has been attributed to the modification by vanadium. The silicide-coated Ta-30Cb-7.5V alloy had good oxidation life at both 1800 and 2700 F with moderate coating thickness, and had no embrittling effect on substrate bend ductility. On the basis of the results shown in the table, this system was chosen for more detailed characterization and will be discussed in more detail later in this paper.

The Si-B coatings on the Ta-30Cb-7.5V alloy exhibited the longest oxidation lives of any system studied in this program. For example, one specimen, shown in Figure 1, survived 32 one-hour cycles at 2700 F and an additional 17 one-hour cycles at 2900 F, with a final oxidation weight gain of 0.5 mg/cm^2. The only apparent surface oxidation product on this specimen was a uniform film of clear glass. At the boron levels included in these coatings, boron-rich intermetallic phases formed in the substrate grain boundaries and caused severe bend embrittlement. Furthurmore, no Si-B coatings of any degree of integrity were achieved on the Ta-10W or Ta-8W-2Hf alloys, because of difficulties in depositing silicon over boron on these two alloys.

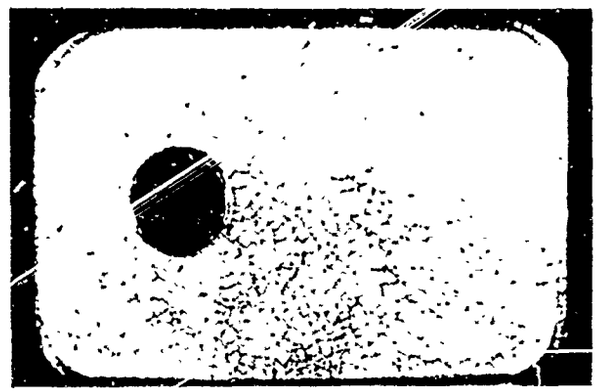

3X

FIGURE 1. Si-57 AT.% B-COATED Ta-30Cb-7.5V SAMPLE AFTER AN ACCUMULATED EXPOSURE OF 32 AND 17 1-HOUR CYCLES AT 2700 AND 2900 F, RESPECTIVELY

The Si-V coating on Ta-10W exhibited good oxidation life at both 1800 and 2700 F and had relatively low weight gains at both temperatures. However, the substrate was embrittled, presumably by the deposition of vanadium, and an investigation was undertaken to determine the cause of this embrittlement. The association of this embrittlement with the vanadizing treatment was based on the following observations:

(1) A net loss in weight of the specimen and the appearance of an intergranular phase in the substrate after first-cycle vanadizing when NaF was used as a carrier
(2) Intergranular cracks and some residual intergranular phase after the siliciding cycle
(3) The intergranular phase was identified as $TaCa_3$.

These characteristics are illustrated in the photomicrograph in Figure 2, along with a summary of the results of an electron-beam microprobe analyses. The specimen shown had been exposed for 101 hours in 2700 F static oxidation and was chosen for analysis because the intergranular precipitate was coarse enough to allow reliable determinations with the microprobe. The results given for the analyses are based on both

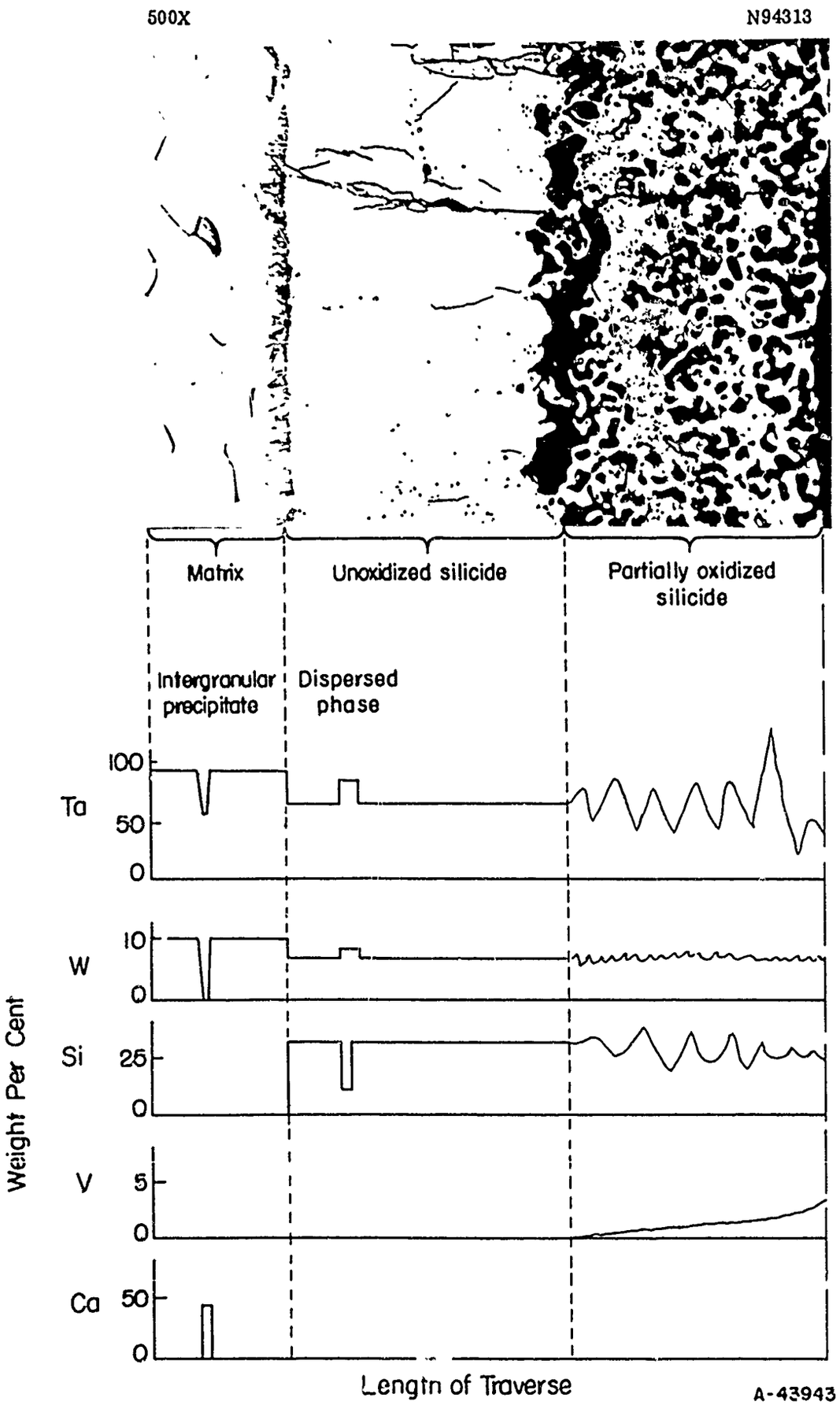

FIGURE 2. SCHEMATIC SUMMARY OF ELECTRON-BEAM MICROPROBE TRAVERSE ANALYSES OF Si-V-COATED Ta-10W

Specimen exposed 101 hours at 2700 F.

traverses and spot analyses, the latter believed accurate to ±2 wt%. The microprobe analyses showed that the calcium was present only in the intergranular phase, in combination with tantalum alone, and in the ratio $TaCa_3$. The compositions of the discontinuous subsilicide phase, adjacent to the substrate (and probably not visible in Figure 2 due to lack of contrast) and the outer silicide layer corresponded to $(Ta\text{-}10W)_{1.1}Si$ and $(Ta\text{-}10W)Si_3$. These silicon ratios were similar to those found in the more extensive analyses conducted on the silicide-coated alloy substrates. Vanadium was found only in the partially oxidized outer layer.

Supplementary coating experiments showed that vanadium deposition could be accomplished using NaI, KI, or NH_4Cl as a carrier without attack of the substrate. It was concluded that the use of Si-V coatings for the protection of Ta-10W would be completely feasible if the proper halide carrier and uncontaminated vanadium were used.

The performance of the last three coatings listed in Table 1 must be qualified with the consideration that all three coatings exhibited poor edge quality due to uneven deposition at edges and corners. Poor edge quality was observed in cases combining two or more of the following conditions:

(1) Small radii on the substrate edges
(2) Rapid deposition rates
(3) Relatively thick coatings.

The specific factors for the coatings listed in Table 1 were the 20-mil thickness of the Ta-8W-2Hf alloy, giving sharper corner radii than the 40-mil thickness of the other alloys, the deposition rates of manganese and silicon, which were the two most rapid encountered in this work, and the fact that thinner (less than 6 mils) Si-Mn coatings on Ta-10W had good edge quality. The advantage of the Si-Mn coatings is apparent in the 2700 F cyclic lives of >7 hours shown by the deliberately defected specimens of Si-Mn-coated Ta-8W-2Hf. The chief disadvantage of the Si-Mn coatings was the very short life at 1800 F.

To illustrate the beneficial effects of vanadium, boron and other silicide modifiers, oxidation weight-gain data are plotted in Figure 3 for a few of the systems studied. Of particular interest are the very low weight gains of the Si-B coating on the Ta-30Cb-7.5V at both 1800 and 2700 F. In contrast to this is the characteristically high weight gain, at 1800 F, of the straight silicide coating on the same alloy. The high weight gain was attributed to some effect of the moderate columbium content of this alloy. Also shown in Figure 3 is the effect of vanadium modification isolated from other influences, i.e., in the straight silicide-coated Ta-5V alloy.

A detailed evaluation was conducted on the straight silicide-coated Ta-30Cb-7.5V alloy. The results of cyclic furnace oxidation tests are listed in Table 2, and show that this system has useful oxidation lives through 2900 F. Oxyacetylene torch tests, with rapid heating and quenching rates, were run at 1800, 2500, 2700, and 3000 F. Failures due to erosion occurred in 3 to 4 half-hour cycles at 3000 F. No failures occurred in 10 half-hour cycles at the lower temperatures. The results of a series of tensile tests on coated and uncoated specimens, listed in Table 3, showed that (1) the coating was protective during 1-1/2 per cent plastic deformation in air at 2200 F and (2) the only detrimental effects of coating were a slight reduction in the yield strength at room temperature and the elongation at 2200 F. Both these effects were attributed to grain growth in the alloy substrate during the thermal exposure of the coating process. No notch sensitivity was present in any of the conditions tested.

TABLE 2. CYCLIC OXIDATION LIVES OF STRAIGHT SILICIDE-COATED Ta-30Cb-7.5V ALLOY SPECIMENS

Exposure Temperature, F	Oxidation Lives of Individual Specimens, hours		Room-Temperature Bend Properties of Substance After Exposure
	Undefected	Defected[a]	
1200	>100, >100, >100	--	0T
1500	>100, >100, >100	--	0T
1800	>100, >100	<1, <1	0T(b)
2000	25-50, 50-75, 50-75	--	Embrittled
2200	>100, >100, >100	--	0T
2500	>24, >24, >24	--	0T
2700	2, 10, 12	<1, <1	--
2900	6, >17, >17	--	0T

(a) 0.020-inch-diameter hole drilled through coating on one side of the sample.
(b) Defected specimens were embrittled.

TABLE 3. TENSILE PROPERTIES OF SILICIDE-COATED Ta-30Cb-7.5V ALLOY

Specimen Geometry	Condition[a]	Test Temp, F	0.2% Offset Yield Strength, ksi[b]	Ultimate Tensile Strength, ksi[b]	Elongation in 1 Inch, per cent
Unnotched	Uncoated	RT	92.0	106.0	>20
Unotched	Uncoated; 16 hours at 2200 F in vacuum (simulated coating treatment)	RT	83.6	100.3	26
Unnotched	Coated	RT	85.7	105.4	13
Unnotched	Coated and exposed 1 hour at 2700 F in air	RT	85.4	102.4	20
Unnotched	Coated and strained 1.5% in 1/4 hour at 2500 F in air	RT	87.6	104.6	27
Notched[c]	Uncoated; 16 hours at 2200 F in vacuum (simulated coating treatment)	RT	-	105.1	3-4
Notched[c]	Coated	RT	-	107.0	3-4
Notched[c]	Coated and exposed 1 hour at 2700 F in air	RT	-	102.6	3-4
Unnotched	Uncoated	2200	30.5	36.5	85
Unnotched	Uncoated; 16 hours at 2200 F in vacuum	2200	38.3	39.6	56
Unnotched	Coated[d]	2200	47.6	50.3	38

(a) All specimens annealed 1 hour at 2200 F in vacuum prior to the treatments listed.
(b) Strengths based on area of substrate core only, data were corrected for substrate consumed during coating formation.
(c) Center-hole notch with a calculated stress-concentration factor of 2.3.
(d) Single specimen, all other values are averages of two specimens.

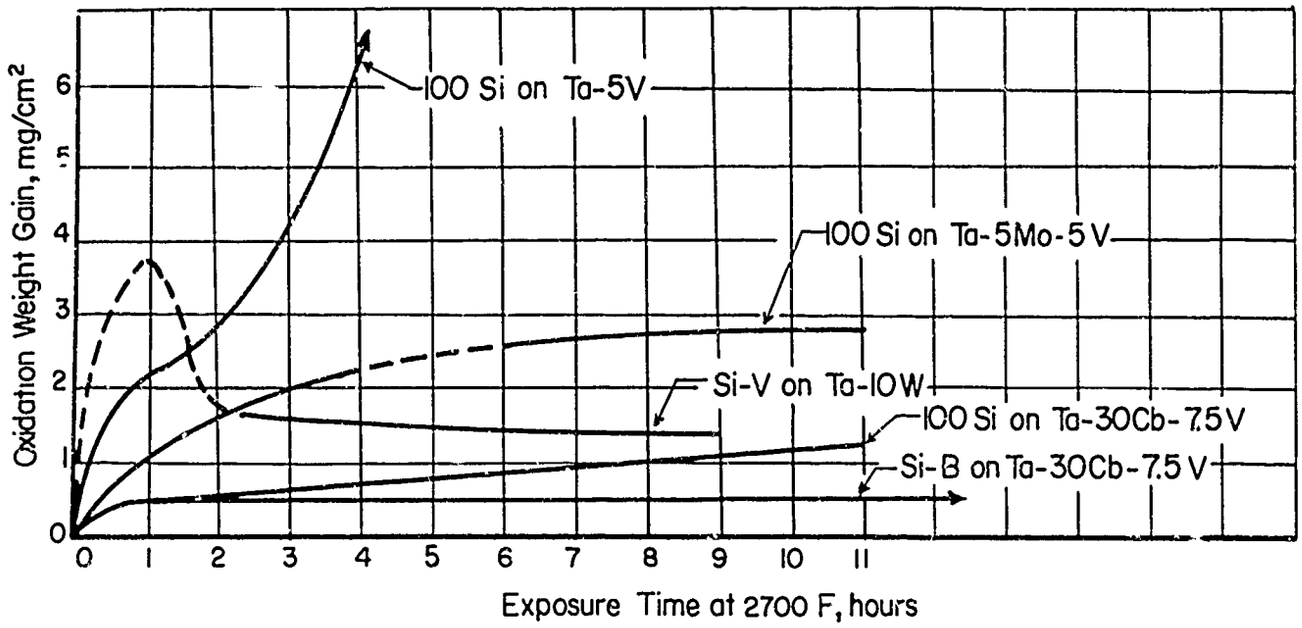

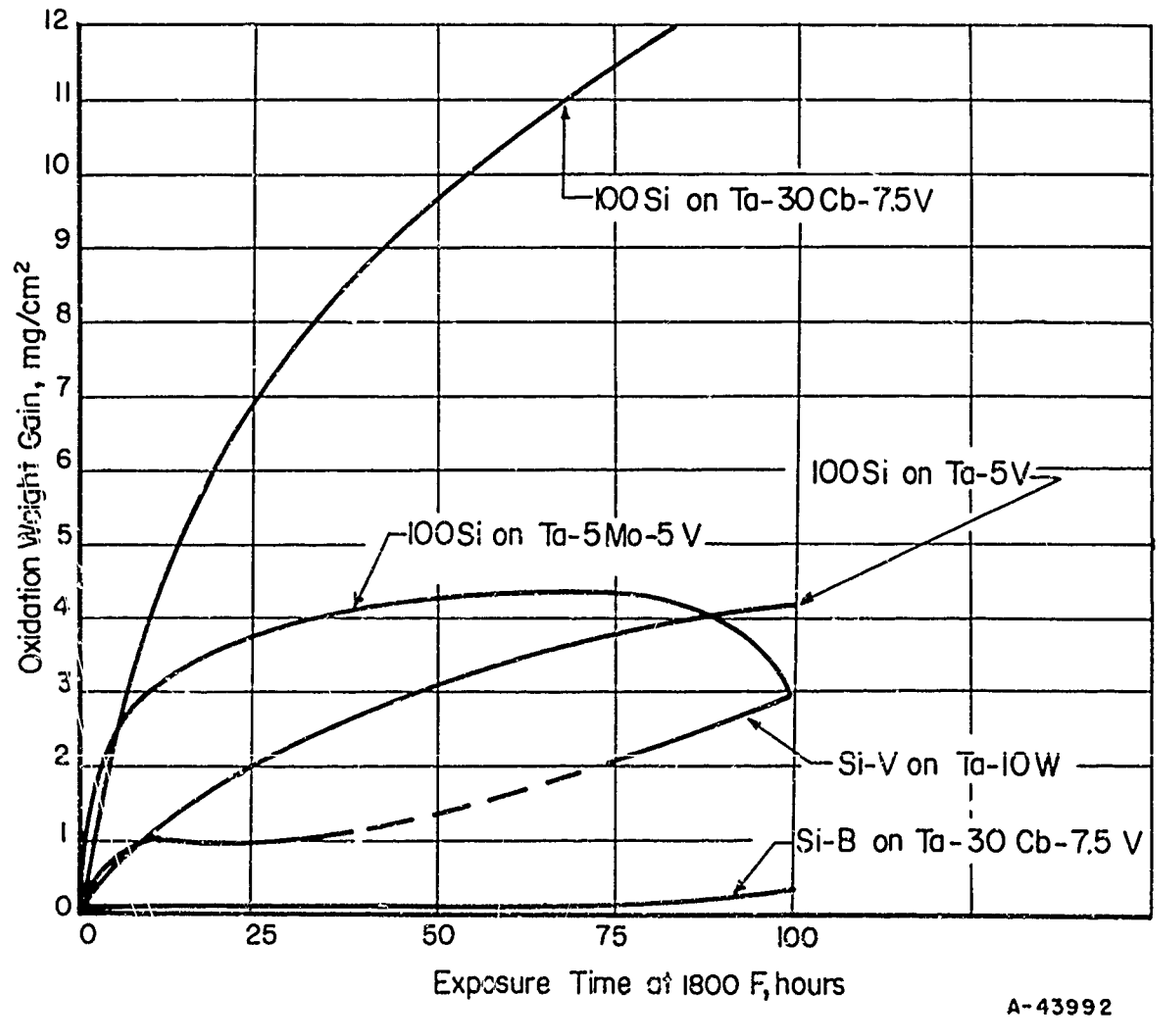

FIGURE 3. OXIDATION WEIGHT GAINS AT 1800 F AND 2700 F FOR SILICIDE-COATED TANTALUM-BASE ALLOYS

CONCLUSIONS

The major conclusions drawn from the work done in this program were:

(1) Vanadium was the most beneficial modifier for silicide coatings on coatings on tantalum alloys and was effective at both low (1200 to 1800 F) and high (2500 to 2700 F) temperatures.
(2) Boron additions, in combination with vanadium, gave further improvements in the degree of protection at both 1800 and 2700 F. However, at the boron levels investigated, substrate bend embrittlement occurred as a result of the presence of an intergranular boron-rich phase.
(3) The capabilities of the straight silicide coating on Ta-30Cb-7.5V alloy included useful lives in cyclic oxidation testing through 2900 F, resistance to thermal shock and oxidation in torch tests up to 3000 F, and protection during 1-1/2 per cent plastic deformation in air at 2200 F.

HIGH-TEMPERATURE PROTECTIVE COATINGS FOR REFRACTORY METALS

Part I - Development of Oxidation Resistant Coatings for Refractory Metals

L. SAMA

Part II - Experimental Study of Factors Important in the Protection of Tungsten above 1900°C

C. D. DICKINSON

General Telephone and Electronics Laboratories

Bayside, New York

PART I

DEVELOPMENT OF OXIDATION RESISTANT COATINGS FOR REFRACTORY METALS

L. Sama

1. INTRODUCTION

The coating work being conducted at this laboratory consists of two parts: Part I is concerned with the practical development of coatings for all of the refractory metals and Part II is a more fundamental program which is directed toward clarification of factors of importance in coatings for tungsten above 1900°C. The objective of this portion of the report is to summarize the work in progress in Part I which covers a fairly broad spectrum of the refractory metals and alloys and, particularly, to give some of the highlights of results obtained on an Air Force-sponsored program [1] on several tantalum-base alloys.

---

[1] L. Sama, "Oxidation Resistant Coatings for Tantalum Alloys and Other Metals, "TR-62-460.7 from General Telephone & Electronics Laboratories Inc. to ASD on Contract No. AF(657)-7339, January 1963

2. COATING DEVELOPMENT AND APPLICATION

The investigations can be divided into three areas: (1) in-house work, (2) Government-sponsored work, and (3) the coating of samples and hardware for outside company evaluation and use. A rather broad range of metals and alloys has been covered under these three programs. Both development and evaluation are continuing on a modified silicide coating for tungsten and tungsten alloys and molybdenum. A number of coatings have been developed or adapted for particular processing and operating conditions for columbium alloys. The coatings consisted of Sn-Al, Ti-Al, Ti-Si, and Ti-Cr-Si. Among the alloys investigated are B-66, X-110, D-14, D-36, D-31, FS-85, Cb-752, and a number of proprietary alloys for several companies. Molybdenum, TZM, and Mo-.5Ti have been coated with Sn-Al with certain modifications. Evaluation samples such as coupons, foil, and tensile bars have been prepared for evaluation. Hardware items such as nozzles, thrust chambers, power conversion devices, and jet engine parts have been coated for outside evaluation and use. Environmental conditions are usually oxidizing and the hardware coated has been evaluated in rocket propellant exhaust streams and in hydrocarbon fuel erosive environments. The types of coatings developed and evaluated, in addition to their varied

composition have also been diverse in their method of application. These consisted of slurries, hot dipping, pack cementation, and pack cementation plus hot dipping.

A year end report has been written covering the results of the development of oxidation-resistant coatings for the refractory metals which was sponsored by ASD. The report was fairly extensive and was concerned primarily with the development and evaluation of tin-aluminum slurry coatings for the refractory metals, particularly for tantalum-base alloys. Since the report was quite extensive and will receive rather wide distribution, only a few of the areas investigated will be touched on here.

An extensive evaluation of the effectiveness of the tin-aluminum spray slurry coating process was conducted on Ta-10W, Ta-30Cb-7 1/2V, and Cb-5 Zr. Some of the data covering stress rupture evaluations, oxidation tests, and reduced pressure environment tests are covered here for 0.040" thick Ta-10W and 0.020" thick Ta-30Cb-7 1/2V. The Ta-10W was coated with Sn-25Al and the Ta-30Cb-7 1/2V was coated with Sn-50(Al-Si). These coating compositions were modified by the addition of both tantalum and molybdenum powder plus excess aluminum to the slurry so that during the subsequent diffusion treatment intermetallic particles were formed, which provided a network for preventing a run-

off of the excess Sn-Al phase. All samples were spray coated with the slurry and then vacuum diffused at 1850°F approximately for 1/2 hour; the process was repeated to build up the coating thickness.

Short time stress rupture data are shown in Fig. 1 for both alloy materials. Data taken from literature for Ta-10W tested in vacuum at the same temperatures are plotted for comparison. At the time of writing, no equivalent data for the Ta-30Cb-7 1/2V tests at 2700°F were available for comparison. The data obtained here for the Ta-10W coated samples at 3000°F appear to fall between two sets of data obtained by other investigators in vacuum tests at 3000°F. The 2800°F data obtained here fall quite close to that plotted from the literature. The stress rupture strength of the Ta-Cb-V alloy is much lower than the Ta-10W, even though the ternary alloy data were obtained at a lower temperature. In fact, the slope of the curve is quite steep for the Ta-Cb-V alloy at 2700°F, and if extrapolated to a 100-hour rupture life, the stress would be about 2000 psi. However, if the data were plotted on a strength-to-weight ratio basis, the Ta-Cb-V alloy would show up much more advantageously. The deformations involved in all cases were quite considerable, amounting to as much as 30 to 40%. Therefore some of the coating tended to chip off or flake off, particularly in the last stages of rupture. However, the only visual evidence of oxidation occurring at or in the vicinity of fracture in these and other

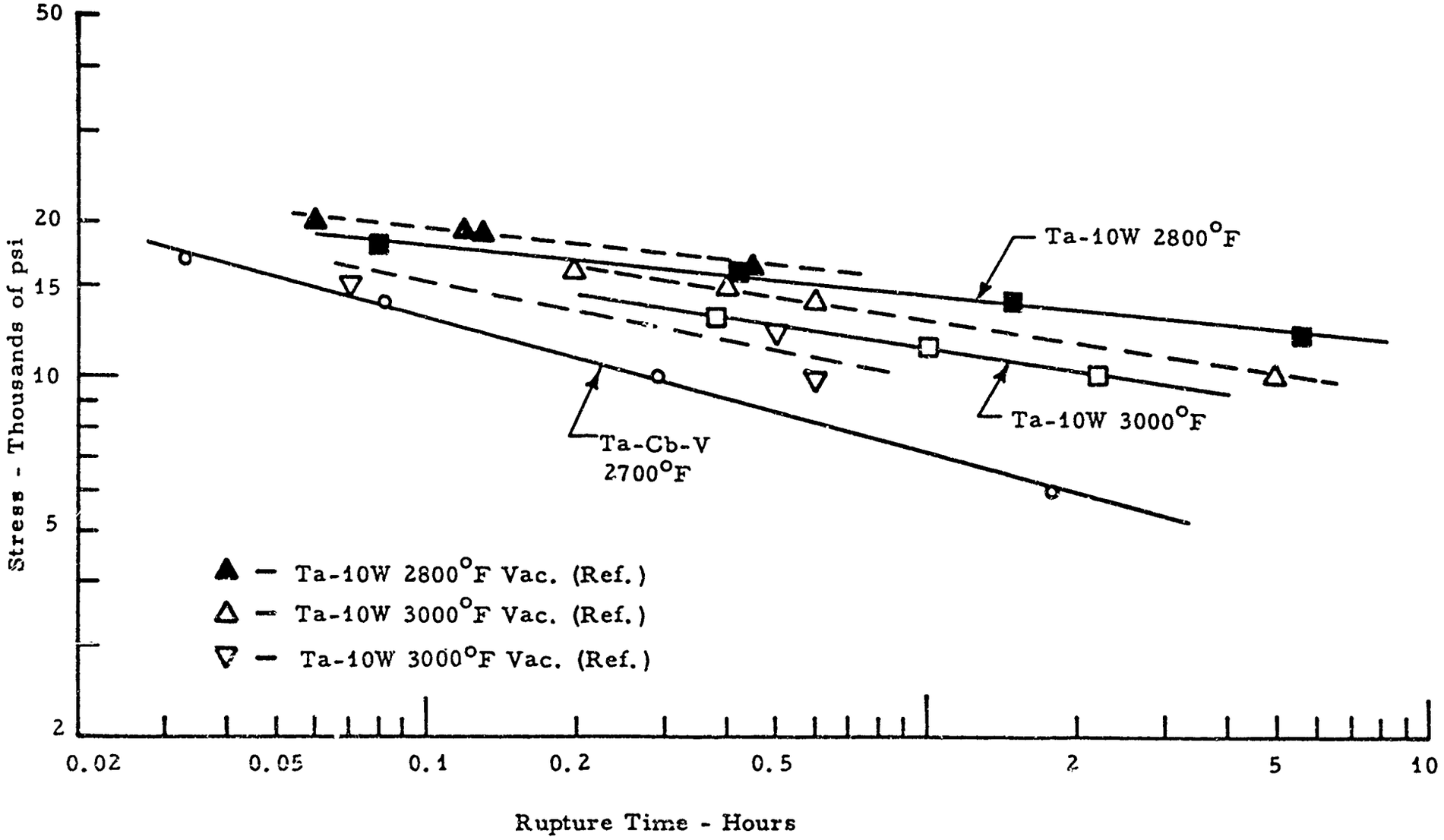

Fig. 1. Stress-rupture curves for Ta-10W and Ta-30Cb-7.5V coated samples tested in air.

tests was in the Ta-Cb-V alloy tested for the longest time, and this was at the tip of the fracture.

Similarly coated coupon samples of each alloy were also tested in batches at tempertures from 1100 to 3000°F in furnaces. Some of the 2500 to 3000°F data are shown here. Life in hours vs. coating weight are plotted in Figs. 2 and 3 for the Ta-10W alloy and in Fig. 4 for the Ta-Cb-V alloy. It was found, in general, that substrate thickness, size, or edge rounding had little effect on oxidation resistance. The most significant effects were due to coating thickness and cycling rate. Failures occurred predominantly at edges at all temperatures. At 3000°F with Ta-10W, oxidation life increases slightly with increased coating thickness. Little effect of sample size is indicated between 3/4" and 1-1/2" long samples. Samples given only one coating had respectable lives of 3 to 6 hours. At 2800°F there was practically a linear relationship between the coating thickness and oxidation life. In fact, the major effect of the molybdenum additive over tantalum is clearly to increase the coating thickness and the data fall in line with the thinner coatings. It can also be seen that the cycling rate has a profound effect on life at 2800°F. In reducing the cycling rate to once a day, lives over 75 hours were obtained.

For the Ta-Cb-V alloy at 2500°F there was a very sharp increase in life with coating thickness. The first batch of samples had lives varying from 40 to over 85 hours. With somewhat thicker coatings

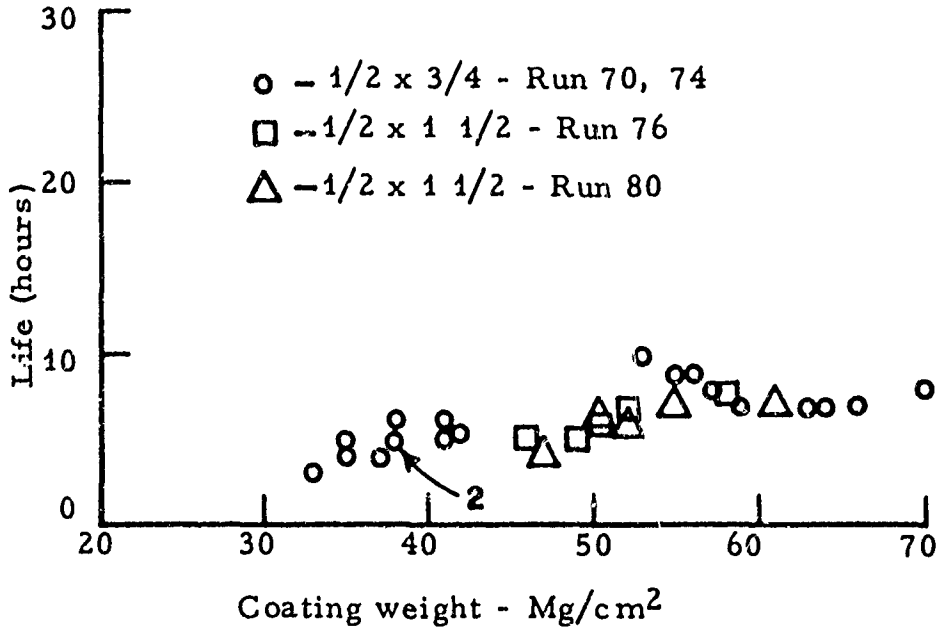

Fig. 2. Oxidation life in furnace tests of Ta-10W samples coated with (Sn-25Al)-10$TaAl_3$ and tested at 3000°F.

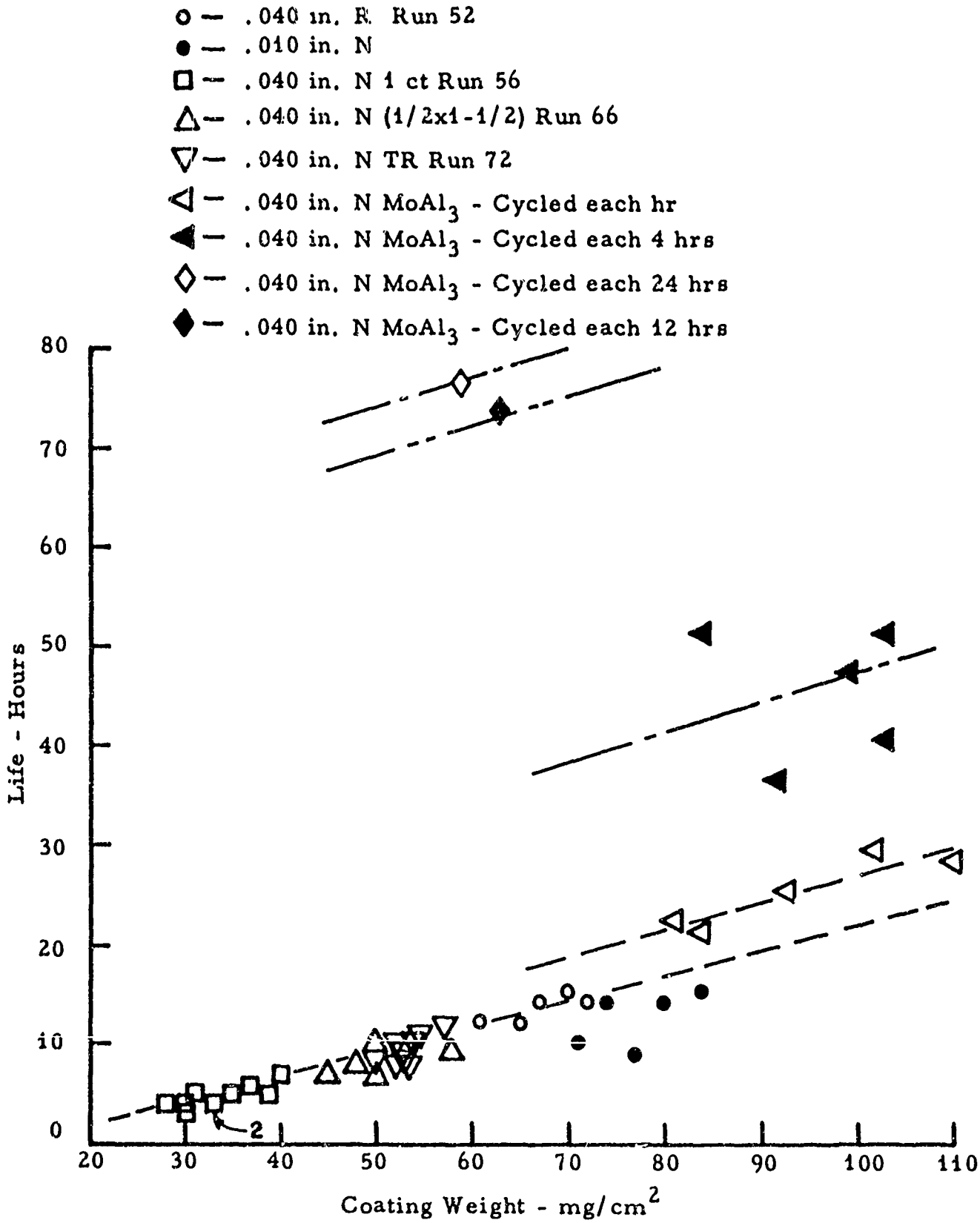

Fig. 3. Oxidation life in furnace tests of Ta-10W samples coated with (Sn-25Al)-10$TaAl_3$ and (Sn-25Al)-10$MoAl_3$ and tested at 2800°F.

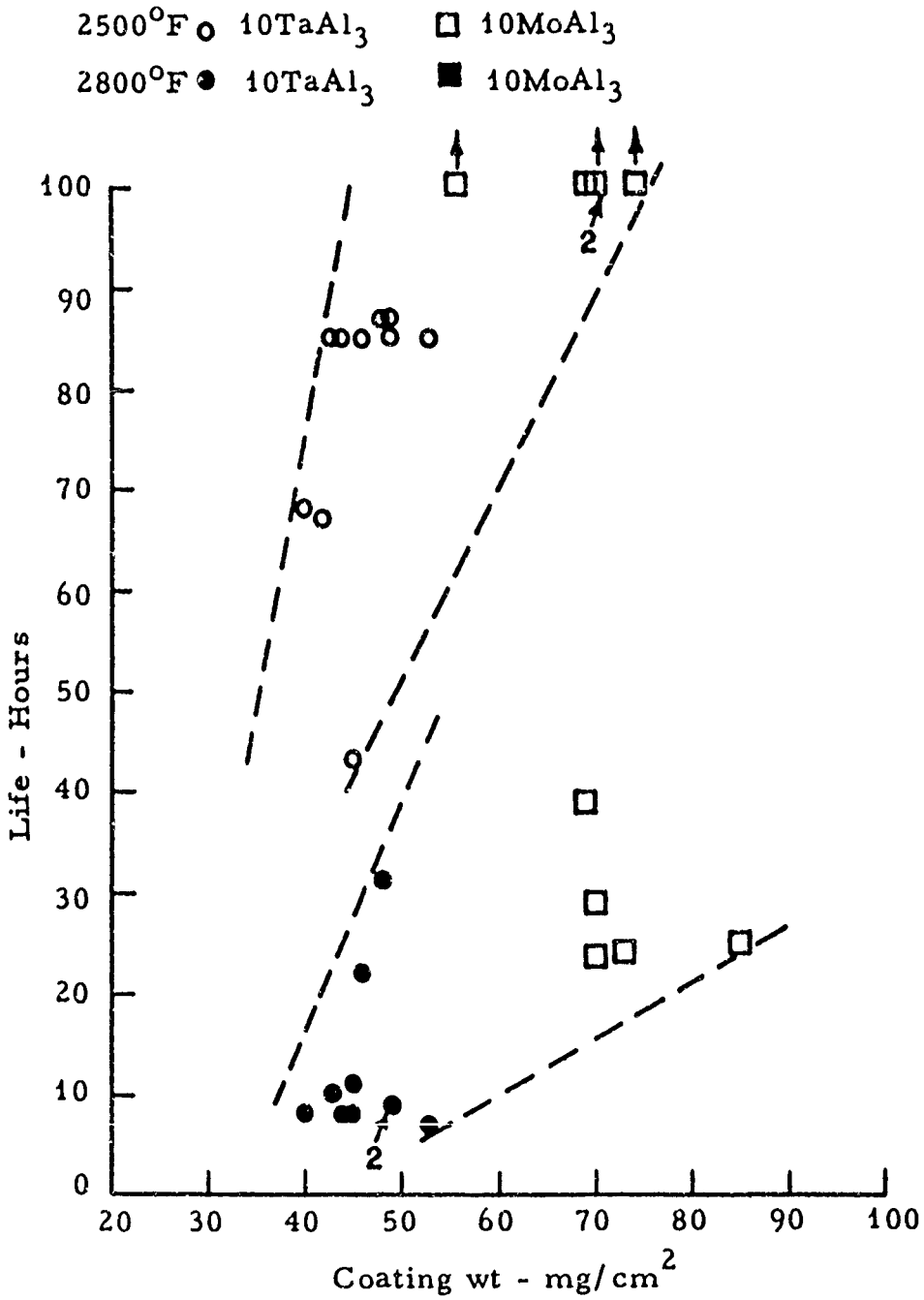

Fig. 4. Oxidation life of Ta-30Cb-7.5V coated samples at 2500 and 2800°F.

provided by the additicn of 10% molybdenum powder to the coating, none of the five samples tested failed in 100 hours at 2500°F. At 2800°F most of the samples failed in 7 to 11 hours, with several lasting up to 30 hours. Coating thickness did not appear to have any particular effect in the range studied. However, the batch of samples with the molybdenum additive had considerably thicker coatings and had longer lives of 24 to 39 hours. In general, the coatings are much thicker than those with equivalent coating weights in the (Sn-25Al)-10$TaAl_3$ composition.

Much more extensive data are given in the final report concerning tensile strength, diffusion effects, and oxidation resistance of coated samples over a wider temperature range.

To study coating stability in the range of 1 to 15 mm of air pressure, a modified Sieverts apparatus was set up together with a resistance heating chamber. A cartesian manostat was used to regulate air pressure in the range of interest. Various attempts were made to minimize the temperature gradient resulting from clamping the specimen in water-cooled electrical grips. Initially this was done by contouring the sample so that the grip ends were narrowest and the sample widened gradually to a maximum of 1/4 in. at the center. Samples of Ta-10W, from 0.01 in. to 0.04 in. thick by approximately 2 in. long were coated with (Sn-25Al)-10$TaAl_3$. Tests showed, however, that the coating thickness variations within the sample test section were sufficient to cause a temperature gradient

in the sample. Therefore, subsequent samples were coated with the molybdenum additive to obtain much more uniform coatings. Additional difficulties were encountered because of the relatively small grip ends which led to hot spots and poor contact. This difficulty was alleviated by using completely rectangular samples, 0.010 in. thick x 1/4 in. wide, but the restraint imposed by the vacuum seals around the grips caused these samples to buckle at the center. In some cases this resulted in shorting out against the wall of the chamber.

Samples were usually exposed for 1/2 hour at temperature, taken out, examined, weighed, reassembled into the apparatus, and re-tested for another 1/2 hour. Many of the samples developed hot spots in some localized area, which resulted in a burnout. Therefore it was not possible to specify the type of failure that occurred. Accordingly, the results plotted in Fig. 5 are those for which a uniform weight loss or weight gain was obtained. None of these samples had failed in the classical sense of an oxidation failure. In fact most of them suffered little change in structure or appearance. It is apparent, however, that at 1.5 mm pressure considerable coating loss occurs in the vicinity of 2570°F in 1/2 hour. Similar losses are obtained at a lower temperature, 2450°F, in one hour. It can be seen from Fig. 5 that the coating is quite stable at approximately 2600°F at 3 mm pressure, at 2780°F at 6 mm pressure, and at 2850°F at 12 mm pressure. The effect of time at temperature is shown in

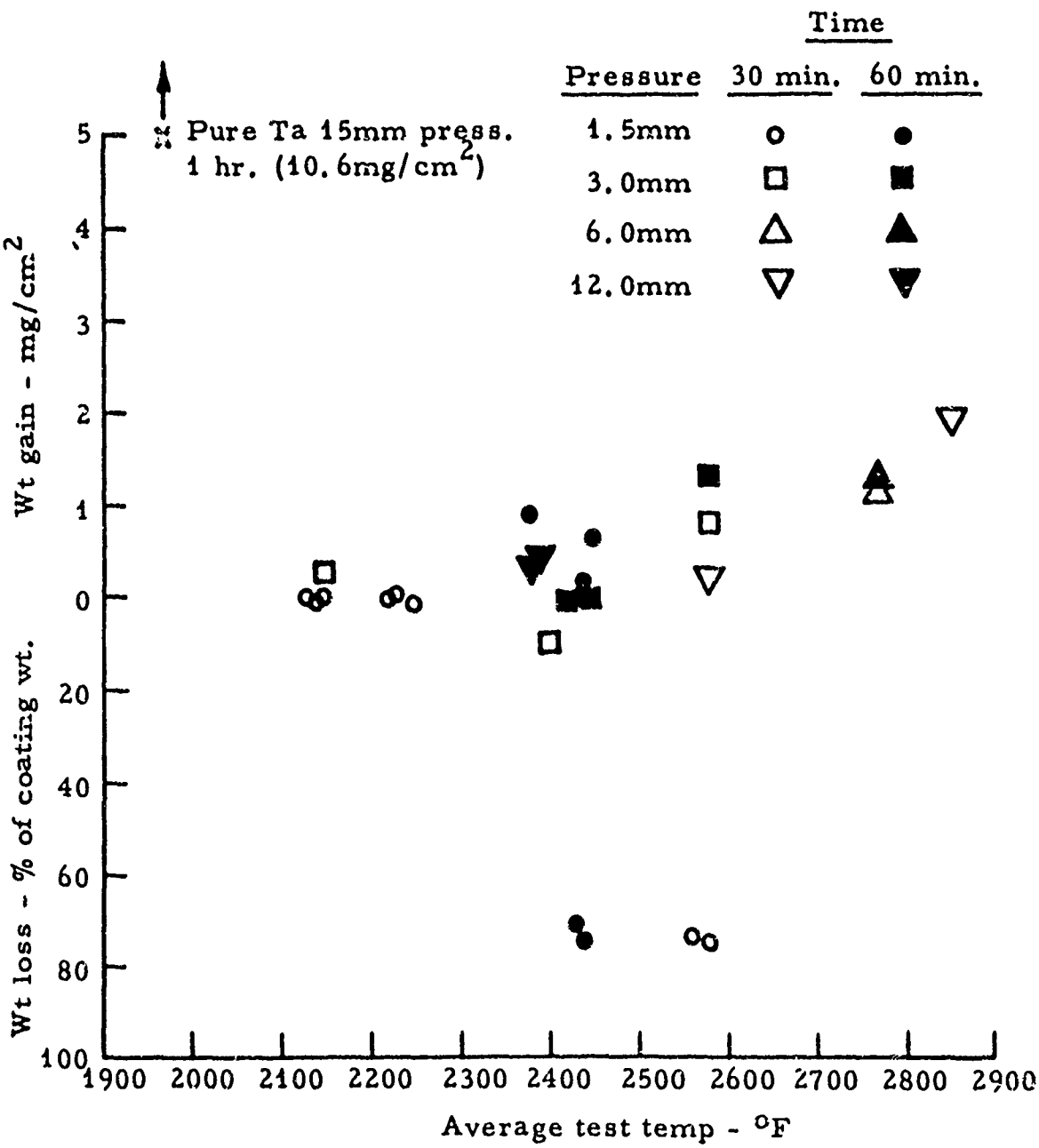

Fig. 5. Weight changes in coated samples at reduced air pressures.

Fig. 6. Where weight gains occur they appear to be continuous. From microstructural changes at 2700°F in 1 1/2 hours it is apparent that local areas can be depleted of the coating within this test time; these depleted areas are probably related to the hot spots within the sample caused by nonuniformities. In order to establish the range of pressures and temperatures at which the coating is stable, it would be preferable to use an outside heating source to attain necessary temperatures.

These studies indicate that where a protective oxide film forms, stability is increased and can probably be increased to temperatures in the vicinity of 3000°F. However, considerably more work would have to be done in order to establish the precise temperature-pressure boundary conditions for stability.

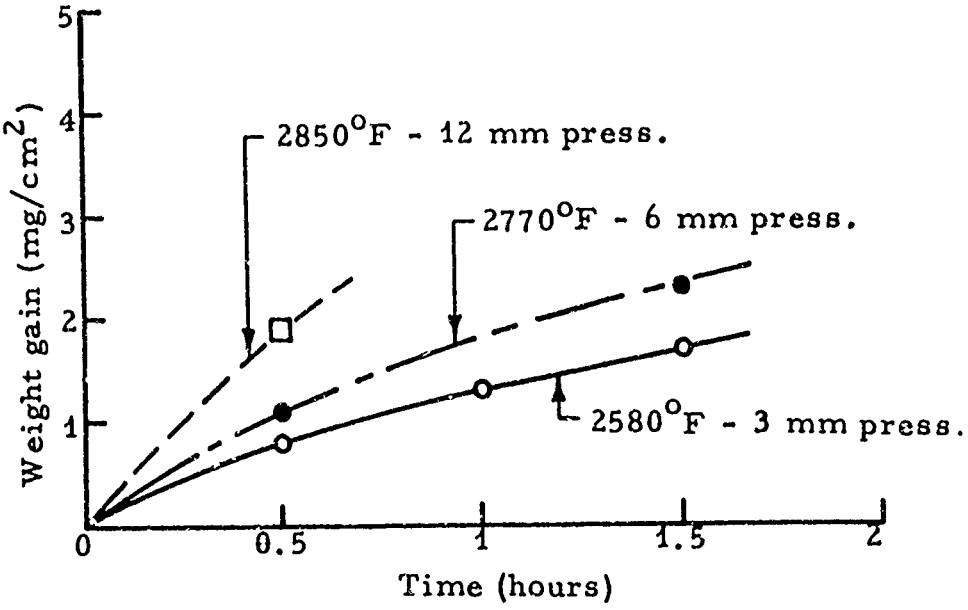

Fig. 6. Weight gains of samples of Ta-10W coated with (Sn-25Al)-10$MoAl_3$ and heated by their own resistance.

PART II

EXPERIMENTAL STUDY OF FACTORS IMPORTANT IN THE PROTECTION OF TUNGSTEN ABOVE 1900°C

C. D. Dickinson

1. INTRODUCTION

Silicide and aluminide-base coatings which adequately protect the refractory metals at temperatures up to 1900°C have a maximum upper temperature limit for protection of about 1900°C. Therefore, knowledge of the growth of protective films of more refractory, less volatile oxides has been the impetus behind investigation of the factors which are important in the growth of refractory oxides as a protective barrier for tungsten. An analysis of the problem was presented at the last Composites Work Group Meeting and five factors were discussed which seem to control the over-all efficacy of a barrier coating of oxide grown from a reservoir coating substrate. A detailed description of analysis of these five factors is given in Ref. 1, 2, 3, and 4 . The survey revealed that there were many areas in which information was insufficient and in which a better understanding would aid in the development of high-temperature coatings. So many areas requiring further study were revealed that some order of priority was required if significant assistance is to be given to development programs

now in existence or projected for the near future. The next objective, therefore, was to define the type of research programs needed and then to assign an order of priority.

Recommendations were made for specific experimental research programs needed to define each of the processes discussed in Ref. 3. The relative importance of these programs was evaluated in terms of the contribution that additional knowledge or information about the particular phenomena could make to coating development programs [4]. It is worthwhile, therefore, to briefly reiterate the five phenomena defined by the analysis of the problem being of major importance and to indicate their relative importance in determining the protectiveness of a coating system.

These phenomena are:

1. The breakaway proneness of the oxide formed.
2. The diffusion paths followed in the ternary oxygen-metal-metal coating environment system.
3. The rates of vaporization of the components of the coating system.
4. The rate of coating-substrate reactions.
5. The rates of cationic and anionic diffusion through the outer oxide layer.

In the final analysis, multicomponent diffusion processes and breakaway are the principal phenomena that initially determine if a coating

is protective, since protection depends on whether refractory oxides of the desired composition and structure are formed as an adherent non-porous film that grows by a diffusion controlled process. Predictions based on the existing knowledge in these two areas should be tested by critical experiments. For example, a demonstration that either the strength or ductility of a substrate affects the high-temperature film-forming characteristics of refractory oxides such as ZrO_2 and HfO_2, or changes the conditions for breakaway, would be an important step toward the better understanding and control of breakaway during the oxidation of refractory and intermetallic compounds. The influence of stoichiometry, as predicted by ternary diffusion, on the oxide formed has important implications for attempts to grow complex refractory oxides, and should be tested. Therefore, experiments have been conducted to provide additional insight on the processes of breakaway and ternary diffusion in oxidation which lead to the formation of refractory oxide films. The results of two experimental studies will be discussed separately in the following sections.

2. STUDY OF BREAKAWAY

The change to linear oxidation rates in the growth of refractory oxides such as Zr and Hf on their own substrate is generally associated with spalling and mechanical cracking of the oxide. Although a variety of

specific mechanisms for breakaway oxidation of individual metals have been proposed and are being investigated, a common denominator is that stresses or strains at the metal-oxide interface seem to be associated with breakaway phenomena in many systems. Therefore, an experimental program was designed to determine if the use of a liquid substrate could prevent breakaway in the growth of various refractory oxides by preventing the transmission of stress or strain from the substrate to the oxide. Achievement of this objective would have some practical implications, since the work of Sama [5] demonstrated that a liquid carrier layer can be used effectively in the formation of Al_2O_3 from coatings on the refractory metals.

2.1 PROCEDURE

The procedure used in the experimental work to be discussed is given in detail in Ref. 4 and will not be repeated. The general experimental procedures used were to melt an alloy of the desired composition in a zirconia or alumina crucible, machine the exposed metal surface and oxidize the sample in the crucible. Temperatures from 900 to 1700°C for various times were used to determine the kinetics of growth by weight gain and thickness measurements. Microprobe and X-ray analyses of the oxidized samples were used to identify specific phases observed metallographically. In all cases, oxides of the diluent used to produce a liquid phase alloy had a lower free energy of formation than the reactive element oxide. Tin and

gold were used as diluents. The growth of HfO_2 and ZrO_2 from a Hf or Zr alloy substrates were studied, using both tin and gold as a diluent. Growth of ThO_2 and Al_2O_3 from Th and Al alloys were investigated, using only tin as a diluent. Study of the oxidation kinetics of the six-liquid alloy system has been completed. Although certain peculiarities in behavior were observed which are characteristic of a specific system, the results which are described in the following section provide information with general implications on the effect of liquid substrates in the growth of refractory oxides without breakaway.

2.2 RESULTS AND DISCUSSION OF RESULTS

The effect of time and temperature on the rate of growth of oxides on Sn-16.7%Hf, Sn-9.3%Zr, Sn-5.3%Th and Sn-16.7%Al alloys are given in Figs. 1 to 4. The resulting curves are a plot of the specific weight gains or metallographically observed thicknesses as a function of the square root of the time of oxidation test. It will be observed in these figures that deviations from parabolic growth do eventually occur at many temperatures at longer times. The oxide films formed (Fig. 5) are compact and adherent at temperature. However, in certain systems, particularly the Au-Zr and Au-Hf systems, stresses generated on cooling caused the oxide to spall after the test had been completed. Even in the cases where the oxides had spalled on cooling, the weight gains indicated that protective growth had occurred during the isothermal test.

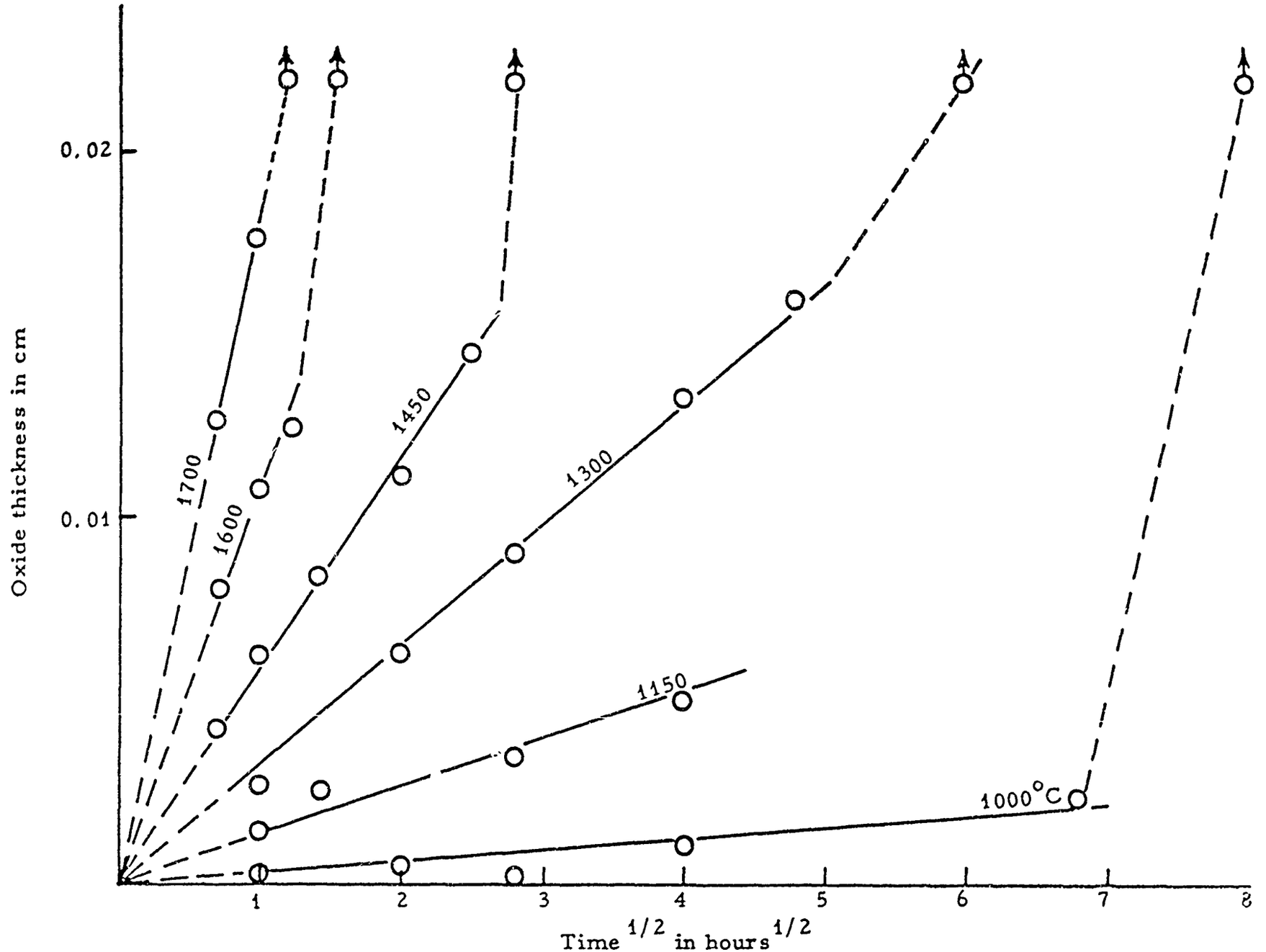

Fig. 1. The thickness of surface films formed on 16.7 w/o Hf-Sn alloy samples in dry air expressed as a function of oxidation time and temperature.

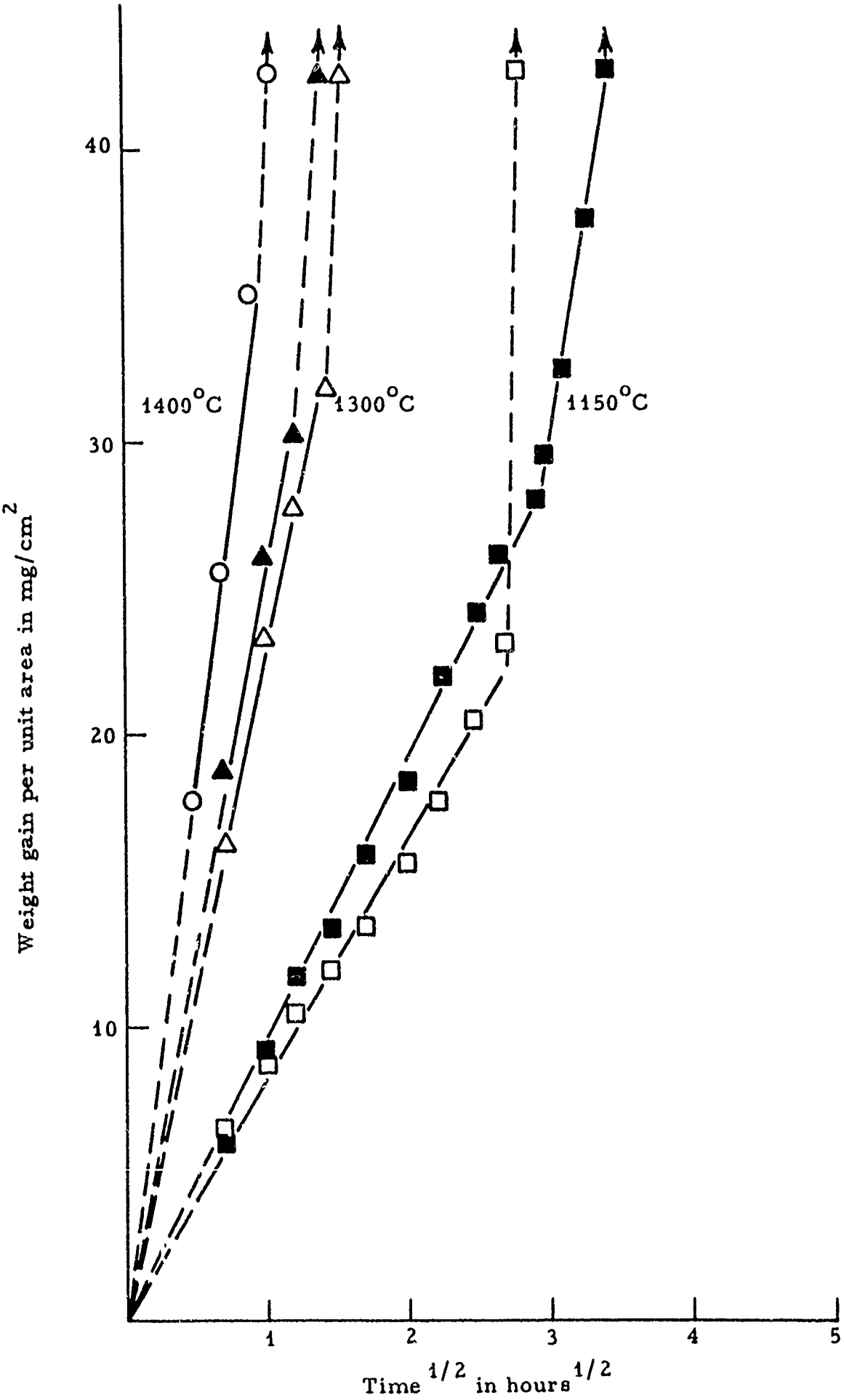

Fig. 2. The weight gains in dry air of 9.3 w/o Zr-Sn alloy samples expressed as a function of oxidation time and temperature.

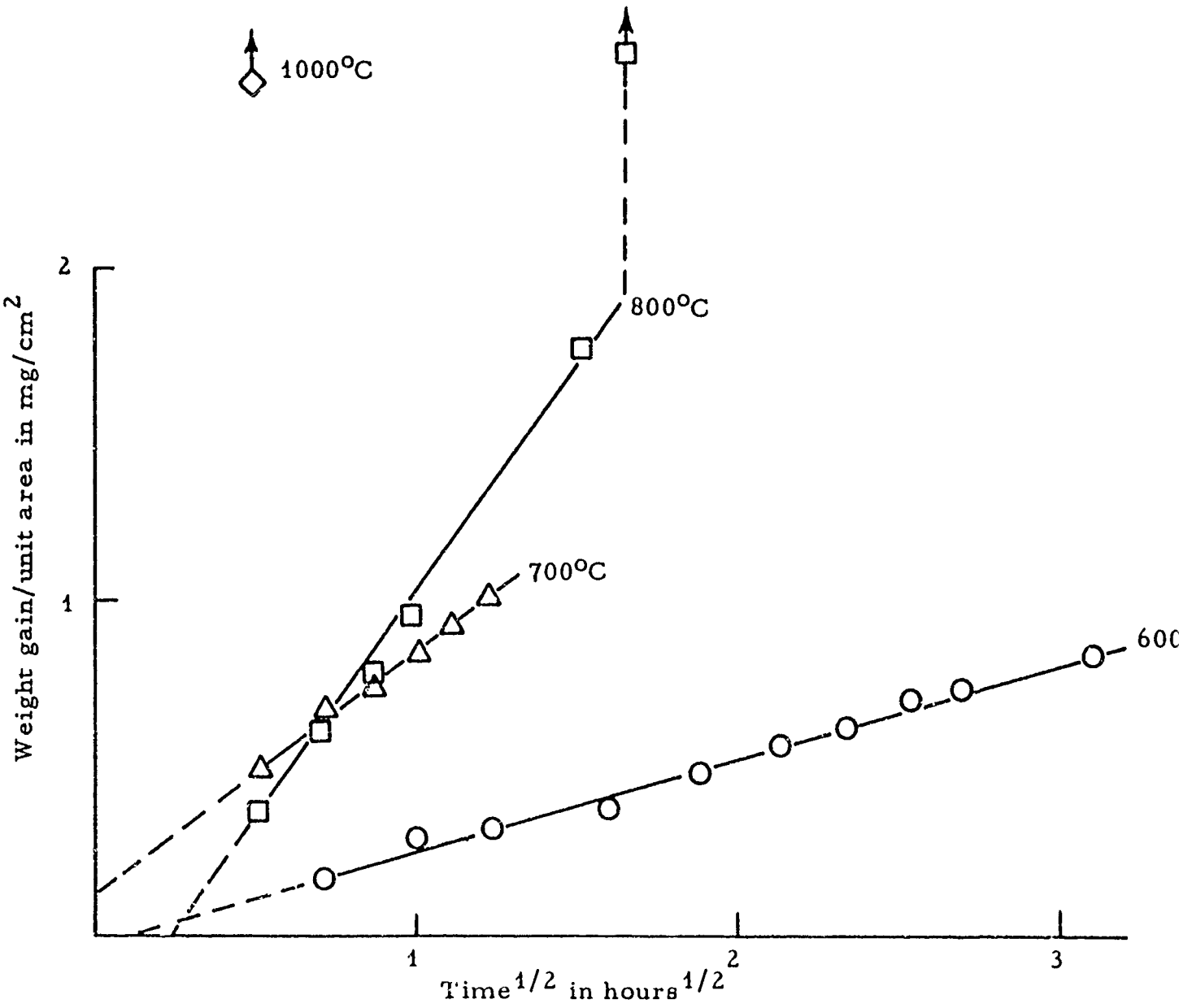

Fig. 3. The weight gains of samples of 5.3 w/o Th-Sn exposed to air, expressed as a function of time and temperature.

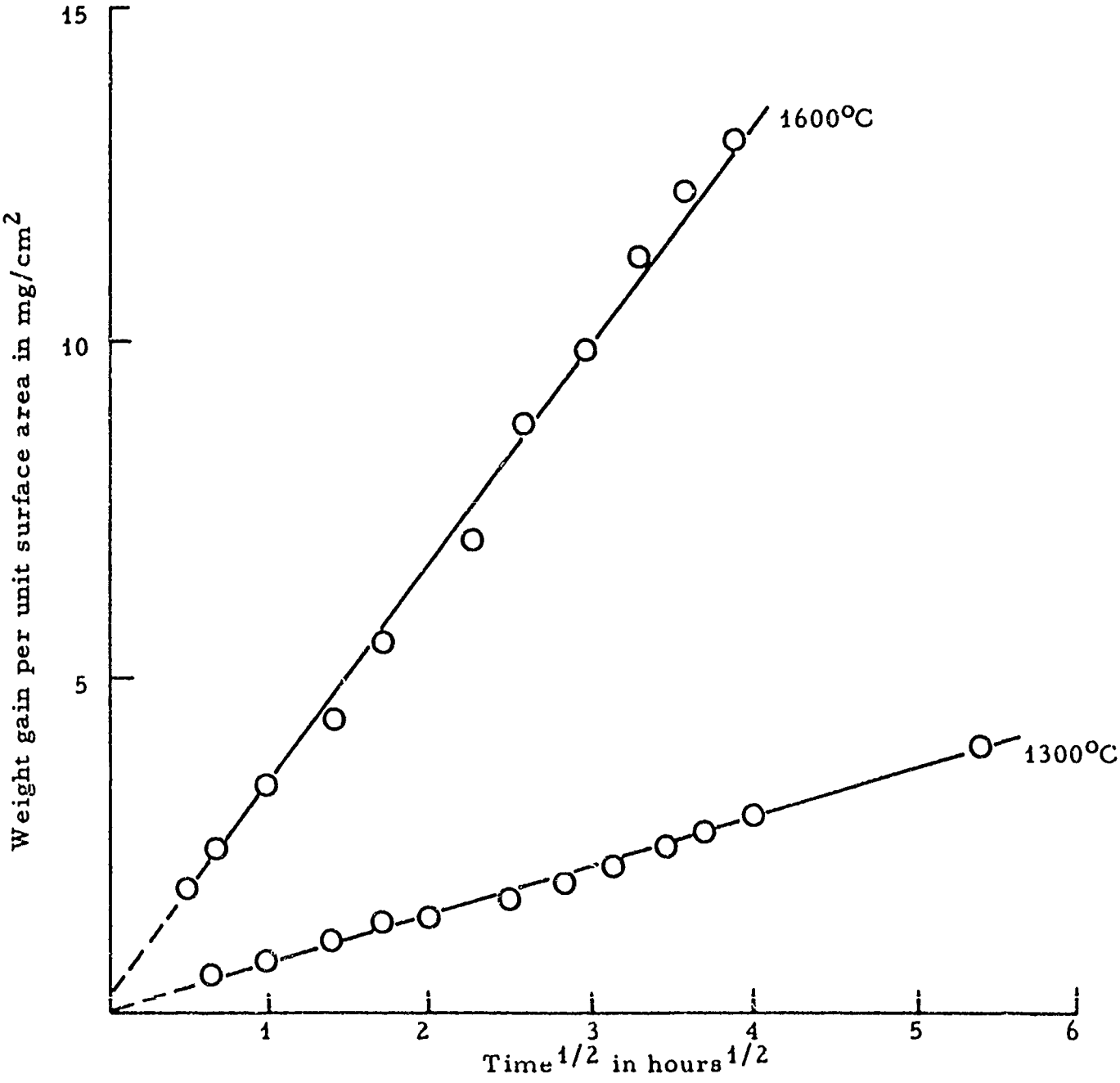

Fig. 4. The weight gains of samples of 16.7 w/o Al-Sn exposed to air, expressed as a function of time and temperature.

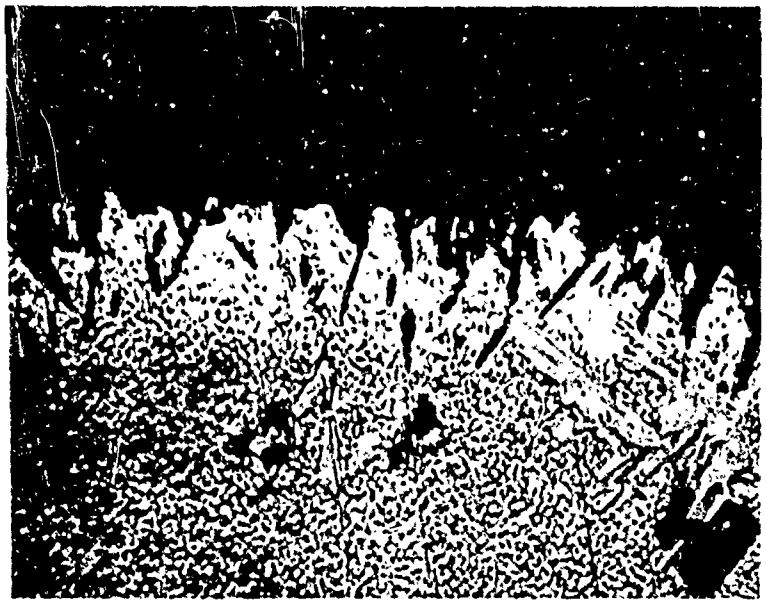

Fig. 5a. The surface of a 16.7 w/o Hf-Sn alloy sample exposed to air for 8 hours at 1150°C. (500X)

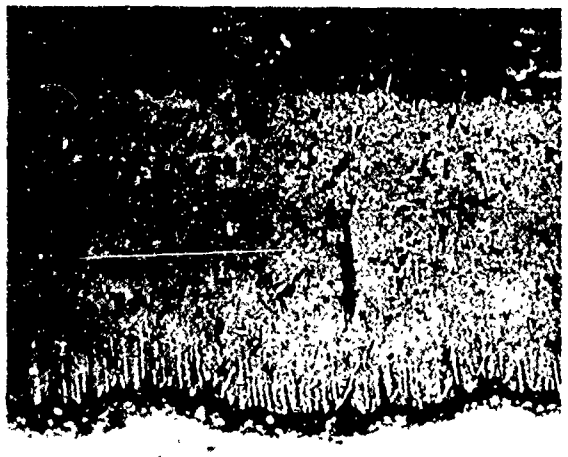

Fig. 5b. The surface of a 16.7 w/o Hf-Sn alloy sample exposed to dry air for 6 hours at 1450°C. (300X)

A comparison was made of the time for breakaway of the oxides on the liquid metal substrates with those reported in the literature for the growth of oxides on the solid, pure reactive metal, and the results indicate that a significant improvement at all temperatures in the time for breakaway resulted from the use of a liquid substrate. Microprobe or X-ray analyses indicated that the oxide formed during the parabolic period of growth was pure HfO_2, ZrO_2, ThO_2 or Al_2O_3. Furthermore the crystal form of the HfO_2 and ZrO_2 formed from Hf and Zr-containing alloys was monoclinic rather than cubic or tetragonal. Therefore, the parabolic growth and the fact that growth of the oxides is less prone to breakaway on the liquid substrates is a direct result of the elimination of stresses at the metal-oxide interface rather than an effect of alloying in the oxide.

Ultimately, however, breakaway does occur. Even though parabolic growth of HfO_2 for one hour at 1700°C is a marked improvement, much longer periods of protective growth will be needed if HfO_2 is to be a component of high-temperature coating systems. It is important to know the cause of the breakaway that occurs ultimately and hence to know whether the data obtained represent the best improvement that can be attained.

Breakaway during the oxidation of reactive-metal tin-base alloys manifests itself by the appearance of a white crumbly mass of tin oxides. The appearance of this other oxide could be the result of two processes; the mechanical breakdown of the protective HfO_2, ZrO_2 and ThO_2 films or

the exhaustion of the reactive metal in the sample by the formation of a thick oxide scale so that further oxidation results in the formation of tin oxides. This second process is believed to be operative on the basis of our experimental data. The times at which the concentration of the dispersed phase in hafnium-tin samples became zero (Fig. 6) were in excellent agreement with the times at which the crumbly oxide was first formed. The microprobe studies showed that hafnium was virtually insoluble in tin at room temperature, therefore all the hafnium content of the samples must have been in the dispersed phase and the times for zero concentration correspond to zero hafnium content.

If reactive metal exhaustion is assumed to be the case of breakaway, the time at which it occurs can be calculated readily. Since oxidation initially proceeds parabolically, the time at which breakaway occurs, t_B, should be related to the initial reactive metal content, m, by the expression

$$(m \times C) = k^{1/2} \, t_B^{\,1/2} , \qquad (1)$$

where

C is the weight gain/unit area or film thickness produced by the consumption of one gram of reactive metal.

A comparison of the observed times at which the Sn-16.7w/oHf samples underwent breakaway with those predicted by Eq. (1), Table I, reveals a good agreement for all temperatures above 1000°C.

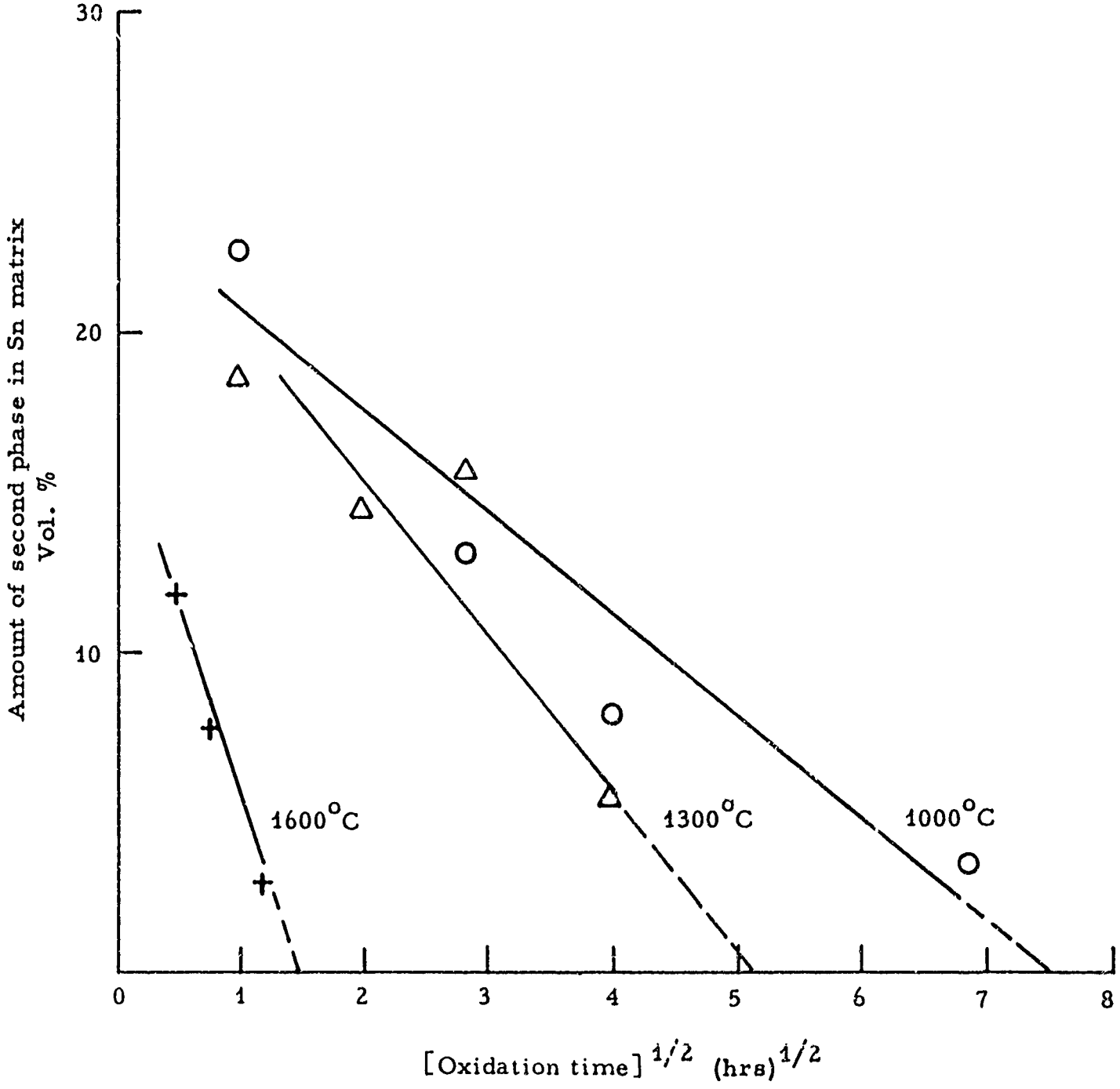

Fig. 6. The effect of oxidation time and temperature on the concentration of the dispersed phases present in samples of a 16.7 w/o Hf-Sn alloy.

TABLE I

The Times at Which Rapid Oxidation of Sn-16.7Hf Alloy Samples Commence

Temperature °C	Observed time * (hours)	Calculated time ** (hours)
1000	46-64	440
1150	-	170
1300	24-36	28
1450	6-8	7.4
1600	1.5-2	2.1
1700	1-1.5	0.9

* Taken from Fig. 8.

** Calculated from Eq. (1) using the average surface area of 14 cm^2. The rate constants were derived from the data presented in Fig. 1.

The good agreement demonstrated by the table provides strong confirmation for the suggested influence of reactive metal content. Further support comes from the fact that data on the effect of zirconium content on breakaway time obey one parabolic relationship over most of the zirconium content range evaluated, and breakaway is related to the initial zirconium content rather than being thickness or time dependent.

Deviations from the suggested parabolic relationship, however, do occur. The cause of the deviation at zirconium contents of 20 w/o or more

is probably due to the existence of solid islands of the zirconium-rich inetermetallic at the oxidation temperature of 1300°C. As shown by the oxidation behavior of the Sn-9.3w/oZr samples at 990 and 1030°C (Fig. 7), the oxidation rate is very high when the solid intermetallic is present and continues to be so until the solid is destroyed. This initial rapid oxidation rate causes an initial rapid depletion of the reactive metal and hence leads to an earlier onset of breakaway. This behavior is believed to be general and not specific to zirconium-tin since breakaway also occurs unusually early for Sn-16.7w/oHf samples oxidized at 1000°C, a temperature at which solid islands of hafnium-rich intermetallic are believed to be present. With the qualification that no solid reactive intermetallic is exposed to the oxidizing environment, the data indicate quite clearly that the times and temperatures for the onset of rapid linear oxidation in Figs. 1 to 3 do not represent the best that can be attained.

This program was not intended to be a study of the oxidation kinetics of tin alloys, but a certain amount of kinetic data have been obtained. It has been suggested that the use of liquid substrates prolongs the low temperature protective growth of the HfO_2, ZrO_2 and ThO_2, and, therefore, it would be interesting to compare the kinetic data obtained in this program with that reported for the protective growth of these oxide films on their parent metals at low temperatures. This comparison is best made in terms of the rate constant, k, which can be derived from the equation

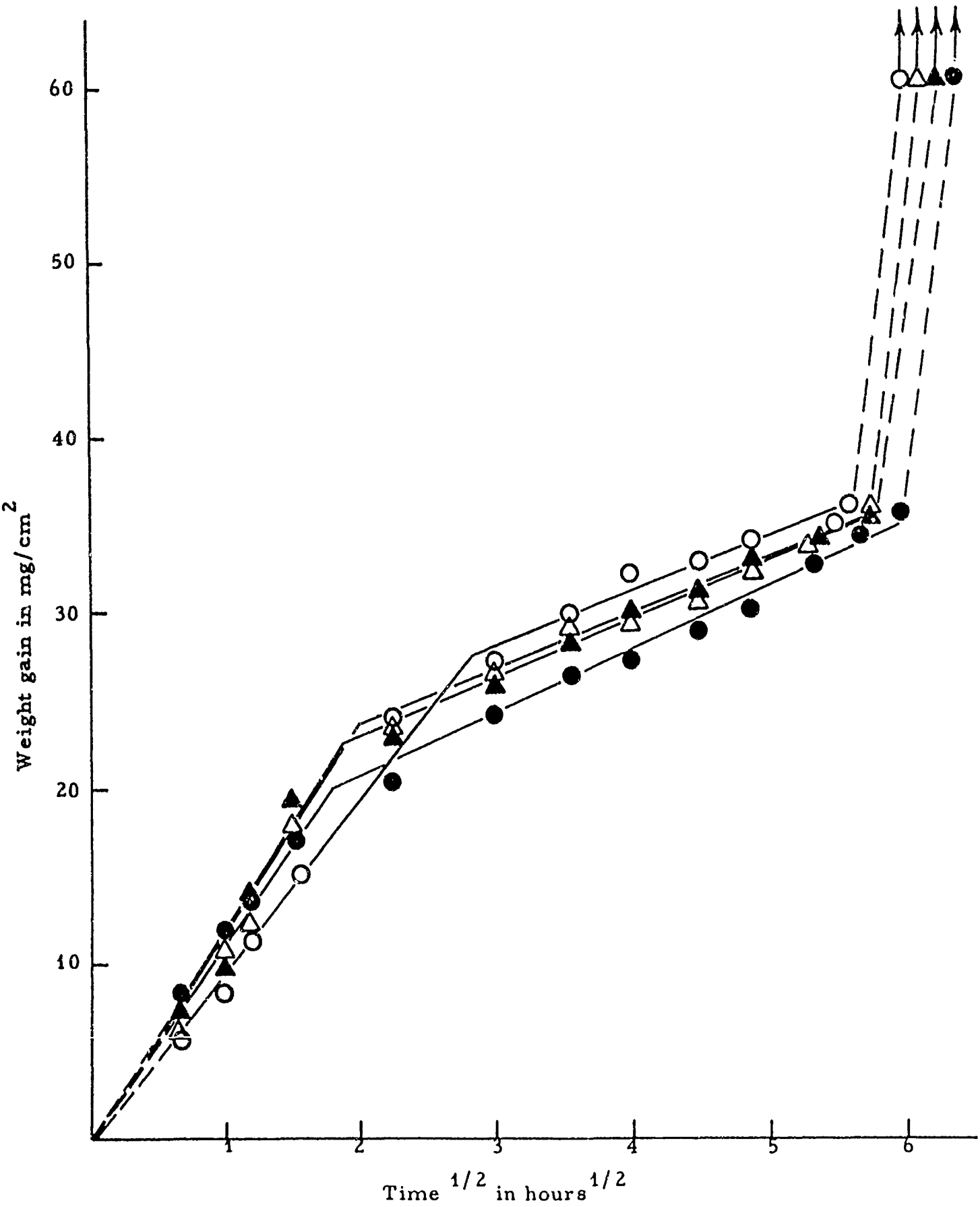

Fig. 7. The weight gains in dry air of 9.3 w/o Zr-Sn alloy samples expressed as a function of oxidation time at 990°C (○,●) and 1030°C (△,▲).

$$X^n = kt,$$

where X is the oxide thickness or weight gain per unit area

n is the reaction index

and t is the time.

The rate constants for the protective growth of the three oxides from liquid tin and solid parent metal substrates are presented in Figs. 8, 9 and 10. The agreement between the various sets of data is good and therefore suggests that the effect of the liquid substrate is to prolong the conditions under which the low-temperature growth mechanism is operative. This is an important inference since parabolic oxidation of zirconium and thorium has been reported to occur at temperatures substantially above those at which breakaway occurs. However, the mechanism of oxidation is not the same at high as at low temperatures. Levesque and Cubicciotti, for example, reported that the low temperature parabolic oxidation process of thorium had an activation energy of 31 k cals/mole (the value derived in this work was 30 k cals/mole) while Gerds and Mallet found that the high-temperature parabolic oxidation process had an activation energy of 62 k cals/mole.

Although there is reasonable agreement between the rate constants of the various sets of data plotted in the three figures, the values of the reaction index are at variance. The index was found to be 2 for the growth of both HfO_2 and ZrO_2 from liquid tin substrates, but values of 2.3 and 1.5 to 3.5 have been quoted for the low-temperature protective growth of

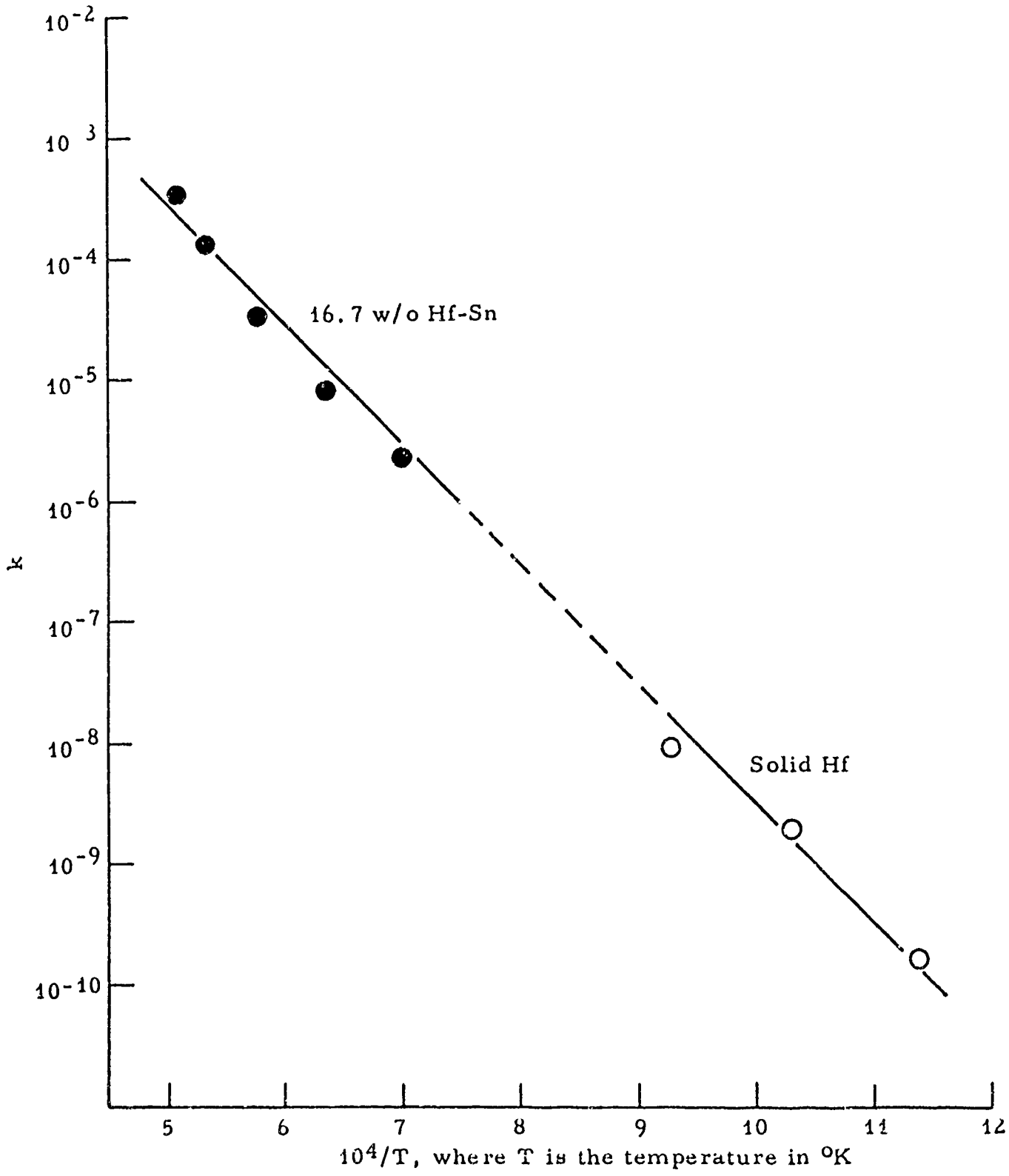

Fig. 8. The rate constants, k, for the growth of HfO_2 films on solid Hf and liquid Sn-16.7% Hf alloy samples exposed to air at various temperatures.

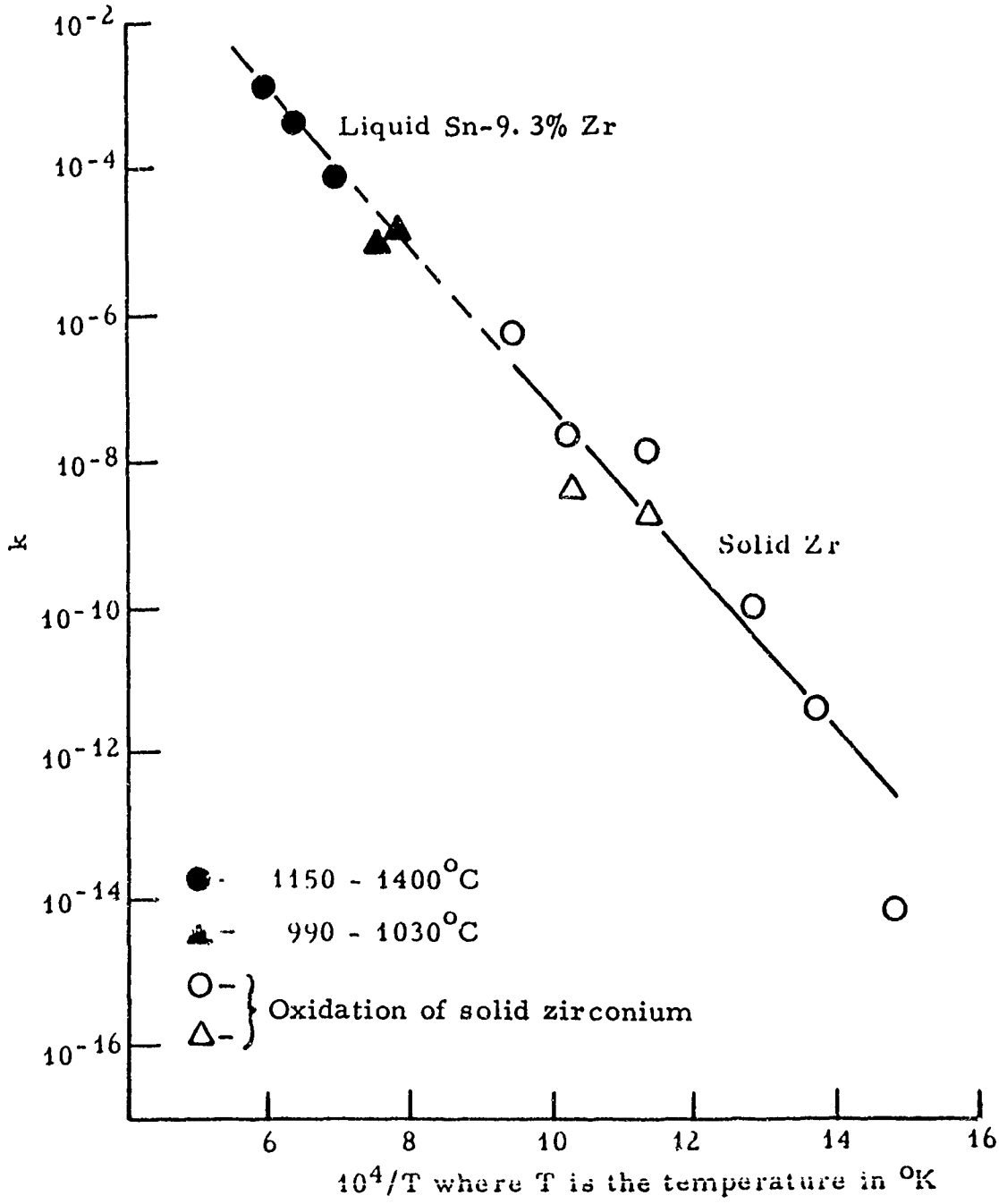

Fig. 9. The rate constants, k, for the growth of protective ZrO_2 films on solid Zr and a liquid Sn-9. 3% Zr alloy exposed to air at various temperatures.

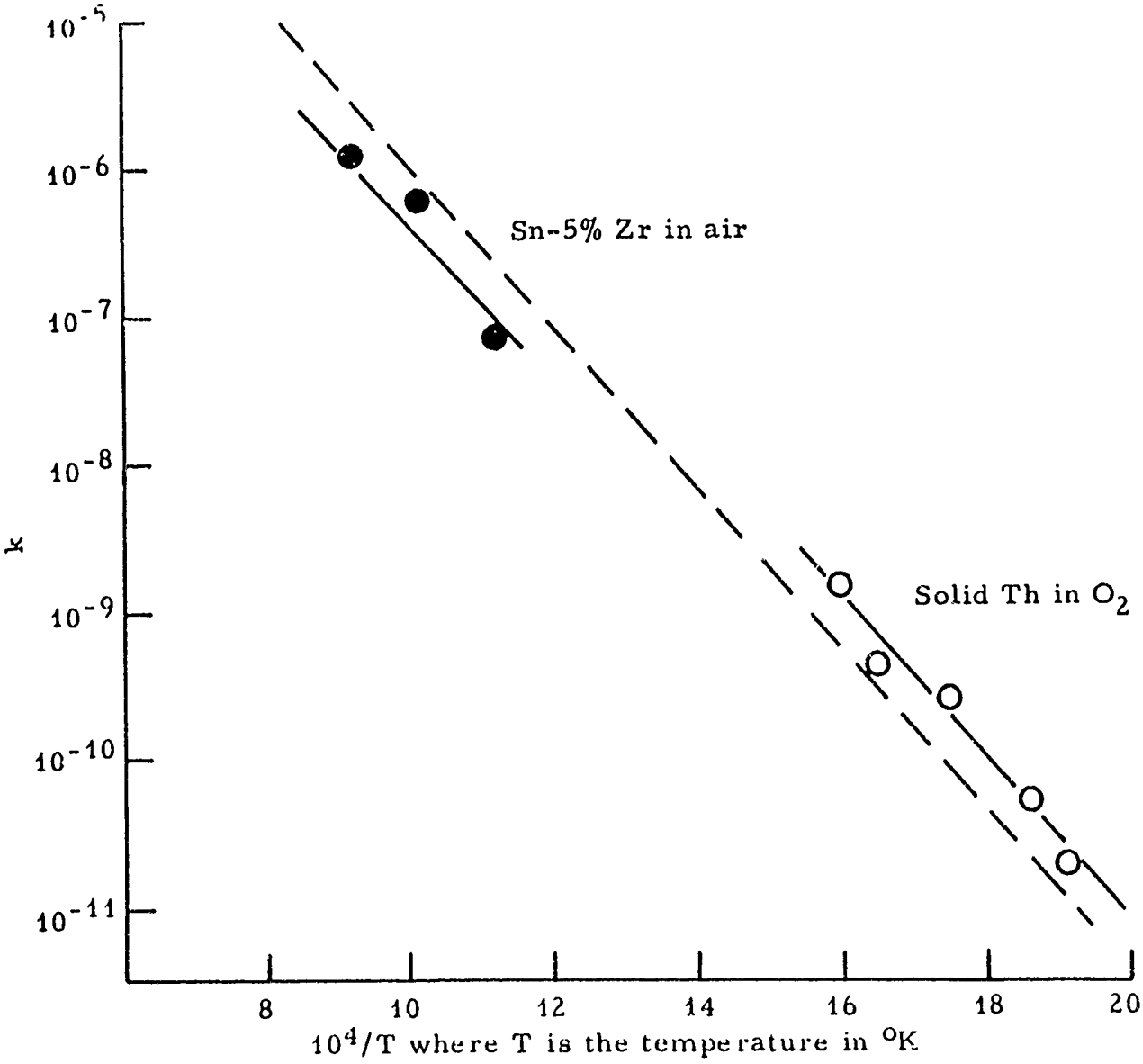

Fig. 10. The rate constants, k, for the oxidation of solid Th and a liquid Sn-5.3% Th alloy.

HfO_2 and ZrO_2 from their solid parent metals. It is difficult, however, to decide whether this difference is of any major significance since variations in the reported values are so large. High reaction index values are usually associated with a significant influence of interfacial processes on the growth of oxide films. If it is assumed that the values derived in this work are indeed lower than those quoted in the literature for solid substrates, it can be deduced that the use of liquid substrates reduces the influence of interfacial processes. The data, however, are not precise enough to make such a deduction more than mere speculation.

Having discussed the major conclusions that can be drawn from the experimental data, it is possible to evaluate the relevance of this work to future coating programs. High-temperature parabolic growth oxides from liquid substrates has been demonstrated before and used by Sama and Lawthers in the development of a successful coating system;[5] however, the oxide (Al_2O_3) grown in that work, is not notably breakaway prone. The demonstration provided by this work that breakaway can be prevented or markedly delayed in the growth of breakaway-prone oxides such as ZrO_2 and HfO_2 now makes it possible to consider use of these oxides in protective coating systems. The utilization of this improvement under actual service conditions should be studied to prove that a wider choice of potential high-temperature coating systems is possible. This duplication, however, would not lead immediately to the development of new coating systems. The

high-temperature parabolic growth rates of HfO_2 and ZrO_2 are greater than those of Al_2O_3 and extrapolation of the present data to 2000°C (Fig. 11) indicates that the rates are probably greater than the tolerable maximum for a high temperature coating. These rates of diffusion controlled growth, therefore, will have to be reduced before practical coating systems can be developed.

Before concluding this discussion, it must be emphasized that it is not believed that any and every breakaway-prone oxide can be caused to grow as a protective film if a liquid substrate is used. An improvement can be expected if stresses at the oxide-metal interface are the cause of breakaway, but this is not always the case. Thorium and magnesium are reported to burn at moderate temperatures and, although some delay has been achieved by use of a liquid thorium-tin alloy, it seems unlikely that ThO_2 and MgO can be grown as protective films at 2000°C. Although not a refractory oxide forming material, liquid tin also fails to form protective films at 1000°C and above. The use of a liquid substrate, therefore, can not guarantee protective film growth for all cases. Nevertheless, it is believed that the use of a liquid substrate can markedly delay the onset of breakaway for the many systems in which breakaway is due to stresses or strains at the oxide-metal interface.

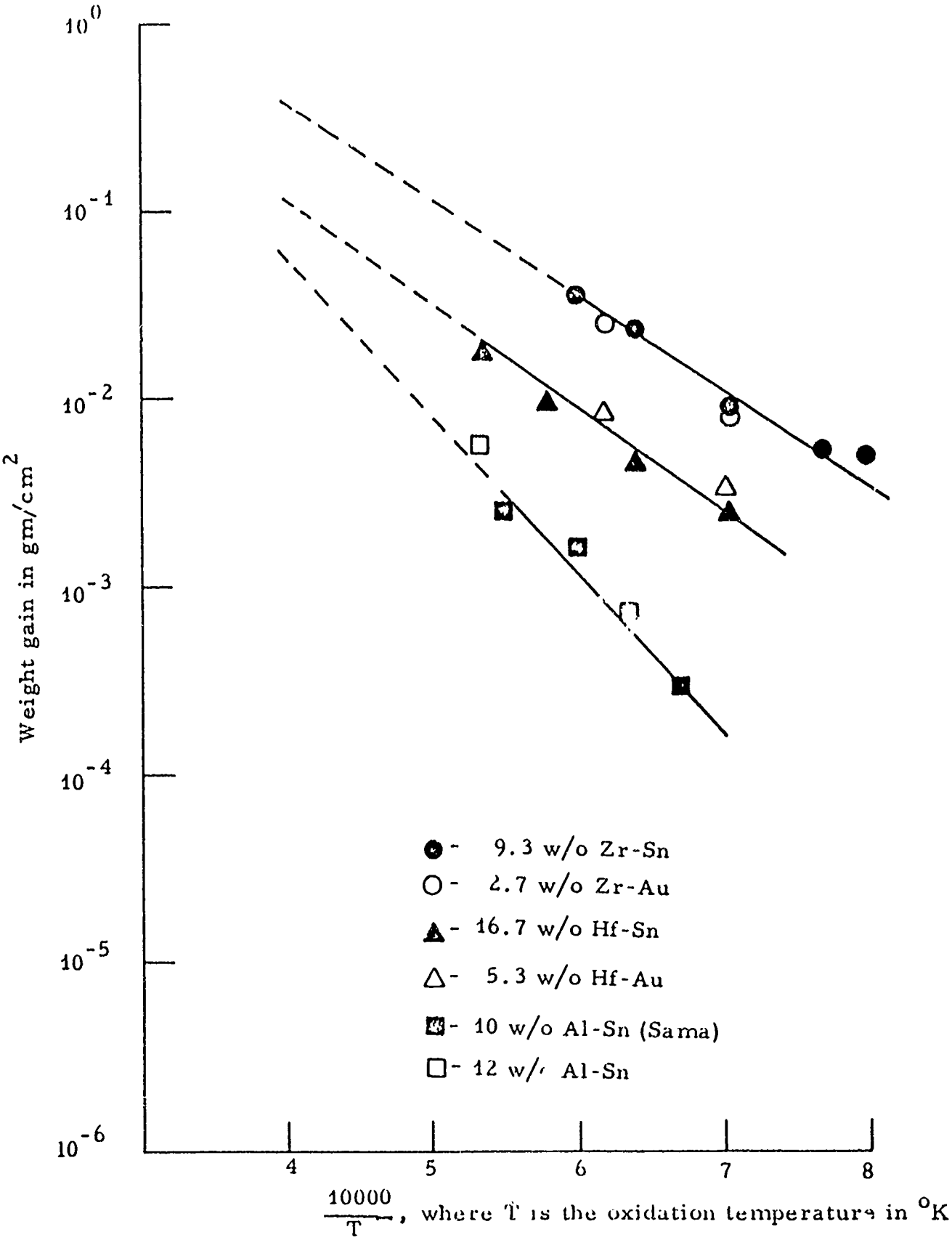

Fig. 11. The extent of oxidation produced by exposing five liquid alloys for one hour at various temperatures.

3. TERNARY DIFFUSION IN THE Zr-Th-O SYSTEM

Most of the successful protective coating systems developed to date depend on an intermetallic compound, diffusion bonded to the substrate, as a reservoir for the formation of a protective oxide. The success of such a coating depends primarily on the ability to form a specific oxide which is protective of the several oxides possible in a given system. The importance of diffusion processes is indicated by the results obtained in the study on silicide pest; the formation of tungsten and silicon oxides are associated with the low temperature, rapid failure.

For a pure metal, the phase sequence of the oxide layers produced on the surface can be predicted from the appropriate phase diagram by simply drawing an isothermal line. The only influence of diffusional processes is to determine the rates of growth of the various layers. With an alloy or intermetallic compound, however, the phase sequence or morphology cannot be predicted on the basis of the phase diagram or thermodynamic data since the relative diffusion rates of the three components of the system (oxygen, metal A and metal B) influence both the compositions of the oxides produced and the morphology of the layers which grow. The oxidation of several binary systems (Th-Zr-O, W-Hf-O and Zr-Y-O) are being investigated to provide further information on the behavior in the growth during oxidation to form fractory oxides of the specific compositions or crystal structure. Some in-

sight is being sought on the influence of the ternary equilibrium diagram, thermodynamics and relative diffusion rates on the behavior analyzed by analysis of the results as a ternary diffusion process. Work is progressing on all three systems mentioned, and the experimental work accomplished to date on the Th-Zr-O system permits some specific conclusions with regard to this system and general conclusions on the analysis of multicomponent oxidation as a ternary diffusion process. These results have implications in the problems of protecting tungsten (and other refractory metals); therefore a brief description of the results obtained to date on the Zr-Th-O system and a discussion of these results are presented.

3.1 EXPERIMENTAL PROCEDURE

Coupons of four Th-Zr alloys containing 30, 55, 70 and 85% thorium were made from mixtures of the Th and Zr powders in appropriate ratios. After blending, the powders were compacted and sintered in a vacuo for one hour at 1300°C. The compacts were arc melted in argon and homogenized by a vacuum anneal for 20 hours at 1200°C. The buttons produced were cold-rolled into strips 0.075 in. thick, with intermediate and final vacuum anneals of five hours at 1200°C. The strips produced were cut into 1/2-in. x 1/4-in. coupons and 1/16-in. diameter holes were drilled near one end. The coupons were then annealed for 5 hours at 1200°C before oxidation testing.

All oxidation tests were made in dry air. The Pt-Rh resistance-wound furnaces described by St. Pierre [6] were used. The solid specimens

were suspended in the furnace by 30% Rh-Pt rods passed through the drilled holes and placed across the top of an Al_2O_3 crucible. Liquid specimens, i.e., the 55, 70 and 85 w/o Th-Zr alloys at 1600°C, were premelted in argon prior to being exposed to air. Both weight gains and oxide thickness measurements were used to determine the extent of oxidation, but greater reliance was placed on thickness than weight gain measurements if both values were obtained. Selected samples were submitted to Battelle Memorial Institute for detailed X-ray and electron microprobe studies as follows:

1. Zr-30%Th alloy oxidized 1/2 and 2 hours at 1200°C and oxidized 20 minutes at 1400°C
2. Zr-55%Th oxidized 1/2 hour at 1200°C
3. Zr-85%Th alloy ozidized 1/2 and 2 hours at 1200°C

The procedure used at Battelle Memorial Institute is given in detail in the Appendix of the Second Progress Report [3]. The general procedure used, however, was to identify the composition of the phases observed in a metallographic cross-section of the specimen by microprobe analysis. The Zr and Th contents were obtained simultaneously, and the composition and the distance from the external surface of the analysis were determined. X-ray diffraction studies of the surface of the specimen and surfaces exposed by removing successive thicknesses gave a similar identification of the structure of the phases as a function of distance from the external interface. In this manner, it was possible to identify the phases formed in various layers and as well to determine the compo on of these phases.

3.2 RESULTS

The rate of oxidation was determined by measuring the weight gain of the specimens after exposure at 750, 1000, 1200, 1400 and 1600°C. The results for each alloy were plotted as shown in Fig. 12 for the Zr-85%Th. The log of the specific weight gain is plotted as a function of the log of time and the reciprocal of the slope of the resulting curve is the index of reaction, n, in the equation

$$\left(\frac{\Delta W}{A}\right)^n = kt \qquad (1)$$

In almost all cases, the data for both noncyclic and cyclic tests for a given temperature and composition are well described by a straight line with a slope of 1 or 2, indicating nonprotective (linear) or protective (parabolic) film growth, respectively. The rate constants presented in Table II were determined from the straight lines of $\Delta W/A$ vs $\overline{t^n}$ plots by assuming that either linear (n=1) or parabolic (n=2) growth best describes the kinetics of the oxidation reaction.

At 750 and 1000°C linear oxidation was observed on all compositions tested, and the oxide formed was externally cracked. The tests were sequential cyclic runs on one sample, but spalling apparently occurred even on the first run as indicated by the fact that for the alloys containing 70-85%Th, the weight gained at 1000°C in the initial run is greater than that gained at 1200°C in the same time.

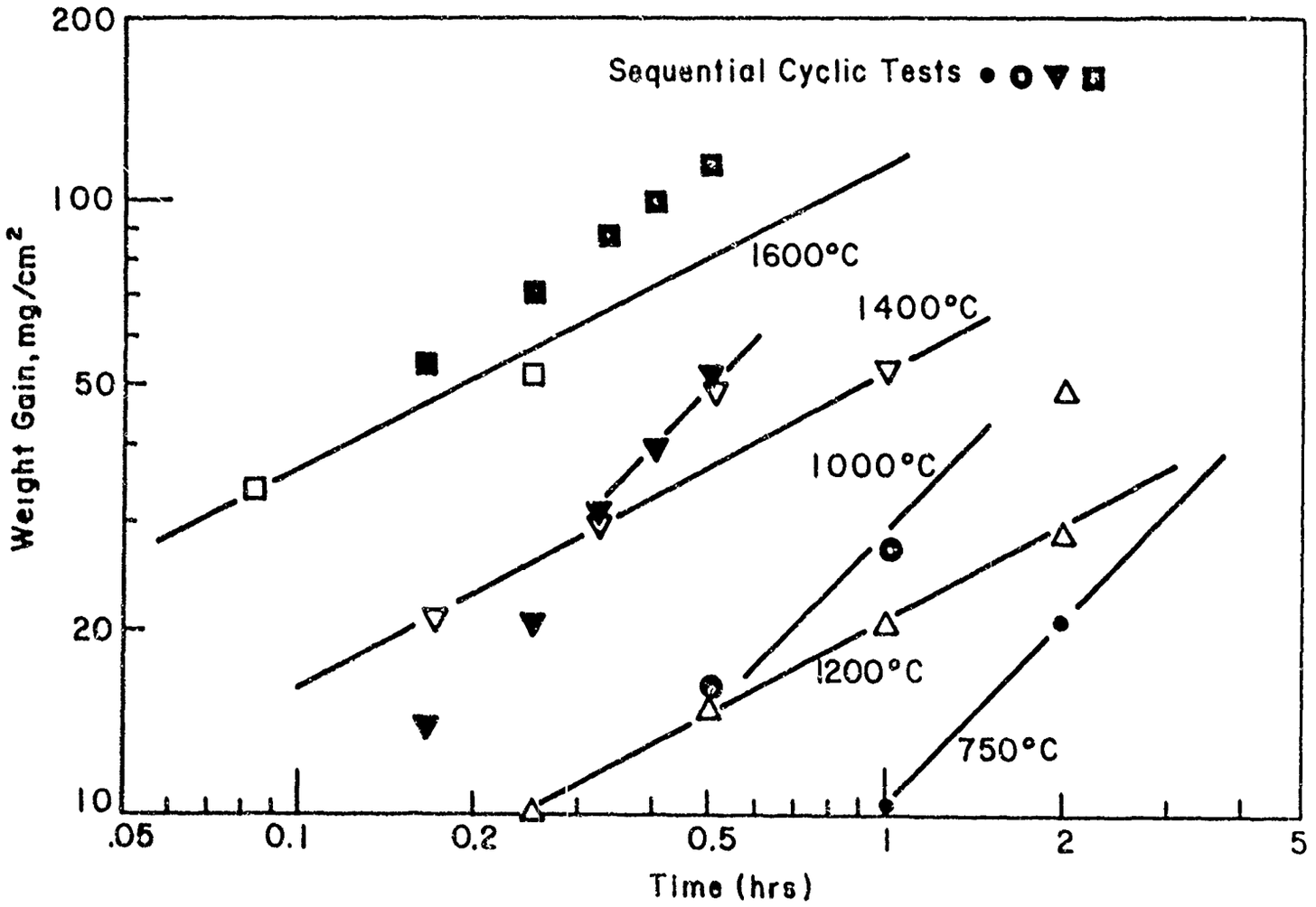

Fig. 12. Weight gained in oxidation of Zr-85%Th sheet in dry air.

TABLE II

The Effect of Temperature and Composition on the Growth Rate in Oxidation of Zr-Th Alloys at 750°C to 1600°C

	Zr-30% Th		Zr-55% Th		Zr-70% Th		Zr-85% Th	
Temp. (°C)	K_l^* gm/cm^2/hr	K_p^{**} gm^2/cm^4/hr	K_l^*	K_p^{**}	K_l^*	K_p^{**}	K_l^*	K_p^{**}
750	2.4×10^{-2}	--	1.5×10^{-2}	--	2.3×10^{-2}	--	2.2×10^{-2}	--
1000	4.2×10^{-2}	--	5.7×10^{-2}	--	5.2×10^{-2}	--	2.9×10^{-2}	--
1200	--	3.14×10^{-3}	--	9.6×10^{-4}	--	4.3×10^{-4}	--	4.3×10^{-4}
1400	--	3.2×10^{-2}	--	6.7×10^{-3}	--	1.6×10^{-3}	--	2.92×10^{-3}
1600	1.7	--	(2.2×10^{-1})	1.02×10^{-2}	--	6.10×10^{-3}	--	1.3×10^{-2}

$^*K_l$ = linear growth rate constant, i.e., $n \cong 1$ in $n \log \frac{\Delta W}{A} = \log Kt$.

$^{**}K_p$ = parabolic growth rate constant, i.e., $n \cong 2$ in $n \log \frac{\Delta W}{A} = \log Kt$.

At 1200°C individual specimens were used for each test and the data can be represented by a line with a slope of 1/2 indicating parabolic growth. The scales appeared to be sound and dense, and the edges and corners were intact in most cases; a sharp corner was retained in the oxide.

At 1400°C both cyclic and individual tests were run, and in the Zr-30Th and Zr-55Th alloy, a line with a slope of 1/2 describes the results of both types of tests. In the Zr-70%Th alloy at 1400°C, the weight gains for individual specimen tests indicated a slope of 1/2, but in sequential tests beyond 0.25 hours the slope changes toward a linear rate, indicating breakaway. In the Zr-85%Th alloy only the individual tests fit a slope of 1/2; the cyclic results indicate breakaway oxidation with a slope of 1. The external appearance of the oxides formed at 1400°C was similar to that observed at 1200°C.

At 1600°C only the Zr-30%Th alloy is solid at temperature. In the noncyclic tests, the rate of weight gain on the liquid Zr-(70-85%)Th alloys is parabolic, but slopes of 0.68 were obtained for cyclic tests. In the solid Zr-30%Th alloy only cyclic tests were run, and a slope of 1 was observed. The results of oxidation of the Zr-55%Th alloy was described by a curve with an initial slope of 1/2 and a slope of 1 for times greater than 0.25 hr. The oxides formed at 1600°C appeared to be dense and sound, but on standing at room temperature the oxides formed on the liquid alloys disintegrated in the atmosphere to form a very fine powder.

3.2.1 Structure of the Surface Layers

3.2.1.1 Metallographic Studies

Metallographic examination reveals that at 750 and 1000°C, oxidation of all alloys proceeds by linear nonprotective growth and the oxide formed contains a large number of cracks parallel to the surface of the specimen, as indicated in the first Quarterly Report.[3] Examination of the metallic substrate of specimens oxidized at 750°C indicates no change in substrate structure, and microhardness tests indicate no increase in hardness of the metal adjacent to the metal oxide interface. Thus the amount of oxygen which penetrates or dissolves in the substrate must be relatively small. At 750 and 1000°C, breakaway due to fracture of the oxide is evidently the controlling process in the rate of oxidation. Oxygen permeates through the cracks to the metal-oxide interface, forming new oxide which, in turn, spalls and does not protect the substrate. Under these conditions, the substrate is oxidized essentially in situ and solid-state diffusion processes do not control the composition of the oxide layer.

Cross-sections through the surface layers of samples that exhibited parabolic growth at 1200 and 1400°C were studied. The thickness of the layers formed were measured and the microstructures after 1 hour in air at 1200°C in Fig. 13 are typical of the structures observed. Photomicrographs of the structures of the Zr-30%Th and Zr-85%Th alloys after 2 hours at 1200°C (Fig. 14) exhibit similar structures.

(a) 30 w/o Th. 100X

(b) 55 w/o Th. 250X

(c) 70 w/o Th. 250X

(d) 85 w/o Th. 250X

Fig. 13. The surfaces of thorium-zirconium alloys exposed to air for 1 hour at 1200°C.

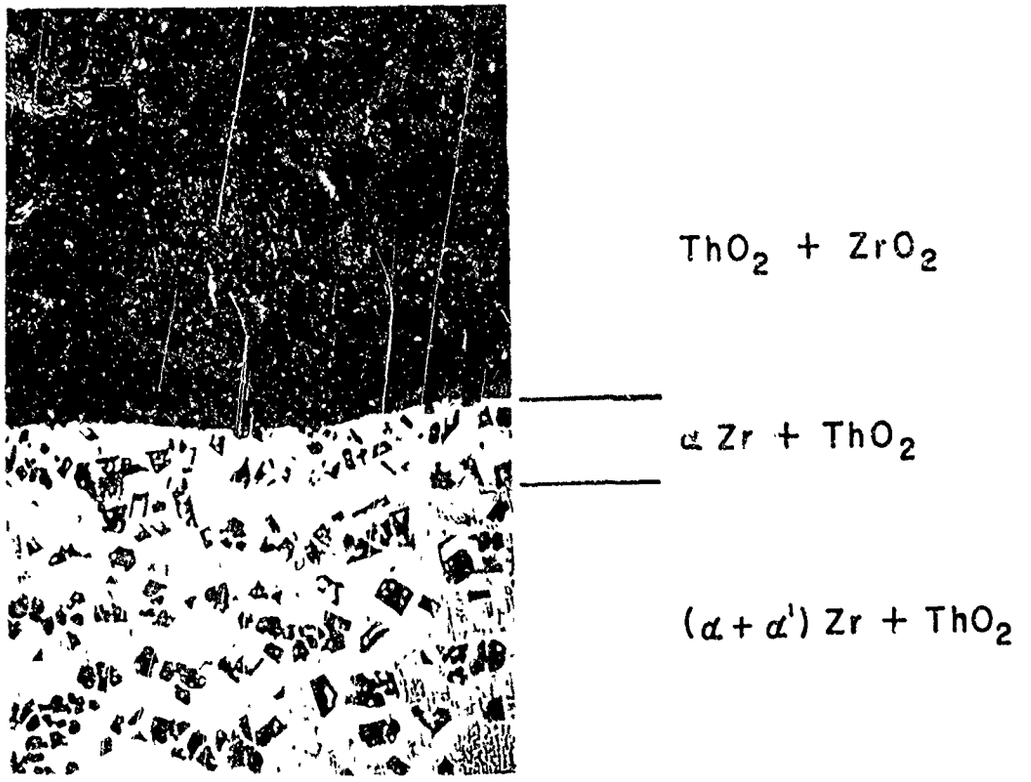

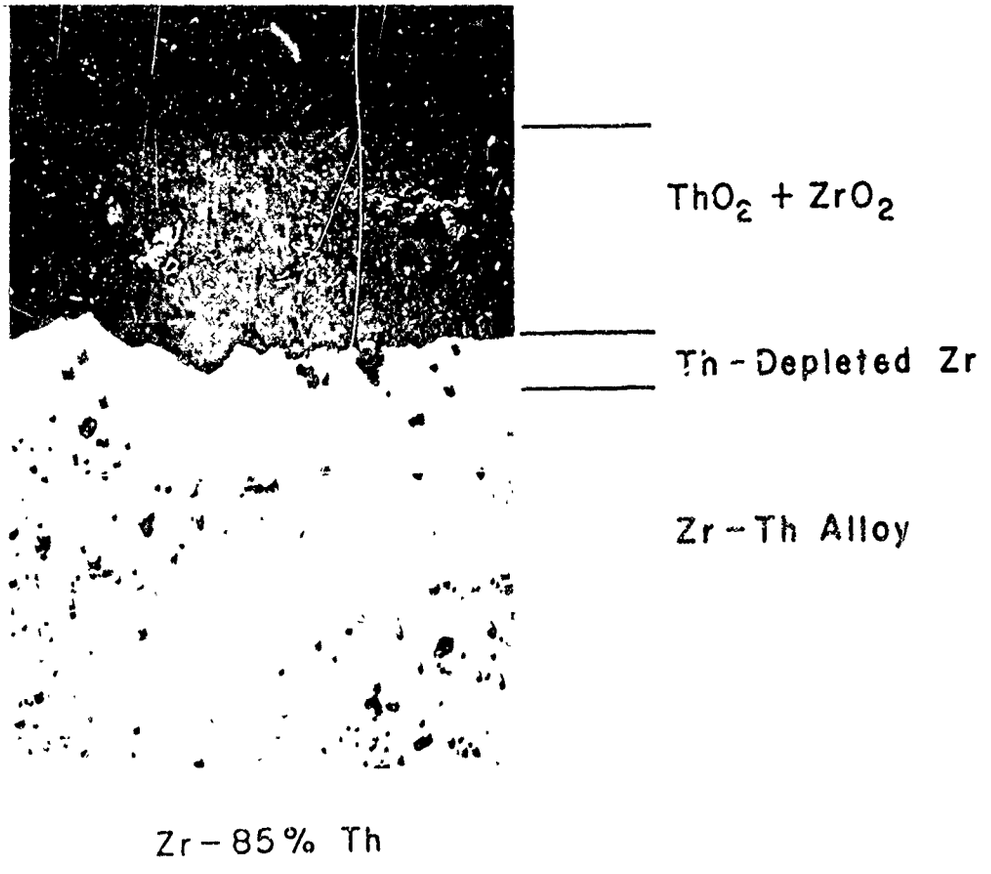

Fig. 14. The effect of alloy content on the sequence of phases observed in Zr-Th samples oxidized in air for 2 hours at 1200°C. (100X)

In general, two types of structures were observed in samples oxidized at 1200 and 1400°C. At 1200 and 1400°C, the rate of growth is apparently diffusion-controlled in all compositions and compact adherent oxides are formed, however, the layers and structures observed in the Zr-30%Th and Zr-55%Th alloys (thorium lean) differ from those in the Zr-70%Th and Zr-85%Th (thorium rich) alloys. In the thorium lean alloys, several layers which thicken with time are observed as follows:

1. An external two-phased oxide;
2. An internally oxidized layer consisting of a single-phase metal matrix containing oxide particles;
3. A transformed two-phase metal matrix containing oxides formed by internal oxidation.

Hardness traverses of the metal + oxide layer observed beneath the oxide in the thorium lean alloys were made on alloys oxidized at 1200 and 1400°C. The single-phase matrix structure has a hardness above 1000 VHN near the oxide-metal interface, and in its entirety is harder than the substrate from which it is formed. The transformed metal + oxide layer is similarly harder than the substrate.

All of the layers thicken with time, and in the Zr-30%Th alloy, which was oxidized 30 minutes at 1400°C, the internally oxidized zone (layer 3) penetrated almost to the centerline of the specimen. In this sample large fissures in layer 2 and in the corners of the outer oxide layer were

observed. The oxide was grossly distorted by growth, but cracks were observed only at corners and in the regions of the support hole in the specimen. In specimens oxidized at shorter times at 1400°C or equivalently shorter time at 1200°C, the corners were essentially intact and formed a sharp corner angle at about 90°.

In the Zr-70%Th and Zr-85%Th alloys, the external oxide is the only layer which grows appreciably, and the rate of growth is considerably less than the rate in the thorium-lean alloys. Some indication of a small amount of internal oxidation at 1200°C may be present in the Zr-70%Th alloy structure (Fig. 13); however, internal oxidation and the solution of oxygen in the metallic matrix do not occur to an appreciable degree in the thorium-rich alloys. No single-phased region in the metallic matrix is observed, and hardnesses immediately adjacent to the metal-oxide interface indicate no hardening from oxygen solution.

At 1600°C observations were complicated by the fact that only the Zr-30%Th alloy was solid at temperature. In addition, the scales that formed on the liquid alloys were initially sound and nonporous but rapidly disintegrated at room temperature so that microstructure observations were not made. However, the disintegrated scales were analyzed by X-ray diffraction to determine their structure, and the following results were obtained:

Zr-55%Th: ThO_2 + 10%ZrO_2 + (ZrN detected $\leq$ 5%)

Zr-70%Th: ThO_2 + $\leq$ 5% (ZrN); (ZrO_2 possibly detected < 5%)

Zr-85%Th: ThO_2 + $\leq$ 5% (ZrN + several unidentified lines - trace ZrO_2 ?)

The oxide that forms at 1600°C on the liquid alloys is predominantly ThO_2. The ZrO_2 observed in the Zr-55%Th alloy may have formed after the composition being oxidized was partially solid. These results indicate that thermodynamic considerations are overriding in the oxidation of the liquid alloys. Chemical analysis of the residual metal of Zr-55%Th samples oxidized for 15 and 30 minutes at 1600°C indicated thorium contents of 45 and 46.7% respectively. An alloy containing 45% thorium would be partly solid at 1600°C, and microscopic examination indicated localized areas where internal oxidation and an oxygen-saturated zone had formed, similar to that observed in the oxidation of the solid alloy.

3.2.1.2 Microprobe and X-ray Diffraction Studies

Microprobe analysis and X-ray diffraction studies of alloys oxidized at 1200 and 1400°C are included in Appendix A of Ref. 3. Several conclusions can be drawn from the results which have direct bearing on the rationalization of the oxidation processes at 1200 and 1400°C. By combining the microprobe, X-ray, metallographic and microhardness results, it is possible to describe the layers formed with greater accuracy, and even

to assign approximate zirconium and thorium ratios of the phases observed. For example in the Zr-30%Th and Zr-55%Th alloys (14 a/o and 31 a/o Th respectively), the sequence of phases at 1200°C observed in order from the external surface towards the center of the sample are as follows:

Layer 1. ZrO_2 (<4 a/o Th) and ThO_2 (Zr content varies). Both cubic and monoclinic ZrO_2 are observed in the Zr-14a/o Th alloy, although the tetragonal phase is stable at temperature. ZrN is present as a discrete phase in the oxide.

Layer 2. ThO_2 (~50 a/o Zr) + α Zr (< 2 a/o Th and up to 30 a/o O_2).

Layer 3. ThO_2 (~30 a/o Zr) + α + β Zr (<3 a/o Th).

Layer 4. A solid-solution zone in which the ratio of thorium to zirconium in the metal increases from 5 a/o and 14 a/o Th to the original alloy compositions of 14 and 31 a/o Th respectively.

In the Zr-85%Th (69 a/o Th) alloy, the sequence of layers or phases and the approximate composition is as follows:

Layer 1. A thin external two-phased oxide (ZrO_2 and ThO_2). The composition of the discrete phases is not defined.

Layer 2. A layer of ThO_2 (X-ray results indicate no ZrO_2 present) which contains 20 a/o Zr (X-ray results indicate some ZrN

as a discrete phase, but the zirconium content in ThO_2 is uniformly high).

Layer 3. A metallic substrate in which the thorium content increases from ~24 a/o Th at the metal-oxide interface to the matrix composition (69 a/o Th).

3.3 DISCUSSION OF RESULTS

The rates of oxidation at 1200, 1400 and 1600°C of the Zr-Th alloys are compared with previously determined rates of formation of ZrO_2 on liquid Zr-Sn alloys and ThO_2 on Th-Sn alloys in Fig. 15. At 1600°C, the parabolic rate constant for the alloys is located directly between the rate constants for the oxidation of Zr and Th in Sn alloys. At 1200° and 1400°C the rates observed for the Zr-30Th and Zr-55Th alloys are considerably higher than a straightline average of the rates for Th and Zr in Sn. This suggests that the occurrence of internal oxidation is important in determining the overall rate constant for these alloys. The rate constants for the Zr-70% alloy at 1200 and 1400°C, and for the Zr-85%Th alloy at 1200°C are between the rate constants for the oxidation of pure Th and Zr. This indicates that the rates observed are an average of the rates determined by the diffusion of oxygen through the Zr and Th-rich two-phase oxide.

Internal oxidation eventually does lead to failure by breakaway in the Zr-30Th and Zr-55%Th alloys but the spalling occurs first in the oxygen-saturated Zr which leads to cracking of the oxide at the ends of the specimens.

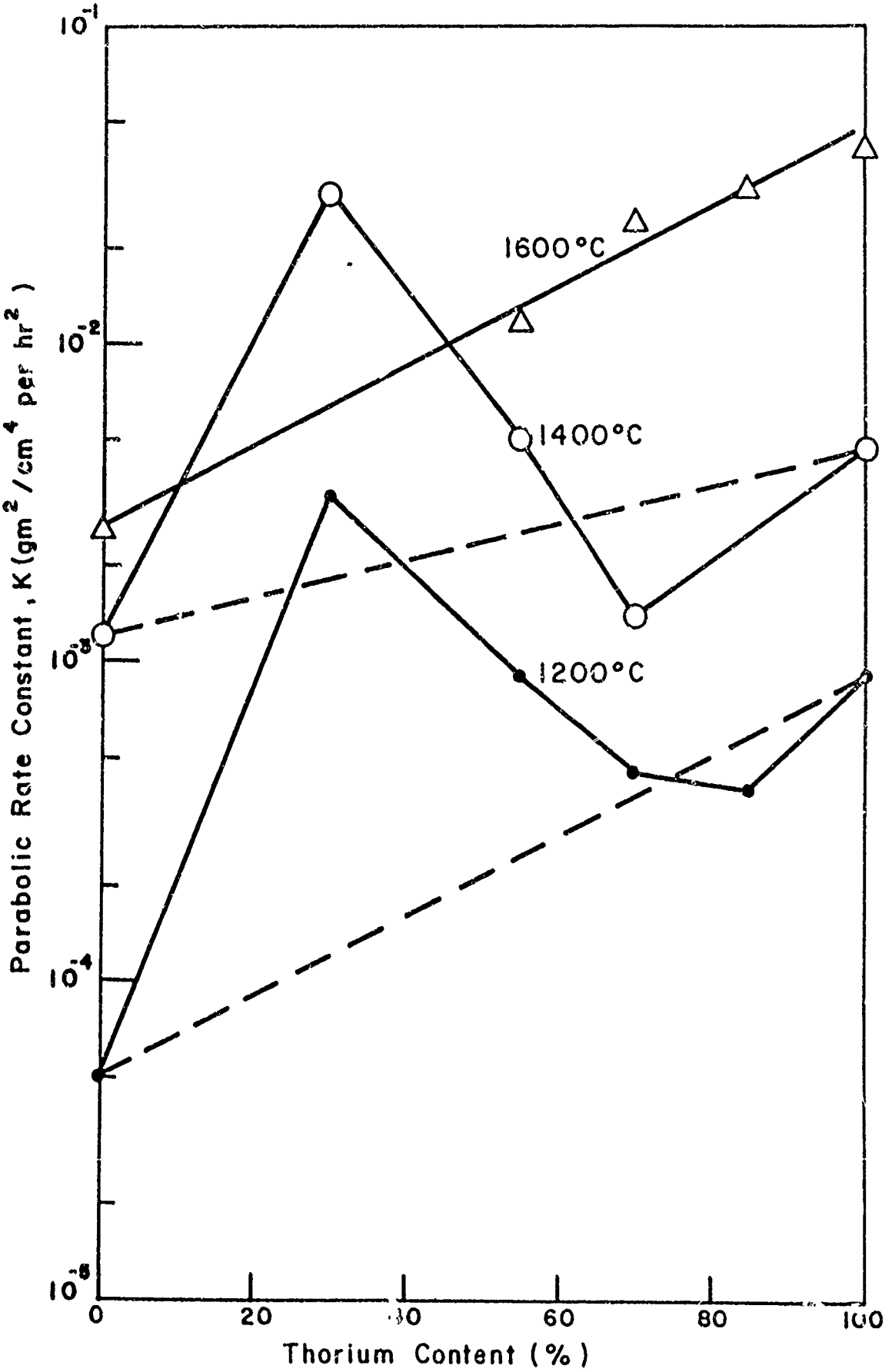

Fig. 15. The effect of thorium content on the parabolic rate constant in oxidation of Zr-Th alloys at 1200 to 1600°C. (Parabolic rates for Zr and Th obtained by interpolation or extrapolation.)

The most surprising fact is that the oxide does not spall in most of the alloys, even though the oxidation process causes a 10% or more increase in the thickness of the specimen. Even the corners of the specimen after 10% increase in thickness are essentially sound, with no indication of corner cracking in spite of the fact that the oxide is apparently being formed by anion diffusion at the metal oxide interface. The fact that the oxide can undergo such distortion without cracking indicates that the two-phase structure of thoria surrounded by a mixture of zirconia or zirconia plus thoria-rich oxides, has considerable ductility at temperatures of 1200°C and above.

If the growth of each layer observed after oxidation at 1200 to 1400°C is truly diffusion-controlled, then all layers should thicken with time, according to equation (1) where $n = 2$ and k is a different constant for each layer. The weight gain should be directly related to the rate of thickening of each zone and to the total thickness. In a plot of the weight gain versus the thickness of the oxide layer, and the oxide layer plus internally oxidized zone, linear relationship is obtained for both at 1200 and 1400°C. The thickness of the oxide layer for a given weight gain is independent of temperature, indicating that the oxide density (and probably composition) does not change with temperature. The thickness of the internally oxidized zone does change with temperature, the layer being thicker for a given weight gain at 1200°C than at 1400°C. In the thorium-rich alloys, only the oxide layer grows with time, and the thickness of the

oxide for a given weight gain is increased which is consistent with the fact that practically all of the oxygen is in the oxide layer in the thorium-rich alloys.

3.3.1 Structure of Surface Zone

In order to discuss the sequence of phases at the air-coating interface in terms of the "ternary-diffusion" concept, it is first necessary to construct a tentative phase diagram for the Th-Zr-O ternary system. The Zr-Th and Zr-O binary diagrams are known and the quasibinary ZrO_2-ThO_2 diagram is also known. The Th-O diagram is not known, but the existence of oxide particles in a melted thorium button containing 1500 ppm O_2 suggests that the solubility of oxygen in thorium is extremely low.

The metallographic, hardness, X-ray diffraction and microprobe results of alloys oxidized at 1200°C define the zirconium-thorium ratio of the phases observed and the structure at temperature or structures which result from transformation on cooling, and permit an estimate of the oxygen gradient in the substrate. These results have been used to construct the tentative 1200° isotherm shown in Fig. 16. The cubic zirconia found in the oxide of the Zr-30%Th alloy has not been included in this diagram since Roy and Mumpton [7] have shown that the cubic zirconia observed in ThO_2-ZrO_2 alloys is a metastable rather than stable phase. It is not known whether the metastable phase is formed at temperature or on cooling, but

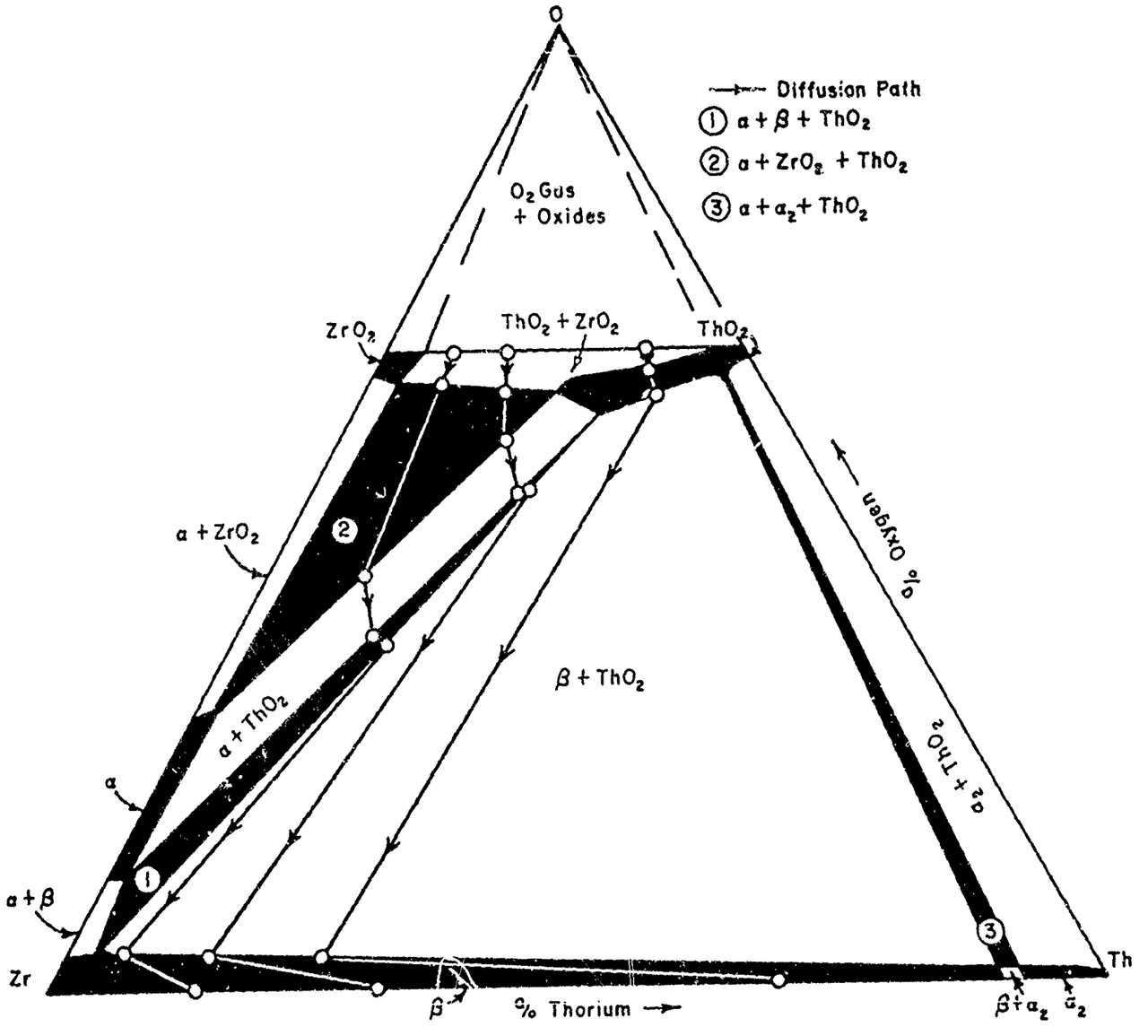

Fig. 16. Tentative phase diagram at 1200°C of Th-Zr-O system based on microprobe, x-ray and microstructure observations in oxidation of three Zr-Th alloys. Composition paths for oxidation of 3 Zr-Th alloys are indicated by arrowed lines.

a three-phased region should not be observed unless one of the phases is metastable.

The low solubility of thorium (<2 a/o) in the oxygen-rich internally oxidized zone of the Zr-14 a/o Th and Zr-31 a/o Th alloys helps to establish the oxygen gradient since the oxygen content of the zirconium-oxygen phases at the limit of solubility of thorium in these phases should not differ greatly from that in the Zr-O binary diagram. The low thorium content between the substrate and the internally-oxidized interface, and the identification of the internal oxide as ThO_2 suggests that the $\beta + ThO_2$ two-phase region exists at very low thorium and oxygen contents. Finally, the high zirconium contents of the ThO_2 in the $\alpha + ThO_2$ and $\beta + ThO_2$ internally oxidized layers in the thorium-lean alloys was used to construct the extended ThO_2 single-phase region with the assumption that this region is qualitatively only slightly oxygen-lean. The three-phase regions were observed as boundaries between layers. The $\alpha_2 + \beta + ThO_2$ and $\alpha_2 + ThO_2$ regions were not encountered in the diffusion couples but must exist at 1200°C.

The tentative diffusion paths of the Zr-14 a/o Th, Zr-31 a/o Th and Zr-60 a/o Th alloys at 1200°C are also indicated in Fig. 16. In the Zr-14 a/o Th and Zr-31 a/o Th alloys the composition paths cross tie lines in the $ThO_2 + ZrO_2$, $\alpha Zr + ThO_2$ and $\beta + ThO_2$ two-phase regions, and thus the internally oxidized layers as well as the two-phased oxide layer is observed in the microstructure. A net material flow of thorium from the unaltered

substrate to form the thorium-lean metallic zone and oxide phases richer in thorium is apparent in all alloys.

In the Zr-69 a/o Th alloy the composition path through the $\beta + ThO_2$ region is also a tie line so that the two-phase region is observed as a boundary between the oxide and substrate rather than an internally oxidized zone. The external layer of the oxide is two-phased ThO_2 and ZrO_2 since tie lines are crossed. The existence of a single-phase zirconium-rich ThO_2 solid solution agrees with the microstructure and initial microprobe results. Although ZrO_2 is observed by X-ray diffraction only in the outer portion of the scale, the presence of large amounts of zirconium in the oxide formed indicates that a layer of single-phase oxide exists in the oxidized specimen. However, further experiments are needed to verify the existence of the zirconium-rich ThO_2 oxide. Nitrogen has been ignored in the analysis of the specimens even though zirconium nitride has been detected in the oxide scales formed.

The diffusion paths and phase diagram in Fig. 16 are reasonably consistent, and speculation on the kinetics of diffusion in certain cases is possible. In the Zr-14 to 31 a/o Th alloys, the flux of thorium to the metal-oxide interface is not sufficient to combine with all of the oxygen, and as a net result, oxygen diffuses into the thorium-depleted metallic substrate until the solubility limit is reached for a given thorium-zirconium ratio. Thorium oxide nucleates and grows as an internal oxide until the

faster diffusing oxygen consumes the thorium available locally and diffuses into the substrate to nucleate additional ThO_2-rich particles at a point further removed from the surface of the specimen.

If this process is active in the Zr-30 to 55%Th alloys, the ratio of the diffusion of oxygen to the diffusion of thorium must decrease with increasing temperature, since the particles nucleate with greater frequency at the higher temperatures. The spatial density of internally oxidized particles in the substrate is greater at higher temperature, and the thickness of the internally oxidized boundary in relation to the thickness of the external oxide decreases with increasing temperature.

The most surprising result is that oxidation at 1200 to 1400°C occurs without breakaway even though stress is generated during oxidation. The corners of the specimens retain a sharp 90° angle, even after the oxide formed causes an increase in thickness of 10% or more. These results indicate that the oxide can accommodate large strains at 1200 to 1400°C without cracking, and thus prevent breakaway or spalling of the oxide which would lead to linear oxidation.

The nonprotective growth of oxides over the alloys at 1000°C and 750°C can now be rationalized if the strains which must be accommodated at the metal-oxide interface during the growth of the oxide are considered. The spalling of the oxide at 750 and 1000°C seems to be the direct result of poor ductility in the two-phase oxides at these temperatures.

The strains due to growth at the metal-oxide interface cause high shear and tensile stresses in the oxide which cause fracture at 750 and 1000°C but apparently cause deformation without cracking in the two-phase oxide at higher temperatures.

4. CONCLUSIONS

The results of our work to date on the oxidation of Zr-Th alloys have led to the following conclusions:

1. Oxidation at temperatures from 750 to 1000°C is linear due to the spalling of the oxide formed, which results from the generation of mechanical stresses during the growth of the oxide.
2. Oxidation at 1200 to 1400°C is diffusion-controlled, and the films formed are compact and adherent.
3. Oxides formed at 1200°C and above accommodate thickness increases of 10% or more without cracking or breakaway oxidation.
4. The rates of diffusion-controlled oxidation are considerably higher for alloys that form internally oxidized zones than for alloys that do not.
5. Insofar as the limited data on diffusion paths and phase diagram are valid:

a. the composition paths in the ternary phase diagram do not cross.

b. two-phased structures are observed when tie lines are crossed, but not when the diffusion path follows a tie line.

c. the morphology and existence of a two-phased internally oxidized zone depend upon the relative diffusion rates of the metals and oxygen, as well as the phase equilibria.

REFERENCES

1. M. Nicholas and C. D. Dickinson, "High-Temperature Protective Coatings for Refractory Metals", Part II, Sixth Meeting of the Refractory Composites Work Group, Dayton, Ohio, 1962.

2. M. Nicholas, A. L. Pranatis, C. D. Dickinson, "The Analysis of the Basic Factors Involved in the Protection of Tungsten Against Oxidation," Part I, ASD-TRD-62-205.

3. M. G. Nicholas, C. D. Dickinson, and L. L. Seigle, "Experimental Study of Factors Controlling the Effectiveness of Oxidation of High Temperature Protective Coatings for Tungsten", First and Second Progress Reports on AF 33 (657)-8787, August 15 and November 15, 1962.

4. M. G. Nicholas and C. D. Dickinson, "An Analysis of the Basic Factors Involved in the Protection of Tungsten Against Oxidation," ASD-TRD-62-205, Part II, September 1962.

5. L. Sama and D. D. Lawthers, ASD Tech. Rep., 61-233

6. P. D. St. Pierre, Bull. of Am. Ceram. Soc., 39, p. 264, 1960.

7. F. A. Mumpton and R. Roy, "Low Temperature Equilibria Among ZrO_2, ThO_2 and UO_2," J. of the American Ceramic Soc., Vol. 43, 1960, p. 234.

RESEARCH IN PROTECTIVE COATINGS FOR REFRACTORY METALS

P. J. CHAO

G. J. DORMER

B. S. PAYNE, JR.

J. B. WHITNEY

J. ZUPAN

The Pfaudler Co.

Rochester, New York

This report summarizes the experimental work performed at Pfaudler since the 1962 meeting of the Refractory Composites Working Group at Dayton, Ohio. The work reported ranges from basic evaluation of electrophoretic properties of particles to scale-up and large scale application of a proven coating, PFR-6. Included in the work was a variety of coating application processes and some coating systems development.

MANUFACTURING METHODS FOR HIGH TEMPERATURE COATING OF LARGE MOLYBDENUM PARTS

General

A major effort under way at the present time is the performance of Contract AF 33(657)-9343 for Manufacturing Technology Laboratory of Aeronautical Systems Division. The purpose of this contract is threefold:

- To advance the state of the art of applying high temperature coatings to large complex refractory metal parts, so as to establish an industrial capability for the application of the protective coating to parts required for aircraft, missile, and spacecraft components.

- To scale-up a representative pack cementation process, PFR-6, in order to attain a capability of coating full size panels and complex components fabricated from molybdenum alloys and thereby provide reliable oxidation protection at temperatures up to 3100° F.

- To establish general principles for future scaled-up operations of pack cementation coating processes.

The equipment and techniques necessary to apply PFR-6 to a fabricated molybdenum alloy part measuring 3 by 4 by 6 ft must be available by Fall of 1963. To date the major effort has been spent in evaluating, selecting, and procuring the proper equipment for performance of this goal. The experimental phase of the contract is underway, but insufficient information is available for the presentation of any conclusions. When the contract is completed, however, considerable knowledge and equipment will be available for the pack cementation coating of refractory metals.

Coating Equipment

Since most of the equipment used is quite straightforward, it will not be described at this time. However, the furnace that has been constructed is probably of general interest and will be described briefly.

Several methods of heating were investigated before a selection was made. Since Pfaudler has a great number of furnaces ranging from laboratory size to a 13 by 13 by 60 ft giant, sufficient experience was available to provide reliable judgment. After due consideration of actual needs, a gas-fired, top-loading design was selected. This furnace was designed and constructed by Pfaudler with help from various material suppliers. Its overall dimensions are about 10 by 8 by 10 ft, permitting a retort of about 5 by 5 by 8 ft to be fired. The largest retort planned for this study will contain over 100 cu ft of pack material and will weigh in excess of 7 tons fully loaded.

Other equipment required for this work will include such items as blenders, hoppers, overhead crane, etch and rinse tanks, ventilation systems, etc.

Thermal Analysis

Since the bulk of the pack used in this process is Al_2O_3, a material of low thermal conductivity, relatively poor heat transfer is experienced within the retort. When retorts up to 42 by 54 by 78 in. are used, the length of time required to attain coating temperature presents practical difficulties. In addition, the thermal gradient within the pack presents further coating problems. The first portion of this investigation lies in determining exactly the thermal characteristics of a large retort, with a minimum of change caused by measuring techniques.

Six different approaches have been studied in an attempt to obtain a suitable method of predicting time-temperature gradients within retorts. In order to provide data to be evaluated by these techniques, various sizes of retorts with thermocouples imbedded in them have been processed through a simulated coating cycle. The data resulting from these runs is now being analyzed. An empirical formula is being derived to permit prediction of the temperature at the mid-point of retorts of various sizes heated in a furnace of a particular configuration. While it was hoped initially that a single universal formula could be derived, it has been found necessary, for reasons of simplicity in calculation, to establish an empirical formula for each furnace configuration. With the final establishment of the curve for one furnace, curves for additional furnaces may be set up with a minimum number of calibration runs. This applies to the large gas-fired furnace as well as to the electric furnaces presently being used.

Pack Reuse

A second area of extreme interest is the reuse of the pack compound. Available data indicates that the coating produced with used pack is not as suitable as PFR-6 with new pack. The oxidation resistance performance is often as good, but the reliability is not satisfactory. Since it is our policy to not jeopardize reliability in order to save money, pack material is not being reused at the present time. However, we are performing a

series of experiments involving the addition of various constituents to the spent pack mixture. These indicate that proper enriching of the used pack will result in performance and reliability as high as with new pack, thus permitting its reuse. Complete data should be available within the next few months.

Coating of TZM Molybdenum Alloy

Another task on this contract is to determine performance data on PFR-6 coated TZM. This will include a series of oxidation tests and mechanical tests. The final tests will probably include temperature, stress, accoustical noise, and possibly shock in an attempt to determine coating performance under conditions more similar to actual end use.

DEVELOPMENT OF NOVEL PRACTICAL TECHNIQUES FOR APPLYING OXIDATION RESISTANT COATINGS TO COLUMBIUM ALLOYS

General

Contract AF 33(657)-8920 has been initiated at Pfaudler under the direction of Directorate of Materials and Processes, Aeronautical Systems Division. The techniques to be developed are to represent the best compromise between simplicity and reproducibility of application on the one hand and the effectiveness and reliability of protection achieved on the other. The processes currently under study are fluidized bed, salt bath deposition, and slurry application. D-14 (Cb-5Zr) alloy is being used as the substrate.

Fused Salt Bath Deposition

Fused salt bath techniques are being utilized for the deposition of chromium and titanium coatings. The fused salt bath reactor is shown in Fig. 1. The samples are contained in a porcelain tube supported by silica within a Hastelloy B retort. A Globar furnace is used as the heat source.

Chromium was deposited from salt baths containing $CrCl_2 - CaF_2 - CaCl_2$; $CrCl_2$-NaCl, Cr-NaCl-NH_4Cl; and Cr-NaCl-NaF. Some substrate embrittlement problems were experienced, but the addition of silicon and tungsten to the Cr-NaCl-NaF bath alleviated the problem and this bath was selected for process variable studies. Since this selection was made, several other salt baths have been evaluated, but the Cr-NaCl-NaF bath still appears to be most suitable. Using this chromium salt bath, a coating was deposited on D-14 in four hours at 1900°F. Average weight gains up to 1 mg/sq cm were attained. Temperature and time are the most influential variables affecting this weight gain.

The deposition of titanium from a fused salt bath has also been accomplished. The bath currently utilized contains 10%Ti, 5-10%I_2 and 80-85%NaCl. Using this bath, coatings of greater than 1 mg/sq cm have been attained in four hours at 2000°F. Temperature, time, and iodine content influence the deposition rate. Fig. 2 is a photomicrograph of a titanium coating deposited from fused salts. Experiments have been initiated for the alternate layer and codeposition of chromium and titanium, but no real progress can yet be reported.

Fluidized Bed Deposition

The fluidized bed facility is used for the deposition of silicon coatings. The bed used for this work (Fig. 3) is approximately 4 inches in diameter. In the initial experiments, TZM molybdenum alloy was used as the base metal, with D-14 being used in later work. Argon is used both as the fluidizing gas and as a carrier for the chlorine or iodine reaction gases. The bed contains alumina, silicon, and, on occasion, metallic additives. Bed height is varied from 10 to 28 inches.

A photomicrograph of silicon-coated TZM is shown in Fig. 4. Preliminary test results indicate life times of 1 to 2 hours at 3050° F in the calibrated oxyacetylene torch test.

The experiments in deposition of silicon on D-14 are more concerned with the evaluation of the effects of process variables than with the development of a modified silicide, high performance coating. Process temperatures, time, gas flow rates, and bed composition are being varied. Figure 5 illustrates the difference between the coating applied within the fluidized bed and the coating applied by vapor deposition above the bed. Figure 6 is a photomicrograph of a coating deposited from a bed containing 5% Si and 95% Al_2O_3 in 3 hours at 2000° F. This coating is about 0.003 in. thick.

Modified silicide coatings have also been applied to D-14 and resulting oxidation test lives of 20 to 200 minutes at 2800° F (optical) have been experienced. These results are preliminary and indicate the scatter expected in early laboratory coatings.

An 8-inch diameter fluidized bed reactor has been designed and is expected to be available this summer. A 22-inch diameter fluidized bed has also been designed, and components are being procured at the present time. This large bed will be used for Pfaudler in-house development of industrial manufacturing technology. It should be operable by mid-summer.

Slurry Application

The purpose of this part of the project is to study processing variables in the slurry application. The work has evolved into three distinct areas: investigation of existing coatings, development of water based slurries, and basic studies of electrophoretic and rheological properties of slurries.

The current coatings used as models in the investigation of organic solvent-containing slurries are the Sylcor 40S and the General Electric LB-2 coatings. Efforts have been concentrated on the effects of different solvents, specific gravity variations, and different types of aluminum and tin particles on the suspension properties of the slurries.

Since porcelain enameling is a slurry technique, a wealth of knowledge and experience in this field is available at Pfaudler. Results to date have demonstrated that a great deal of improvement can be achieved in these coatings. Therefore, a basic study of the electrophoretic and rheological properties of particles has been initiated in an attempt to improve the performance and suspension properties of the coatings.

The approach for this study is based on work performed previously at the University of Rochester. This work has indicated a direct correlation between particle electrokinetics and rheology of suspension. Two of the investigators, Dr. G. J. Su and Dr. D. H. DeClerck are now associated with The Pfaudler Co. and are engaged in this particular effort. A detailed description of the work is beyond the scope of this paper, but the resultant data should be useful to anyone interested in slurry techniques.

The third area of interest is the development of water-based slurry systems for obvious reasons of practicality and economy. Water-based slurries containing aluminum and tin in approximately the LB-2 ratio with extremely good suspension properties have been developed. Hydrogen is not evolved from the slurry as it is presently compounded. Initial results indicate no substrate embrittlement using D-14, but this factor is being checked extensively. Samples tested in the oxyacetylene torch test facility have exhibited oxidation resistance of 2 to 3 hours. A great deal of work is still required, but progress to date has been encouraging.

COATINGS FOR COLUMBIUM ALLOYS

Several columbium alloys have been coated by the pack cementation process. In recent months, efforts have been chiefly on B-66, FS-85, and Cb-752 alloys. These coatings are two-cycle pack cementation coatings using a chromium alloy first layer and a modified silicide second layer. Since others will be reporting on the performance of these coatings, no data is included in this report.

COATINGS FOR TANTALUM BASE ALLOYS

Single-cycle and two-cycle pack cementation coatings are being developed for tantalum base alloys. Since these coatings are in a very early stage, present results are not particularly noteworthy. Performance times of one to two hours at 2800°F (optical) have been experienced in the oxyacetylene torch test, but higher performance is required. A new development in this area may come from the use of a titanium pre-coating layer. Figure 7 illustrates a titanium coating on Ta-10W alloy. This coating, incidentally, was deposited in four hours from a fused salt bath at 2000°F. Adequate thickness can readily be attained by using newly developed techniques. The advantages of this coating have yet to be explored.

FURTHER INFORMATION ON PFAUDLER STUDIES

More detailed information on the Air Force sponsored portion of the Pfaudler work is available from quarterly reports submitted to Wright-Patterson Air Force Base. These reports are available from:

Mr. N. Geyer ASRCMP-3: Contract AF 33(657)-8920

Mr. D. Harleman ASRCTC: Contract AF 33(657)-9343

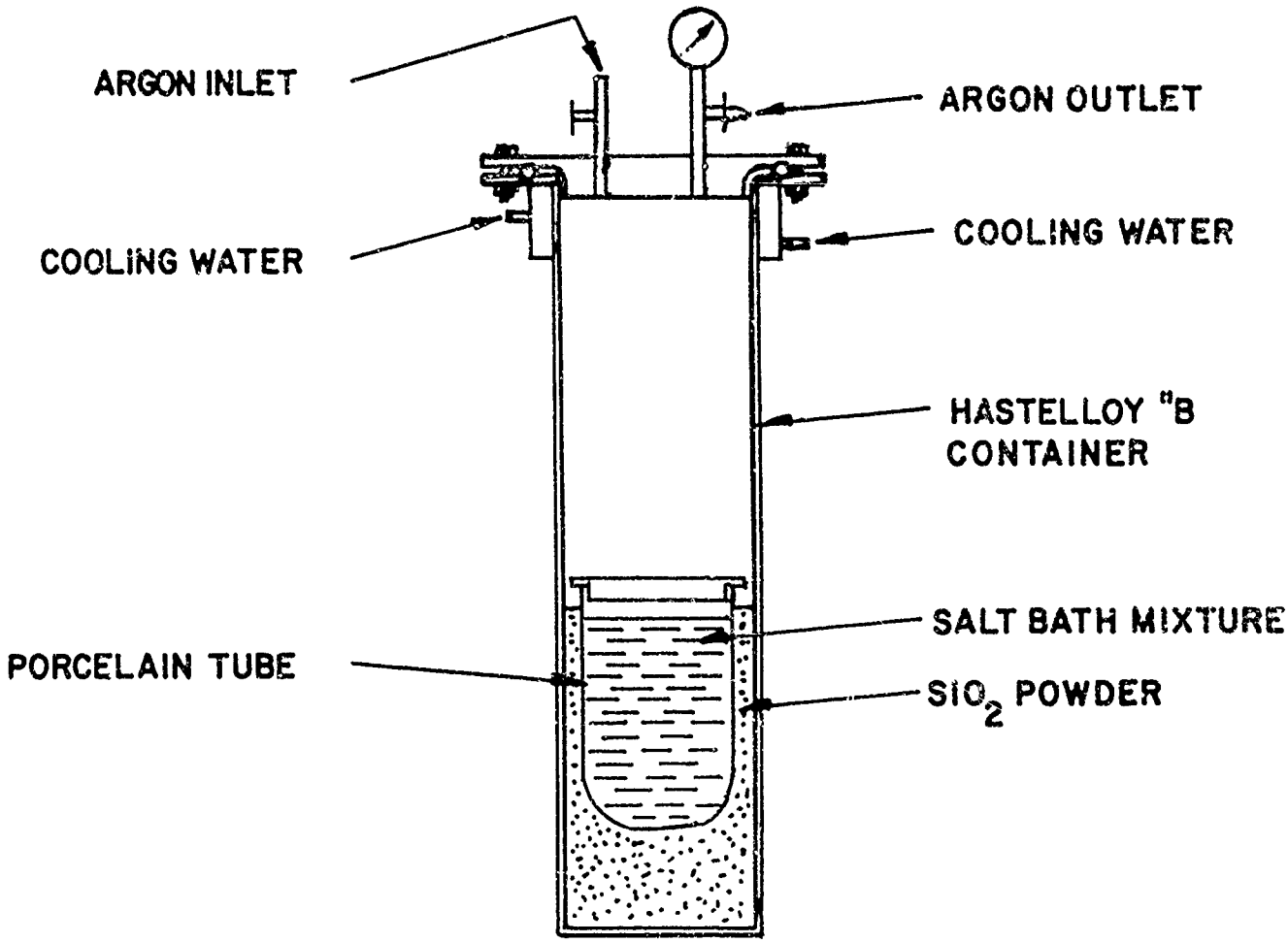

Fig 1 Fused Salt Bath Reactor

Fig. 2 Titanium coating deposited in run Ti-25 of the fused salt bath deposition process on D-14 columbium alloy.

250X (H-1008)

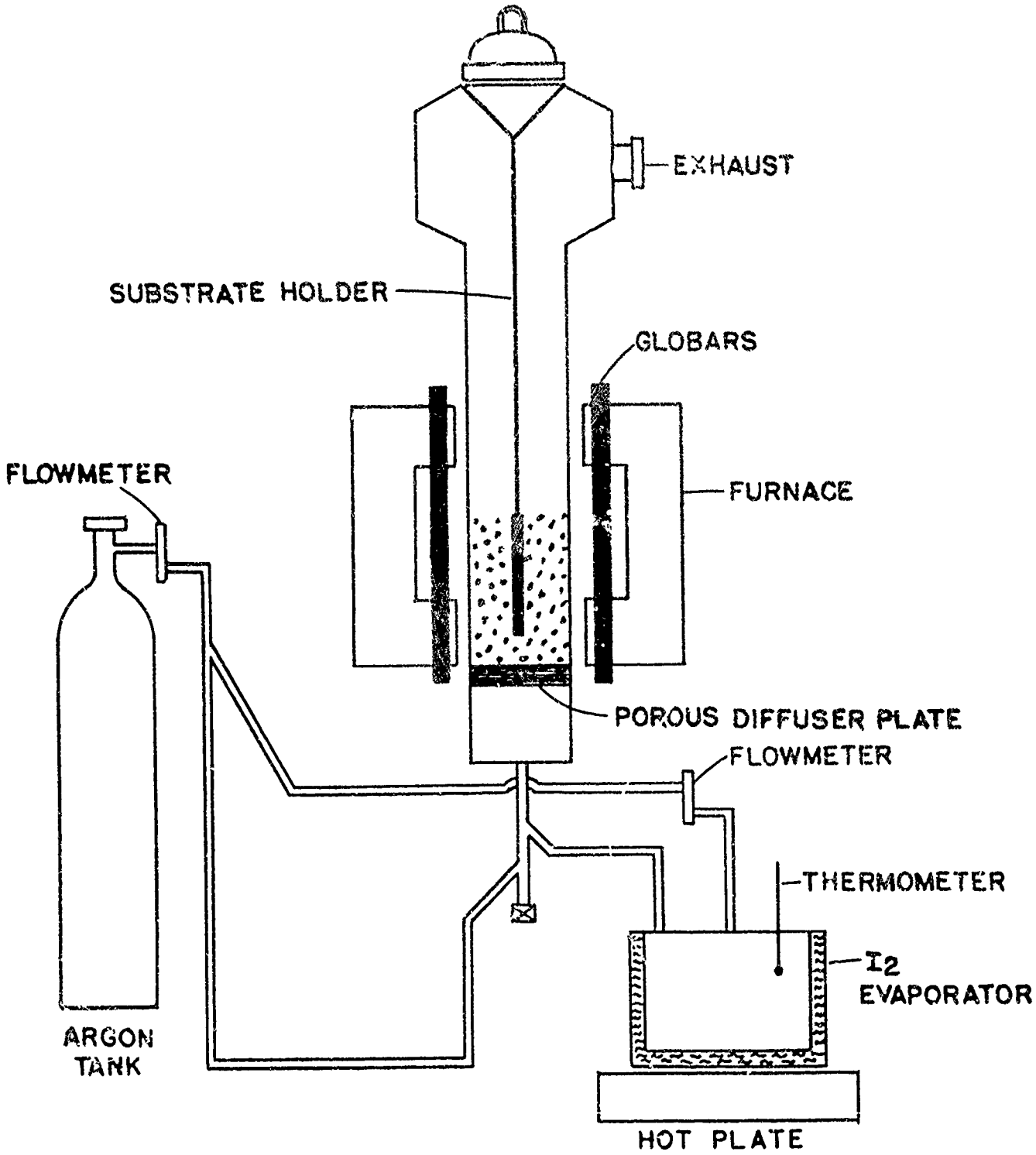

Fig. 3 Fluidized Bed Facility

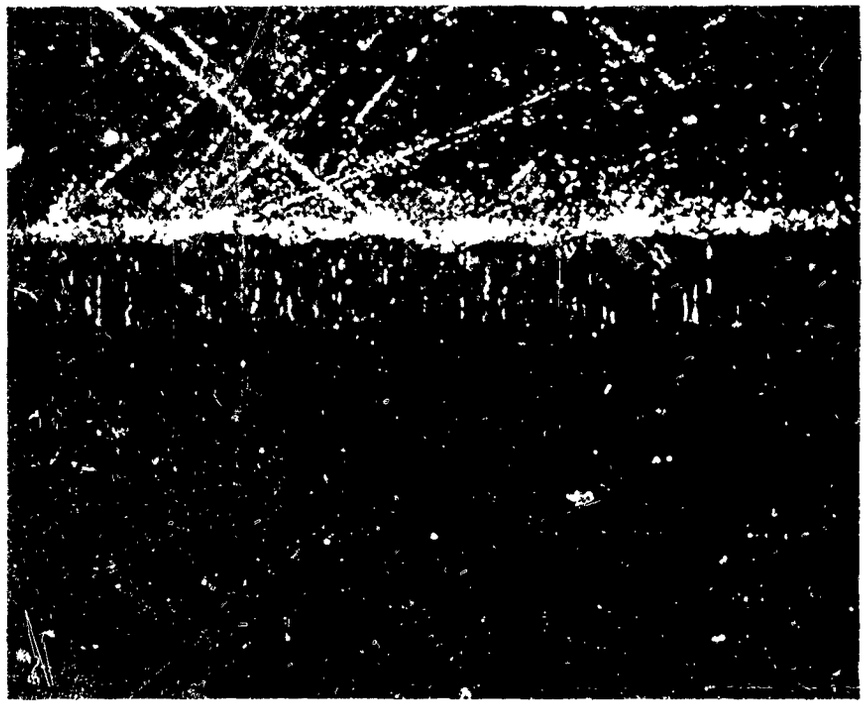

Fig. 4 TZM sample coated in fluidized bed reactor at 2150°F for 2 hr
Potassium ferricyanide etchant, 250X (H-1005)

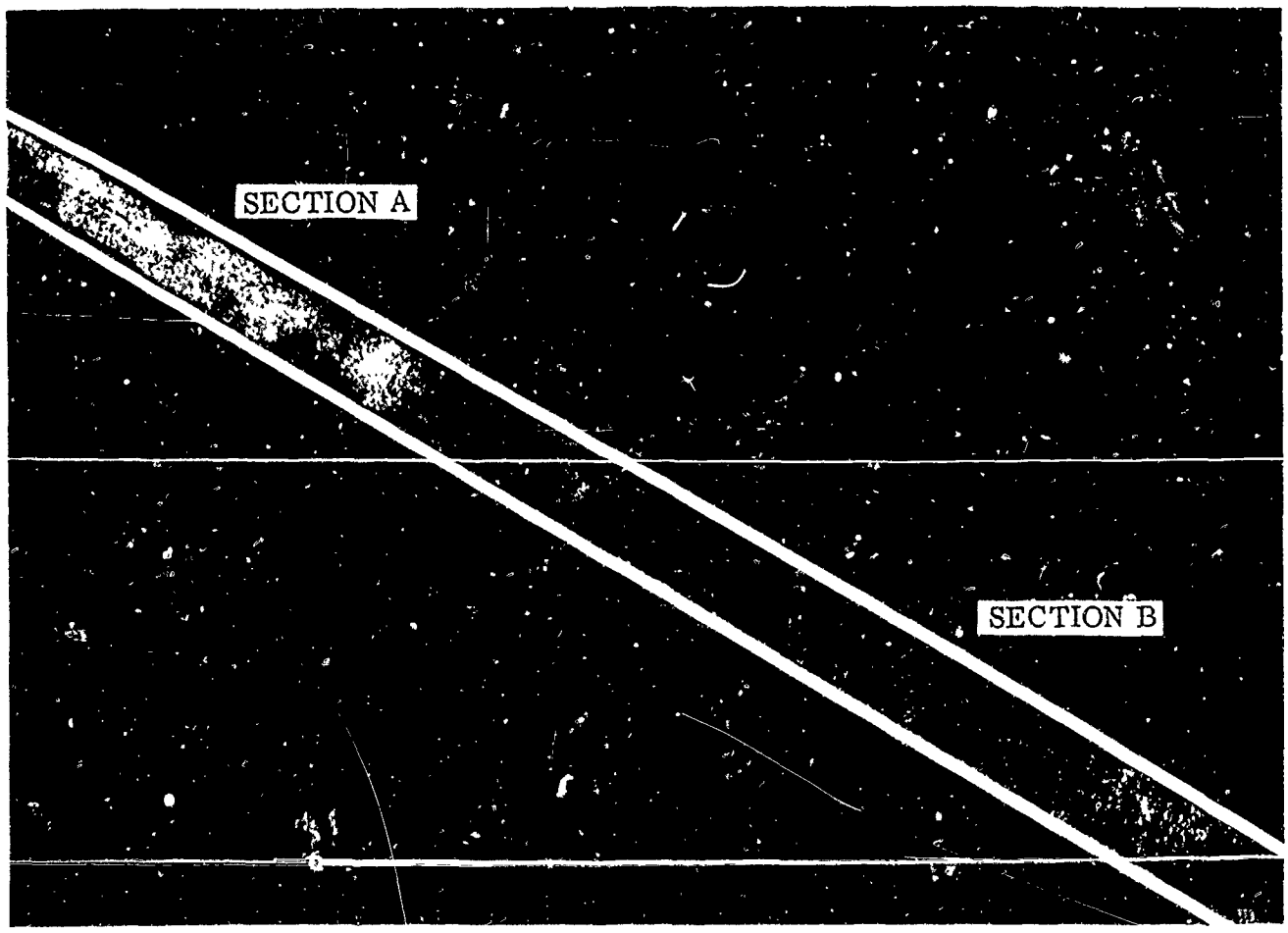

Fig. 5 Surface appearance of coatings formed within fluidized bed (Section A) and above fluidized bed (Section B). Section A coating is smooth adherent, and 2.5 mils thick. Section B coating is rough, somewhat nonadherent, and about 4 mils thick.

(H-1010)

Fig. 6 Coating deposited from a bed containing 5% Si, 95% Al_2O_3 in 3 hours at 2000°F (H-1012)

Fig. 7 Titanium coating on Ta-10W alloy from fused salt bath in 4 hours at 2000°F (H-1013)

HIGH TEMPERATURE PROTECTIVE COATINGS DEVELOPMENTS

J. E. BURROUGHS

P. F. GHENA

General Dynamics

Fort Worth, Texas

I. Objective

The coating program being carried out at GD/FW is being done on a continuous basis. This report covers the program for the last fiscal year for presentation to this group. The various portions of the research are presented at their present stage of development. The overall object of our investigation, which has not been realized as yet is to develop and evaluate a slurry or spray-on intermetallic coating (Sylcor type) for elevated temperature oxidation protection of refractory metal alloys subjected to re-entry vehicle environments. The thermal environment considered was 5 hours at 3300°F for the tantalum alloy and 20 hours at 2300°F for the columbium alloy.

II. Background

The pack cementation process and its application to refractory metal alloys was studied in FY1961. Variables such as time, temperature and elemental ratios from available reports were analyzed to try to optimize pack variables in processing. Three types of coatings appeared to be most promising: chromium plus

titanium, chromium plus titanium plus silicon, and chromium plus silicon. Work accomplished in FY1961 consisted of numerous pack cementation runs to establish the best techniques for lay-up, packaging, cleaning of details, etc. Coatings obtained have shown steady improvement as evidenced by appearance and microstructure. Due to the limited funds available the coated specimens were examined visually and some limited oxidation tests were conducted.

At the SAMPE-ASD sponsored "Ceramics and Composite Coatings Symposium" in Dayton November 1961, the preliminary results of Sylcors work on slurry-dip, paint, or spray-on intermetallic diffusion coatings were reported. In addition, the Martin-Marietta Company representative reported on utilizing this type of coating on their ASD contract "Refractory Metal Structure" (brazed and welded sandwich) for 3300-3400°F operation.

This intermetallic diffusion coating on tantalum has exhibited some resistance to over 3000°F for short time exposures. The Martin Company personnel also reported exposure to

3450°F for fifteen (15) minutes and with some self healing characteristics. It has been theorized that the aluminum in this coating induces self-repair by being transported from the $TaAl_3$ layer through the liquid Sn-rich phase to the Al_2O_3 barrier.

Because of the encouraging results obtained by this technique, and ease of application it was decided to investigate the Sylcor type coating in FY1962 instead of continuing the more combersome three component pack cementation development. The Sylcor diffusion type coating would lend itself more readily to large, complex components than the other processes.

III. Program

A. Development of Intermetallic Coatings

During the last year the Al-Sn intermetallic coating for columbium and tantalum alloys was investigated at GD/FW. D-31 and FS-82 columbium and Ta-10W tantalum alloys were used in the investigation. Initial efforts were intended to produce a workable coating by establishing the processing variables, ie., vehicle, vehicle thinning, vehicle-powder

mixture, diffusion temperature and time at temperature. Once the coating had been produced and effects of variables were known, additional research was initiated to modify this coating with more refractory elements or compounds to increase its resistance to elevated temperature for longer periods of time. As the program progressed investigations into duplex diffusion coatings were also conducted to obtain greater thickness.

The coatings were diffused in a tube furnace under purified argon atmosphere.

Screening tests used in coating development were:

1. Thickness
   (a) coating
   (b) diffusion layer
2. Appearance
3. Microstructure
4. Bend ductility
5. Oxidation Resistance: Center of 1/2 x 1 inch specimen heated by natural gas-oxygen flame in air to temperatures up to 2500°F as determined by optical pyrometer readings taken on unheated side of specimen.

B. Evaluation of GD/FW Developed Intermetallic Coating

The more promising coatings for columbium and tantalum alloys were evaluated by the following tests.

1. Oxidation resistance at elevated temperature in moving air.
   a. Continuous exposure
   b. Thermal shock resistance to multiple exposure.
2. Self-repairability - Scribe lines were marked on oxidation specimens and ability to self-repair was observed.
3. Tensile test at temperature.
   a. The best coating for each alloy was evaluated by coating columbium and tantalum tensile specimens and testing at the following temperatures.
      D-31 columbium alloy RT, 1500, 2500°F
      Ta-10W alloy RT, 1000, 2000, 2800, 3300°F
   b. General Telephone & Electronics Laboratory (Sylcor) coated tensile specimen were also evaluated at the same test temperatures.

IV. Summary of Results

Saturated solutions (refluxed overnight) of PVA in water, methyl alcohol, isopopyl alcohol, and acetone were found to be unsatisfactory for coating application. A commercial grade of lacquer was used for the greater portion of the program with some degree of success, but in many cases duplex treatments were necessary to obtain a coating of adequate thickness. The use of a low residue lacquer, Raffi and Swanson No. 1830, greatly simplified the application of the coatings.

Early in the program it appeared that the columbium base alloys would be more easily coated than the tantalum alloys. Portions of D-31 and Ta-10W which were dipped into molten 50Al-50 Sn at 1900°F for one hour are shown in Figure 1. The diffusion zone on the D-31 is even and clearly defined. The tantalum had a narrow diffusion zone along most of the specimen, but highly localized attack occurred adjacent to the liquid surface. In the application of slurry dipped coatings, the tantalum was more easily coated. It appears that a small amount of

oxide enhances the diffusion in tantalum.

A composition of 50 Al-50 Sn was found to be more resistant to oxidation, but 75Sn-25Al was a more easily applied coating. Work has not been completed in this area, as yet, but it is felt that a composition between these two will produce the optimum coating for this system. The 50Al-50Sn coating on D-31 columbium alloy has withstood 2000°F for 100 hours, 2300°F for 4-8 hours, and 2500°F for 10-15 minutes. The same coating on Ta-10W withstood 2300°F for up to 50 hours and 2500°F for 3 hours. Failures usually originated from the holes used to suspend them during coating. The edges had been carefully rounded and the holes chamfered.

A typical failure, shown in Figure 2, occurred after 4 hours at 2200°F to the 50 Al-50Sn coated FS-82 columbium alloy specimen. The areas shown in the two micros are identical, only the method of lighting is different. The diffusion layer which appears bright and only slightly different in color from the substrate under bright field, appears as either

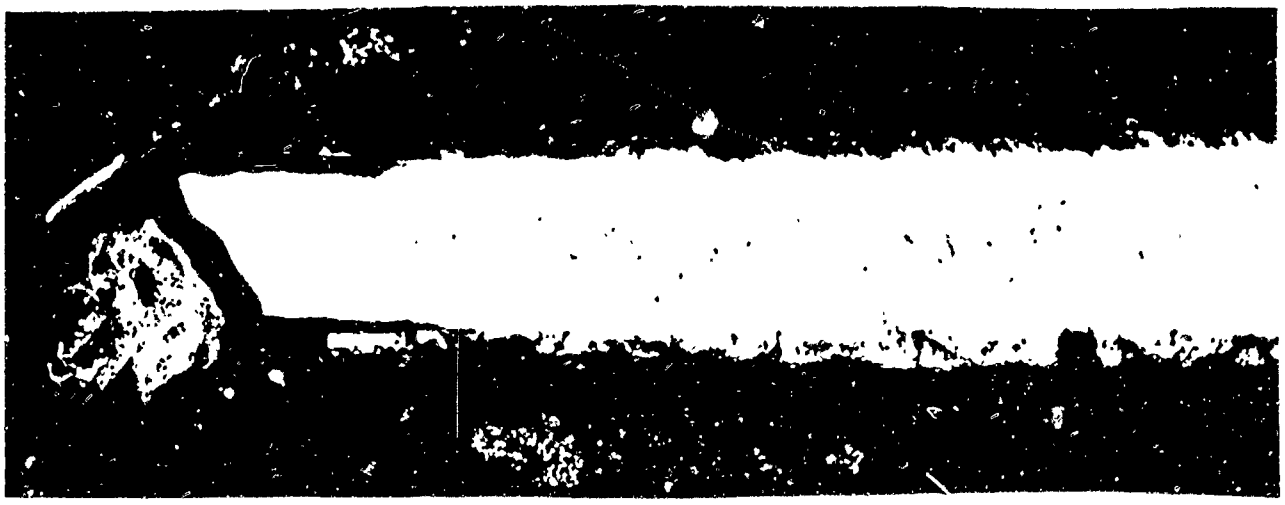

dark or light grains under polarized light. This birefringence is due to the anistropic nature of the intermetallic, probably $CbAl_3$. The areas which appear dark under bright field and speckled under polarized light are the oxidized portions of the coating. Note the blob of oxide formed on the edge of the specimen and the under cutting of the coating adjacent to the failure. The oxide build up which had started only minutes before was growing at a very rapid rate when the specimen was removed from the furnace. Note also that the coating has been oxidized to the substrate in one area of the specimen face. Failure was probably imminent at this point.

The basic tin-aluminum coating was modified with additions of copper, chromium, titanium and zirconium. The latter two elements were not absorbed into the alloy on diffusion when added as elemental powders. Subsequent additions were made in the form metal hydrides. The limited alloy modification work done to this time can only be considered to be indicative, but the most promising additions have been chromium and titanium.

The latter formed a visible oxide very quickly, but it seemed to be quite tough and resistant to further oxidation.

The tensile testing, to date, has been limited to D-31 columbium alloy to 2200°F in partial vacuum. The controls for this heat of material have not been tested as yet, but based on other heats that have been tested there is no extremely deleterious effect. The greatest effect is to the yield strength which is somewhat lowered. The ultimate strength is reduced only slightly and ductility remains excellent.

V. Current Efforts

During the coming year work will be continued on the aluminum tin system and its modifications. The new low residue lacquer seems to impart a greater fluidity to the coating on diffusion which will necessitate a further investigation of these variables. Although the aluminum-tin coating provides excellent protection to 2000°F, above this temperature it seems to be deteriorating rapidly. The possibility of utilizing another

eutectic to provide for better self healing characteristics will be investigated. Copper forms a higher melting eutectic with aluminum and in addition forms solid solutions with some of the other elements. Silicon has been used by several investigators with some success. Attempts to improve the oxidation resistance of the coatings with chromium, titanium, and zirconium will be continued and hafnium will be included. The effect of the coatings on the mechanical properties of the substrate will be further investigated. Tests will be made on the effect of low temperature on coatings containing tin. Tin undergoes a transformation to its enantiotropic form, a tin powder, which might preclude its use in cold environments.

Planning is complete and hardware is available for a creep oxidation resistance test set-up. The coated specimen will be resistance heated in moving air while loaded to a stress that will cause creep. Programming will be included for the three variables, temperature, loading and atmosphere, to permit cycling in addition to steady state effects. This should be an

excellent test of the coatings ability to withstand service conditions.

EVALUATION OF COATED REFRACTORY METAL FOILS

A. R. STETSON

V. S. MOORE

Solar Research

San Diego, California

I. INTRODUCTION

Future Air Force procurement will continue to be directed toward the exploration and utilization of space. Missiles will play an important strategic role, but there will be an increasing emphasis on more versatile vehicles which can perform the functions of aircraft but operate in space. Size, complexity, and cost of the projected vehicles require that they be re-usable for a large number of exits and re-entries with only relatively minor rework between missions.

Aerospace vehicles of the future will probably be of extremely large size and of rigidized lightweight construction. The skins of the vehicles must have temperature capability to withstand and re-radiate the energy absorbed by aerodynamic heating and since weight is at a premium, the skin must also be a structural member. The high temperature, light weight, and structural requirements make refractory metal foils prime candidates for these surfaces.

Honeycomb sandwich and ribbed structures are typical of the rigidized configuration that must be constructed of refractory metal foils if the various current concepts are to reach the hardware stage. Numerous unknowns present themselves when considering these structures and materials which can be best discussed by reference to schematics of the foil structures as shown in Figure 1. Both structures must be coated for oxidation resistance. The sandwich structure requires protection on the outer surface only, but the ribbed panel requires complete coating coverage. Both panels require development of brazing or welding techniques for joining and protection of these joints. Specific problems that must be investigated with both structures are:

Coated Material

- Reliability
- Time-temperature life
- Coatings-joining interaction
- Effect on substrate properties
- Design data

Joining Process

Design data

Basis Material

Design data

The most critical material problem is associated with the performance of coated and joined foil. The Air Force, recognizing this problem, awarded Solar a program (AF33(657)9443) to determine the state of the art of coatings as applied to columbium and molybdenum alloy foil. This report is a brief summary of the screening test results on virtually all the commercially available refractory metal coatings for columbium and molybdenum alloys.

Alloys used in the screening tests were D36 (Cb-10Ti-5Zr), B66 (Cb-5Mo-5V-1Zr), and TZM (Mo-0.5Ti-0.08Zr-0.02C) in a nominal thickness of 0.006 inch. This thickness was chosen because it was thin enough to demonstrate the problem of foil coating, but thick enough to be considered as a facing material for structural applications. Columbium alloys were supplied by Metals and Controls Incorporated, a Division of Texas Instruments Incorporated, and the TZM by Universal-Cyclops Steel Corporation. Compositions of the alloys are shown in Table I and a set of screening test specimens, prior to coating, is shown in Figure 2.

Coating vendor selection for the screening tests was very broad. Inquiries were sent out to all known coating vendors to determine their interest in the program. All organizations expressing an interest in participating in the program were included. Boeing and Pratt & Whitney (CANEL) declined to participate. The coating vendors and the type coating applied are shown in Table II.

The screening tests were not selected to produce design data but rather to bring out differences in coatings, illustrate the problem of coating foil, and show the time-temperature capabilities of the various coating systems. Tests selected are:

- Receiving Inspection
  - Weight change on coating
  - Mechanical properties
  - Bend ductility
  - Metallography

    Substrate and coating thickness and hardness

- Oxidation Tests
  - Cyclic oxidation at 2000 F and 2500 F
  - Cyclic oxidation at 2000 F and 2500 F with pre-strain
  - Plasma torch oxidation at 2000 F and 2500 F
- Bend Tests After Static Oxidation at 2000 F and 2500 F
- Metallography After Oxidation Tests

In addition to the screening tests, a preliminary study was conducted on the coating-joint interaction with a silicide pack cementation process.

II. TEST RESULTS

2.1 RECEIVING INSPECTION

2.1.1 Appearance

The foil specimens as returned from the coating vendors were, in general, in fair condition. Fallout on the larger specimens, such as the 3/4 inch by 9-inch tensile specimens, was greater than on the 3/4-inch by 1-1/2-inch specimens. Vendors receiving more than one set of specimens invariably had less fallout and warpage on the second set.

All vendors applying modified silicide coatings by pack cementation methods (Chromizing Corporation, Vought, TAPCO, General Technologies Corporation(GTC), Pfaudler, Chromalloy Corporation, and American Machine & Foundry (AMF)) experienced some reaction between the pack and the specimen. Reaction sites were pits or projections. TZM coatings were, in general, more uniform in appearance than coatings on D36 and B66.

The aluminum-or tin-based coatings of General Telephone & Electronics (GT&E) were quite uniform on B66 and TZM, but on D36 a large bead of residual alloy formed on the lower edge of each specimen.

2.1.2 Weight Change

The 3-inch by 3-inch specimens were weighed before and after coating to determine the weight change resulting from the coating process. The results are tabulated in Table III and shown graphically in Figure 3. Weight change varied from a minimum of 4.6 percent to 51.6 percent with the GT&E and TAPCO coatings showing the maximum weight gains and the less complex pack silicides the minimum gains in weight.

2.1.3 Metallograph

Residual substrate thickness, substrate hardness, and coating thickness and hardness were measured on specimens after coating. The results are shown in Table III.

Loss of substrate, as measured by the distance between the diffusion fronts on each side of the specimens, was appreciable for all coatings. Examples of maximum coating penetration are TAPCO's on D36 with a 57.5 percent substrate loss, GTC's on B66 with a 45.5 percent loss, and Vought's on TZM with a 36 percent loss. The aluminum-based coatings of GT&E showed the least substrate loss on all alloys with a maximum coating penetration of 14.4 percent.

Contamination of the D36 and B66 alloys and recrystallization of the TZM alloy was minor as determined by appearance and microhardness measurements at the center of the coated foil specimens. The D36 alloy showed the greatest increase in hardness with TAPCO and GTC coatings. It exhibited a hardness of 214 and 249 DPH, respectively, compared to 170 DPH for the uncoated alloy. Except for the Vitro coated specimens, the TZM alloy showed no evidence of recrystallization.

Coating thickness, including diffusion zones, range from 100 percent (GT&E-D36 alloy) to 18 percent (Chromizing-TZM alloy) of uncoated substrate thickness. Coating hardness ranged from the extremely soft aluminum-tin coatings (19 DPH) to the modified $MoSi_2$ coatings at approximately 1500 DPH.

2.1.4 Mechanical Properties

Tensile tests and bend tests were performed on the "as coated" specimens. Results are shown in Table IV and mechanical properties are presented graphically in Figure 4 as a ratio of the uncoated foil properties. Condition of the tests were:

Mechanical Properties

Temperature	RT (70 to 75 F)
Strain rate	
to 0.2 percent yield point	0.005 in/in min
to failure	0.050 in/in min

Results are based on uncoated specimen dimensions.

Bend Test

Temperature	RT (70 to 75 F)
Specimen	3/4 inch by 1-1/2 inch

Supports	15 t (0.090 inch)[1]
Ram radius	4 t (0.024 inch)
Ram speed	0.030 inch min

The yield and tensile strength of the alloys after coating occasionally exceed the base metal properties, e.g., GT&E and TAPCO on B66 and Chromizing and GT&E on TZM. On columbium-based alloys this is probably due to substrate alloy contamination and to the actual strength of the coating; however, on TZM the variation is probably due to different initial substrate thickness which on this alloy varied ± 0.0006 inch. A nominal 6 mils in thickness was used to calculate strengths on TZM.

The strength-weight ratios on all alloys were reduced by coating. As a whole, the reduction was in proportion to the loss in substrate, and the gain in weight during coating. The minimum reduction was for silicide coatings on TZM and the maximum reduction on the silicide coatings on D36 (up to 45 percent).

Elongation was reduced on all coated foil. One silicide coating lowered this property on columbium-based alloys to less than 30 percent of the base-line properties, and with several coatings to less than 1 percent elongation. Generally, the aluminum-tin based coating had the least effect on this property.

A rather anomolous performance was noted between bend test and elongation results (Table IV). For example, the TAPCO coating with very poor tensile elongation consistently passed the bend test; whereas, three coatings on B66, which exhibited much better tensile elongation, failed this test. There is no obvious explanation for this behavior but since bend performance, after oxidation testing, improved over the "as coated" condition on the Vought, Pfaudler, and GTC coatings on B66, hydrogen may be responsible for the poor bend ductility (Table VII).

2.2 OXIDATION TESTS

Three oxidation tests were used in screening the refractory foil coatings:

---

[1] Based on uncoated foil thickness nominal 0.006 inch

1. Cyclic furnace oxidation in flowing dry air at 2000 and 2500 F

2. Cyclic plasma torch oxidation in a simulated air environment at 2000 F and 2500 F

3. Isothermal oxidation at 2000 F and 2500 F in flowing dry air.

The third test was performed primarily to obtain specimens for bend testing that were free of substrate oxidation and for this reason was limited in furnace time to 85 percent of the cyclic oxidation life. The descriptions of tests 1 and 2 are given below.

Cyclic Furnace Oxidation

Specimens	D36, B66 and TZM 0.006 inch by 0.75 inch by 1.5 inch - triplicate specimens
Supports	Alundum boats - Mullite tube
Test Cycles	18 - one-hour cycles 7 - one-hour cycles followed by a 16-hour soak. This sequence to be repeated until failure or 75 hours.
Atmosphere	Dry air (d.p. - 60 F or lower) at 4 CFH
Heating Rate	Rapid - charge into hot furnace
Cooling Rate	Air cool

Plasma Torch Oxidation

Specimens	D36, B66, TZM 0.006 inch by 3-inch by 3-inch-single or duplicate specimens
Support	Alundum bricks (see Figure 5)
Test Cycle	2000 ± 15 F - four minute cycles [1] 2500 ± 20 F - eight 15 minute cycles [1]
Atmosphere	54 percent A, 26 percent N_2, 20 percent O_2
Heating	Rapid
Cooling Rate	Air cool
Gas Velocity	2000 F 190 fps 2500 F 250 fps

[1] Temperatures were uncorrected back surface optical readings using a micro-optical-pyrometer.

In the furnace cyclic oxidation tests, specimens were tested in the "as received" and pre-strained condition. Prestraining was accomplished by bending to the knee in the load deflection curve as shown in Figure 6.

Criteria of failure, as used to determine cyclic oxidation life is obvious evidence that the substrate is being attacked. This may take the form of oxide growth or loss of material, or a major inflection in the weight change curves. On many specimens, however, testing was continued long after a small defect developed.

2.2.1 Furnace Oxidation Results[1]

Graphical representation of the furnace cyclic oxidation test results are shown in Figure 7. Protection of the D36, B66, and TZM at 2000 F for more than 50 hours can be effected by a number of the coating systems. At 2500 F, only the Vitro coating on TZM and the TAPCO coating on D36 and B66 were capable of affording 50 hours of protection without gross failures.

Results of the cyclic oxidation test and results of prestrained specimens are shown in Table V. At 2000 F on the D36 alloy only the TAPCO coating showed no apparent loss in oxidation resistance with prestraining; however, on the B66 alloy only the GT&E coating had reduced life as a result of prestraining. On the TZM alloy at 2000 F, all coatings were adversely effective by prestraining exhibiting virtually no useful life except for the GT&E coating with a 5.6-hour life.

Test at 2500 F after prestraining on D36 and B66 followed the pattern of the 2000 F results, with the TAPCO coating exhibiting no adverse effect from prestraining. The other coatings either had very little life at this temperature or the life was considerably reduced by prestraining. On TZM only Vought and GT&E coatings showed up to five hours life. The other coating withstood less than one hour of testing before failure.

---

[1] Stetson, A. R., Moore, V. S., Evaluation of Coated Refractory Metal Foils. Quarterly Progress Report No. 1 and 2. Solar Report RDR 1325-1 and 1325-2 (5 October 1962, 21 January 1963).

2.2.2 Plasma Torch Oxidation Tests

The plasma torch cyclic oxidation test (Table VI) brought out some interesting results. One coating on D36 failed in the low temperature region rather than in the hot zone indicating a pest condition. Two of the other coatings on D36, one silicide and one aluminum-tin type, were too mobile in the torch and burned through at 2500 F. On B66, three of the coatings burned through at 2500 F, two silicide and one aluminum type, with the more mobile coating suffering the greatest attack. No catastrophic failures were experienced on coated TZM in the plasma torch test. Two of the coatings exhibited small pinholes after the test, but these did not result in a major burn through.

In the subject test, an uncoated D36 panel burned through in four seconds at 2500 F; whereas, an uncoated TZM specimen lasted 25 seconds. The rapid burn through of the D36 specimen is probably the result of ignition since the oxidation rate of columbium alloys should be less than the molybdenum alloys due to the formation of a high melting point oxide.

2.2.3 Bend Test After Static Oxidation

Specimens were heated for a period of time at 2000 F or 2500 F in dry air and subsequently bent at room temperature using the procedure described in Section 2.1.4. The time at temperature was not necessarily the same for each coating-substrate composite. The time of exposure was selected, based on cyclic oxidation results, as a time at which no coating damage could be noted in testing.

Results of the bend tests are given in Table VII. On D36, the GT&E and TAPCO coatings failed the bend test after testing at 2000 F and 2500 F, respectively. Of the silicide coatings tested on D36, the TAPCO coatings exhibited the lowest ductility even when tested for the very short times shown in Table VII.

Coating diffusion rates appeared to be slower in the B66 (see section 2.2.4) than in the D36 alloy and consequently all of the coatings tested, excepting the aluminum-based GT&E coating, exhibited ductile bend performance. The Vought, Pfaudler and GTC were more ductile after testing than in the "as coated" condition (compare results in Tables IV and VII).

Bend test results on TZM were erratic. None of the silicide coatings could be consistently bent to an angle of 90 degrees after 2000 F exposure. After 2500 F exposure, bend ductility of all silicide coated specimens improved and two coatings, Pfaudler and Chromizing, withstood bending to 90 degrees on at least two of the three specimens tested. The aluminum-tin coatings exhibited excellent bend ductility but furnace times were very short.

The improved bend ductility of the TZM specimens after exposure to 2500 F was unexpected. Full recrystallization occurred in less than one hour at this temperature; whereas, at 2000 F recrystallization was nil after 72 hours. Thus, the wrought structure is not necessary for ductility in TZM.

2.2.4 Substrate Changes After Oxidation Testing

Substrate hardness and the distance between diffusion interfaces was measured after oxidation tests to indicate the rate at which the coating diffuses into the substrate.

The diffusion results reported here should be looked upon as preliminary, indicating trends, rather than as basic diffusion data. Errors in the data can result from:

- Measurement of substrate thickness prior to oxidation testing not being made on the same specimen that was oxidation tested. Results are, therefore, subject to error from both the substrate thickness variation and the coating thickness variation.

- Diffusing species not being known. They may be oxygen and/or one or more coating constituents.

- The fact that diffusion coefficients are determined, in general, for very short times and from as few as two thickness measurements.

- Diffusion boundaries on coatings such as TAPCO and GT&E being determined by recrystallization and grain growths as well as by a distinct movement of boundaries. With the TAPCO coating, particularly, considerable diffusion can be of the solid solution type; e.g., titanium in columbium, which is difficult to distinguish by metallographic examination.

Substrate Hardness

Substrate center line hardness is shown in Table VIII for coated D36, B66, and TZM foil specimens after test. The 2000 F results on all alloys and coatings show only relatively minor hardness changes in the residual substrate. The one exception is the GT&E coating on D36 which showed an increase in hardness of 118 DPH units after test. The GT&E coating also showed the greatest rate of diffusion into this alloy of all coatings tested.

At 2500 F the D36 alloy was the most affected by diffusion. The GT&E coating showed no substrate after only 11 hours of test. The TAPCO coating exhibited severe substrate hardening, which resulted from saturation and precipitation of a phase, perhaps $CbCr_2$, after only seven hours. The less complex silicide coatings such as applied by Vought and Chromizing exhibited the lowest rate of substrate hardening.

Test times at 2500 F on the B66 alloy were quite short, but the results indicate that the rate of penetration of all coatings into the alloy is much slower than for the D36 alloy.

Substrate hardness of the coated TZM alloy decreased during the 2500 F test as a result of recrystallization. The rate of hardness loss was a variable which was probably influenced by the interaction of the substrate, coating, and prior heating in the coating process cycle. The GT&E coating showed the slowest rate of recrystallization.

Diffusion Rate

An indication of the rates of diffusion of the coatings into the various alloys was obtained by assuming the parabolic relationship $X^2 = K't$ to be valid. K' (mils^2/hr), which is linearly related to the diffusion coefficient, was then determined as the slope of the straight line plot. The depth of diffusion, X, was determined metallographically as one-half the difference in the substrate thickness before and after test. Extrapolation of the measured 2000 and 2500 F results to 3000 F was performed by assuming that the modified diffusion, coefficient K' varied with temperature according to the Arrhenius rate expression

$$K'_t = K'_o e - \frac{\Delta H}{RT}$$

By plotting log K' against the reciprocal temperature at 2000 F and 2500 F, K' could be determined at 3000 F.

Rate plots and diffusion coefficients are shown in Figure 8 for the various coating-substrate combinations at 2000 F, 2500 F, and 3000 F (extrapolated). In several of the plots, two or more coatings of similar types were plotted as a single coating because of the paucity of data; e.g., Chromizing, Vought, and Pfaudler coatings on B66, and Chromizing and Vought coatings on D36. Rate plots of the TAPCO coating on D36 are not included because of insufficient data.

Of the coatings evaluated, the aluminum and tin-based coatings exhibited the most rapid diffusion rates, the slightly modified silicides the slowest rate, and the TAPCO chromium-titanium-silicon coating an intermediate rate. Diffusion rates into the D36 alloys were considerably higher than for the B66 alloy.

Rates of diffusion of the silicide type coatings (including TAPCO's) are slow enough at 2000 F to permit operation for at least 100 hours without considering the change of base-line properties as the result of diffusion. At 2500 F, however, on foil gage alloys, penetration in only 10 hours is a high percentage of the residual substrate. For example, on 0.006 inch foil at 2500 F.

Alloy	Percent	Substrate Penetration (hr)
D36 (GT&E)	100	10
TZM (GT&E)	62	10
D36 (Vought, Chromizing)	33	10
D36 (TAPCO)	100	10
B66 (Vought, Chromizing, Pfaudler)	25	10
B66 (TAPCO)	47	10
TZM (Vought, Pfaudler, Chromalloy)	26	10

These percentages are in addition to the loss of substrate during the actual coating process.

Diffusion into the substrate of the aluminum-tin coating results in complete loss of base-line mechanical properties; however, diffusion of the silicide coatings and particularly the TAPCO chromium-titanium-silicon coating may not result in the same percentage loss of mechanical properties as loss in original substrate. The diffusion product of coating and substrate may have useful mechanical properties.

III. COATING-JOINING PROCESS INTERACTION

There is essentially no published information on the compatibility of refractory metal coatings and joining processes, and the effect of joint configuration on coating appearance and performance. Butt welds are an exception to this statement since it can be concluded from Reference 1 that clean, butt-type welds can be coated as satisfactorily as sheet materials. If a honeycomb or ribbed structure is to be fabricated from refractory metals, the interaction and interplay of potential joining processes and joint configurations must be evaluated in detail. The experimental work to be described in this section will illustrate the magnitude of the problem and recommend the type of joining process required.

3.1 SPECIAL PROBLEMS IN COATING JOINED STRUCTURES

Overlapping spotwelding and brazing are the two methods being considered for joining ribbed structures, similar to the one shown in Figure 1B. The principal effort has been directed toward brazing because of the greater possibility of completely bonding the faying surfaces.

Prior experience with mechanical joining using rivets has shown that it is essential to double coat a structure to get 100 percent reliability. The structure must be coated before joining and recoated afterward. If this procedure is not followed, the probability of having uncoated areas between the unjoined faying surfaces is very great. The throwing power of the cementation processes is inadequate to prevent oxidation in these unbonded areas. Coating of a welded structure can only approach 100 percent reliability when the welds completely cover the faying surfaces, i.e., where throwing into the unbonded zone is not required. Since such a joint is nearly impossible to make, it is doubtful that coated refractory metal structures joined by this technique can be realized.

Brazing minimizes the throwing power requirement of the coating because the flow and fillet formation provides a smooth, uniform surface to coat in the area of the faying surfaces. The major unknown, which is currently under investigation, is the effectiveness of the existing commercial processes on protecting the braze alloy and the

braze alloy refractory metal interfaces.

Eutectic melting may occur between the coating material and the braze alloy, which could result in severe undercutting of the foil. For example, the titanium-silicon and zirconium-silicon systems which form the base for several braze alloys, have eutectic temperatures of 2426 F and 2480 F, respectively. The ternary and quaternary systems can be expected to have lower melting points. Solution of the coating problem of joints is not expected to be an easy one and may require development of a process for pre-coating the braze fillets or the entire foil structure with a material to minimize the interdiffusion of the coating and braze alloy.

3.2 EXPERIMENTAL PROCEDURES AND MATERIALS

Specimens used in this investigation were 10 mil D36 alloy fabricated into U-channels and flat plates to simulate the corrugated structure shown in Figure 1B.

The two pieces of the specimen were joined together by one of the following processes:

a. Diffusion Bonding
   (1) without intermediate alloy
   (2) with 0.3 mil pure Ti foil intermediate alloy
   (3) with 0.14 mil pure Zr foil intermediate alloy

b. Brazing
   (1) Solar RGN-15, Zr-base alloy
   (2) Martin Ti-8.5Si alloy
   (3) General Electric AS537, Zr-V-Ti alloy

c. Spot Welded

   For ease of welding, two flat plates were bonded using very fine overlapping spot-welds. After this operation, the re-entrant angles of 45 degrees were formed. These angles provided a much more favorable situation with this joining process since joining out to the re-entrant angle was not required.

   After joining, all specimens were siliconized using a standard pack cementation process:

Pack composition:	silicon metal and alumina
Pack activator:	sodium fluoride
Pack temperature:	1850 F
Pack cycle:	16 hours
Pack pressure:	1 Torr

This pack was selected because it was available at Solar and is typical of the processes in current use. Oxidation life of this coating on D36 alloy foil is greater than 50 hours at 2000 F under thermal cycling conditions.

After joining and coating, one specimen of each joining process was metallurgically examined. Up to three additional specimens were subjected to 2000 F under thermal cycling conditions in dry air until failure or for 40 hours.

3.3 TEST RESULTS

Photomicrographs of two coated specimens prior to oxidation testing are shown Figure 9. The most significant item is the decrease in coating thickness near the re-entrant surface from two mils to essentially zero in the diffusion bonded specimen (Fig. 9A). The decrease in thickness is the result of lack of vapor transport in or near the unbonded faying surface. This problem is inherent in the pack coating process and can only be overcome by joint design and very rigid controls of the joining process.

The specimen (Fig. 9B) brazed with the Martin Ti-8.5Si alloy, shows adequate coverage at and near the re-entrant angle. This is a result of fillet formation and flow which eliminates any unbonded faying surface. Specimens brazed with Solar RGN15 and GE AS537 alloys also exhibited adequate coating coverage, and were similar in appearance to the Martin alloy. Welded specimens showed extreme coating thinning at the re-entrant surface due to the very acute re-entrant angle immediately preceding the welded nugget; however, the entire bond area appeared to be coated.

Oxidation tests at 2000 F showed that the brazed specimens gave the most consistent resistance to oxidation in the re-entrant area. Spot welded and diffusion bonded (titanium intermediate layer) specimens, in that order, had lower oxidation lines.

The diffusion bonded specimens, particularly the ones with zirconium and titanium intermediate alloy, appeared well coated. However, oxidation test results showed

that the entire faying surfaces were not well bonded. Considerably more development must be put into this new but extremely promising joining process before it can be considered for complex structure fabrication.

Photomicrographs of the Martin and GE brazed specimens after oxidation testing are shown in Figure 10. Both braze systems performed satisfactorily with no apparent oxidation of the braze areas after 40 hours of exposure at 2000 F. Slight reaction between the AS537 braze alloy and the silicide coating is apparent in Figure 10B, however, porosity or diffusion into the substrate is not apparent. The Ti-8.5 Si braze joint is essentially unchanged as a result of testing.

Additional laboratory work is continuing with the simple test panels used in this coating-joining compatibility study before more complicated panels are constructed. Efforts will be concentrated on compatibility studies of the silicide coating and braze alloy systems. Oxidation test temperatures will be extended to 2500 F. Work on spot-welded structures will be continued only if brazing compatibility problems cannot be resolved.

IV. CONCLUSIONS

It cannot be concluded that one of the silicide coatings is necessarily better than the other as the oxidation results would tend to indicate. If coating life is plotted against thickness (Fig. 11), the thickest coatings have the longest life. The type of coating that is needed for foil will have the oxidation resistance of the TAPCO coating, the thickness of the Chromizing coating on TZM, the elongation of the GT&E coatings, and a lower rate of interdiffusion than any of the coatings tested.

On specific coatings, it is possible to draw several conclusions. The high boron coatings such as Vought and GTC are not as protective at 2500 F as silicide coatings with more refractory modifiers. Aluminum-based coatings have high diffusion rates and are generally not as protective at 2500 F as the silicide coatings, particularly on the columbium-based alloys. The TAPCO coating exhibited outstanding oxidation resistance at temperatures up to 2500 F with and without prestrain, but also exhibited one of the highest rates of interdiffusion, the highest weight increase on coating, and the greatest thickness of any silicide coating.

Fusion welding and brazing appear to be the only satisfactory methods for joining foil structures prior to coating. Clean fusion welds are as readily protected as sheet material and at 2000 F several braze alloys can be adequately protected. No tests have been run on coated braze alloys above 2000 F but eutectic melting may limit the maximum-use temperature to considerably less than 2500 F.

Bonding methods, such as resistance welding, which do not completely bond the faying surface cannot be reliably coated by pack cementation processes due to throwing power limitation. Fusible coating, e.g., aluminum-tin, will probably protect this type of joint, but oxidation life is less than for the silicide coatings.

V. FUTURE WORK

Future work on this program will include:

- Improvement of the coating-substrate composite by reducing interdiffusion. Barrier layers of slow diffusion elements such as tungsten, rhenium, and tantalum will be interposed between the coating and the substrate.

- Creep and fatigue tests to determine the change in mechanical properties of coated foil with exposure to elevated temperatures, and an oxidizing environment.

- Coating-joining compatibility studies of the silicide coating and braze alloy systems, particularly those braze alloy systems that are titanium or vanadium based, e.g., Ti-8.5 Si, V-35Cb.

ACKNOWLEDGEMENT

The authors gratefully acknowledge the support extended to them by the Directorate of Materials and Processes, ASD under Contract AF33(657)-9443. They also wish to thank Captain Charles Lee and Lieutenant William Payne for their interest, helpful discussions, and permission to publish these data.

LIST OF FIGURES

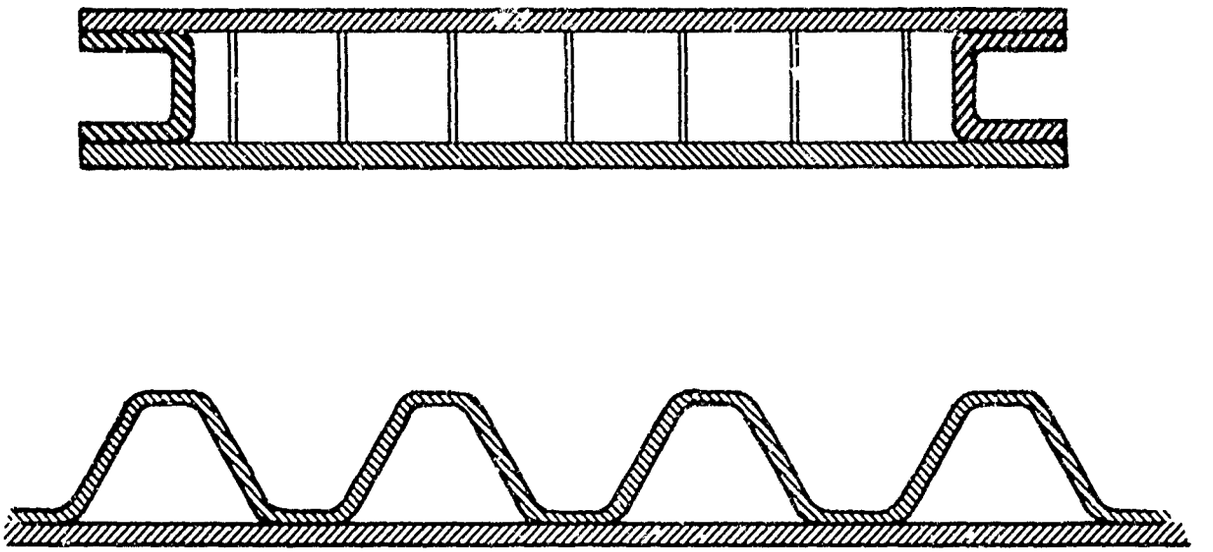

FIGURE 1. SCHEMATIC OF PROPOSED REFRACTORY METAL STRUCTURES

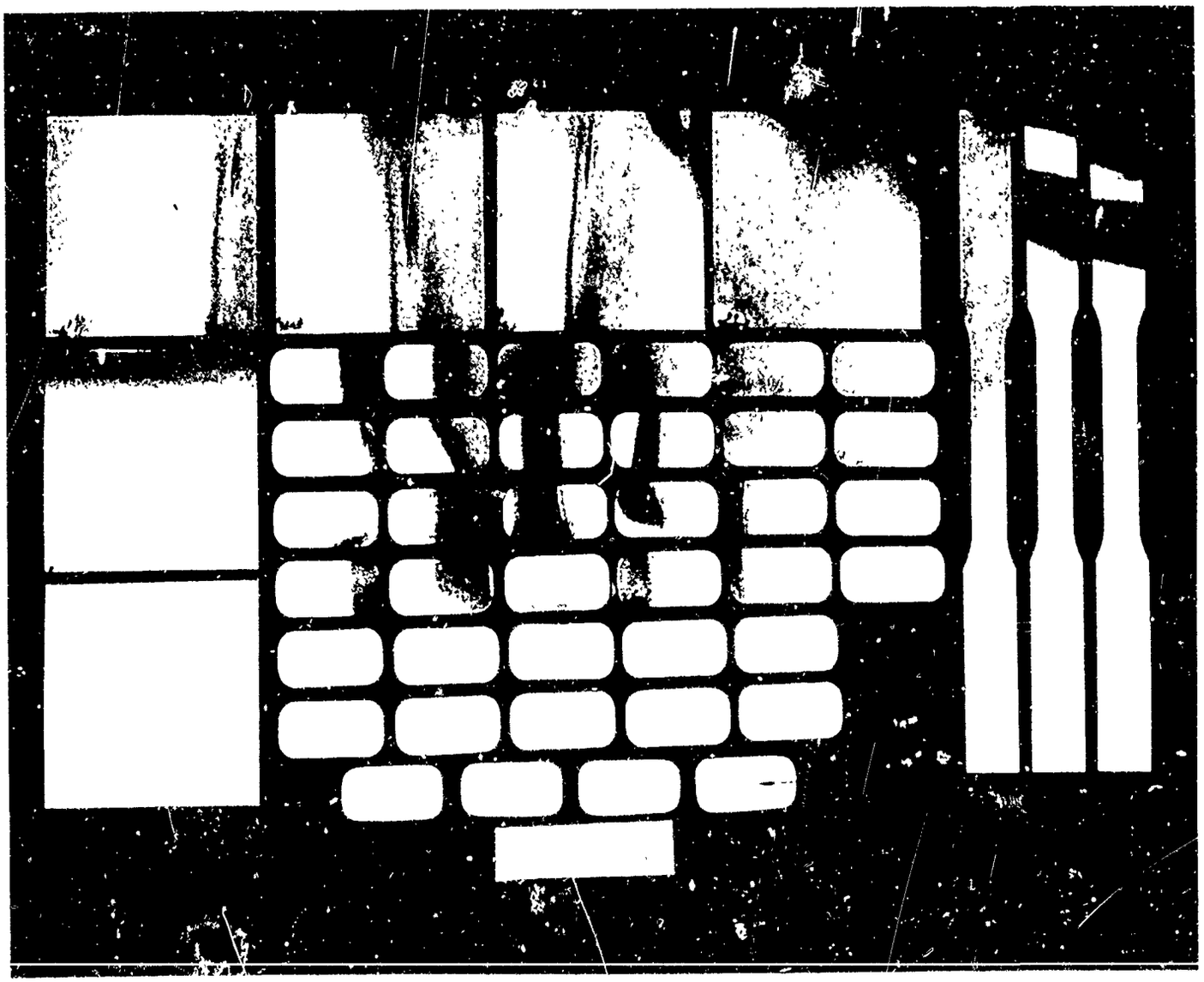

FIGURE 2. SET OF SCREENING TEST SPECIMENS BEFORE COATING

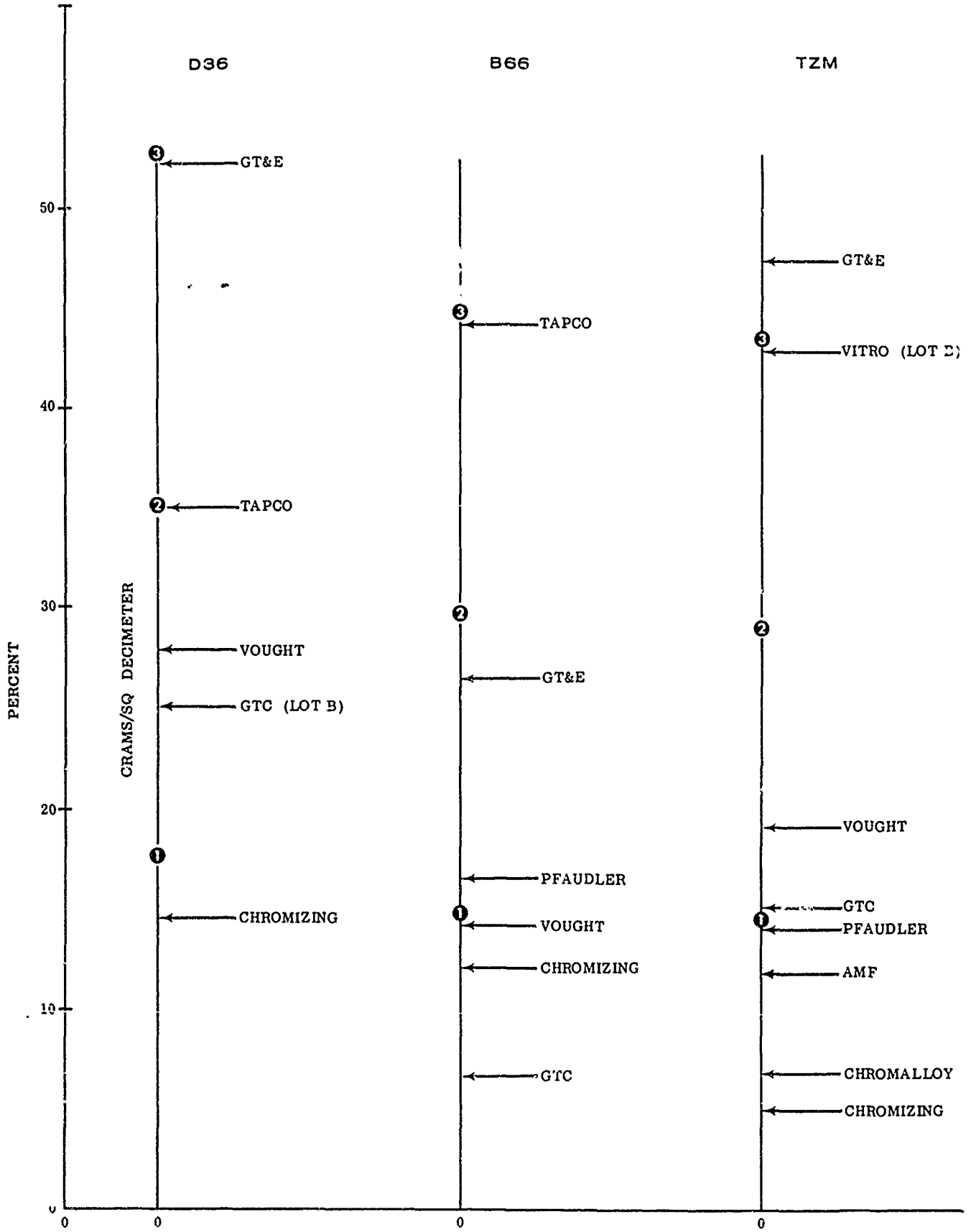

FIGURE 3. WEIGHT GAIN RESULTING FROM THE COATING PROCESS

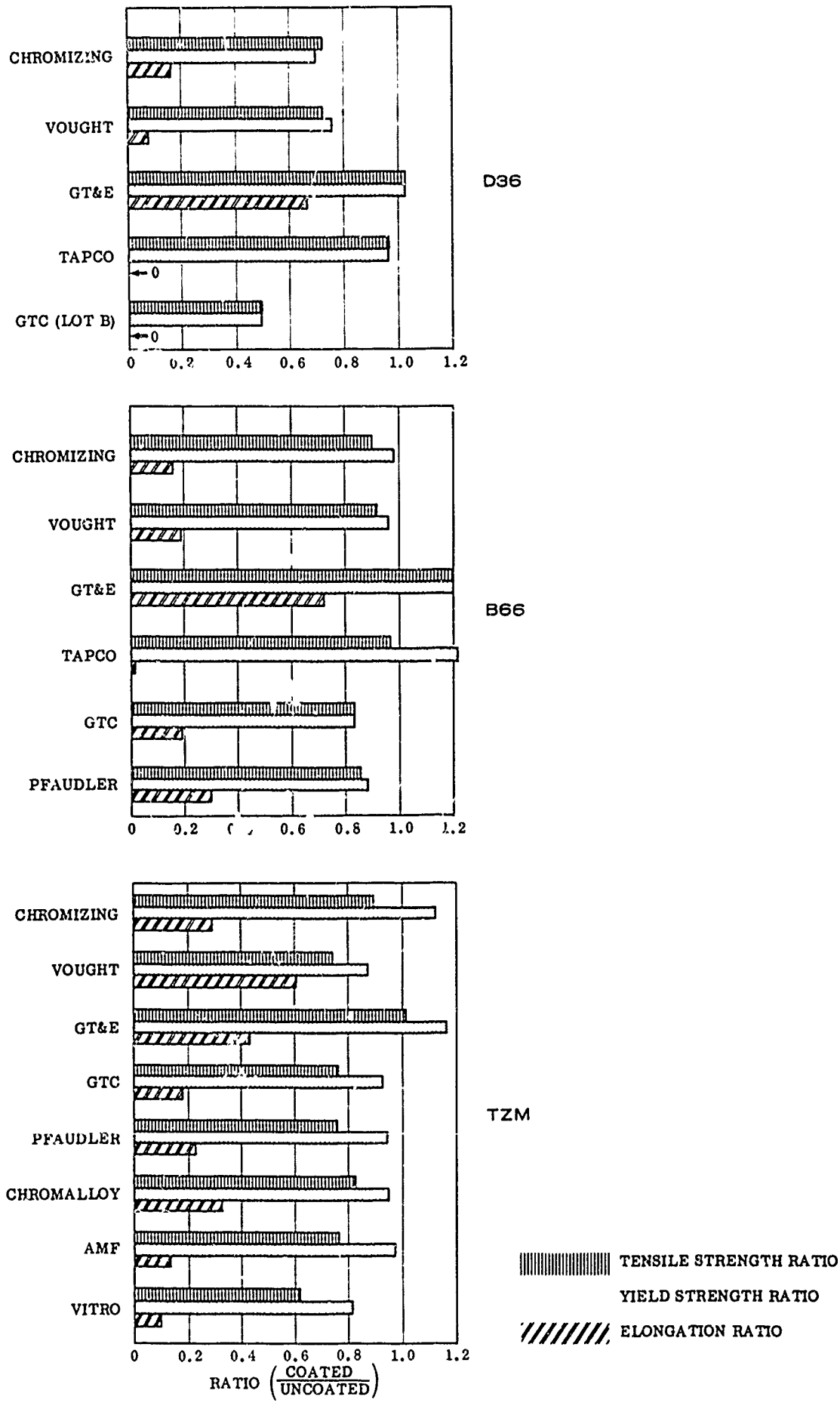

FIGURE 4. SUMMARY OF ROOM TEMPERATURE MECHANICAL PROPERTIES OF "AS COATED" D36, B66, TZM FOIL

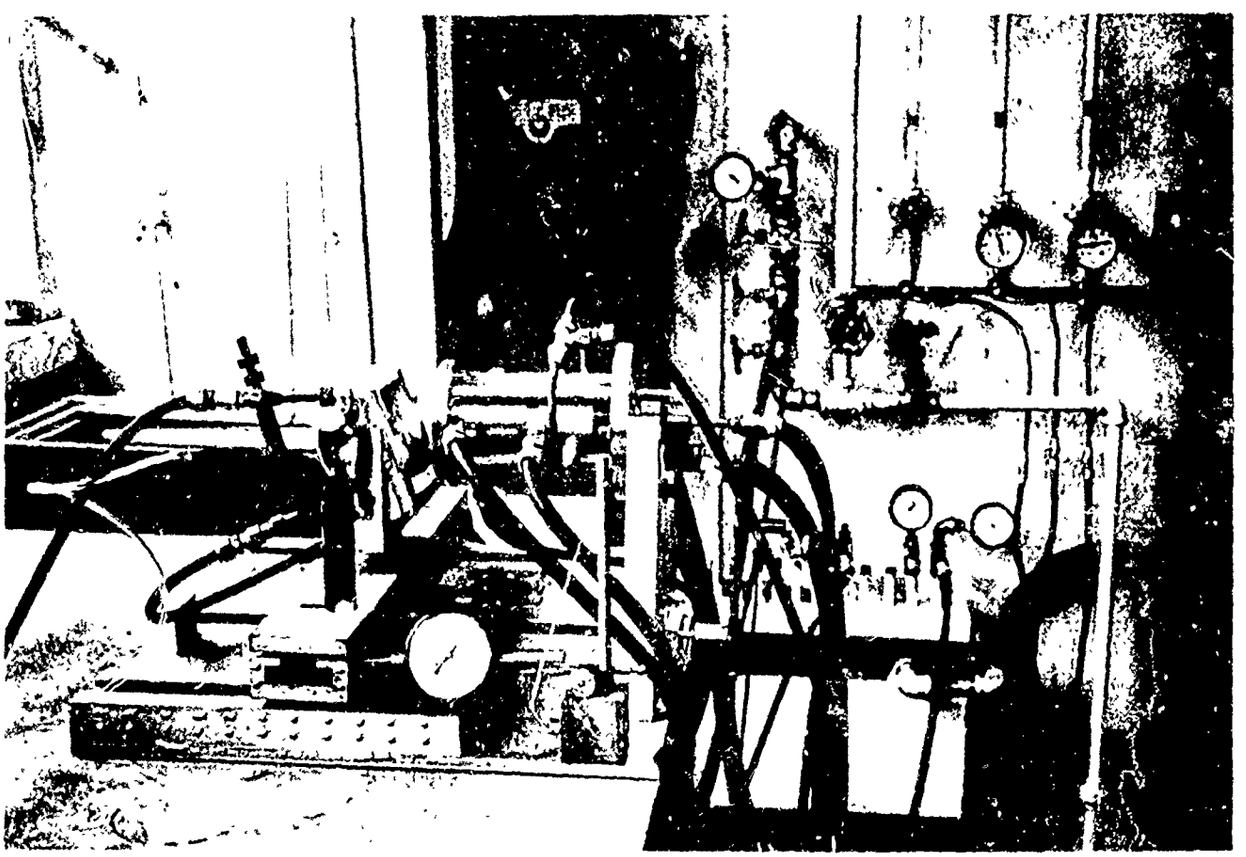

FIGURE 5. PLASMA TORCH TEST SETUP

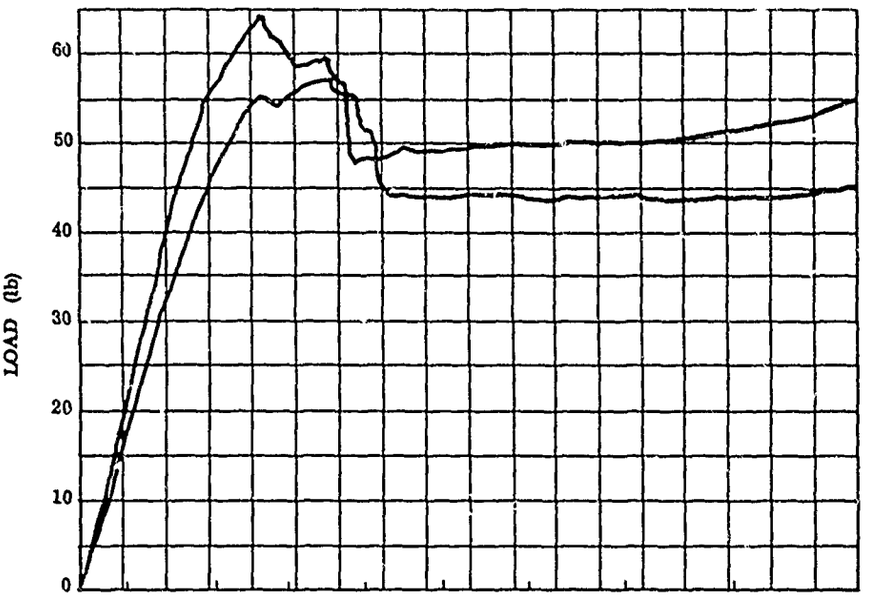

TYPICAL LOAD DEFLECTION CURVE OF A COATED ALLOY IN BEND TESTING

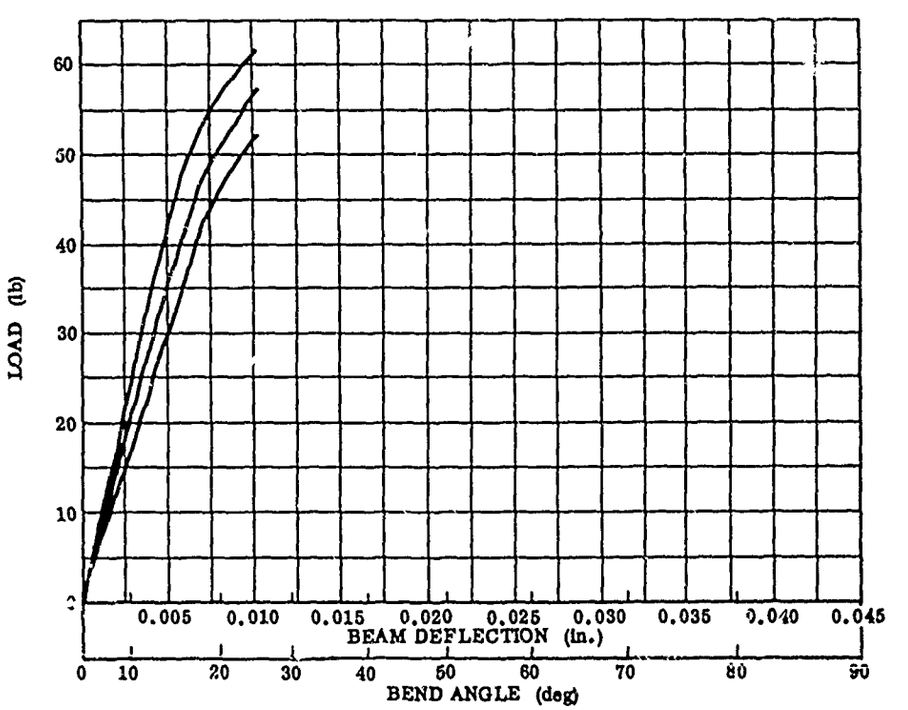

TYPICAL LOAD DEFLECTION CURVE FOR PRESTRAINING A COATED SPECIMEN

FIGURE 6. TYPICAL BEND TEST AND PRESTRAIN CURVES

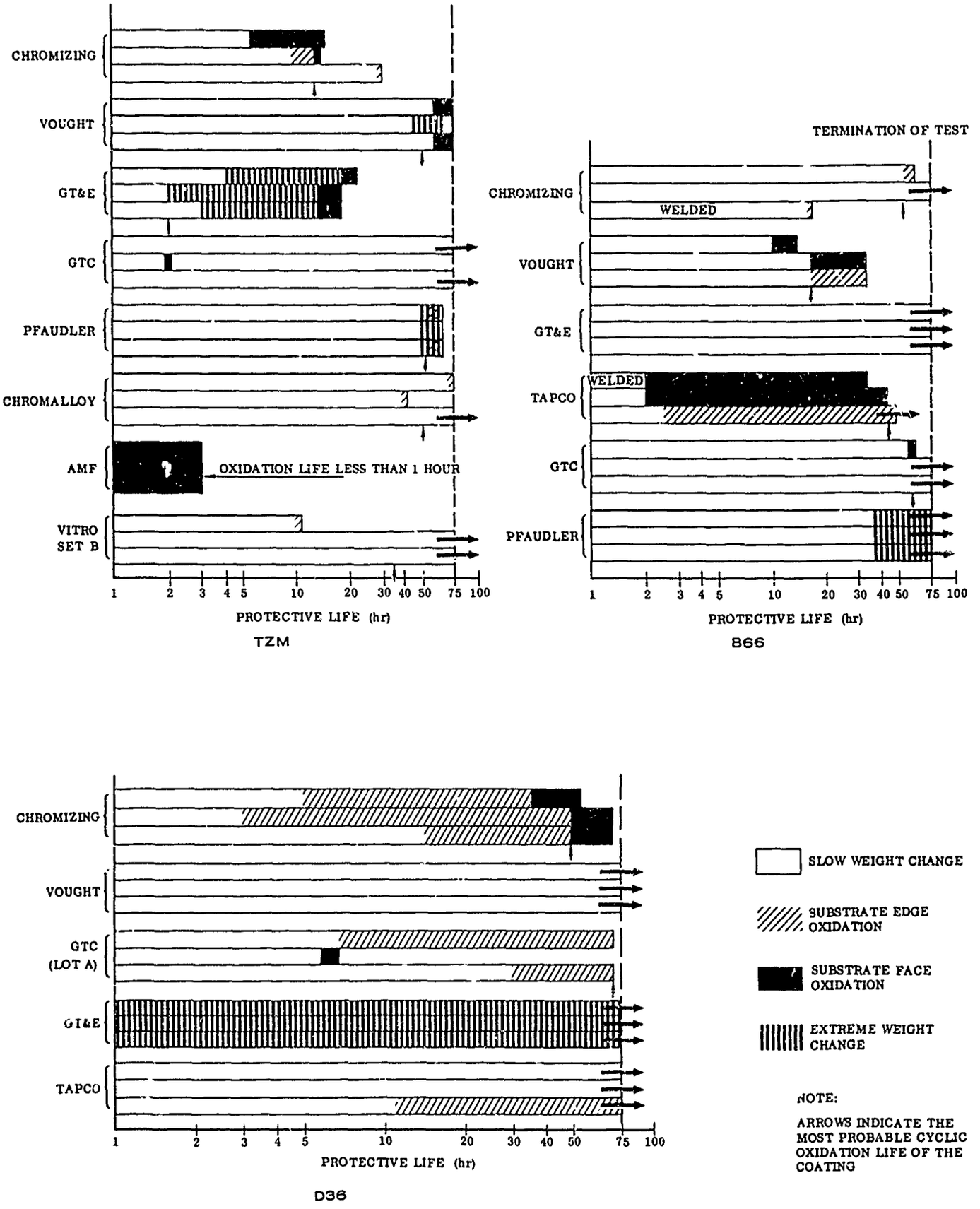

FIGURE 7. SUMMARY OF CYCLIC OXIDATION TESTS AT 2000 F
Coated D36, B66, and TZM Alloy

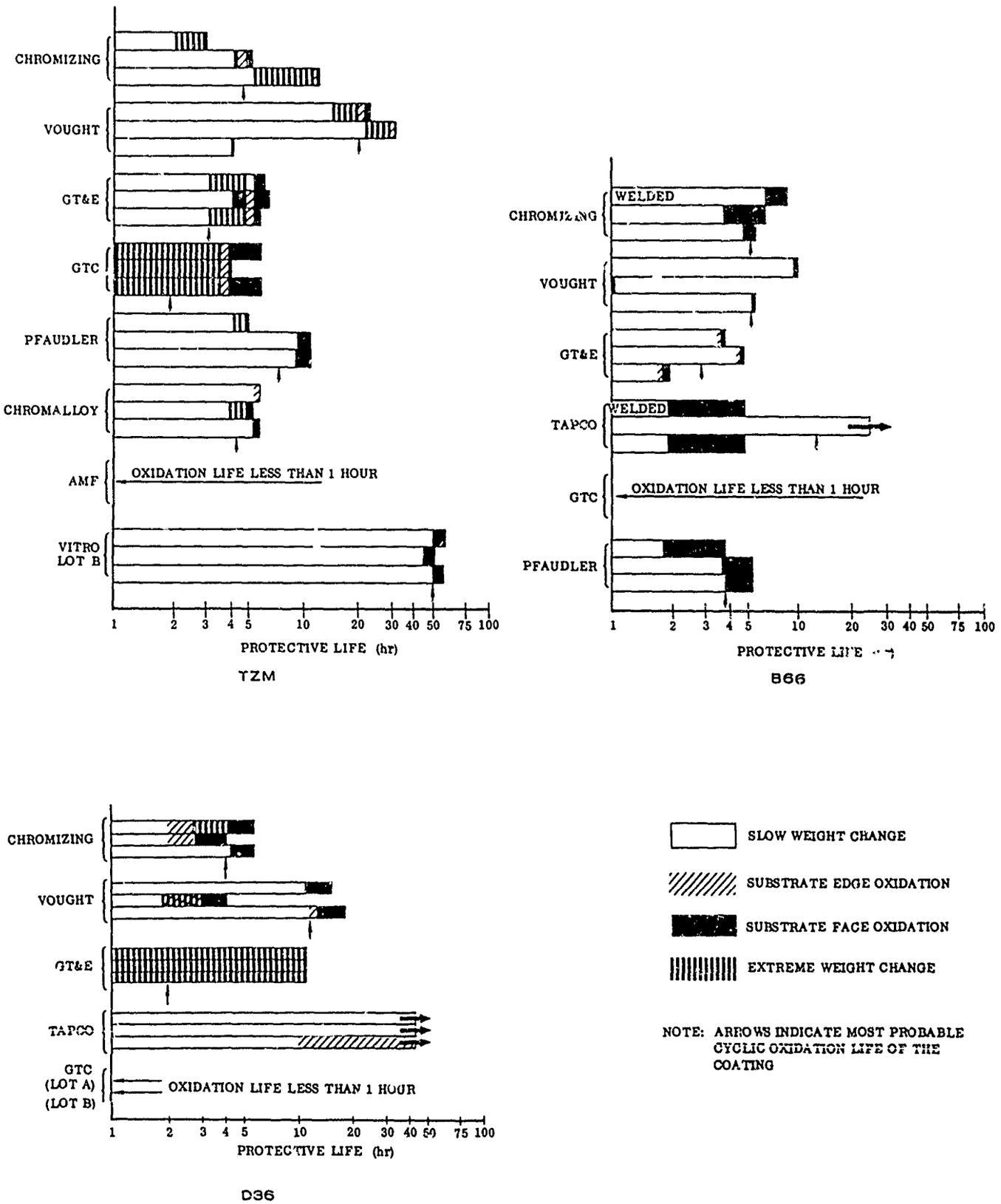

FIGURE 7. SUMMARY OF CYCLIC OXIDATION TESTS AT 2500 F; Coated D36, B66, and TZM Alloy

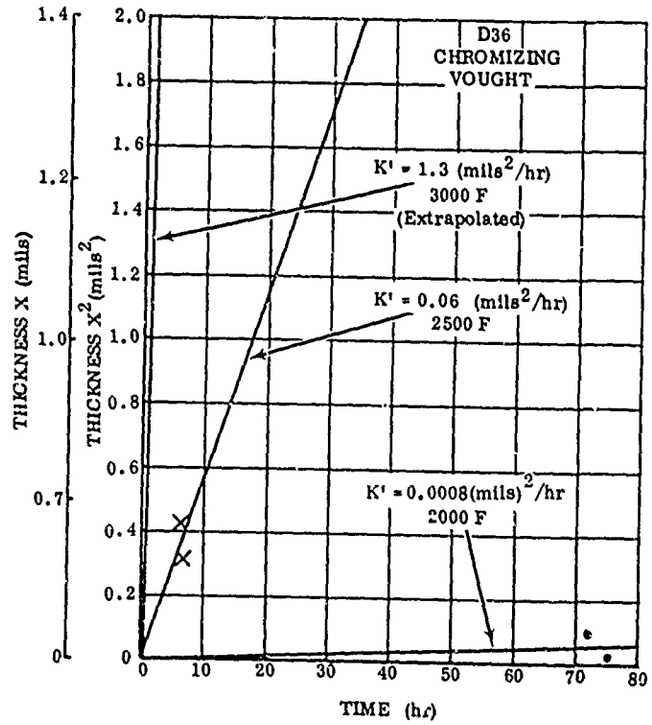

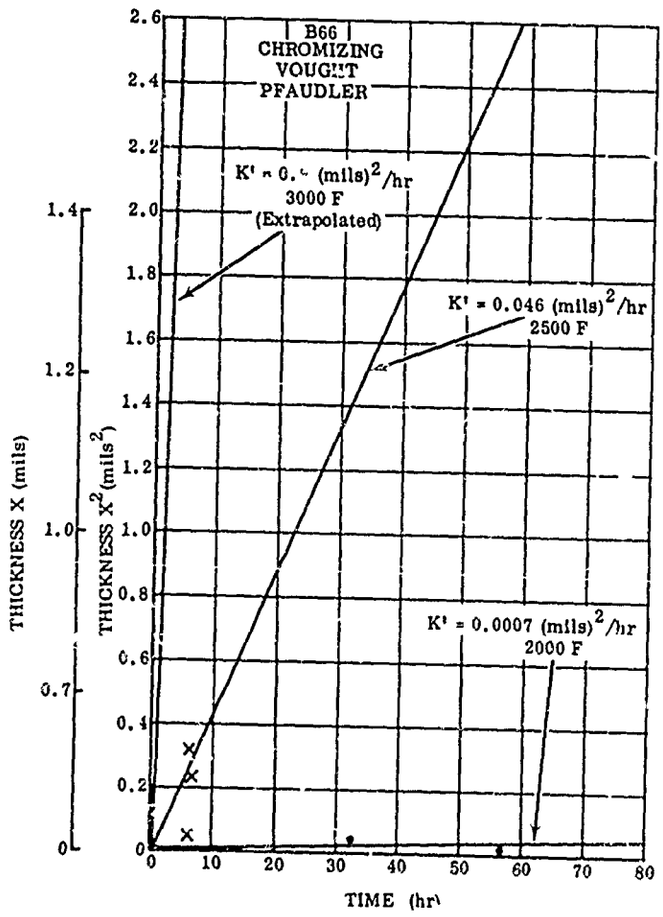

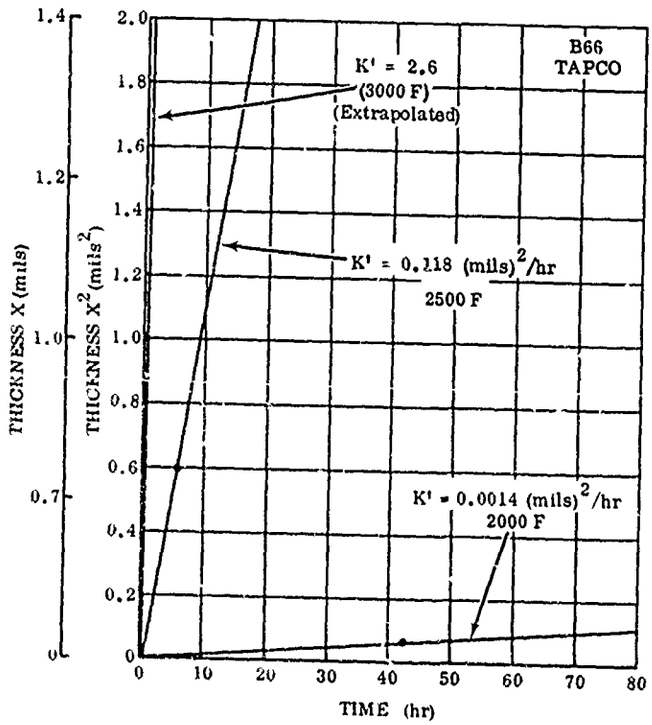

FIGURE 8. DIFFUSION OF COATINGS VERSUS TIME; D36, B66, and TZM Foil

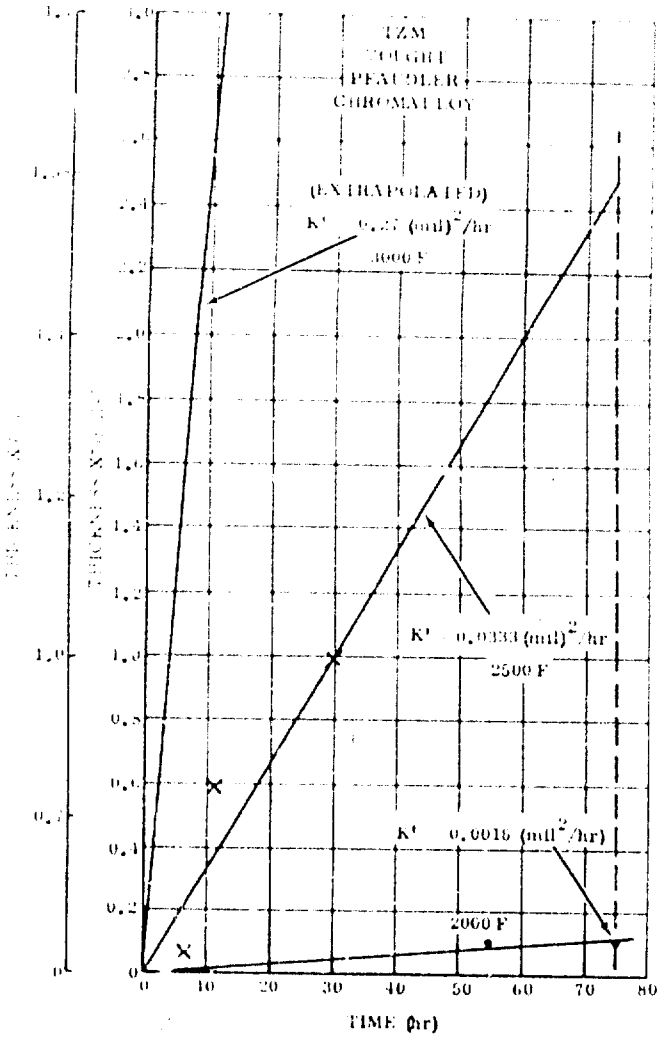

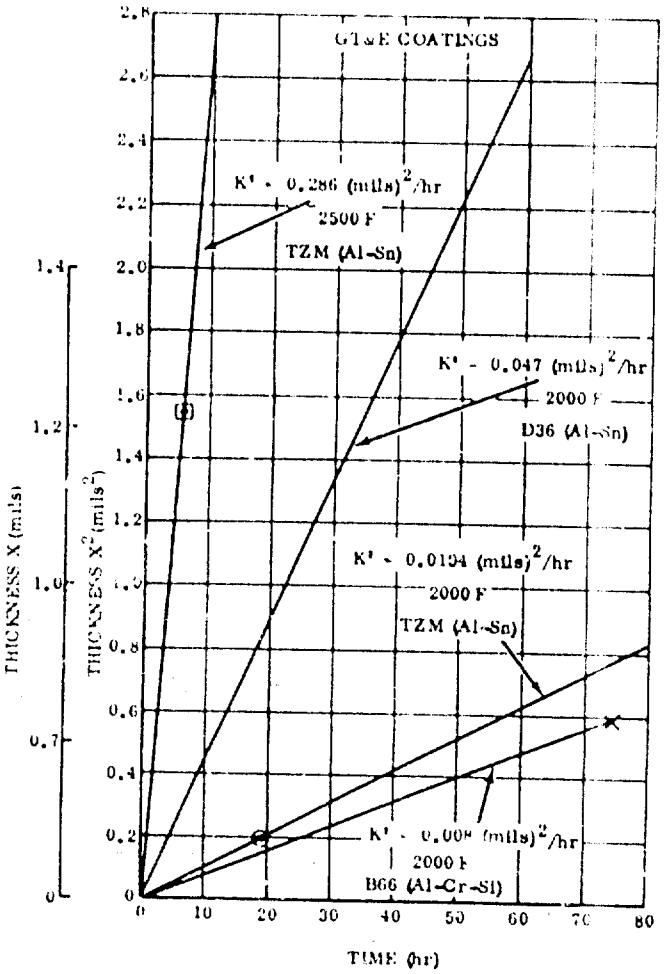

FIGURE 8. DIFFUSION OF COATINGS VERSUS TIME; D36, B66, and TZM Foil

A. DIFFUSION BONDED (NO INTERMEDIATE ALLOY)

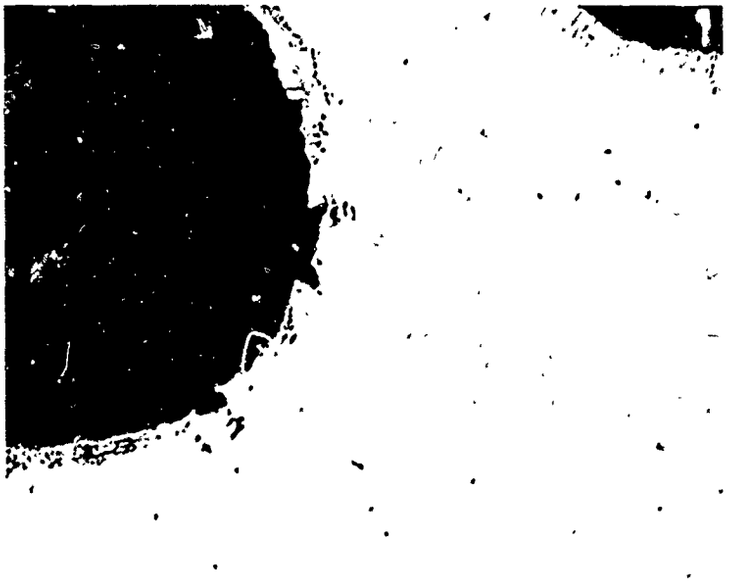

(MAG. 100X)

B. BRAZED-MARTIN Ti-8.5Si

FIGURE 9. MICROSTRUCTURE OF JOINED AND COATED D36 ALLOY "AS PROCESSED"

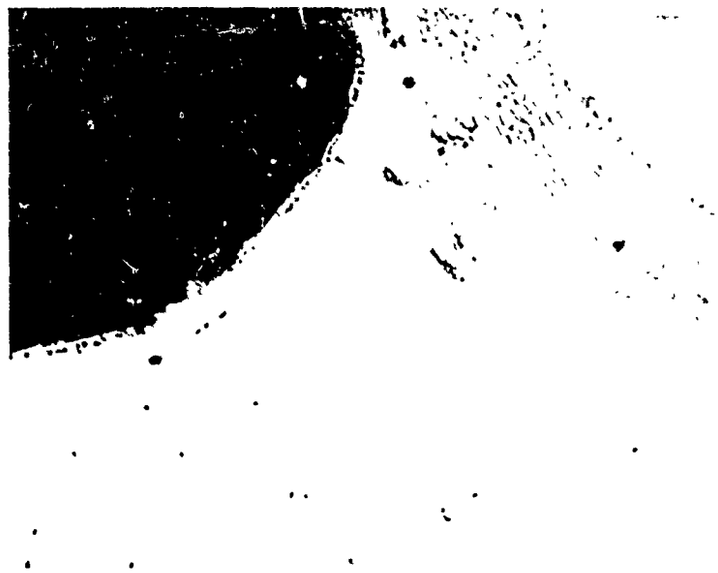

A. BRAZED-MARTIN Ti-8.5Si (40 HOURS)

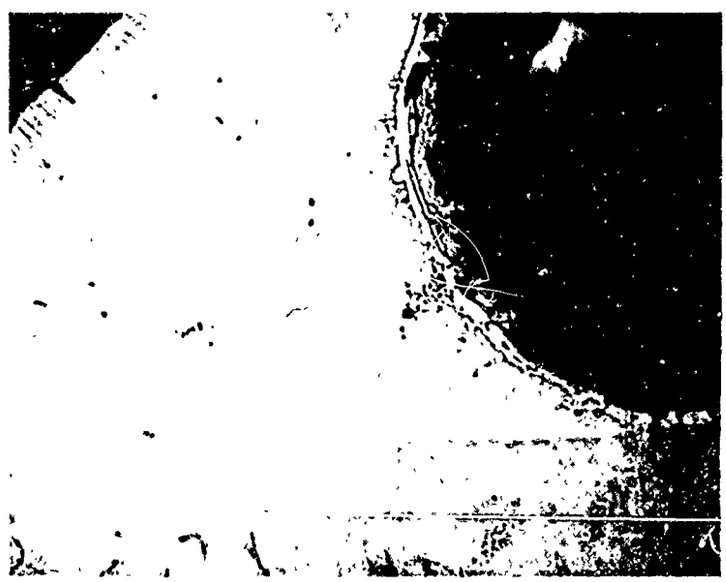

(MAG. 100X)

B. BRAZED-GE AS537 (40 HOURS)

FIGURE 10. MICROSTRUCTURE OF JOINED AND COATED D36 ALLOY AFTER 2000 F OXIDATION TEST

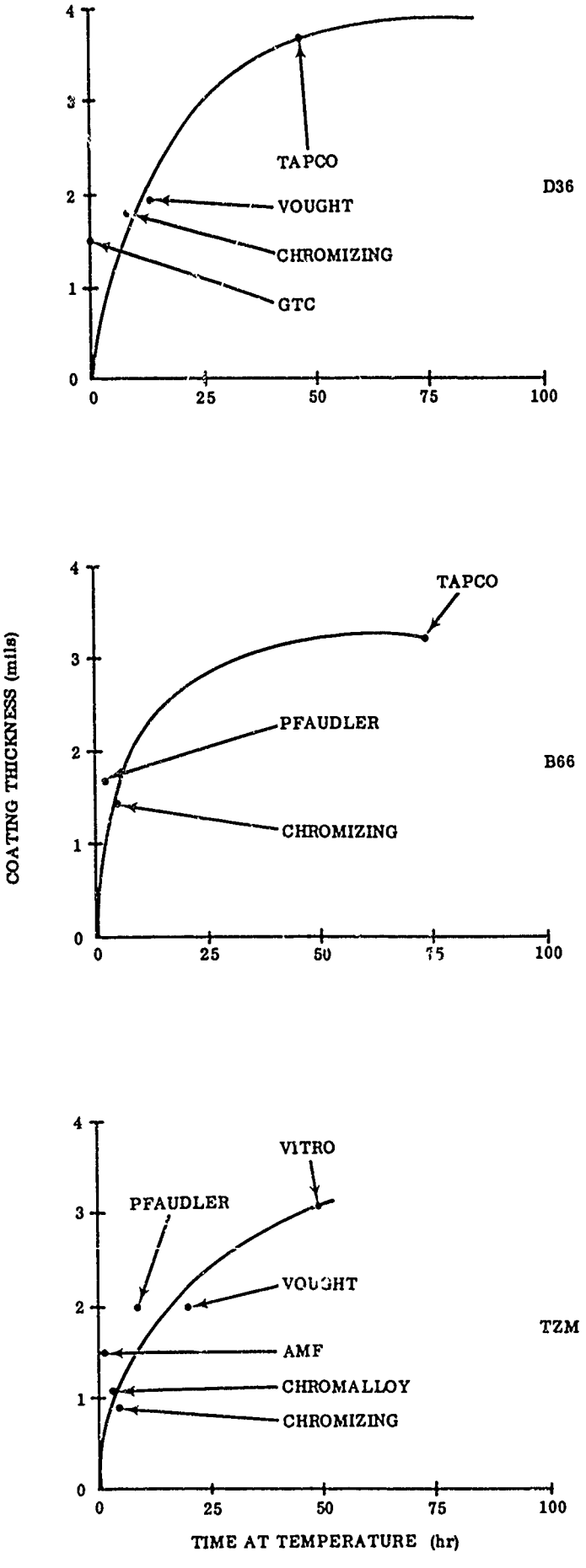

FIGURE 11. COATING THICKNESS VERSUS OXIDATION LIFE AT 2500 F; Silicide Coated D36, B66, and TZM Foil

LIST OF TABLES

TABLES

TABLE I

CHEMICAL ANALYSIS AND BASE-LINE MECHANICAL PROPERTIES
Uncoated D36, B66, and TZM Alloys

CHEMICAL ANALYSIS [1]

Alloy	Heat No.	Parts per Million				Weight Percent					
		C	N	O	H	C	Ti	Zr	Fe	Ni	Si
D36	36-164-01	130	67	80	10		10.2	5.0			
B66	DX-526	145	65	80	5						
TZM	980-A					0.029	0.43	0.072	0.0016	0.001	0.005

MECHANICAL PROPERTIES (R.T. LONGITUDINAL) [2]

Alloy	Heat No.	Average Tensile Strength (ksi)	Average 0.2% Yield Strength (ksi)	Average Elongation in 2.0 inches (%)
D36	36-164-01	80.0	75.0	19.5
B66	DX-526	102.5	78.8	24.5
TZM	980-A	126.6	91.3	7.3

(1) Chemical Analysis of D36 and B66 alloys by Metals & Controls, Inc.
Analysis of TZM alloy by Universal Cyclops.

(2) Solar Data (Ref. 2 and 3)

TABLE II

COATING VENDORS AND PROCESSES

Vendors	Alloys and Coating Type (Ref. 1) D36	B66	TZM
The Chromizing Company (Chromizing)	DURAK-KP Mod. silicide (max. temp. 1850 F)[1]	DURAK-KA Mod. silicide (max. temp. 1850 F)	DURAK-B Mod. silicide
Ling-Tempco-Vought Aeronautics Div. (Vought)	Mod. silicide 1st Coat - Si 2nd Coat - Cr-B (max. temp. 1950 F)	Mod. silicide (Same as D36) (max. temp. 2000 F)	Vought IV (Same as D36) (max. temp. 2000 F)
General Telephone & Electronics (GT&E)	Al-Sn-Ta Two Coats - Slurry (max. temp. 1900 F)	Ti, Al-Cr-Si Molten Dip (max. temp. 2000 F)	Sn-Al-Mo-Si Slurry (max. temp. 1900 F)
Thompson Ramo Wooldridge, Inc. TAPCO Group (TAPCO)	Mod. silicide 1st Coat - Cr-Ti 2nd Coat - Si (max. temp. 2300 F)	Mod. silicide Same as D36	----
General Technologies Corp. (GTC)	Mod. silicide 1st Coat Cr-Ti 2nd and 3rd Coat - Complex silicon, etc. pack. (max. temp. 2200 F)	Mod. silicide 1st - Ti 2nd - Cr-Ti 3rd - Complex silicon, etc. pack. (max. temp. 2100 F)	Mod. silicide Two-cycle pack (max. temp. 2000 F)
The Pfaudler Company (Pfaudler)	Process not applicable to this alloy.	Mod. silicide 1st Coat - Cr, etc. 2nd - Si, etc. (max. temp. 2050 F)	
Chromalloy Corporation (Chromalloy)	Process not applicable to this alloy.	----	W-3 Mod. silicide Two-cycle pack
Vitro Laboratories (Vitro)	----	----	Mod. silicide Electrophoretic deposition. Press. 10 to 20 ksi (max. temp. 2300 F)
American Machine & Foundry (AMF)	----	----	AMFKote 2 Mod. silicide Single-cycle pack (max. temp. 1975 F)

(1) Temperature in ( ) indicates maximum process temperature

TABLE III

RECEIVING INSPECTION TESTS ON
"AS COATED" D36, B66, AND TZM ALLOYS

Vendor	Weight (%)	Change (gm/dm^2)	Residual Substrate (mils)	Coating Thickness (mils)	Substrate Hardness (DPH)	Coating Hardness (DPH)
D36 Alloy			Avg. 5.75(1)		170	
Chromizing	14.2	0.85	4.66	1.78	191	1095
Vought	27.3	1.58	4.45	1.98	192	995
GT&E	51.6	2.98	5.04	5.14	170	19-426(3)
TAPCO	34.8	2.00	2.44	3.83	214	1290-424(3)
GTC (lot B)	24.8	1.44	4.20	1.55	249	1197
B66 Alloy			Avg. 6.6(1)		227	
Chromizing	11.8	0.79	5.30	1.50	233	1145
Vought	14.4	0.98	4.95	1.53	239	1225
GT&E	26.4	1.75	5.65	2.25	234	407-689(3)
TAPCO	44.3	2.93	4.65	3.30	228	1283-689(3)
GTC	6.5	0.43	3.60	2.60	239	909-1254(3)
Pfaudler	16.2	1.09	5.20	1.75	228	1006
TZM Alloy			Avg. 6.0(2)		331	
Chromizing	4.58	0.34	4.68	0.83	345	1486
Vought	18.9	1.40	3.84	2.05	324	1443
GT&E	46.5	3.66	5.50	3.15	317	28-625(3)
GTC	14.9	1.09	4.25	1.95	337	1345
Pfaudler	14.6	0.96	4.70	2.00	303	1185
Chromalloy	6.06	0.50	5.10	1.05	333	1345
Vitro (Lot B)	40.3	2.98	4.45	3.10	274	625-1225(3)
AMF	11.3	0.37	4.55	1.40	333	1564

(1) Thickness varied ± 0.0004 inch
(2) Thickness varied ± 0.0006 inch
(3) First figure is coating hardness, second figure is diffusion zone hardness.

TABLE IV

MECHANICAL PROPERTY TESTS ON
"AS COATED" D36, B66, AND TZM ALLOYS[4]

	Coating Vendor	YS (ksi)[1] (Min)	(Max)	TS (ksi)[1] (Min)	(Max)	Elong. (% in 2 inches) (Min)	(Max)	Bend Angle (deg)[2] 1	2
D36	Uncoated alloy	71	77	79	81	19	20	90	90
	Chromizing	49	57	53	62	2.5	4.5	90	90
	Vought	54	56	54	62	0	1.3	90	90
	GT&E	76	77	81	83	11.0	13.0	90	90
	TAPCO	64[3]	91[3]	64	91	0	0	90	90
	GTC (Lot B)	16	59[3]	16	59	0	0	36	45
B66	Uncoated alloy	76	82	100	105	24	25	90	90
	Chromizing	76	79	87	99	3.0	5.0	90	90
	Vought	73	80	91	102	3.5	6.0	44	45
	GT&E	92	98	120	125	17.0	19.0	90	90
	TAPCO	94	98	95	100	0.5	1.0	90	90
	GTC	64	68	82	90	6.5	7.5	42	48
	Pfaudler	66	72	83	91	4.0	5.0	42	53
TZM	Uncoated alloy	91	92	125	129	4.5	10.5	90	90
	Chromizing	89	124	102	131	0.5	3.0	90	90
	Vought	74	84	84	100	2.0	6.0	90	90
	GT&E	102	111	122	131	1.5	6.0	90	90
	GTC	76	92	85	106	0	2.5	90	90
	Pfaudler	80	91	90	102	1.5	2.0	90	90
	Chromalloy	85	96	90	107	0	3.5	90	90
	Vitro (Lot B)	56	89	56	103	0	2.5	90	90
	AMF	85	96	92	107	0	1.5	19	19

(1) Based on original uncoated cross section (nominal 0.006 inch foil)
(2) Angle at fracture or 90 degrees
(3) Failed before 0.2 percent offset
(4) Results are based on testing of three specimens of each alloy/coating combination

TABLE V

CYCLIC OXIDATION AFTER PRESTRAIN

Vendor	Prestrained Life 2000 F (hr)				Average Cyclic Life 2000 F (hr)	Prestrained Life 2500 F (hr)				Average Cyclic Life 2500 F (hr)
	Specimen No.					Specimen No.				
D36	1	2	3	Avg.		1	2	3	Avg.	
Chromizing	5	2	2	3	42	4	3	3	3.3	4.2
Vought	3	2	3	2.6	75+	2	4	2	2.6	11
GT&E	13	13	13	13	75+	2	2	2	2	2
TAPCO	24	26+	26+	26+(1)	75+	26+	22	25+	24.3+(1)	42+(1)
B66										
Chromizing	75	70	70	72	68	10	4	4	6.0	6.0
Vought	16	20	20	19	15	1	1	3	1.6	6.0
GT&E	11	7	22	13	74+	3	9	--	6.0	3.0
TAPCO	75+	75+	75+	75+	46+	75+	75+	75+	75+	13+
Pfaudler	75+	75+	--	75+	75+	2	7	--	4.5	4.0
TZM										
Chromizing	1	1	1	1	14	1	1	1	1	3.2
Vought	2	3	1	2	63	9	4	1	4.6	18.3
GT&E	6	6	5	5.6	19	6	6	4	5.3	5
GTC	9	4	21	11	75	2	1	2	1.6	2
Pfaudler	1	1	1	1	59	1	1	1	1	6.6
Chromalloy	1	1	1	1	63	1	1	1	1	4.3
Vitro Lot (B)(2)					75					50
AMF(2)					1					1

(1) Removed from test for inclusion in report.
(2) Prestrained oxidation test not performed. AMF specimens exhibited low oxidation protection. Insufficient specimens from Vitro.

TABLE VI

SUMMARY OF PLASMA TORCH OXIDATION TESTS

	2000 F (1)	2500 F (2)
D36		
Chromizing	Failed (pest)	Failed (pest)
Vought	Passed	Passed
GT&E	Passed	Failed (burned through)
TAPCO	Passed	Passed
GTC	Passed	Failed (burned through)
B66		
Chromizing	Passed	Passed (some pits)
Vought	Passed	Failed (2 of 3 specimens burned through)
GT&E	Passed	Failed (burned through)
TAPCO	Passed	Passed
GTC	Passed	Failed (burned through)
Pfaudler	Passed	Passed
TZM		
Chromizing	Passed	Passed
Vought	Passed	Passed
GT&E	Passed	Passed
GTC	Passed	Passed
Pfaudler	Passed	Passed
Chromalloy	Passed	Failed (small pinhole)
AMF	Passed	Failed (number of pinholes; also uncoated edge)

(1) Test duration: four 15-minute cycles.
(2) Test duration: eight 15-minute cycles.

TABLE VII

BEND TEST AFTER STATIC OXIDATION

	2000 F (1)				2500 F (1)			
	Test Hours	Specimens			Test Hours	Specimens		
		1	2	3		1	2	3
		Bend angle (deg)				Bend angle (deg)		
D36								
Chromizing	42	90	90	90	7.0	90	90	
Vought	64	90	90	90	7.0	90	90	
GT&E	64	20	28	30	1.7	90	90	
TAPCO	64	90	90	90	7.0	20	20	
B66								
Chromizing	22	90	90	90	4.5	90	90	90
Vought	32	90	90	90	4.5	90	90	90
GT&E	55	90	90	90	1.7	82	85	62
TAPCO	29	90	90	90	1.7	90	90	90
GTC	55	90	90	60	(2)			
Pfaudler	30	90	90	90	1.7	90	90	90
TZM								
Chromizing	9	30	90	20	5	68	90	90
Vought	38	90	19	15	17.6	80	72	76
GT&E	15	90	90	90	1.7	90	90	90
GTC	56	18	19	18	2.3	18	21	90
Pfaudler	30	19	90	21	6.8	90	90	90
Chromalloy	36	12	22	21	2.5	19	90	79
Vitro (Lot B)	35 (3)	90	90	90	50 (3)	31	34	40

(1) 90 degrees or angle at fracture
(2) No protection at 2500 F during cyclic oxidation test.
GTC specimens not included in 2500 F static oxidation tests.
(3) Bend tests performed on cyclic oxidation test specimens.

TABLE VIII

SUBSTRATE HARDNESS AFTER OXIDATION TESTS

		2000 F		2500 F	
		Test Hours	Hardness (DPH)	Test Hours	Hardness (DPH)
D36	Uncoated	0	170	0	170
	Chrominizing	72	203	7	220
	Vought	75	207	7 and 14	336 and 233
	GT&E	75	288	11	No substrate
	TAPCO	75	207	7 and 42	429 and 396
	GTC (Lot B)	(2)	(2)	1	(1)
B66	Uncoated	0	227	0	227
	Chromizing	57	234	6	219
	Vought	33	225	6	227
	GT&E	74	249	2	249
	TAPCO	43	228	5	233
	GTC	75	232	1	(1)
	Pfaudler	75	232	6	232
TZM	Uncoated	0	331	0	331
	Chromizing	15	324	6	244
	Vought	75	337	31	239
	GT&E	18	336	6	303
	GTC	75	336	6	232
	Pfaudler	59	336	11	227
	Chromalloy	72	336	7	290
	Vitro (Lot B)	75	(2)	56	249
	AMF	3	303	1	290

(1) Specimens melted during test
(2) Tests not completed in time for inclusion in report

DEVELOPMENT AND EVALUATION OF REFRACTORY METAL COATINGS

R. L. HALISE

S. C. COLBURN

R. E. MIHALCO

General Dynamics

Pomona, California

I. INTRODUCTION

During the past year General Dynamics/Pomona has been activily engaged in the development and evaluation of refractory metal coatings. Three principal areas have been investigated; namely (1) the development of silicide coatings for columbium and tantalum, (2) elevated temperature creep testing of coated 0.5 Ti-Mo alloys, and (3) performance tests on coated FS 82 columbium alloys.

II. COATING DEVELOPMENT

All specimens in this investigation were coated using the pack cementation process. In this process, the metal substrate to be coated was placed in a pack of 80 percent - 325 mesh silicon and 20 percent sodium fluoride and heated in a furnace under a controlled atmosphere. This caused silicon to diffuse into the substrate material with the final result being a thin silicide layer.

The specimens used for preliminary evaluation were 1/4" diameter, columbium and tantalum rods approximately one inch long. These one inch specimens had one side ground flat for more accurate readings with the x-ray diffraction unit. All specimens were placed in fireclay boats approximately two inches long and one half inch deep. The boats were then filled with the pack as described above. The specimens used for high temperature oxidation tests were 1/4 inch diameter columbium and tantalum rods 9 1/2 inches long. The sodium fluoride in the pack promotes diffusion, in a reducing atmosphere, in the following manner:

$$4\,NaF + Si \rightarrow SiF_4 + 4Na$$

$$SiF_4 + 2H_2 \rightarrow Si + 4\,HF$$

Apparently Si in this form can be more readily diffused into the metal than Si added as the pack.

The fireclay boats containing the specimens and pack were then placed in a Burrell muffle furnace that had been purged with argon gas. The muffle tubes were provided with tightly fitting ends so that a closed system could be maintained. After the specimens were placed in the furnace, the argon was allowed to flow for a few minutes to insure the exit of all oxygen, Hydrogen was then allowed to flow into the muffle furnace at different gas flow rates.

A large number of variables exist in this type of system. Those which were investigated during this period were:

1. Furnace temperature
2. Time at temperature
3. Furnace atmosphere
4. Effect of adding SiF_4 gas

During this portion of the investigation several short tantalum and columbium specimens were coated varying the furnace atmosphere. SiF_4 gas was introduced to see what effect it would have on the coating. It was through that the reaction of this gas with hydrogen would produce silicon metal that would diffuse more readily into the substrate. This did not occur as evidenced by visual examination. It was decided to use just hydrogen gas as an atmosphere. Furnace temperature and time at temperature was then investigated. Temperatures varied from 1850°F to 2200°F and time at temperature was varied from 1/2 hour to 4 hours.

Using x-ray diffraction the composition of the diffused layer was determined. Figures 1, 2 and 3 show an x-ray diffraction pattern and photomicrographs of a columbium silicide coating. Figures 4, 5 and 6 show an x-ray diffraction pattern and a photo micrograph of tantalum samples. From these preliminary

screening tests and x-ray diffraction patterns of the columbium coating, the optimum coating conditions were determined.

They are:

Furnace temperature: 2100°F

Time at temperature: 1 Hour

Hydrogen gas flow: 4 Cubic ft/hr.

The x-ray diffraction patterns for the tantalum coatings were almost identical so that the optimum coating conditions could not be determined. It was decided to coat long specimens with a wide range of variation in furnace temperature and time at temperature for testing in the high temperature test unit.

Cyclic oxidation testing was performed on coated specimens 1/4 inch in diameter and 9 1/2 inches long in the General Dynamics developed high temperature resistance heated test unit. The ends of the coated specimens were sand blasted to bare the substrate metal so that electrical contact could be made with the grips of the test unit. The specimens were heated to 2980°F and held for 5 minutes and cooled to room temperature. The columbium specimens which were coated using the optimum coating conditions withstood four of these cycles in still air without failure. The coated tantalum specimens were tested under the same cyclic conditions for two cycles in still air. After testing they were visually inspected for oxide and reweighed to obtain a weight gain due to the oxide formation. There was no apparent correlation between weight gain and the ability of a coating to afford protection to the substrate. It is felt that weight gain may occur in both protective and non-protective coating systems in the following manner.

In a good coating the silicide is oxidized and forms a protection glass according to the equations:

$$4TaSi_2 + 13O_2 \rightarrow 2Ta_2O_5 + 8SiO_2$$

$$4Ta_5Si_3 + 37O_2 \rightarrow 10Ta_2O_5 + 12SiO_2$$

Some of the Ta_2O_5 is dissolved in the silica while some is volatilized. The net result is that the tantalum substrate is protected by the silicate glass, while a weight gain has taken place due to the oxidation mechanism.

On the other hand, in a non-protective coating, weight gain may also occur. If there are cracks in the coating, or if there is insufficient silicon present in the coating to form a protective glass, the substrate will be oxidized as follows:

$$4Ta + 3O_2 \rightarrow 2Ta_2O_3$$

Under prolonged exposures to elevated temperatures the oxide will be lost by volatilization with a resulting weight loss. However, for relatively short exposures it can be seen that weight gain has taken place in both protective and non-protective coatings.

The coating that appeared best was coated using the following conditions:

Furnace temperature	1950°F
Time at temperature	3 hours
Hydrogen gas flow	4 Cubic ft./hr.

Temperature measurements at elevated temperatures are difficult to accurately determine. The optical pyrometer, which was used during this investigation, compares the color of a heated tungsten filament to the color of the radient heat from the specimen. To obtain a true temperature of the specimen from the optical pyrometer it must be assumed that the emissivity of the specimen is that of a black body or 1.0. Since most silicide coatings reported in the literature have emissivities in the range of 0.7 to 0.8 an assumed emissivity of 0.78 was used

for temperature corrections. Based on this assumption the measured temperature of 1590°C was adjusted to 1638°C or 2980°F. No correction was made for the reduction in radiation through the view port in the test facility. It can be seen that several assumptions were made in arriving at the temperature at which the specimens were tested, thus these figures must be taken as only an approximation of the true temperature.

III. ELEVATED TEMPERATURE CREEP TESTING OF COATED 0.5 Ti-Mo ALLOY

The purpose of this test program was to evaluate the creep rupture properties at 2800°F of coated 0.5 Ti-Mo alloy specimens. A total of twelve specimens were tested, four coated with the Thermonet T-55 coating and eight coated with the Pfaudler PFR-6 coating. All tests were conducted in air under conditions of creep to rupture under constant load.

The specimens were 8 1/2 to 10 1/2 inches long, approximately 0.450 inch wide, and the thickness varied from 0.040 to 0.069 inch. To assure good electrical contact for the resistance heated test unit and sufficient area to support a tensile load, approximately 1 1/2 inches was sand blasted from each end of the specimens. The tests were performed on the General Dynamics/Pomona developed elevated temperature testing equipment. With this unit an AC current heats the specimen to temperature at pre-selected rates which can be controlled by varying the power input. A small preload is applied, the specimen is heated to the desired temperature, and the two inch gauge length extensometer is zeroed to eliminate the effects of thermal expansion. The specimen is then loaded hydraulically through a servomechanism to a pre-selected load to give a specified stress. Records of load vs. time and stress vs. time are then recorded on a Sanborn Recorder. Figure 7 is a photograph of the test unit itself during a typical test.

Temperature measurements were made on the coated specimens using a Pyro Micro Optical Pyrometer made by the Pyrometer Instrument Company. The measurements made assumed an emissivity of .90 for both types of coatings.

All twelve specimens were creep rupture tested at 2800°F. The tests were performed in the following sequence. After the specimen was inserted in the test equipment, a preload of fifteen pounds was applied. The specimen was then heated to 2800°F in fifteen seconds, held for fifteen seconds, the extensometer zeroed, and then the load applied in .2 second. Since no set up specimens were available, the first stress level selected was 5700 psi, which was somewhat below the expected stress of 6000 psi, to produce rupture in thirty minutes. The stress levels selected for subsequent tests were then based on the results of the preceeding tests. After the application of the load, strain time or creep deformation was measured on the Sanborn Recorder for thirty minutes or rupture, whichever came first. If the specimen did not rupture in thirty minutes, the load was increased to a higher stress level, the extensometer zeroed, and creep deformation was then measured starting from zero time, and zero deformation. If more than one stress level was used on a single specimen, the subsequent test specimens and results are labeled a, b, c, etc. The percent deformation reported is that portion based on creep only, and does not include the strain due to thermal expansion or the strain due to the initial application of the load.

The results of the tests are tabulated in Tables I through III. For those specimens which did not rupture in thirty minutes and were subject to further testing at higher stress levels, the percent deformation would be accumulative. For example, the total creep deformation before failure of the coating on specimen 14 would be 4.60% + 2.30%, or a total of 6.90%. For specimen 14 the total deformation would be 6.70%, etc.

Footnotes in Tables I through III indicate the time of initial coating failure and the time to rupture. It is interesting to note that specimens 13, 14, 15, 2 and 20 were quite uniform in thickness over their length and all broke in the middle of the gauge section. Specimens 9 and 10 broke at the edge of the gauge length while specimens 3, 4, 7 and 8 all of which exhibited a pronounced thickness taper from end to end, broke outside the extensometer.

Both coatings appear in general to have the ability to protect the 0.5 Ti-Mo alloy at 2800°F for periods of over thirty minutes. The coatings tested are capable of creep deformation of from two to ten percent before coating failure. The typical deformation obtained before coating failure is four to six percent. In general, a stress level of 6000 psi at 2800°F is not sufficient to produce rupture within thirty minutes, while stress levels of 6800 to 7400 psi are sufficient to produce rupture within the range of five to thirty minutes.

IV. PERFORMANCE TESTS ON COATED FS 82 COLUMBIUM ALLOY

Table 4 lists the results of the preliminary tests performed on the coated FS 82 columbium alloy. These tests evaluated coatings by four different companies; General Electric, Sylcor, Pfaudler, and TRW. With the exception of specimen T3, which had a chipped coating before testing, all of the specimens appeared to hold up equally as well before the load was applied. The test conditions used were as follows:

Heating Rate	Heat to temperature in 10 sec.
Soaking Time	10 sec.
Strain Rate	as indicated
Atmosphere	Air

Temperature measurements were made with an optical pyrometer using the following emissivities:

General Electric	.70
Sylcor	.55
TRW	.85
Pfaudler	.88

The limited test results indicate the following rating for the coatings tested:

1 - General Electric LB-2

2 - Sylcor Al-Sn

3 - Pfaudler

4 - TRW Cr-Ti-Si

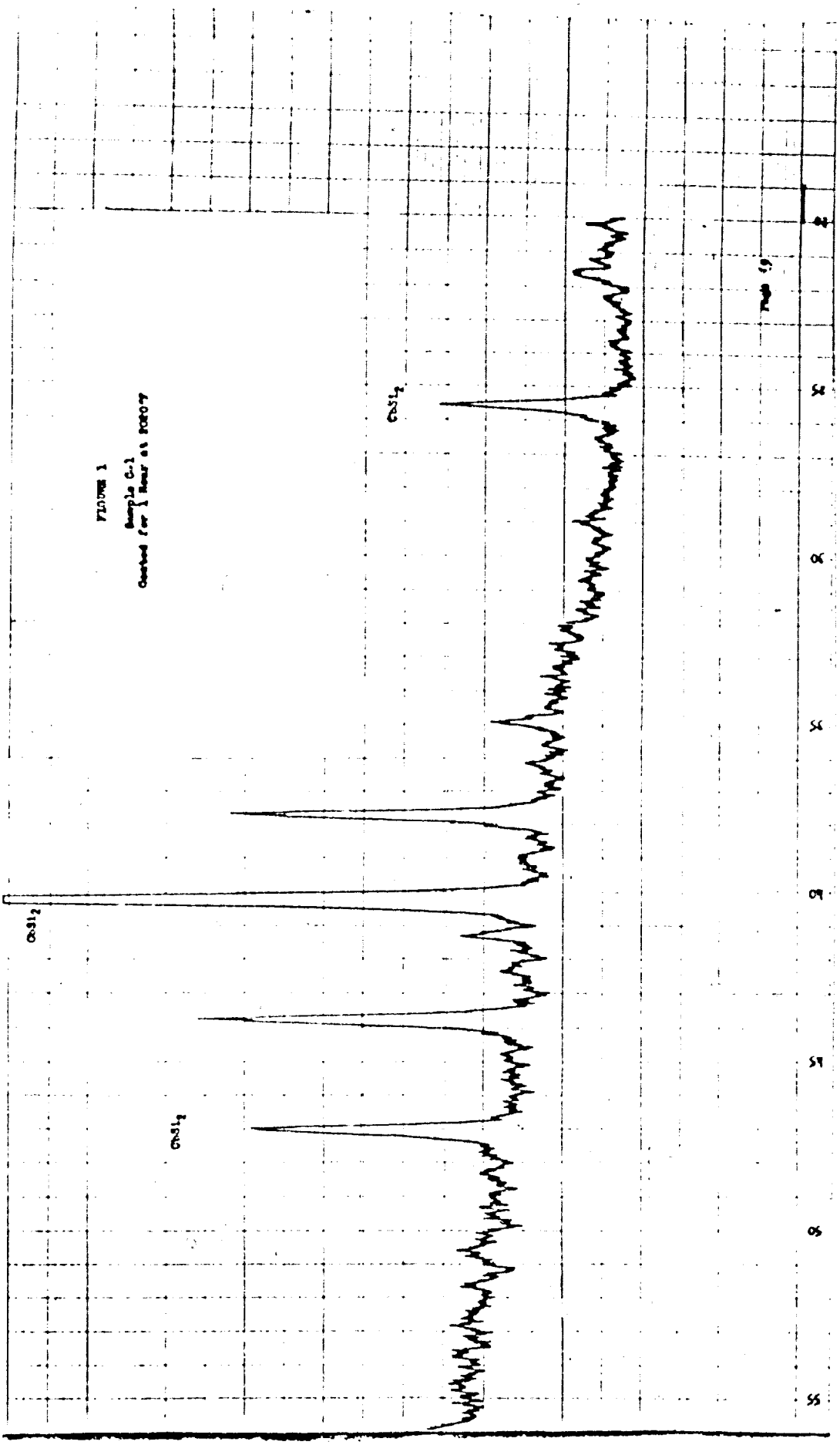
FIGURE 1
Sample C-1
Cooked for 1 Hour at 800°F
$CaSi_2$
$CaSi_2$
$CaSi_2$

FIGURE 2

Specimen A-1, Coated for 1 Hour at
2110°F for 1 Hour - 250X

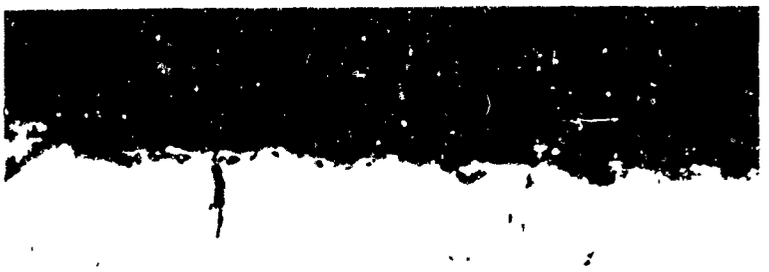

FIGURE 3

Specimen 2-44, Coated for 2 hours
at 2110°F - 250X

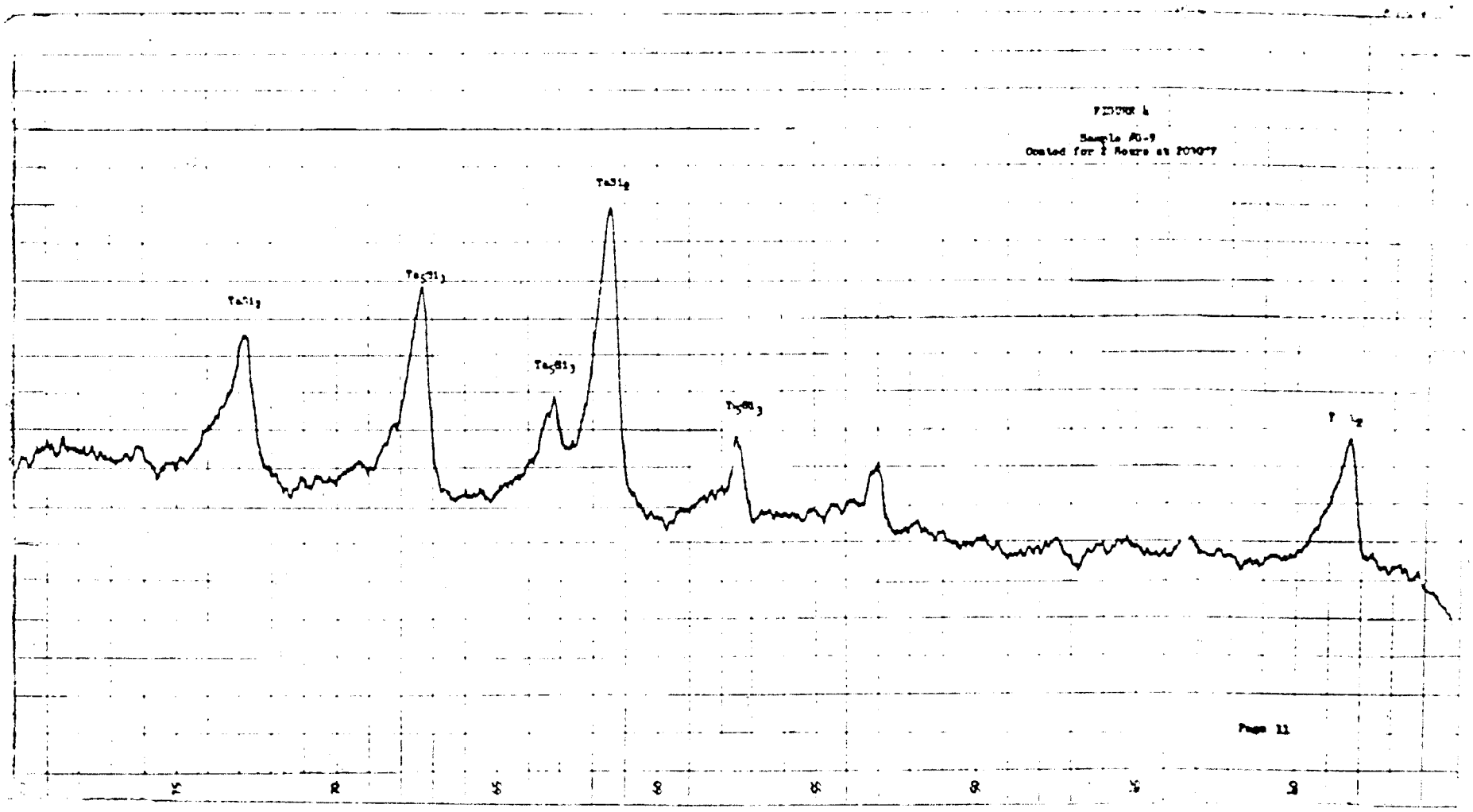
Sample #0-9
Page 11

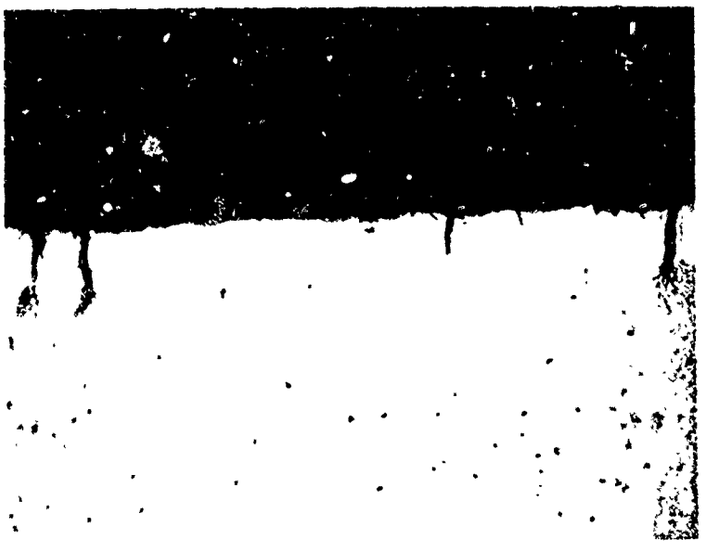

FIGURE 5

Specimen G-1, Tantalum Specimen
Coated for 1 1/2 Hour at 1925°F - 250X

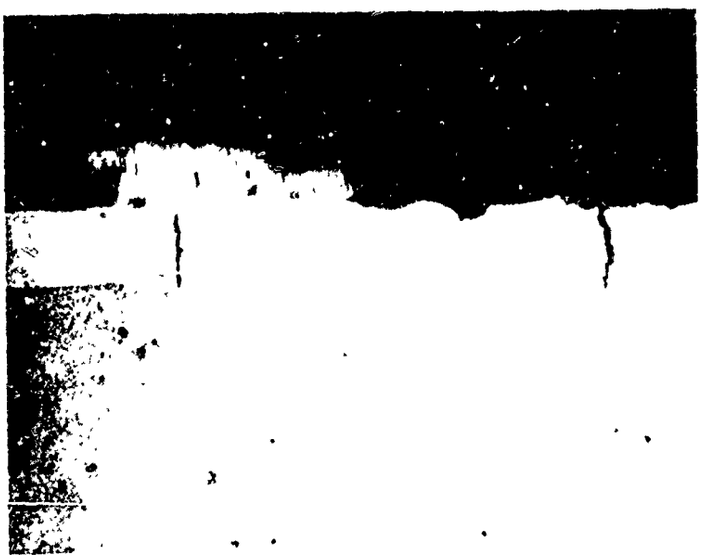

FIGURE 6

Specimen G-9, Tantalum Specimen
Coated for 2 Hours at 2030°F - 250X

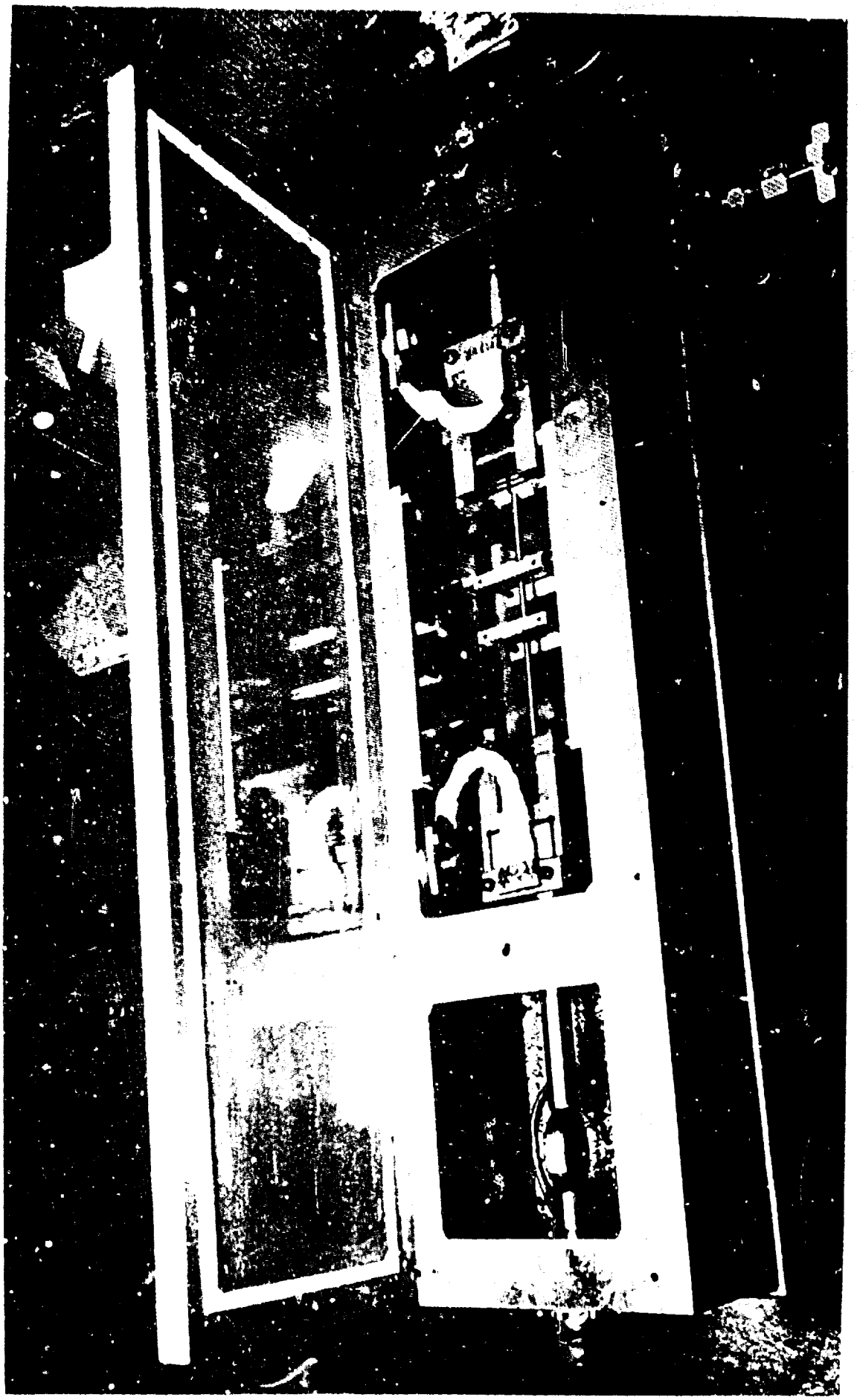

FIGURE 7
HIGH TEMPERATURE VACUUM CHAMBER

TABLE I
Creep Rupture Tests
0.5 Ti-Mo Coated Specimens

Type of Coating	Spec. No.	Temp. °F	Stress psi	% Creep Deformation in: 30 sec.	1 min.	2 min.	5 min.	10 min.	15 min.	20 min.	25 min.	30 min.
Thermomet T-55	13	2800	5700	0.20	0.30	0.50	1.0	1.65	2.20	2.80	3.60	4.60
	13 a	2800	6300	0.25	0.45	0.85	2.3	*				
	*Smoking began at six minutes and specimen ruptured at six minutes 45 seconds with 4.4.% deformation											
Thermomet T-55	14	2800	6000	0.10	0.20	0.25	0.35	0.55	0.75	0.95	1.15	1.45
	14 a	2800	6400	0.10	0.20	0.25	0.40					
	14 b	2800	6800	0.10	0.20	0.30						
	14 c	2800	7400	0.10	0.25	0.40						
	14 d	2800	7800	0.20	0.40	0.60						
	14 e	2800	8300	0.25	0.50	1.05						
	14 f	2800	8900	0.45	0.95	2.50	*					
	*Smoking began at two minutes thirty seconds and specimen ruptured at four minutes ten seconds.											
Thermomet T-55	15	2800	6000	0.30	0.50	0.90	1.50	2.30	*			
	*Smoking began faintly at 4 minutes 20 seconds, began to smoke noticeably at 10 minutes and specimen ruptured at 12 minutes 30 seconds.											
Thermomet T-55	16	2800	6000	0.05*	0.10	0.20	0.35	0.45	0.60	0.75	0.90	1.10
	16 a	2800	6400	0.10	0.20	0.40	0.65**					
	*After heating to temperature and before load application, specimen was smoking very slightly from a pinhole outside the gauge length.											
	**Smoking began vigorously at 2 minutes and specimen ruptured at 5 minutes 20 seconds.											

TABLE II
Creep Rupture Tests
0.5 Ti-Mo Coated Specimens

Type Coating	Spec.No.	Temp. °F	Stress psi	% Creep Deformation in: 30 sec	1 min.	2 min.	5 min.	10 min.	15 min.	20 min.	25 min.	30 min.
Pfaudler	10	2800	6000	0.05	0.10	0.15	0.25	0.40	0.60	0.80	1.00	1.20
	10 a	2800	6800	0.10	0.15	0.25	0.55	1.10				
	10 b	2800	7600	0.10	0.20	0.40	0.95	1.85				
	10 c	2800	8300	0.15	0.30	0.65	1.55	*				
	*Smoking began at 5 minutes 20 seconds and specimen ruptured at 7 minutes 10 seconds with 2.30% deformation.											
Pfaudler	9	2800	7300	0.05	0.30	0.60	1.20	2.10	3.10	4.10	*	
	*Smoking began at 21 minutes and specimen ruptured at 22 minutes 20 seconds with 4.45% deformation.											
Pfaudler	8	2800	7400	0.30	0.55	1.00	2.00	*				
	*Specimen broke abruptly at 8 minutes 10 seconds.											
Pfaudler	7	2800	7600	0.10	0.20	0.45	1.00	1.80	2.60	3.40	4.00	*
	*Smoking began at 24 minutes and specimen ruptured at 26 minutes ten seconds with 4.10% deformation.											

TABLE III
Creep Rupture Tests
0.5 Ti-Mo Specimens

Type Coating	Spec.No.	Temp. °F	Stress psi	% Creep Deformation in: 30 sec.	1 min.	2 min.	5 min.	10 min.	15 min.	20 min.	25 min.	30 min.
Pfaudler	4	2800	7500	*								
	*Specimen broke abruptly outside extensometer with 0.8% deformation in 20 seconds. Specimen was extremely tapered from one end to the other.											
Pfaudler	3	2800	6800	0.15	0.35	0.70	1.55	2.40	3.40	4.35	5.25	6.15 *
	* Smoking began at 29 minutes 30 seconds and specimen ruptured in 33 minutes 30 seconds with 6.6% deformation.											
Pfaudler	2	2800	7200	0.10	0.20	0.35	0.85	1.65	2.45	3.20	3.95	4.75
	2 a	2800	8000	0.15	0.35	0.65	1.70	*				
	* Smoking began at 5 minutes 30 seconds and specimen ruptured at 6 minutes 50 seconds with 3.05% deformation.											
Pfaudler	20	2800	7000	0.10	0.15	0.30	0.70	1.60	2.40	3.20	3.95	4.75
	20 a	2800	7200	0.10	0.20	0.45	1.15	2.45	3.75	5.35	*	
	*Smoking began at 22 minutes 30 seconds and specimen ruptured in 23 minutes 40 seconds with 7.95% deformation.											

FORM 6 - 3 81

TABLE IV

COATED RS-"2 COLUMBIUM ALLOY TESTS

COMPANY	Spec. No.	Area in.²	Temp. °F	Ftu ksi	Fty ksi	E x 10⁻⁶ psi	Strain rate "/"/min.	% Elong. in 2 inche
General Electric	GE 1	.02047	2400	22.4	11.0	12.2	.0056	21.0
	GE 2	.02060	2190	24.5	14.0	14.0	.0033	27.0
	GE 3	.02060	1800	41.7	30.5	14.4	.0070	9.0
Sylcor	S1	.0280	2400	18.7	11.5	11.5	.0060	17.0
	S2	.02086	2215	23.5	14.2	12.3	.0039	21.0
	S3	.02111	1810	41.2	30.8	17.1	.010	12.2
Pfaudler	P1	.02027	2380	16.0	10.1	12.6	.0050	34.0
	P2	.01995	2205	23.8	14.0	---	.0047	24.5
	P3	.02047	1795	35.1	22.9	13.3	.0020	12.2
Tapco	T1	.02063	2380	15.8	7.7	12.8	.0056	39.5
	T2	.02115	2200	21.2	11.3	14.1	.0150	28.0
	T3 *	.02130	1775	29.5	17.6	17.6	.0049	5.5

* Specimen had coating chipped before testing

PLASMA-SPRAYED OXIDE AND VAPOR-DEPOSITED NITRIDE COATINGS ON TUNGSTEN AS A MEANS OF ACHIEVING OXIDATION PROTECTION

J. L. BLITON

J. J. RAUSCH

Armour Research Foundation

Chicago, Illinois

PLASMA-SPRAYED OXIDE AND VAPOR -DEPOSITED NITRIDE COATINGS ON TUNGSTEN AS A MEANS OF ACHIEVING OXIDATION PROTECTION

I. INTRODUCTION

This paper describes current studies in which attempts are being made to utilize refractory oxide and nitride coatings as a means of protecting tungsten from oxidation. This work is part of a program directed to developing effective coating systems for refractory metals at temperatures above 3600°F for use in low-pressure, liquid-fueled, rocket engines*. Oxide coatings were applied by plasma spraying, and the nitride coatings by chemical vapor deposition. Methods of improving adherence, coating density, uniformity, and thermal shock resistance are being investigated, and protective capability is being evaluated.

Experimental effort on these coating systems is continuing, and this paper is presented at this meeting merely in the form of a progress report.

II PLASMA-SPRAYED OXIDE COATINGS

This phase of the program is to produce mechanically and thermally stable, closed-pore, oxide coatings by plasma spraying. Stabilized zirconia (5w/o CaO), partially stabilized hafnia (5w/o Y_2O_3), and strontium zirconate have been evaluated; thoria is yet to be studied.

Two main problems encountered were tensile cracking of the coating and poor coating-to-substrate bonding; both are believed due to the differences in thermal expansion between the oxides and the tungsten substrate.

---

* Contract No. NAS7-113

A. Coating-to-Substrate Bond Strength

The common surface preparation practice of grit blasting with No. 20 grit SiC was found inadequate for zirconia coatings applied directly on tungsten. With substrate temperature during coating in the range of 1250°F to 1350°F the interfacial stresses during cooling were great enough to cause the coatings to spall. The use of a 43 w/o W-57 w/o ZrO_2 layer between the grit-blasted tungsten and the ZrO_2 cover coat eliminated this problem. Such coatings, however, were subject to localized blistering when tested with the blast of an oxygen-hydrogen torch. This problem was overcome by spraying a thin layer of large grit, 74 to 44 micron, tungsten on the substrate. The undercoat, 3 to 4 mils in thickness, formed a rough irregular surface allowing better coating-to-substrate bonding. The increase in adhesion gained from the rough undercoat with hafnia-type coatings is shown in Table I. Tensile bond strength data were obtained by coating one end of 3/4 inch diameter tungsten cylinders, cementing them with epoxy to similar uncoated cylinders and stressing the couplet in tension. Further bond strength studies using photoengraving and electrolytic etching techniques for substrate preparation are in progress.

B. Coating Systems

Three basic coatings systems have been or are presently being evaluated; these are listed in Table II. The coatings are produced from refractory oxides with a particle size range of -25+5 microns and tungsten particles approximating 5 to 6 microns in diameter. The coatings are formed in a 3 v/o hydrogen-argon atmosphere with an SG-3 Plasmadyne torch. Argon is used as the stabilizing gas, 3 v/o hydrogen-argon as the powder feed gas, and the operating power is approximately 6 kw.

The severity and prominence of a mosaic crack pattern in the oxide cover coatings is in direct proportion to the difference in thermal expansion between the oxide and tungsten, i.e., stronium zirconate and zirconia (CaO stabilized) the worst with crack-free hafnia coatings being achieved periodically. When the substrate thermal expansion was increased by use of Ta-10W instead of tungsten, crack-free hafnia coatings were

Table I

TENSILE BOND STRENGTH DATA

FOR TUNGSTEN-HAFNIA COATINGS * ON TUNGSTEN

Surface Preparation	Tensile Strength, psi	Remarks
No. 20 grit Sic blasted surface	1080-2330	Average of 5 tests was 1770 psi
3 mils of sprayed 74 x 44μ W over grit-blasted surface	2270-2670	Average of 5 tests was 2, 420 psi

* First layer 40 w/o W-60 w/o HfO_2, second layer HfO_2.

Table II

TYPICAL PLASMA-SPRAYED COATINGS SYSTEMS

ON TUNGSTEN

Series	Composition
I	Tungsten substrate 3-4 mils of 74 to 44μ 5 mils of 43 w/o W-57 w/o ZrO_2 5-10 mils of ZrO_2
II	Tungsten substrate 3-4 mils of 74 to 44μ 5 mils of 40 w/o W-60 w/o HfO_2 3-5 mils of 10 w/o W-90 w/o HfO_2 5-10 mils of HfO_2
III	Tungsten substrate 3-4 mils of 74 to 44μ 3-4 mils of 40 w/oW-60 w/o HfO_2 5-10 mils of $SrZrO_3$

obtained, even when substrate temperatures of 1900°F were used during coating.

C. Oxidation Testing

Tungsten plates, 3 x 3 x 0.1 in. coated with any of the three systems listed in Table II, have successfully withstood oxidation testing with one oxygen-hydrogen torch (specimen surface temperature 3600° - 3800°F) for 5 minutes. The oxidation rate of bare tungsten under these conditons is 30 mils/min. Only the tungsten-hafnia coatings (Series II, Table II) have been subjected to two oxyhydrogen torches (4100° - 4200°F surface temperature, 48 mils/min oxidation of bare tungsten). The coatings protected the substrate throughout the 5-minute test. After either type of exposure, the coatings will crack and will spall when retested.

III. PYROLYTIC NITRIDE COATINGS

A. Introduction

Pyrolytic coatings of TiN and HfN were applied to 0.125 in. diameter tungsten rods by hydrogen reduction of the tetrachloride in the presence of nitrogen. Plating temperatures were varied between 2730° and 3630°F. The TiN coatings were relatively free of cracks after deposition, and specimens of this type were generally tested in the as-coated condition. Hafnium nitride coatings, however, contained large radial cracks, which cannot be eliminated by variation in coating deposition temperature. This prompted us to study methods of partially dissociating the nitride in order to obtain crack-free coatings.

B. Hafnium Nitride Dissociation Studies

Hafnium nitride is quite unstable in vacuum (10^{-4} torr) at 4120°F. A coated specimen heated under these conditions for 5 minutes underwent a weight loss of 3.50% of the original coating weight. Since nitrogen comprises 7.84% of the weight of stoichiometric HfN, this weight

loss can be considered particularly significant if the bulk of the loss is attributable to nitrogen evolution. The structure of the coating after this treatment is two-phase, with an apparent third phase existing as a continuous layer at the tungsten surface. X-ray diffraction analysis indicates the presence of hafnium, nitrogen-deficient HfN, and a minor quantity of W_2Hf. Heating the nitride for 5 minutes at 2820°F in vacuum causes no apparent dissociation or interaction with tungsten. By heating at high temperatures and moderate pressures (100-500mm Hg), dissociation of the nitride can be controlled so that the primary structural change that occurs in the coatings is grain growth and partial loss of nitrogen. Crack-free structures of this type have been produced.

C. Oxidation Testing

Oxidation tests have been performed in static air on TiN-coated tungsten at 3090° and 3630°F. At the lower temperature a protective oxide forms; the rate of oxidation is approximately +22mg/cm^2/min during the early stages. This corresponds to a surface recession rate of about 0.5 mils/min for the original coating. Bare tungsten oxidized under these conditions loses weight at a rate of 110 mg/cm^2/min. The oxide, which forms on the nitride, appears glazed and may contain tungsten. At 3630°F, oxidation of the TiN-coated samples proceeds far more rapidly, and specimens lose weight at a rate of 122 mg/cm^2/min. during a 30-second exposure. The rate of weight loss for bare tungsten is 360 mg/cm^2/min under these conditions.

When HfN-coated tungsten specimens are oxidized in the as-coated condition, a molten oxidation product is formed at temperatures as low as 2200°F. Formation of the liquid appears to originate at coating defects. When the coating is partially dissociated in a low-pressure nitrogen atmosphere, subsequent oxidation causes pure HfO_2 to form as a solid scale on the nitride surface. The protective capability of coatings of this type is currently being investigated under a variety of oxidizing conditions.

OBSERVATIONS ON METALLURGICAL BONDING BETWEEN PLASMA SPRAYED TUNGSTEN AND HOT TUNGSTEN SUBSTRATES

S. J. GRISAFFE

W. A. SPITZIG

Lewis Research Center

NASA

Cleveland, Ohio

INTRODUCTION

While considerable work has been carried out on plasma sprayed coatings, very little effort has been directed toward a critical examination of the resultant particle-to-substrate bonds. Since the characteristics of the initial bond generally determine the adherence and strength of bonding of any applied coating, improved bonding from one of mechanical interlock to one that is truly metallurgical is important. Therefore, an investigation was undertaken to explore the type and quality of coating-to-substrate bonds which can be obtained during plasma spraying. This work is a portion of a larger effort to characterize more fully the plasma-spray deposition phenomenon and to develop improved plasma-spray coatings.

In general practice, powder of one material is plasma sprayed on the roughened surface of a different material. In this investigation, however, tungsten powder was deposited on metallurgically polished tungsten substrates in order to minimize some of the variables involved in coating-substrate bonding. Admittedly, using the same material for coating and substrate and using highly polished substrate surfaces do not simulate general coating practice. However, these conditions were chosen so that the bond could be studied without undue complications. In this way, physical property variables such as thermal conductivity, linear coefficient of thermal expansion, relative melting temperatures, etc., were eliminated. Also, eliminating

surface roughness excluded the questions of total roughness, roughness variation, and as-roughened surface composition. In addition, the smooth surface allowed additional deductions to be made on particle properties, such as plasticity, and permitted more controlled observations of effects on the substrate.

A preliminary investigation (unpublished) showed that plasma-sprayed tungsten particles did not adhere to metallurgically polished tungsten specimens that were not preheated. However, tungsten particles did adhere to substrates of lower thermal conductivity, which reduced the quench rate of the particles and allowed them to cool at a slower rate. Therefore, this investigation was conducted on tungsten substrates that were preheated to relatively high temperatures, in order to reduce the quench rate of the particles and enhance their adherence.

To gain the maximum information from this investigation, the number of particles deposited on the substrate, in each test, was kept at a minimum. This was done to observe the characteristics of the individually sprayed particles rather than the characteristics of a gross deposit.

APPARATUS AND PROCEDURE

Commercial tungsten powder, 74μ to 30μ particle size (Metco XP-1106), was sprayed on metallurgically polished tungsten coupons, 1 by 1 by 0.017 inch thick. These coupons were ground from as-received tungsten sheet, mounted in a cold castable mounting material, and metallurgically polished. After polishing, the specimens were broken out of their respective mounts and stored in a desiccator to prevent surface contamination. The particles were sprayed on the 1- by 1-inch surface that was metallurgically polished.

The coupon thickness was kept to a minimum in order to permit rapid heat transfer to the back side for temperature monitoring.

All runs were made with a Thermal Dynamics F-40 torch operating in an environmental chamber (utilizing nitrogen) under the following fixed conditions:

Number 1 nozzle - 7/32-inch I.D.

450 amperes

60 volts

80 SCFH[1] high purity dry nitrogen
10 SCFH hydrogen
} Plasma gas

10 SCFH high purity dry nitrogen - carrier gas

11.9 setting on Continental Coatings hopper

Each tungsten coupon was mounted by fitting two diagonally opposite specimen corners into spring-loaded alumina tubes. Each specimen had a Pt-Pt - 13-percent-Rh thermocouple spot-welded to the back face and the temperature was monitored through the preheat and spray cycle by means of a recorder with a response of a few milliseconds. A schematic of the spray setup is shown in figure 1. The test sequence was as follows:

(1) Set coupon to torch distance

(2) Evacuate chamber to 20μ and backfill to atmospheric pressure with high-purity dry nitrogen

(4) Roll torch into position and permit plasma gas to preheat tungsten coupon

[1]Standard cubic feet per hour.

(5) When specimen temperature reaches equilibrium (2 to 3 sec), activate powder spray for approximately 1 second

(6) Roll torch out of position and shut down

(7) Permit specimen to cool to room temperature and open tank

The total time involved for specimen preheating, spraying, and cool down to 400° F was approximately 30 seconds.

Average particle velocity measurements were made at various torch-to-substrate distances with a rotating disk velocimeter similar to that used in reference 1.

RESULTS AND DISCUSSION

During preheating with the plasma gas, the substrate temperature varied with torch distance as shown in figure 2. Also shown on this figure are the back side substrate temperatures during spraying.

The average particle velocity data are shown in figure 3. Notably there is little difference in average particle velocity between 4 inches (240 ft/sec) and 7 inches (215 ft/sec).

The actual deposition patterns and cross-sectional views are shown in figures 4, 6, 8, and 9, and will be discussed in order of increasing torch-to-substrate distance. Before these cross sections are examined, it must be remembered that the particles were sparsely deposited on the substrate to permit easy examination of the particle configuration. For this reason, a cross section will not show a series of particles side by side, but only isolated particles. Also, the deposition efficiency decreases as torch-to-substrate distance increases, so that the 4-inch specimen shows several particles on top of the same spot while lower particle concentrations are seen at increasing torch-to-substrate distances.

4-Inch torch-to-substrate distance. - At a distance of 4 inches the plasticity of the particles is maximum for the range investigated. Most of the particles which struck the substrate were deformed into flat, almost circular disks and had sufficient plasticity to fold over previously deposited particles (fig. 4(a)). Most of the particles were, therefore, at high temperature as evidenced by the relatively few pits blasted into the substrate surface. The pits which are present were not filled by the flow of material from the particles next to them. This may indicate that dynamic resistance to flow (as governed by surface tension, velocity, temperature, etc.) is still sufficiently high to prevent such a discontinuous flow. This may well point to a reason for difficulties when spraying on grit-blasted surfaces, where numerous surface discontinuities are present.

A cross-section view of the deposit and substrate (fig. 4(b)) reveals large columnar grains perpendicular to the recrystallized structure of the substrate. The original interface has been almost completely eliminated. This appears to have occurred by each substrate surface grain growing into the coating. In some areas it is apparent that this growth continued even into the subsequent particles that landed on the first particle, i.e., the columnar grain boundaries are continuous through the rows of voids which mark interparticle boundaries. This continuity of columnar grains is better illustrated in figure 5, which is an electron micrograph. Here it can be seen that the columnar grains do grow through the original particle-to-particle interfaces, which appear as rows of voids in this figure. These voids are thought to be caused by surface oxides or absorbed gases. They should not be due to the presence of tungsten nitride since this compound is thermodynamically unstable at these temperatures as is discussed in reference 2.

5-Inch torch-to-substrate distance. - In the 5-inch distance, the particles were similar to those at 4 inches; however, both the number and the size of the pits increased. The amount of undeformed particles[2] had increased slightly (fig. 6(2)).

The cross section (fig. 6(b)) shows that the particle-to-substrate interface has been completely eliminated while maintaining an essentially "as-worked" structure in the substrate. Consistent with this, the columnar grains in the coating are smaller. Some evidence of particle-to-particle interfaces can be seen, but they are not sharp lines of demarcation. Figure 7 is an electron micrograph showing the coating and the substrate.

The original substrate surface is evidenced by the row of voids, but a metallurgical bond exists and there is continuity between grains of the substrate and of the coating. This situation exists even though there is essentially no recrystallization of the substrate. The relative size decrease in the columnar grains which occurred at this distance as compared to the size of the grains which occurred at 4 inches may be seen by comparing figures 5 and 7.

6-Inch torch-to-substrate distance. - The coupon surface (fig. 8(a)) showed larger pits and a greater amount of undeformed particles than seen in figure 6(a). The particles still exhibited a considerable amount of plasticity as can be seen by the amount of particle overlap. However, in spite of this plasticity, some particle cracking was observed.

---

[2]The undeformed particles were determined to be raised portions on the substrate by microscopic analysis of focus points.

The cross section (fig. 8(b)) is similar to that obtained at 5 inches but the columnar grain structure is much finer. (The dark line is a delamination of the tungsten substrate.)

7-Inch torch-to-substrate distance. - The greater distance of 7 inches produced many undeformed particles (fig. 9(a)), and most of those that did deform show cracks. The size of the pits is increasing but their number is decreasing slightly (as compared to fig. 8(a)). The increase in the pit size and the decrease in number of pits indicate that only the larger particles have sufficient energy to cause pitting of the colder substrate at this distance.

The particle-to-substrate bond is not complete (fig. 9(b)), but a metallurgical bond still exists over a great portion of the interface. The interparticle interfaces are more obvious and the columnar structure can still be seen.

SUMMARY OF RESULTS

From an examination of the plasma-sprayed particles on preheated substrates over a substrate temperature range of 2050° to 2700° F, certain trends are observed:

1. The amount of undeformed particles increases slightly with increasing torch-to-substrate distance.

2. Cracks are present in the particles deposited at greater distances.

3. The number of pits is a minimum at the shortest distance investigated.

4. The pit size increases with increasing torch-to-substrate distance.

From examination of the coating substrate cross sections, certain trends can also be seen:

1. The columnar grain size of the coating decreases with increasing torch-to-substrate distance.

2. Up to a 6-inch torch-to-substrate distance, good metallurgical bonds exist between the coating and the substrate, and at 7 inches a metallurgical bond exists over a considerable portion of the interface.

CONCLUSIONS

1. Metallurgically bonded tungsten coatings can be achieved by plasma spraying on polished tungsten substrates, without prior roughening of the substrate surface, if the substrate is first heated in an inert atmosphere (the substrate temperatures investigated ranged from 2050° to 2700° F).

2. It is possible to deposit such coatings while retaining the high-strength properties of an as-worked substrate, i.e., a metallurgical bond can be achieved at a substrate temperature below the substrate recrystallization temperature.

3. The type of columnar grains which appear in all the cross sections indicates that the coating-substrate bond is the result of substrate surface grains growing into the coating.

4. Even under very short-time conditions, almost complete elimination of the original coating-to-substrate interface can be achieved. This indicates extremely rapid short-range diffusion occurred at this interface.

REFERENCES

1. Meyer, H.: Flame Spraying of Alumina. Library Trans. 943, British RAE, Apr. 1961.

2. Stokes, C. S., and Knipe, W. W.: The Plasma Jet in Chemical Synthesis. Ind. and Eng. Chem., vol. 52, 1960, pp. 287-288.

E-2078

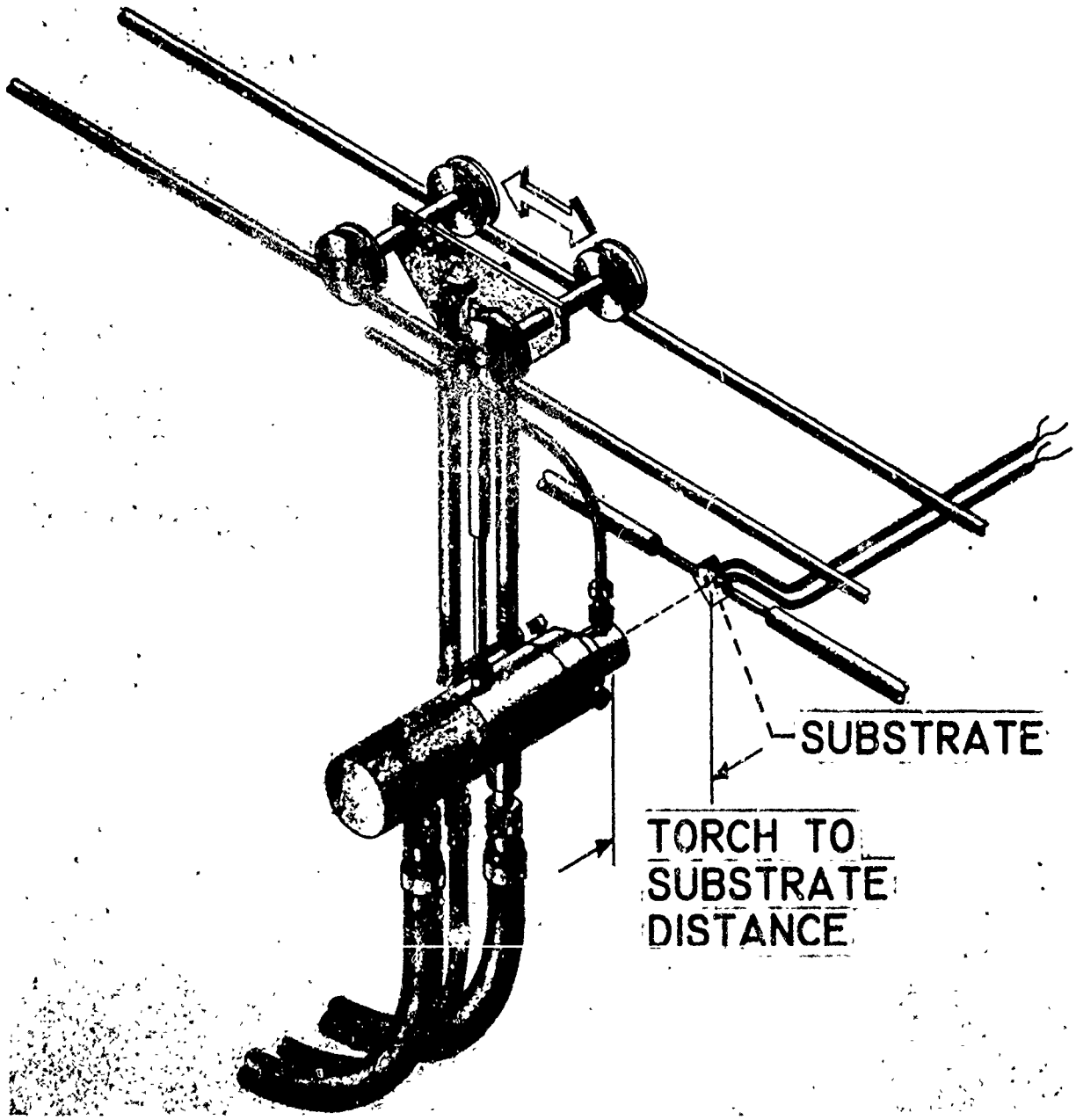

Fig. 1. - Apparatus in inert chamber.

E-2078

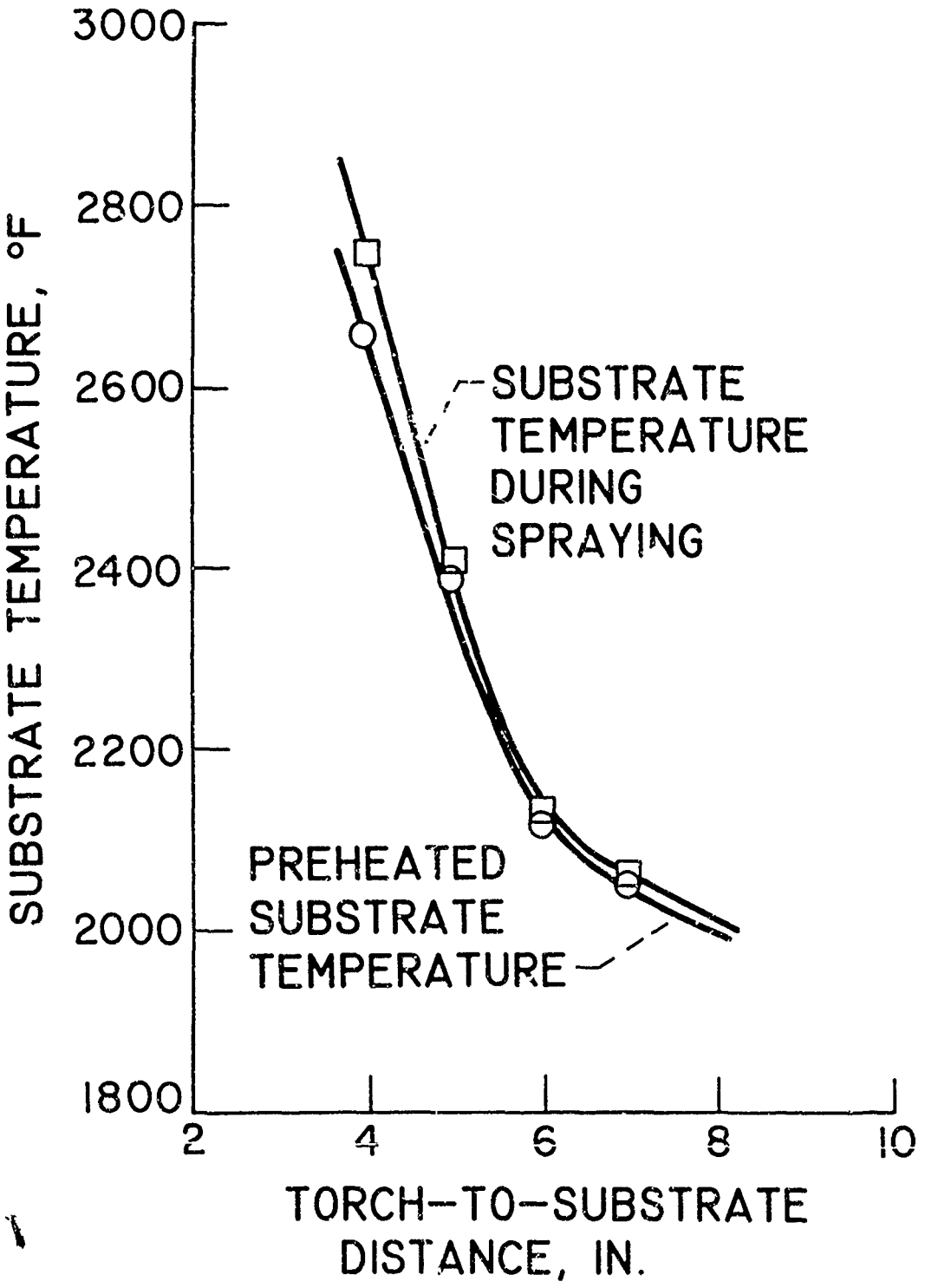

Fig. 2. - Variation of substrate temperature with torch-to-substrate distance.

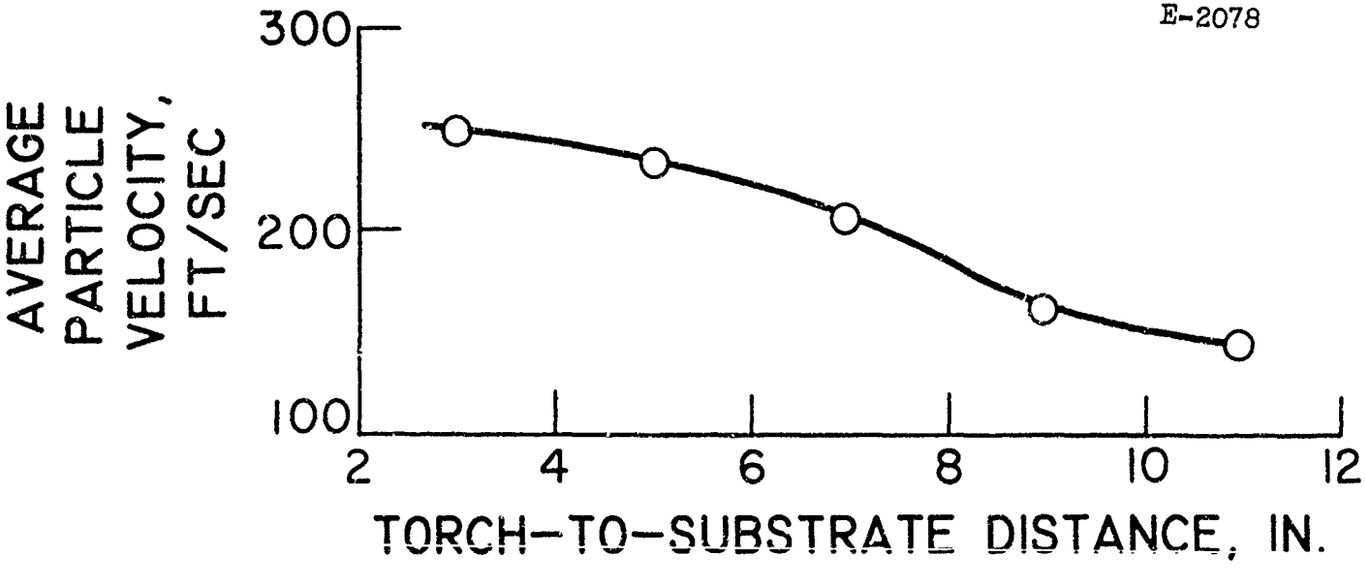

Fig. 3. - Variation of average particle velocity with torch-to-substrate distance.

E-2078

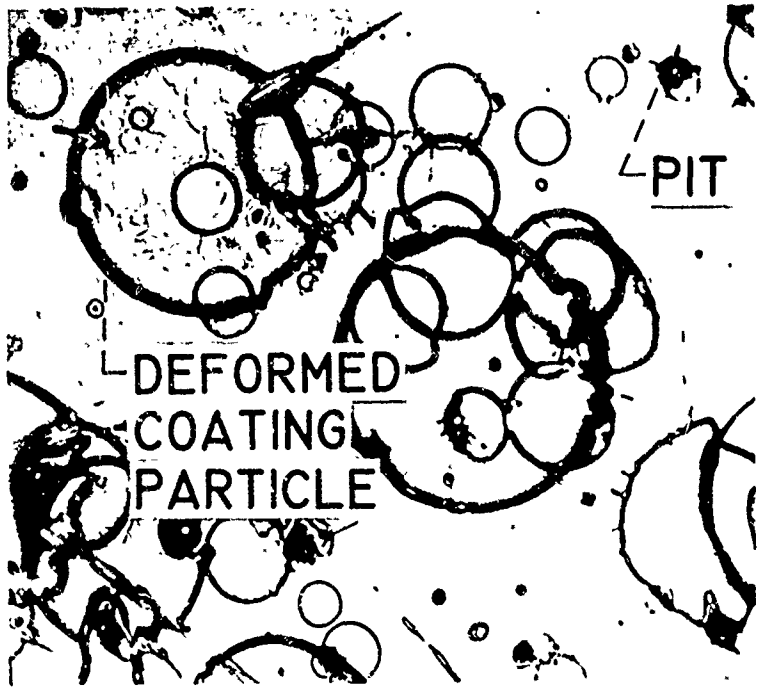

(a) Particles on substrate. Etchant, Murakami's reagent; X250.

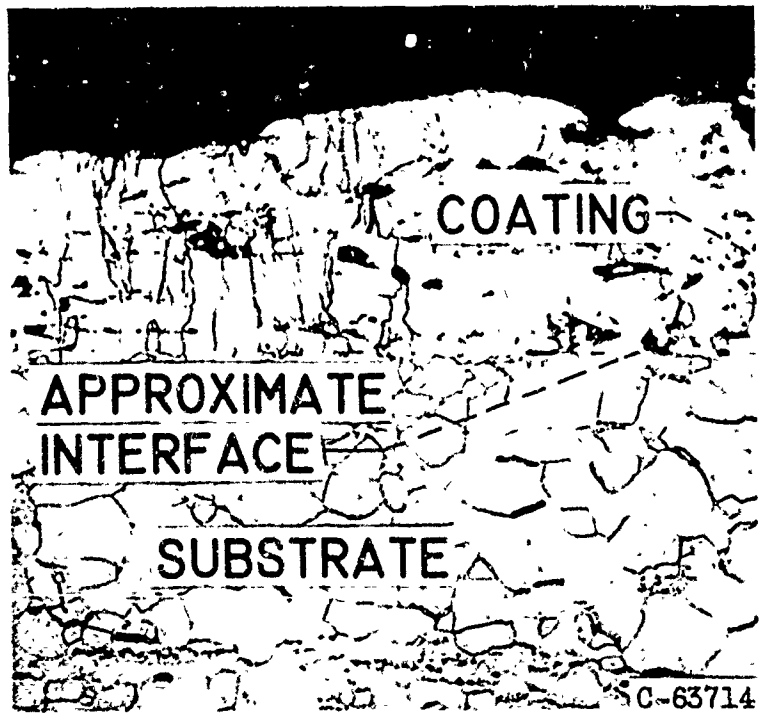

(b) Particle cross-section. Etchant, Murakami's reagent; X500.

Fig. 4. - As-sprayed and cross-section views for a 4-inch torch-to-substrate distance. Substrate temperature, ~2700° F.

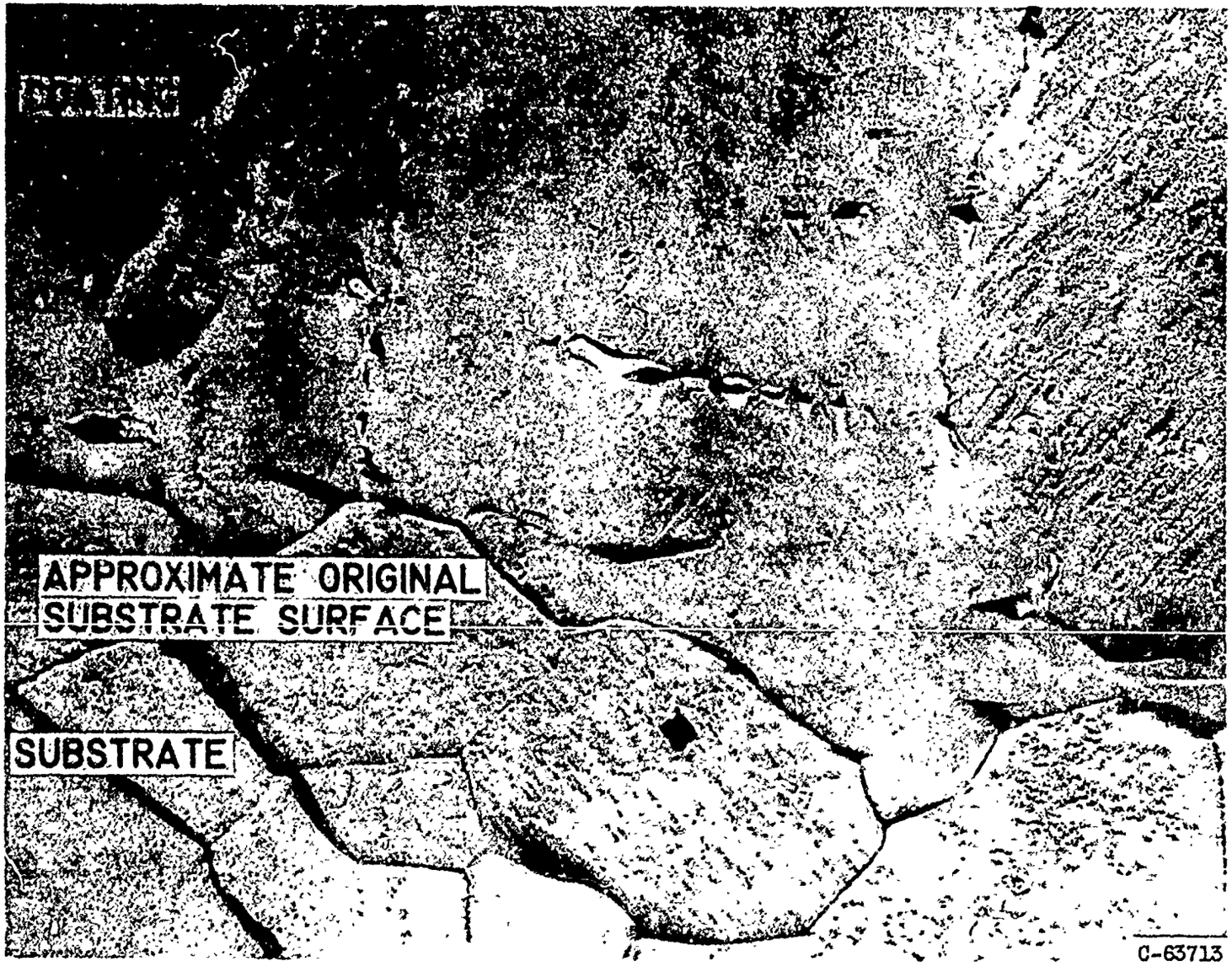

Fig. 5. - Electron micrograph of a cross-section of the coating and substrate for a 4-inch torch-to-substrate distance. Etchant, Murakami's reagent; ×20,000.

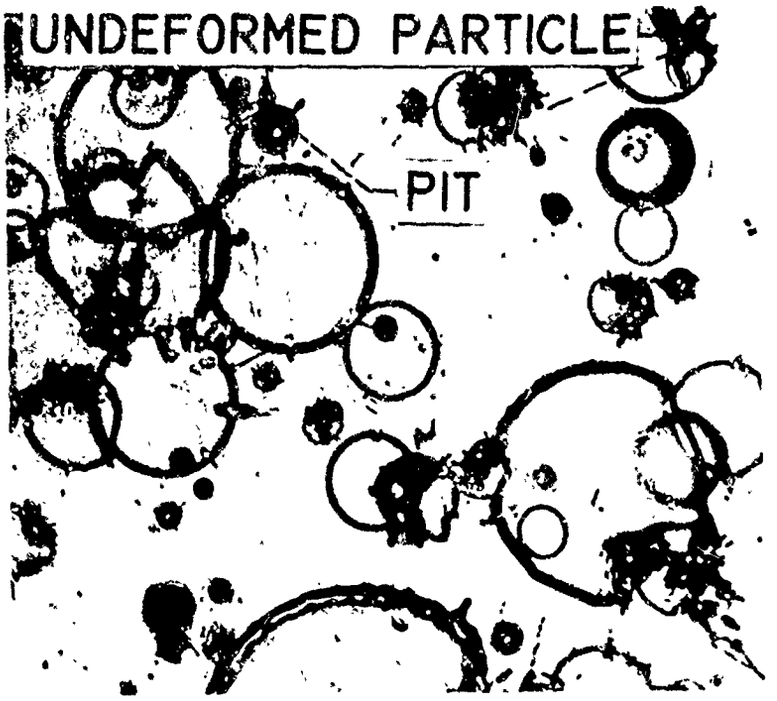

(a) Particles on substrate. Etchant, Murakami's reagent; X250.

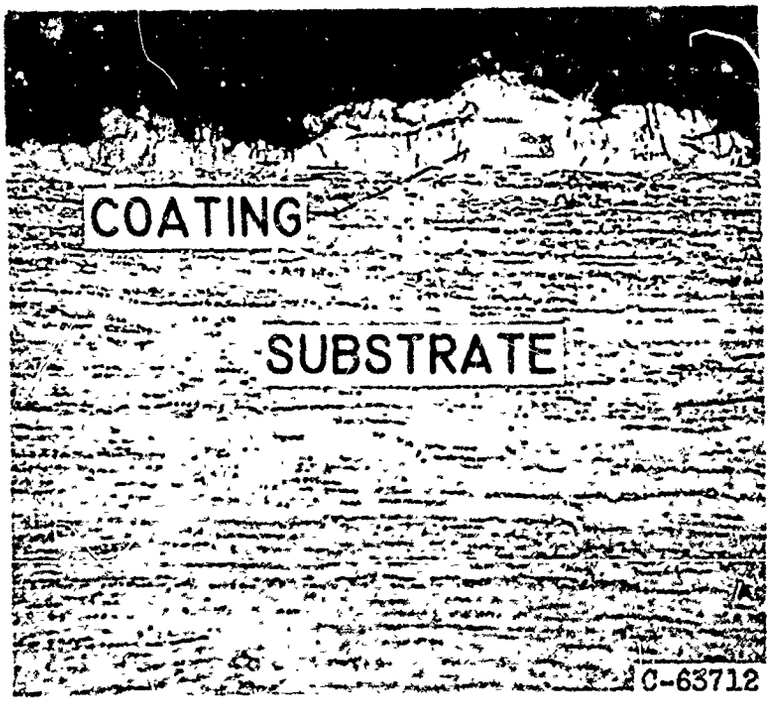

(b) Particle cross-section. Etchant, Murakami's reagent; X500.

Fig. 6. - As-sprayed and cross-section views for 5-inch torch-to-substrate distance. Substrate temperature, ~2400° F.

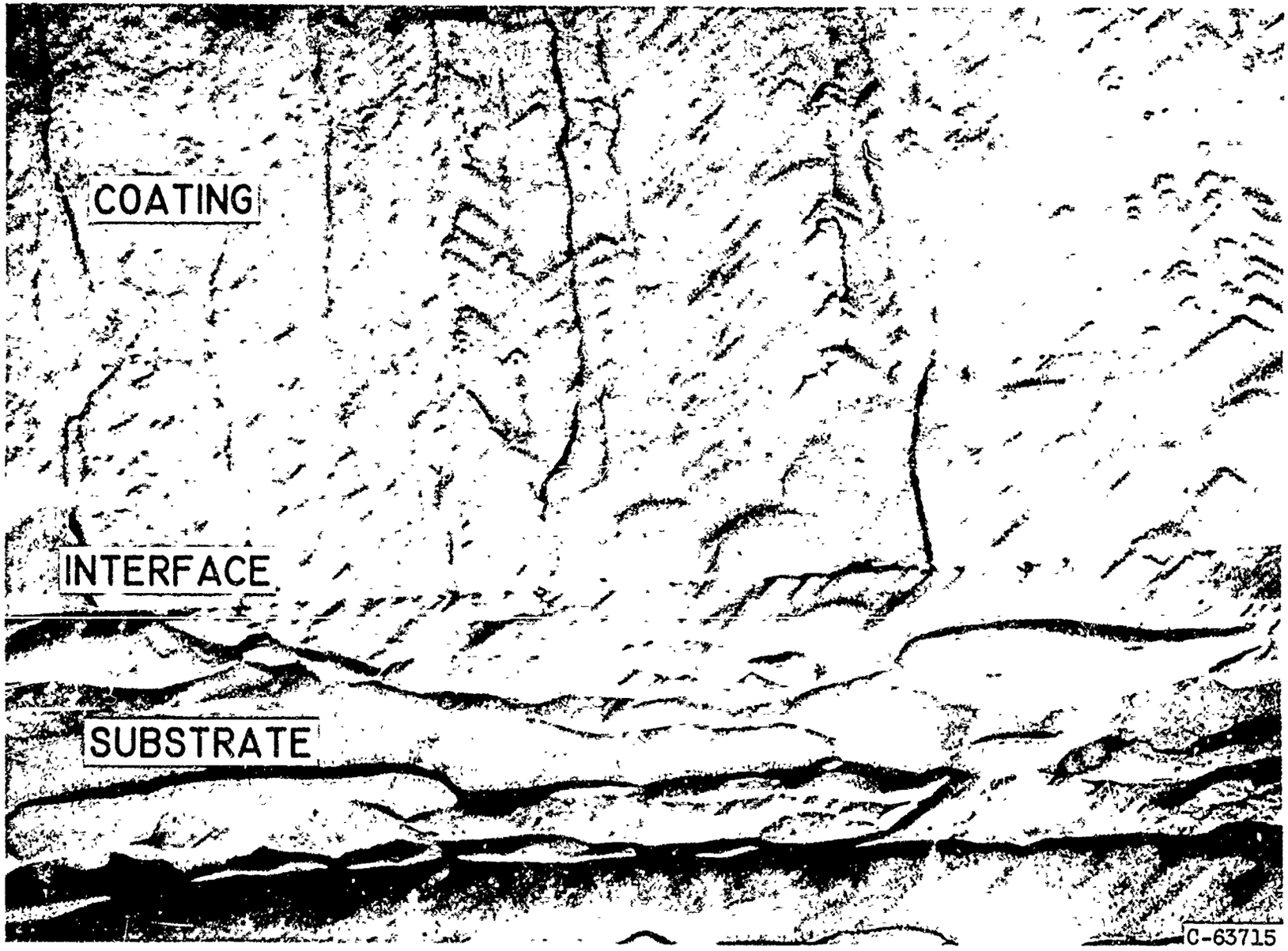

Fig. 7. - Electron micrograph of a cross-section of the coating and substrate, for a 5-inch torch-to-substrate distance. Etchant, Murakami's reagent; ×20,000.

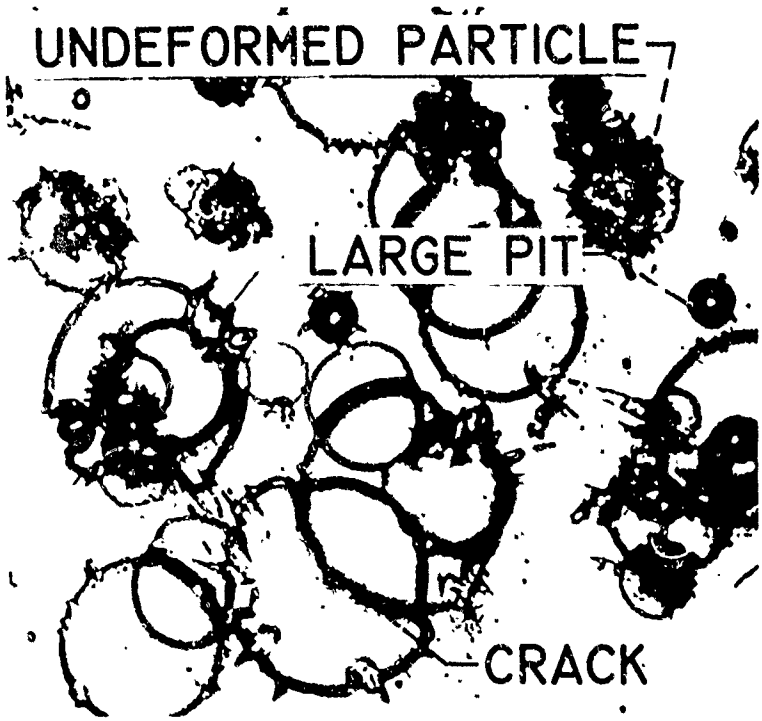

(a) Particles on substrate. Etchant, Murakami's reagent; ×250.

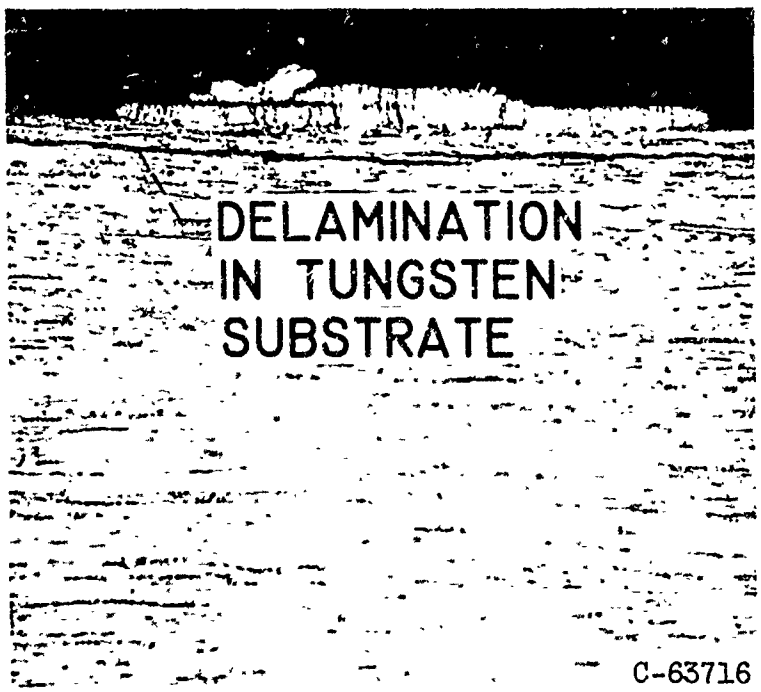

(b) Particle cross-section. Etchant, Murakami's reagent; ×500.

Fig. 8. - As-sprayed and cross-section views for a 6-inch torch-to-substrate distance. Substrate temperature, ~2100° F.

E-2078

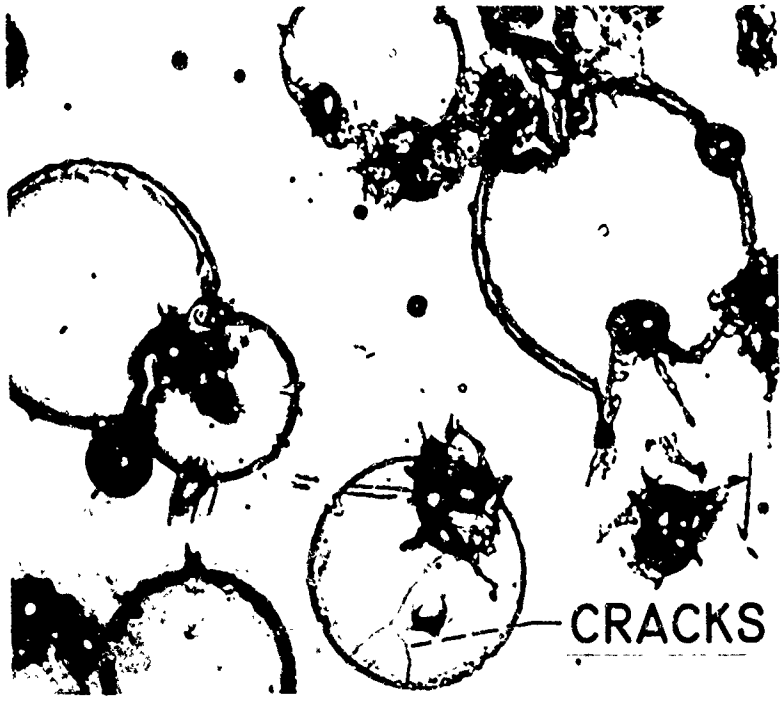

(a) Particles on substrate. Etchant, Murakami's reagent; X250.

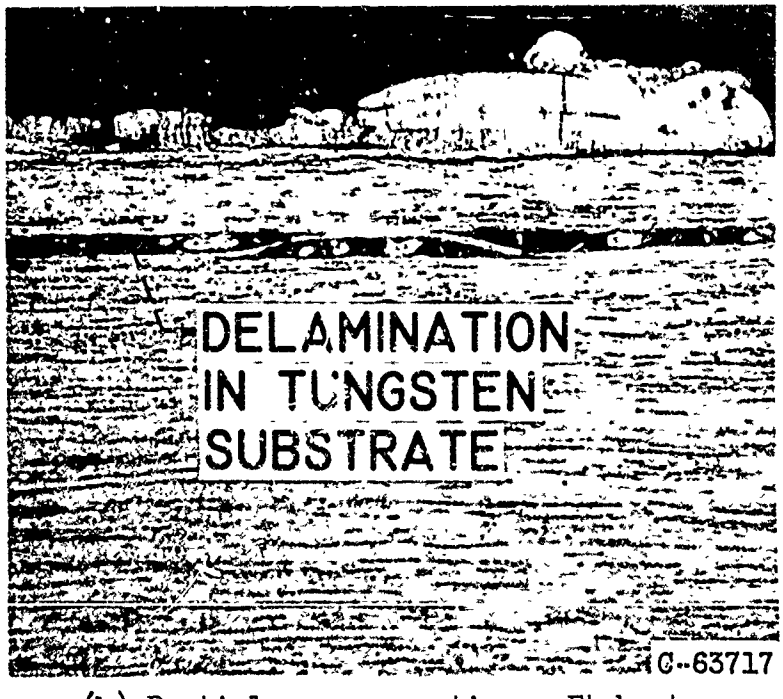

(b) Particle cross-section. Etchant, Murakami's reagent; X500.

Fig. 9. - As-sprayed and cross-section views for a 7-inch torch-to-substrate distance. Substrate temperature, ~2050° F.

NASA-CLEVELAND, OHIO E-2078

REFRACTORY METAL COATING SYSTEMS UTILIZED ON A TYPICAL HYPERSONIC GLIDE RE-ENTRY VEHICLE

J. D. CULP

McDonnell Aircraft Corp.

St. Louis, Missouri

INTRODUCTION

McDonnell Aircraft Corporation is presently under contract to the Air Force to design, fabricate and fly a hypersonic glide re-entry vehicle. The main purpose of the vehicle is to define structural deflections and determine such flight dynamics characteristics as temperatures and pressures experienced in hypersonic glide re-entry. This paper will describe the refractory metal coating systems employed on this research vehicle and summarize the evolution of these systems.

The vehicle, in general, is a delta plan form with a flat bottom canted at a 10° angle. The instrumentation package is covered by a modified conic heat shield structure. The vehicle, as pictured in Figure 1, is approximately 6 feet long, 5 feet wide at the aft end, and weighs approximately 1100 pounds.

Materials employed range from zirconium oxide at the nose cap to aluminum in the instrumentation package and inner-stage. The nose assembly is composed of a zirconia nose cap attached to a molybdenum nose skirt by means of a molybdenum bulkhead. Forward leading edges are of siliconized graphite while the aft two leading edges are of columbium. The forward lower body is made of molybdenum heat shield panels and the aft lower body is of columbium heat shield panels. The forward upper body is a modified conic, single faced corrugated assembly fabricated from columbium. The aft upper body is of similar design and fabricated from L-605. Columbium and titanium compose the primary structure. The forward bulkhead, side beams, aft beam and trusses are of columbium and the stringers, floor and aft bulkhead are of titanium. The interstage assembly which does not re-enter with the vehicle, is made of aluminum.

MOLYBDENUM STRUCTURES

In order to understand the nature and problems of the molybdenum coatings, a more detailed description of those portions of the vehicle fabricated from molybdenum is in order. The most forward metallic structure is the molybdenum nose assembly which holds the zirconia nose cap. This assembly, shown in Figure 2, is machined from an unalloyed molybdenum forging and a TZM alloy bulkhead holds the nose cap to the nose skirt. Molybdenum sheathed thermocouples and molybdenum pressure pickup tubing complete the detail parts of this assembly.

The second major portion of the vehicle fabricated from molybdenum is composed of TZM fittings which secure the graphite leading edges to the primary structure. The third group, and most complex of the molybdenum assemblies, is composed of the forward lower body and the rail assemblies which attach them to the primary structure. These assemblies are of a TZM alloy and are shown in Figures 3, 4 and 5. The panels are of a riveted, single faced corrugated design and are instrumented for temperature and pressure measurements. The rail assemblies are of a hat section or channel design.

The molybdenum fasteners used on this vehicle are purchased in the coated condition. The molybdenum bolts and nuts are supplied by the Standard Pressed Steel Company and are coated by the Pfaudler Company with the PFR-6 system. The molybdenum rivets are supplied by the Voi Shan Manufacturing Company and are Durak B coated by the Chromizing Corporation. The major molybdenum components (those assemblies previously mentioned) are coated with the Chromalloy Corporation's W-3 system. The choice of the coating vendor for the main portions of the molybdenum structure was a difficult one. The technical criteria used for making this choice, in increasing order of importance, are as follows:

(a) Size and nature of facilities and size and competence of the staff.
(b) Coating performance as exhibited by coupon testing.
(c) Volume and complexity of typical hardware previously coated.

During the course of this program a wide variety of testing has been conducted. Some of the highlights of the molybdenum test work will be presented. One of the initial tests made on the Chromalloy W-3 coating was to determine what minimum coating thickness was acceptable. This testing was performed primarily at the Chromalloy Corporation in an air atmosphere tube furnace at 3100°F, 100°F over the maximum predicted design temperature. These tests were terminated after two hours with no failures occurring. The minimum coating thickness was established at 1.3 mils per surface

Physical property tests in the form of tensile strength determinations were used to insure that the coating produced no deleterious effects upon the substrate and that the design allowables previously used were satisfactory. It was assumed, for strength calculations, that all the substrate remaining after the formation of the silicide coating was load bearing material. This assumption proved to be correct as the strengths obtained compared very closely with the predicted strength reductions caused by consumption of substrate material during formation of coating.

It had been previously shown that some coating vendors had difficulty coating internal surfaces with restricted access such as tubing and pressure pickup fittings. Therefore, special testing was performed to demonstrate that reliable coatings of sufficient thickness could be obtained on surfaces in such poorly accessible areas. Figure 6 and Figure 7 show the comparison between acceptable and unacceptable coating thickness on the internal surface of a molybdenum pressure pickup fitting.

A series of tests was performed in order to determine general design information. Since the coating buildup on the interior of the holes can be expected to be different from that produced on the surface of a sheet, the specific buildup in holes and countersinks was determined. A test panel composed of a corrugation and skin having a large number of mate drilled holes was fabricated and coated to establish that warpage or relaxation during the coating process or during an oxidation check test would not be a problem. Chemical compatibility couples were made and tested on virtually all materials known to contact the coated molybdenum. In general, most materials contacting the W-3 coating were chosen such that they would be chemically compatible within the range of their specific requirements. This was substantiated by testing.

Since it has been shown that the failure of refractory metal coatings is accelerated at elevated temperatures by reduced pressures, all refractory metal coatings used on the vehicle were tested at the respective maximum temperature and minimum pressures. This testing was conducted in the modified Marshall vacuum tube furnace shown in Figure 8. The test procedure involved projecting the specimen into the furnace on a zirconia rod, heating the furnace to the desired test temperature at a pressure of 1×10^{-4} mm of mercury, continuously introducing air or oxygen into the furnace, holding the desired test pressure for a specified time and then cooling the furnace at a pressure of 1×10^{-4} mm of mercury. It was determined that the Chromalloy W-3 coating system on TZM alloy proved satisfactory for 30 minutes at 3000°F and a pressure of 7×10^{-2} mm of mercury. Unalloyed molybdenum tubing produced by power metallurgy techniques and W-3 coated failed within ten minutes under the previously specified test conditions. Figure 9 illustrates the type of failure encountered, Figure 10 illustrates an interesting result obtained in this test. The specimen used was a molybdenum sheathed thermocouple having one end welded shut. It can be seen in Figures 10 and 11 that the coating produced on the welded end proved satisfactory while the coating on the shank portions of the tube failed. The metallurgical structure of the welded tip is no longer that of a sintered material, but is approaching that of arc cast material.

Problems encountered with the molybdenum portions of the vehicle were mainly those of fabrication. The common problem of exfoliation, or delamination, in the manufacture of detail sheet metal parts from molybdenum has plagued this project. The manufacturing techniques of chemical blanking and edge preparation by means of chemical deburring and vibratory finishing have helped to decrease the large number of man-hours usually required in hand finishing. However, delaminations still persist. The time consuming and tedious job of inspection with stereo binocular microscope has proven to be the most satisfactory means of detecting delaminations and

other edge and surface defects before coating. Even so, this method is subject to the severe limitations of individual interpretation and operator fatigue. This, coupled with the necessity of producing large numbers of parts, has proven to be rather troublesome. Some coated detail parts having edge delaminations have been judged to be flight-worthy based upon the results of oxidation check testing at 2000°F for 30 minutes in an air atmosphere furnace. Since the test temperature is relatively low, uncorrectable damage to defective parts usually does not occur, and the degree of self-healing exhibited at this temperature is small enough to afford a measure of conservatism to the test. Since service temperatures are in the range of 2800° to 3000°F, the silicide coatings show a much higher degree of self-healing ability; however, reduced pressure effects now under study may modify this position. Through the testing of large numbers of detail parts, a qualitative understanding of which defects will or will not self-heal has been obtained. Future plans call for the testing of typical defects in a molybdenum coating system in an attempt to quantitatively study this problem. Qualitatively speaking, delaminations and other edge defects are considerably less critical with the Chromalloy W-3 coating system than originally believed at the outset of this program. However, a major concern in making use of parts with delaminations is their susceptibility to handling damage.

The coating work performed by the Chromalloy Corporation has been quite satisfactory. The only difficulty arising has been with one panel which, upon the completion of the second coating cycle, showed a scaly condition in a localized area (see Figure 13). Clean-up of this area and subsequent reprocessing made this scaly condition more generalized. Oxidation check testing showed the coating in these scaly areas to be quite inferior. The specific cause for the condition of this panel has not yet been determined. One technical explanation is that it was caused by generalized surface contamination between coating cycles and that the contamination probably occurred in M.A.C. facilities. This incident illustrates the fact that fabrication and coating of such assemblies is, to a large measure, an art rather than a science.

COLUMBIUM STRUCTURES OPERATING OVER 2500°F

The forward bulkhead and the aft leading edges along with their associated fittings, rivets, etc., comprise the major portion of coated columbium parts operating over 2500°F. The forward bulkhead is approximately 13 inches wide and 12 inches tall and it is the portion of the primary structure through which the nose assembly is attached to the vehicle. The aft leading edges shown in Figure 12 are integrally stiffened sections of Cb-1Zr alloy, have a 4-inch radius, and are approximately 14 inches long. Pressure pickups for these leading edges are unalloyed columbium tubing which is welded into the leading edges before coating.

The choice of a columbium coating vendor for these assemblies was a long, difficult task. It is discussed here in order to demonstrate certain weaknesses in commercially available columbium coating systems. These test results should not be used as a basis for comparison of columbium coating vendors since the test conditions are specific to the requirements of M.A.C. This testing has already initiated improvements in the general state-of-the-art of columbium coatings since several shortcomings have been subsequently removed or significantly improved by the coating vendors after the shortcomings were revealed.

Initial coating tests were made in the three following distinct areas:

(a) Torch testing was performed to obtain qualitative understanding of the refractoriness of the coating system by heating specimens for 10-minute time increments in 100°F temperature increases between 2600° and 3100°F.

(b) Coupon testing was carried out in an air atmosphere furnace at 2500°F for five one-hour cycles. Coupons were of Cb–5Zr, Cb–1Zr and unalloyed columbium tubing.

(c) The metallographic sectioning of tube samples which were 1/8" O.D. and 6 inches long and contained two right angle bends was done to determine the ability to coat internal surfaces.

Participation in the second phase of the testing was restricted to three coating vendors and followed the following types of testing:

(a) Oxidation testing for two hours at 2800°F, 2000°F and 1400°F. Again, the alloys of Cb–1Zr, Cb–5Zr and unalloyed tubing were used for specimens.

(b) Additional tubing samples to determine internal coating quality.

(c) Stepdown oxidation cycles for 30 minutes at 2800°F, 30 minutes at 2500°F, 30 minutes at 1400°F. The three previously mentioned alloys were again used.

The purpose for running the stepdown oxidation tests was an attempt to approximate the expected conditions when the vehicle is heated quite rapidly to the maximum temperature and then cools off relatively slowly.

Table 1 summarizes the results of this testing and Figure 14 shows typical failures in stepdown oxidation tests. It is evident that no vendor was able to satisfy the requirements in either the initial or final testing. The TAPCO coating system, which showed promising results in the oxidation testing portions, had not yet demonstrated an ability to realiably coat the tubing. In addition, TAPCO did not have operating facilities that would accommodate the forward bulkhead. However, in light of the problem involved in improving the silicide coatings, it was decided that the most reliable end product would be achieved by appropriate redesigns to accommodate the the TAPCO process and facilities. The forward bulkhead was therefore redesigned in two pieces and the tubing in the leading edge segments was reduced to approximately three inches in length, which the TAPCO process could reliably protect.

The same general type of testing as previously described in the molybdenum section was conducted with satisfactory results. In addition, testing has been initiated to supplement oxidation tests in which the specimen simultaneously experiences the time, temperature and pressure conditions anticipated in the flight. It is believed that this testing will yield more understanding of the nature of the failures experienced in the low temperature range after that system has experienced an elevated temperature exposure.

Generally, the results experienced with the TAPCO coating have been satisfactory. However, there have been two leading edge assemblies returned to M.A.C. with a scaly surface conditions(see Figure 15). TAPCO expressed concern about these assemblies and suggested that M.A.C. perform appropriate testing to insure their quality. Fortunately, some TAPCO-coated

TABLE I

SUMMARY OF TESTING PERFORMED TO AID IN THE SELECTION
OF A COLUMBIUM COATING VENDOR FOR STRUCTURES OVER 2500°F

COATING VENDOR	INITIAL OXIDATION RESULTS SATISFACTORY (2500°F)	COATING THICKNESS IN TUBING SATISFACTORY	ABSENCE OF SUBSTRATE EMBRITTLEMENT SATISFACTORY	STEP DOWN OXIDATION RESULTS SATISFACTORY	2800°F OXIDATION RESISTANCE SATISFACTORY
Company 1	No	No (2)	No	Not Run	Not Run
Company 2	No (1)	Yes	Yes	No	Yes
Company 3 (4)	No	No	Yes	Not Run	Not Run
Company 4	Yes	No (3)	Yes	No	Yes
Company 5	Yes	No (3)	Yes	Yes	Yes

(1) Later results were satisfactory.

(2) Ability to coat tubing had been demonstrated on molybdenum tubing.

(3) Improvements were made in later stages of the evaluation.

(4) Results were unusual enough to render the validity of the test questionable.

(5) Torch test results showed no significant differences.

shims were available with an analogous surface condition present. These shims failed in oxidation within two hours at 2500°F, demonstrating that this condition was quite inferior to the standard coating quality. The leading edges were disassembled and returned to TAPCO for complete reprocessing. Through extensive testing, TAPCO has been able to duplicate this surface condition, thereby determining the cause and eliminating the problem. Again, this demonstrates the complexity of consistently applying uniform and satisfactory coatings. The TAPCO coating is generally recognized as being one of the best commercially available columbium coatings and is considered to be one of the most standard and stable systems available. One might be surprised to find temporarily unexplainable coating conditions occurring in such a process. This might serve as a warning to newcomers in the refractory coating business that patience and caution are necessary.

One additional problem was encountered in the coating of columbium sheath thermocouples containing W–5Re versus W–26% Re thermocouple wires. Recrystallization of the W–5%Re wire occurred and so embrittled the wire that junctions to it could not be made. This is not the fault of the TAPCO coating since M.A.C. knew of the high processing temperature required. However, in this instance, it has proven to be a shortcoming of the TAPCO process.

COLUMBIUM STRUCTURES OPERATING AT OR BELOW 2500°F

Columbium structures operating at or below 2500°F are protectively coated with the LB–2 system, an aluminum cold slurry process originally developed for M.A.C. by the General Electric Company. Briefly, the process involved the application of an aluminum alloy to the columbium substrate by means of an organic vehicle system and painting techniques. The structure is then heated in an argon atmosphere to approximately 1900°F for one hour. During this time the aluminum and columbium react to produce a protective coating which is primarily columbium aluminide. The LB–2 was originally developed for the Air Force sponsored refractory structures program which found ultimate utilization in the protection of a fin-rudder structure. This fin-rudder structure, shown in Figure 16, was quartz lamp heated to 2500°F for one hour and simultaneously loaded at 150% of the design loads. This successful program formed the basis for the selection of the LB–2 system for this vehicle.

The portions of the vehicle which are protectively coated with the LB–2 system are as follows:

(a) The aft lower body panels – these are flat single faced corrugated assemblies which are resistance welded together and protectively coated after completion of the assembly procedure. These panels are shown in Figure 17.

(b) The side beam assembly – this is the primary longitudinal structure to which the floor, upper body and leading edges are attached. The side beam, as shown in Figure 18, is partially resistance welded and partially rivited together. The areas containing the rivets receive a partial application of the LB–2 slurry before the two halves are joined.

(c) The aft beam and truss assembly – as shown in Figure 19, this is a set of trusses and angles which comprise the primary structure to which the aft bulkhead, upper body, aft leading edges and floor assemblies are attached. As in the case with the beam assembly, the aft beam and truss is partially slurry coated prior to installation of the rivets.

(d) The forward upper body – this is a modified truncated conic section of single faced corrugated design. It has two longerons on the inside and a reinforced zee section connecting the corrugations to the skin on the bottom side, thus closing the corrugation. This assembly, shown in Figures 20, 21 and 22 is approximately 29 inches in width at the major diameter, 10 inches in width at the minor diameter, and approximately 42 inches long. It is completely fabricated prior to the application of the coating.

(e) Other miscellaneous pieces – these are an antenna assembly which is mounted on the aft upper body, fairings between leading edges and the upper body assembly, washers, fittings, keepers, columbium sheathed thermocouples, etc. All the parts are of D–14 alloy (Cb–5Zr) except the columbium thermocouple sheaths which are unalloyed.

The results of the first attempt to protectively coat a curved single faced corrugated test assembly representing the forward upper body are illustrated in Figure 23. It can be seen that this attempt did not produce successful results. Figure 24 shows the extensive coating buildup on the exterior surfaces, insufficient buildup on the interior of the corrugations, and little, if any, coating on the faying surfaces. In addition to the obviously undesirable condition of substrate loss through oxidation, the panel became warped because of formation of columbium pentoxide on the faying surfaces. This condition was considered completely intolerable because of the catastrophic results which would occur if an edge were to warp in flight, protrude into the airstream, and produce extremely high temperatures in such a local area. Figure 25 illustrates the magnitude of such warpage that occurred in the faying surface of a rivited joint which failed during thirty minutes of oxidation testing at 2500°F. It was concluded that a positive means of uniformly coating the interior of the corrugations and faying surfaces had to be developed.

The two solutions considered to this problem were electrophoretic deposition of the columbium aluminide coating or vacuum inpregnation techniques using the present LB–2 slurry. Because there was doubt about the degree of success which could be expected on such a complex structure by the use of electrophoresis, and because of the relative simplicity of the vacuum impregnation techniques, the initial studies were made with the vacuum impregnation method. In order to have reasonably representative yet economical specimens with which to work, several specimens like the 3-inch by 6-inch single faced corrugated test specimen shown in Figure 26 were designed and fabricated. These specimens contained a single corrugation, one skin, and two end reinforcing zee sections to close off the ends of the corrugations.

These specimens were fabricated and coated under a wide variety of manufacturing and processing sequences. In general, the best results were obtained by pickling the detailed parts, assembling under white room cleanliness conditions, hand sanding copper contamination and oxidation from the spot welds, solvent scrubbing and then LB–2 coating. The LB–2 coating is effected by vacuum impregnation of the first slurry application at approximately 5 psia, force drying at 120°F for one hour, reapplication of the slurry at ambient pressure followed by diffusion at 1900°F for one hour. Should cleanliness conditions require an additional short acid pickle prior to coating, a technique of pickling assemblies as assemblies has

been evolved. This procedure, applicable to assemblies containing no LB-2 coating, involves a 24-hour hot water rinse for the purpose of diffusing any trapped acid products back out of the poorly accessible areas. The key to success of the assembly pickling procedure appears to be an initial rinse in distilled water. This fills the faying surfaces with distilled water by the capillary forces involved, rather than filling them with an acid of comparatively high concentration. Figure 27 shows one of six curved upper body test sections which were fabricated, coated and furnace tested at one atmosphere in order to substantiate the quality of the pickling and coating procedures derived.

In order to effect the vacuum impregnation coating on the required production parts, the 160 gallon slurry tank and other support equipment shown in Figures 28, 29 and 30 were constructed. All of the parts except the forward upper body are manually dipped. Because of the size and complexity of the forward upper body assembly and the obvious difficulties of hand dipping, a motor driven spit was built into the dip tank to allow a constant immersion and exit rate of this assembly and to thereby obtain the desired slurry coating uniformity. All of the LB-2 coated parts for the first vehicle have now been successfully coated as have most of the parts for the second vehicle.

Through several months of working with four different batches of LB-2 slurry in the laboratory, it was discovered that the top coat was subject to aging. This aging effect is somewhat dependent on the amount of use which is made of the slurry. However, in each batch of the top coat used, the effect has been noted after a minimum time of approximately six weeks and a maximum time of approximately three months. Figure 31 illustrates this aging effect. The "as diffused" coatings show no apparent difference by visual observation, but upon experiencing oxidizing environments, the exterior oxide layer becomes white and scaly. Oxidation testing of such coatings at 2500°F shows no appreciable decrease in coating life; however, in the area of 1400°F, the coating life is substantially reduced. Because of this reduction in low temperature oxidation resistance and the formation of an exterior oxide layer (aluminum oxide) with a low emittance, it was considered to be intolerable.

Based on the results of a MAC sponsored LB-2 study program, a test was initiated to prove that the top coat (30-LN paste) could be replaced by multiple applications of the base coat slurry (LS-866 paste, 88Al-2Si-10Cr alloy). This test required that oxidation tests be made on each alloy to be used on the vehicle at both 2500°F and 1400°F. In addition, specimens representing critical configurations, such as tubing and corrugated assemblies, were evaluated in order to determine that the double base coat modification was satisfactory. The results of these tests, in all cases, showed the double base coat application to be equal to, or better than, the base coat – top coat combination in protecting both the alloys and configurations involved. In addition to resolving the problem of the aging effect in the top coat slurry and the obvious economic advantage of having to deal with only one slurry in production facilities, it has been found that a more uniform and reliable coating system is produced.

The specific reason for the aging effect was not determined since the top coat was found to be unnecessary. Initial attempts to renew the usefulness of the top coat slurry by restoring

the original chemical balance of the four-part organic vehicle was unsuccessful. Nevertheless, the destruction of this chemical balance through evaporation of the solvent appears to be the only logical reason for this effect since oxidation, or destruction of aluminum through other chemical reactions is very unlikely. It has been noted on photomicrographs of coatings produced with slurries in the advanced stage of this aging effect that a high degree of porosity in the exterior portions of the coating exists. The conclusion is that sub-surface coating oxidation occurs to produce the heavy scaly exterior aluminum oxide layer rather than a thin tenacious layer. Large batches of the base coat slurry have been in use at M.A.C. for approximately one year with no evidence of this aging effect.

Another interesting modification of the basic LB-2 slurry process has been in the diffusion temperature. The occurrence of problems with the degradation of physical properties of the D-14 alloy due to coating repair cycles made it desirable to reduce the diffusion temperature. Expansion and evaluation of previously M.A.C. sponsored work on the effects of time and temperature on the diffusion cycle for the LB-2 process showed that coatings of equal quality could be produced at 1700°F for 90 minutes. The major difference in the diffusion temperatures is the nature of the surface produced. The coatings produced using the multiple base coat application modification and diffusion at 1700°F produce a surface containing a large number of small metallic nodules of aluminum. Subsequently, oxidation of such surfaces at ambient pressure produces tiny nodules of aluminum oxide which can be expected to lower the emittance of the system (see Figure 31). It has been found that a short pickle in hydrochloric acid will remove these aluminum nodules. Low pressure testing under the previously stated conditions produces a surface which is darker than that of a coating diffused at 1900°F and which has been similarly treated. (Testing is presently being conducted to determine the differences in emittance of the two coating conditions). Since the coatings diffused at 1700°F appear to be equal, or superior, in protective qualities to the coatings diffused at 1900°F, all repair cycles are presently being performed at 1700°F. The metallic nodules are not considered to be a problem since they can easily be removed if high pressure oxidation exposures are required, or they can be advantageously left on the surface if low pressure oxidation conditions are required.

One problem with the LB-2 system which has resisted all attempts at solution has been the bare spot problem. This problem is not new as General Electric experienced the same phenomenon on the columbium structures program. Approximately one-half of the assemblies coated emerge from the process with a few spots which are void of the coating. The spots give the impression that the aluminum alloy present in a molten form during the diffusion cycle simply does not wet the columbium in local areas. It is believed that the basic cause is the lack of cleanliness prior to coating. A geometric effect has also been noted but is partly related to the cleanliness. Areas affording particular difficulty are those whose geometry is such that contamination can easily become trapped. These same areas are the hardest to effectively clean by solvent scrubbing. The bare spot problem has proven to be more of an aggravation than a technical difficulty to this project since an effective repair procedure is available. This repair procedure requires alumina grit blasting the area needing repair and reapplication of the LB-2 slurry by brushing or dipping followed by a diffusion cycle. This procedure has always made an effective repair.

CONCLUSION

This paper has briefly described the refractory metal coating systems utilized on a typical hypersonic glide re-entry vehicle. It has become obvious to M.A.C. that the successful completion of such a project requires the integration of design, fabrication and coating processes. Since each project has its individual design peculiarities and final mission, a relatively large amount of testing must be expected. As production of a refractory metal structure having the complexity of a glide re-entry vehicle proceeds, the infancy of the refractory metal coating technology becomes very obvious. As a general rule, the application of refractory metal coating technology to the aerospace field has been greatly oversimplified and a realistic understanding of the problems involved has not been demonstrated. It is believed that the basic direction and philosophies of protecting refractory metal structures will have to be modified before they can be efficiently utilized by the aerospace industry.

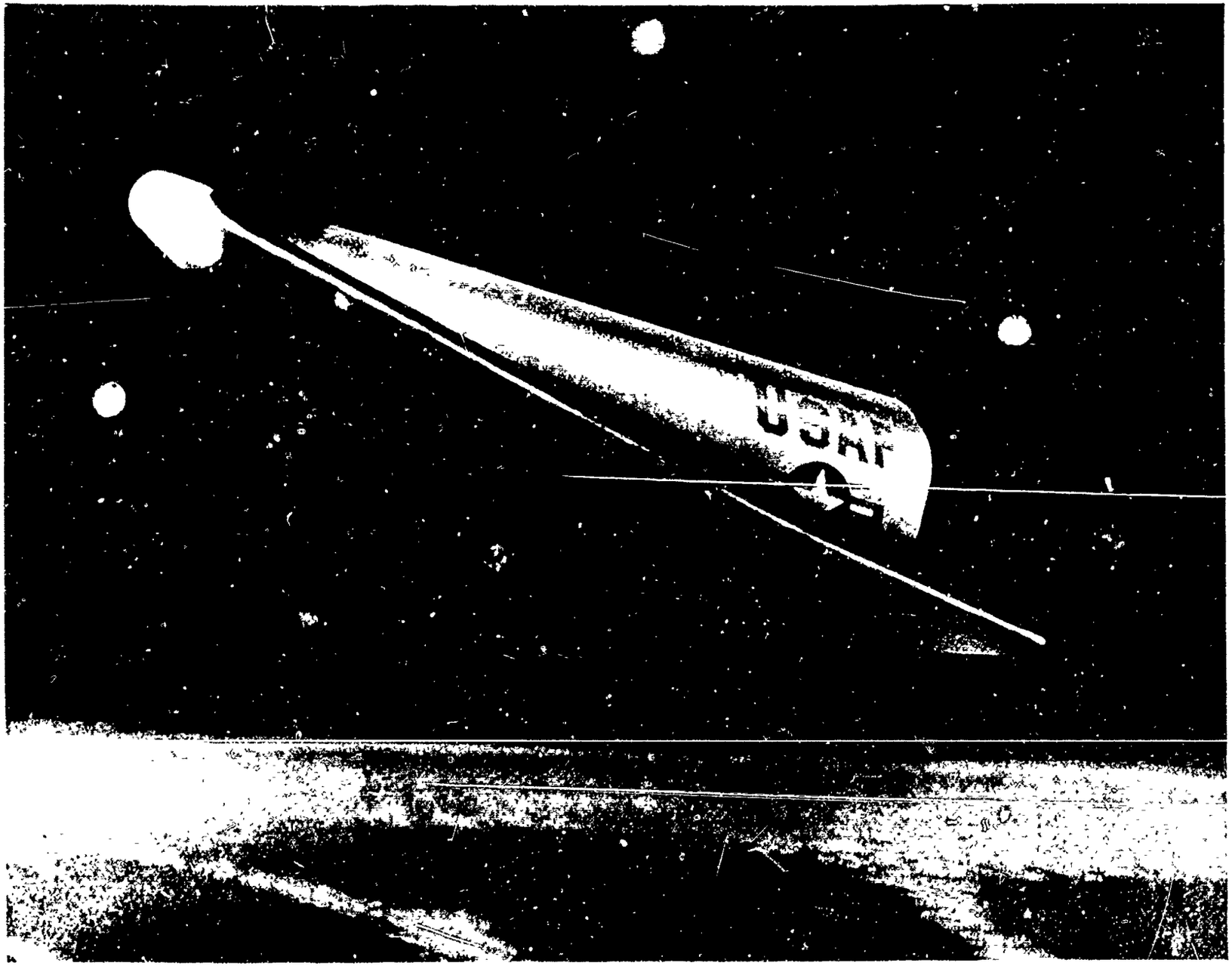

Figure 1 – Artists Concept of the Typical Hypersonic Glide Re-Entry Vehicle Presently Being Fabricated by McDonnell.

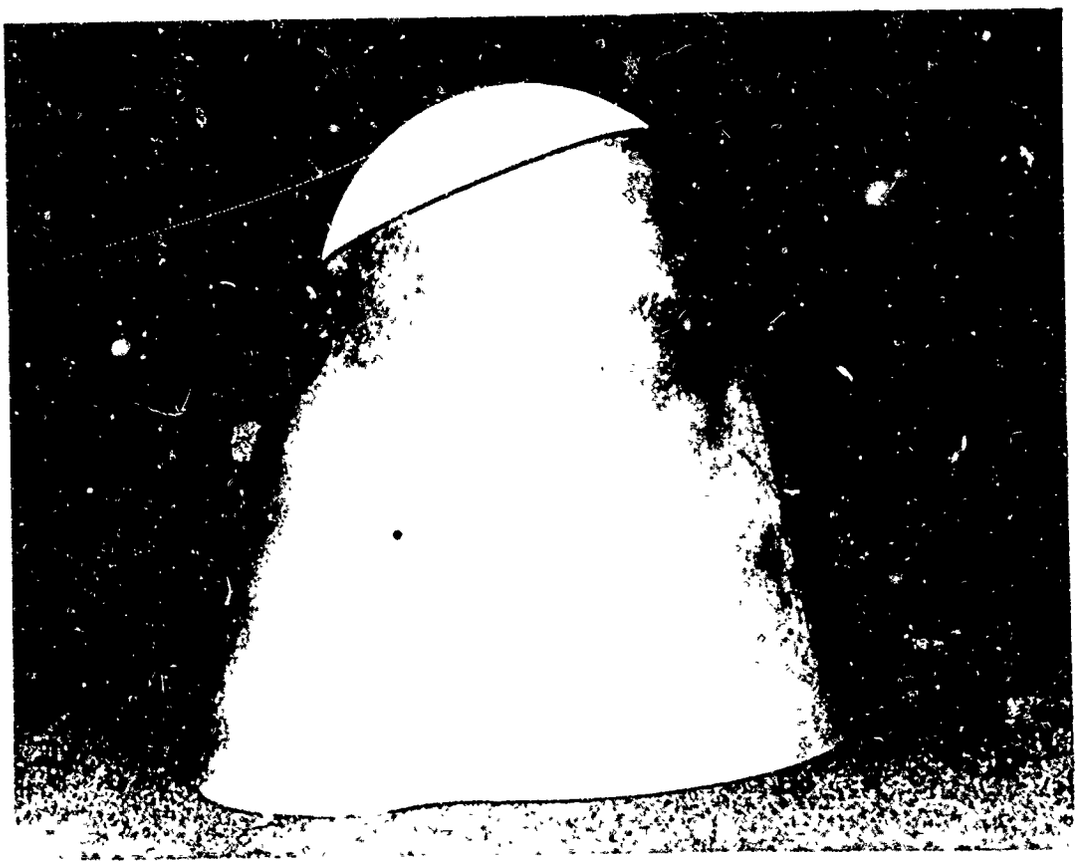

Figure 2 – Nose Cap Assembly Showing Molybdenum Skirt and Zirconium Oxide Skull Cap.

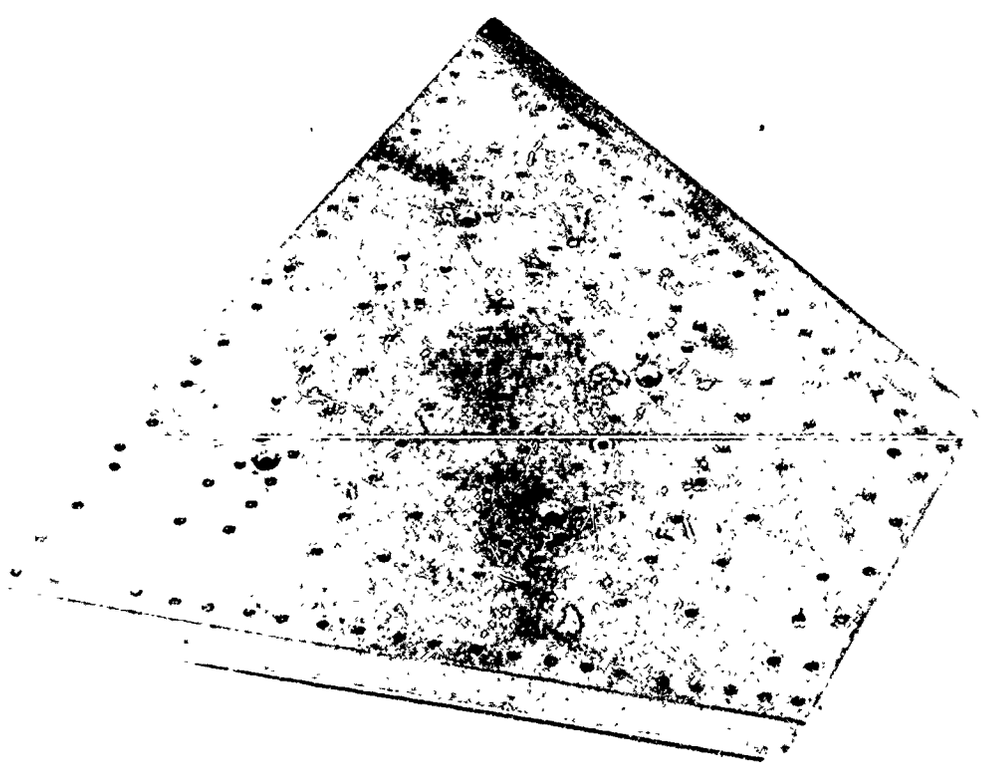

Figure 3 – One of the Six W–3 Coated Molybdenum Lower Body Heat Shield Panels.

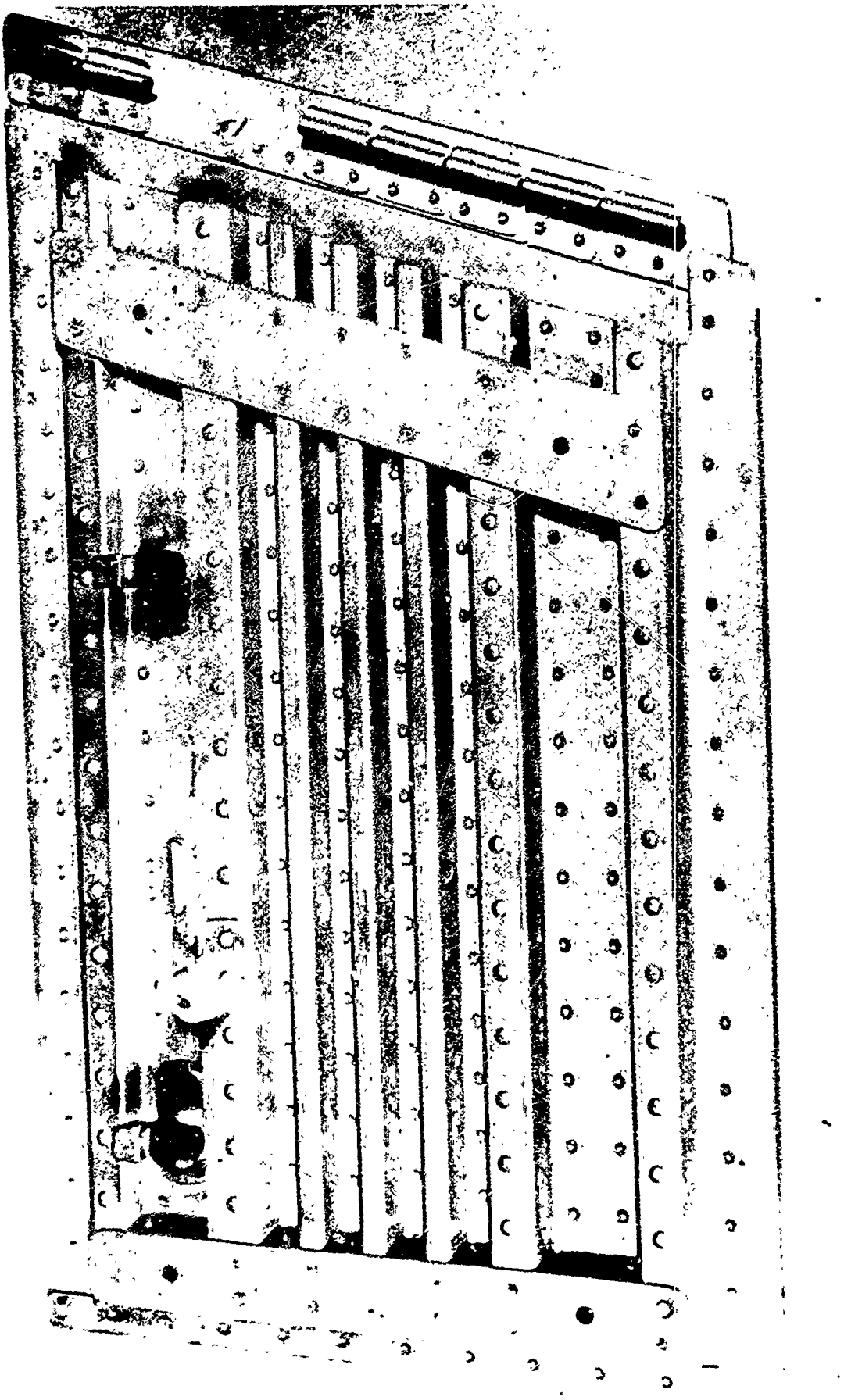

Figure 4 – Inside of a W–3 Coated Molybdenum Heat Shield Panel.

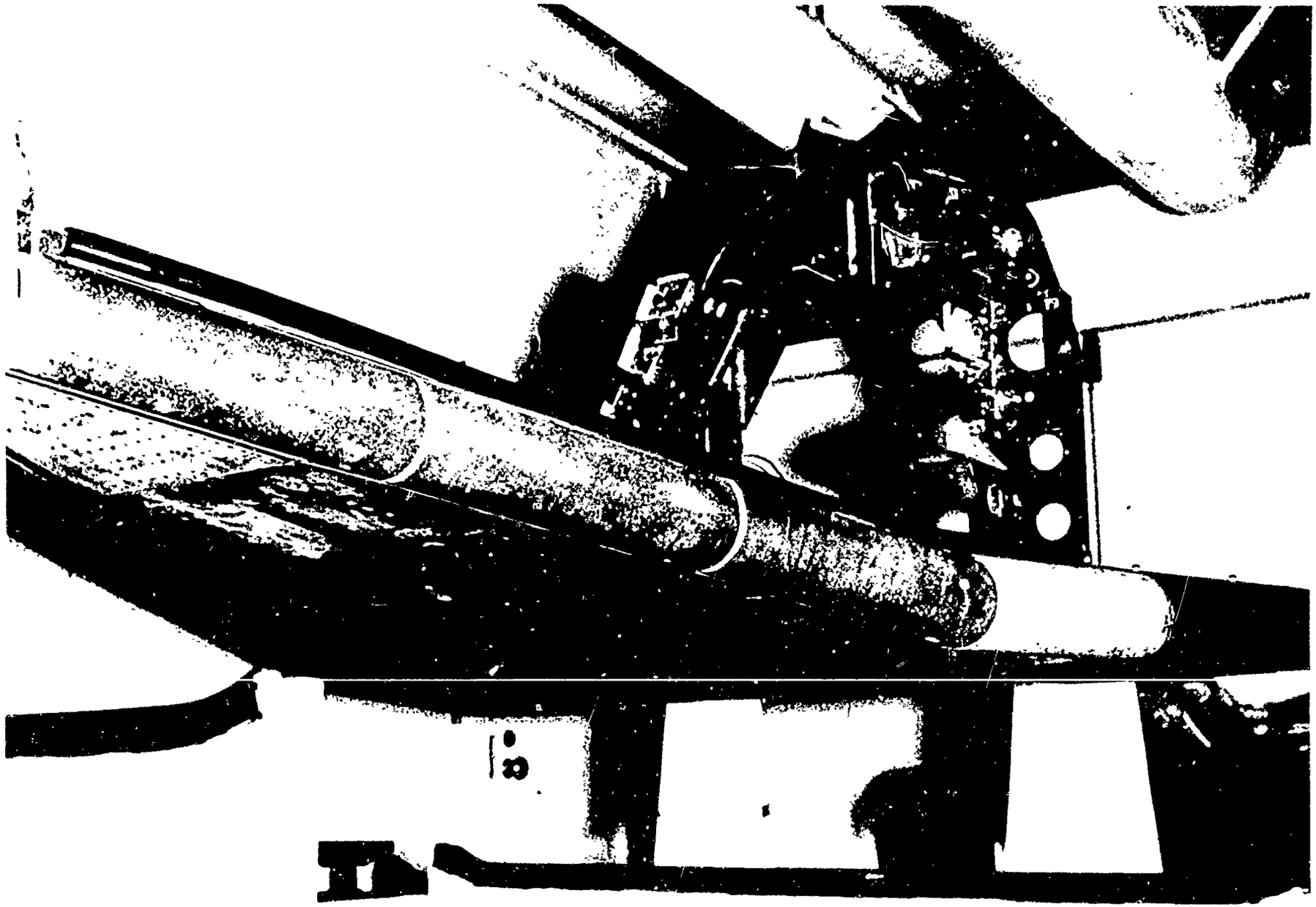

Figure 5 – Lower Body Panels Installed on Vehicle. Forward Six Panels are W–3 Coated Molybdenum and Aft Panels are LB–2 Coated Columbium.

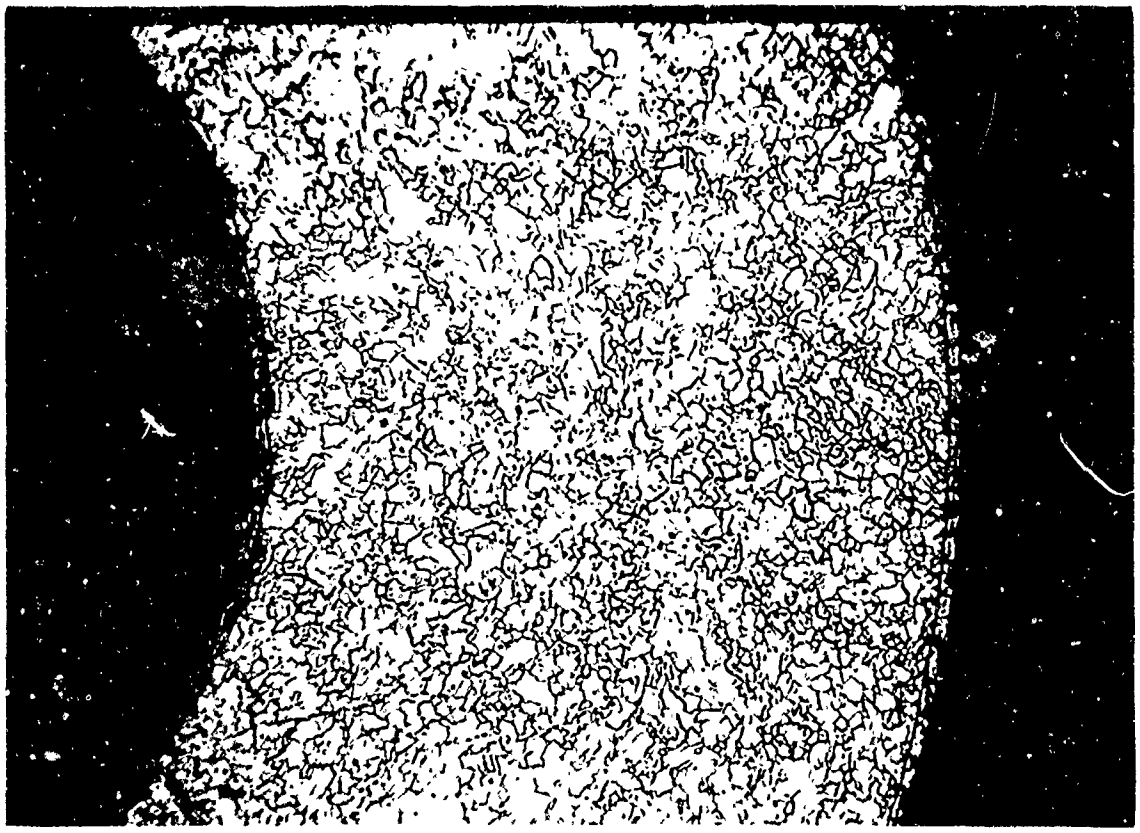

Figure 6 – Unsatisfactory Silicide Coating Thickness on Internal Surface Surface of a Molybdenum Pressure Pick-up Fitting. Mag. 100X.

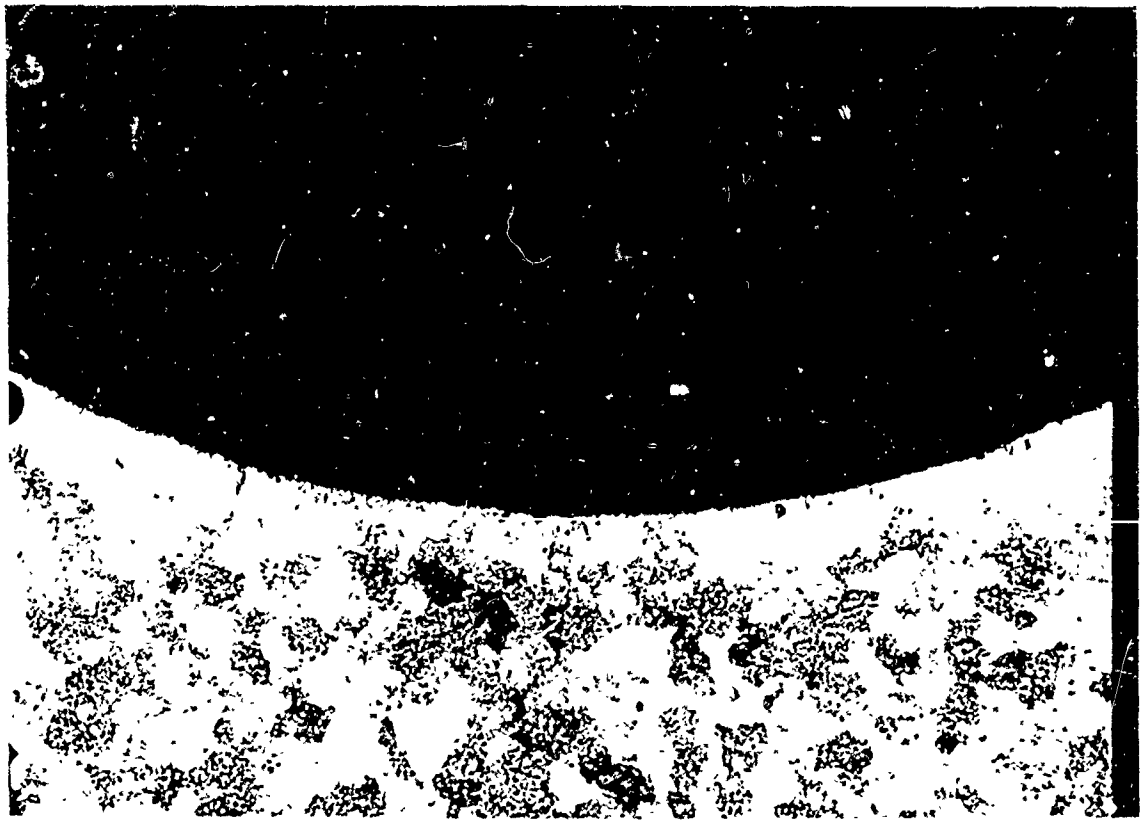

Figure 7 – Satisfactory Silicide Coating Thickness on Internal and External Surfaces of a Molybdenum Pressure Pick-up Fitting. Mag. 50X.

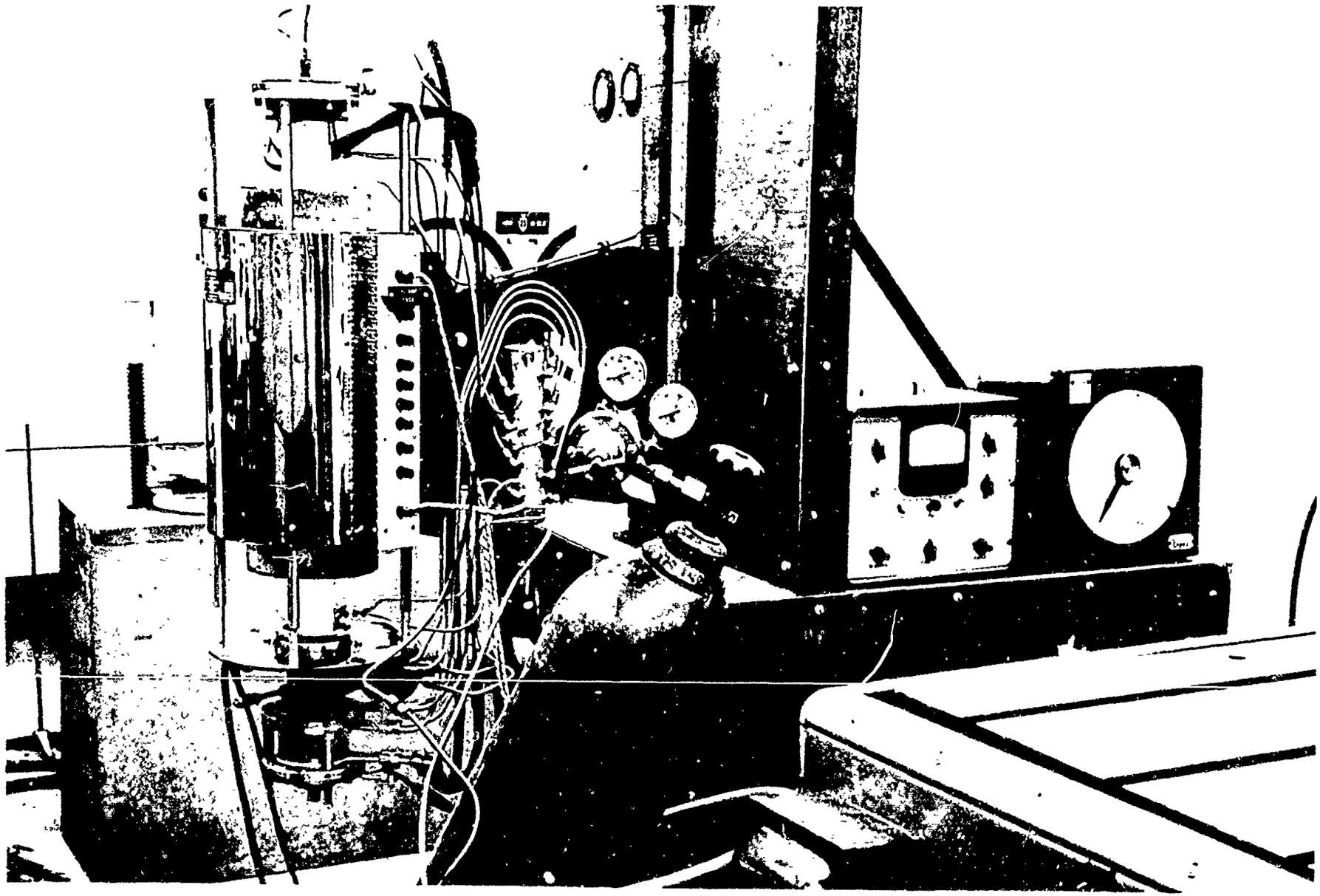

Figure 8 – Elevated Temperature – Reduced Pressure Test Apparatus Capable of 3000°F and 2×10^{-4} mm Hg Total Pressure.

Figure 9 – W–3 Coated Unalloyed Sintered Molybdenum Thermocouple Sheath which Failed Within 10 Minutes at 3000°F and 7×10^{-2} mm Hg Total Pressure of Oxygen. Mag 500X.

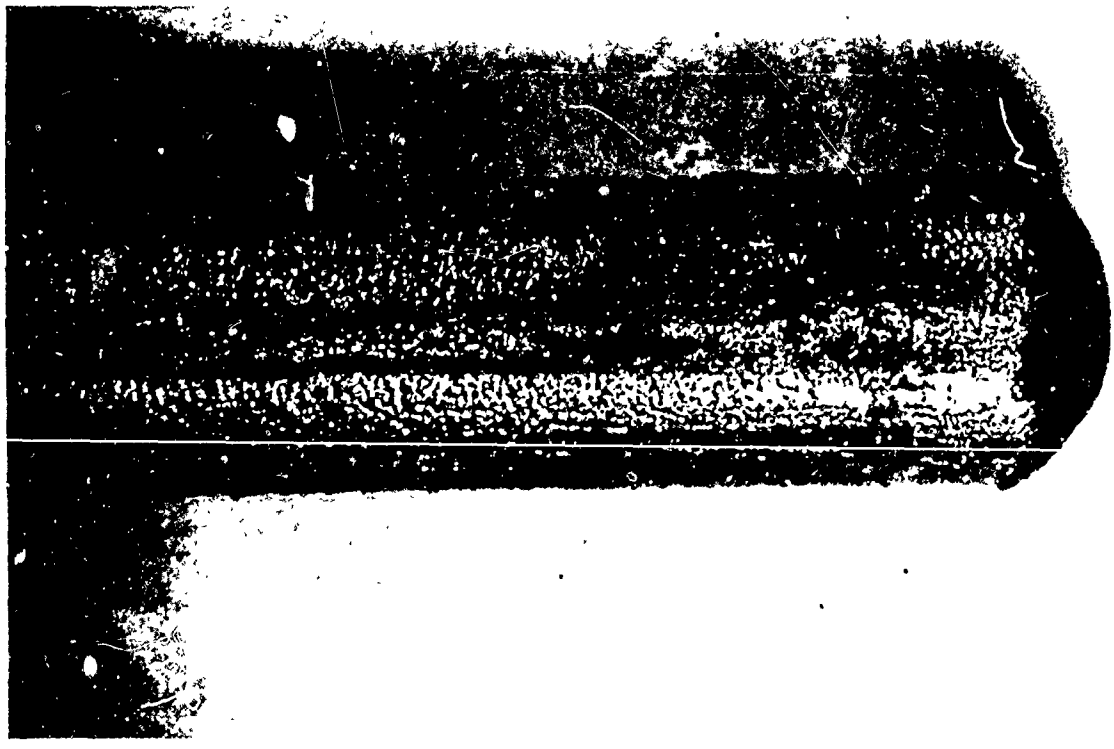

Figure 10 – Over-all View of Specimen Shown in Figures 11 and 13. Note the Differences in the Protectiveness of the W–3 Coating on the Welded Tip and Sintered Shank. Mag 15X.

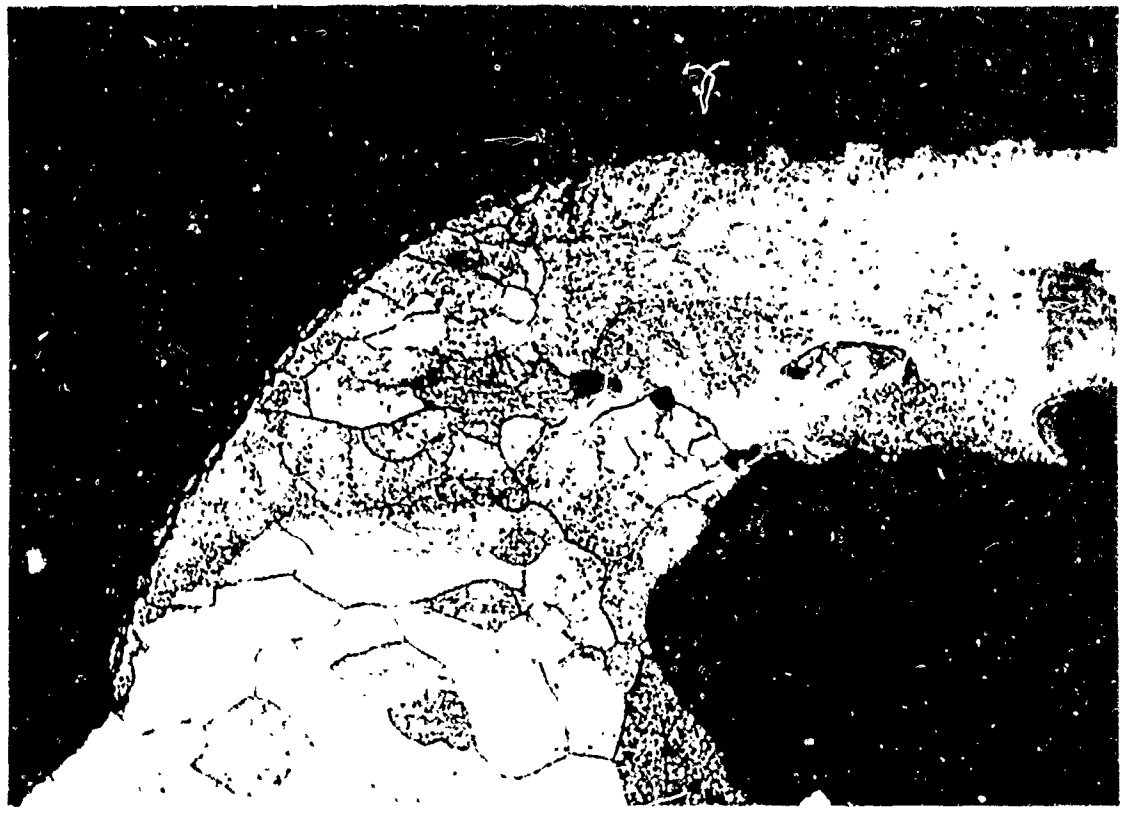

Figure 11 – Photomicrograph of Specimen Shown in Figure 12 at the Transition Point Between the Shank and Welded Tip.

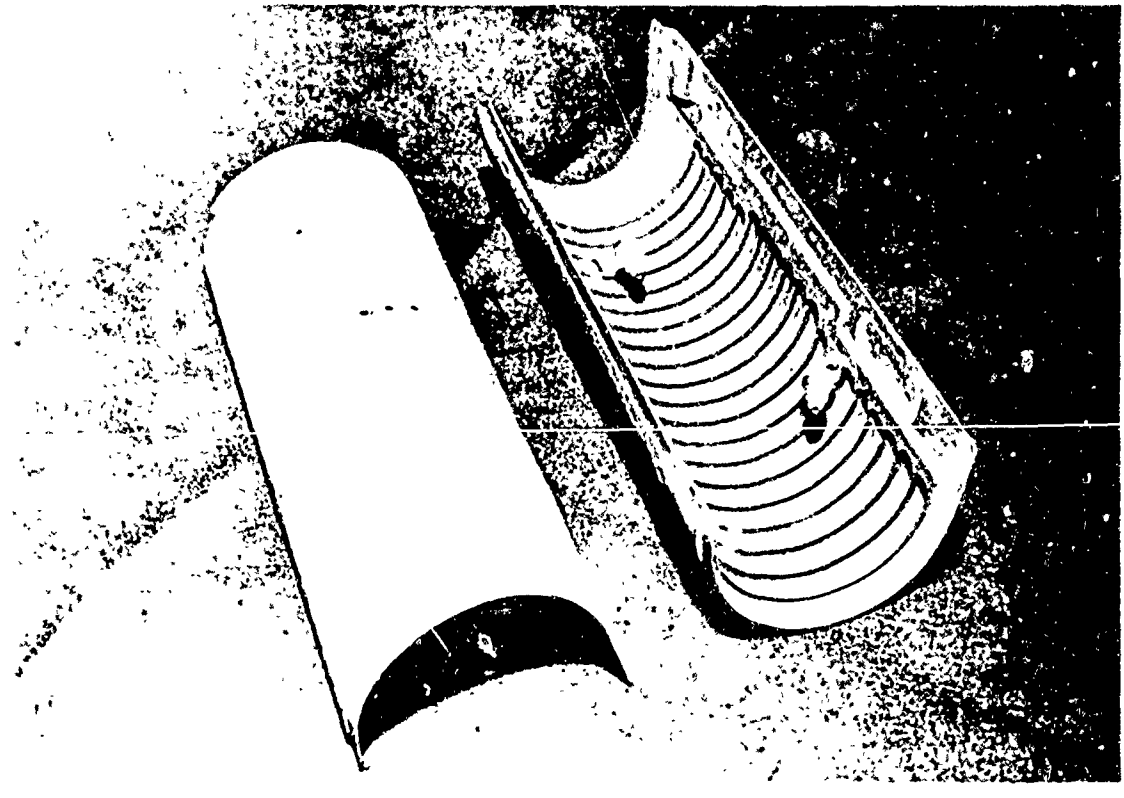

Figure 12 – Columbium Aft Leading Edge Assemblies Showing Internal and External Features.

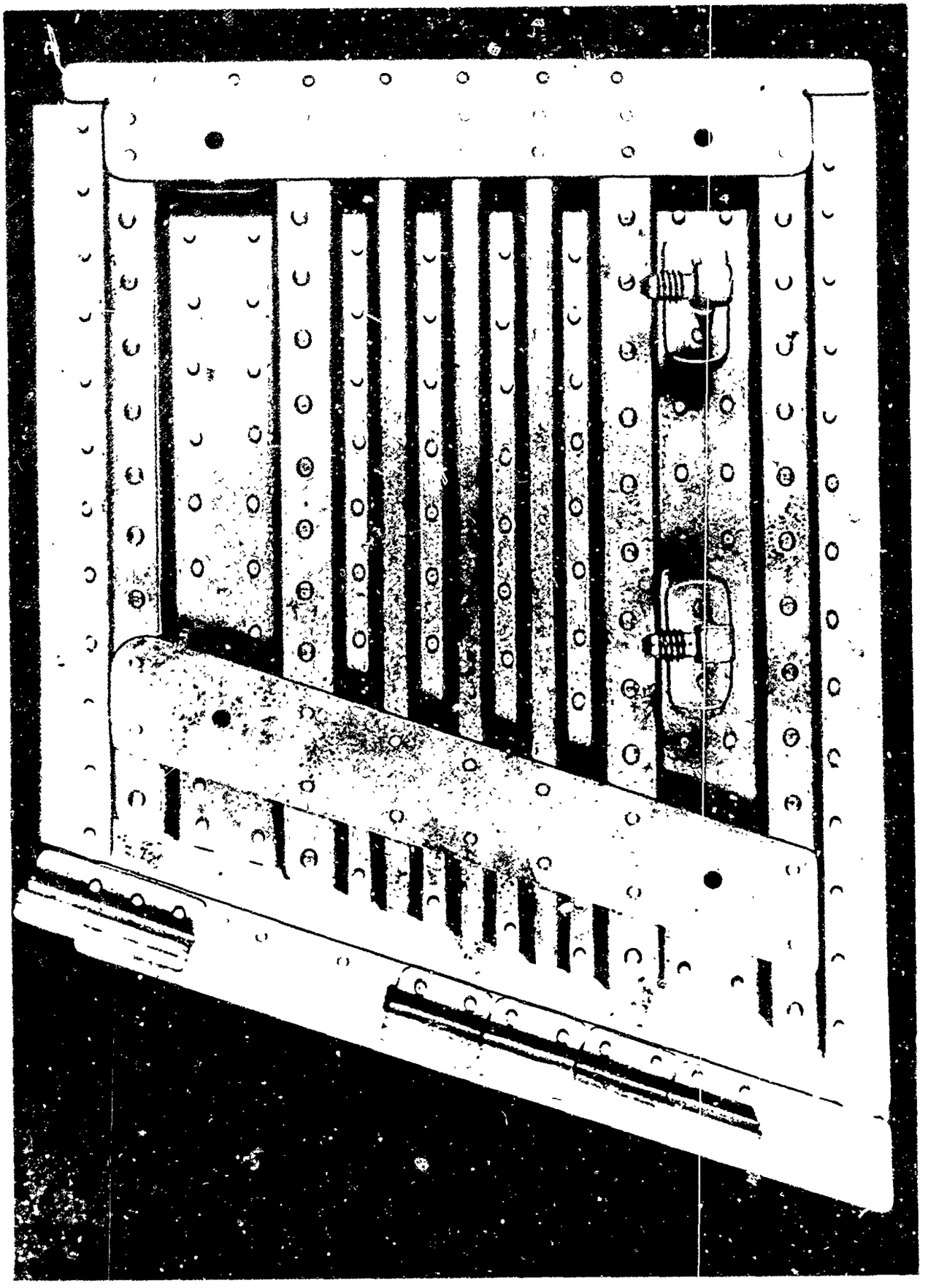

Figure 13 – Scaly W–3 Silicide Coating on a Molybdenum Heat Shield Panel.

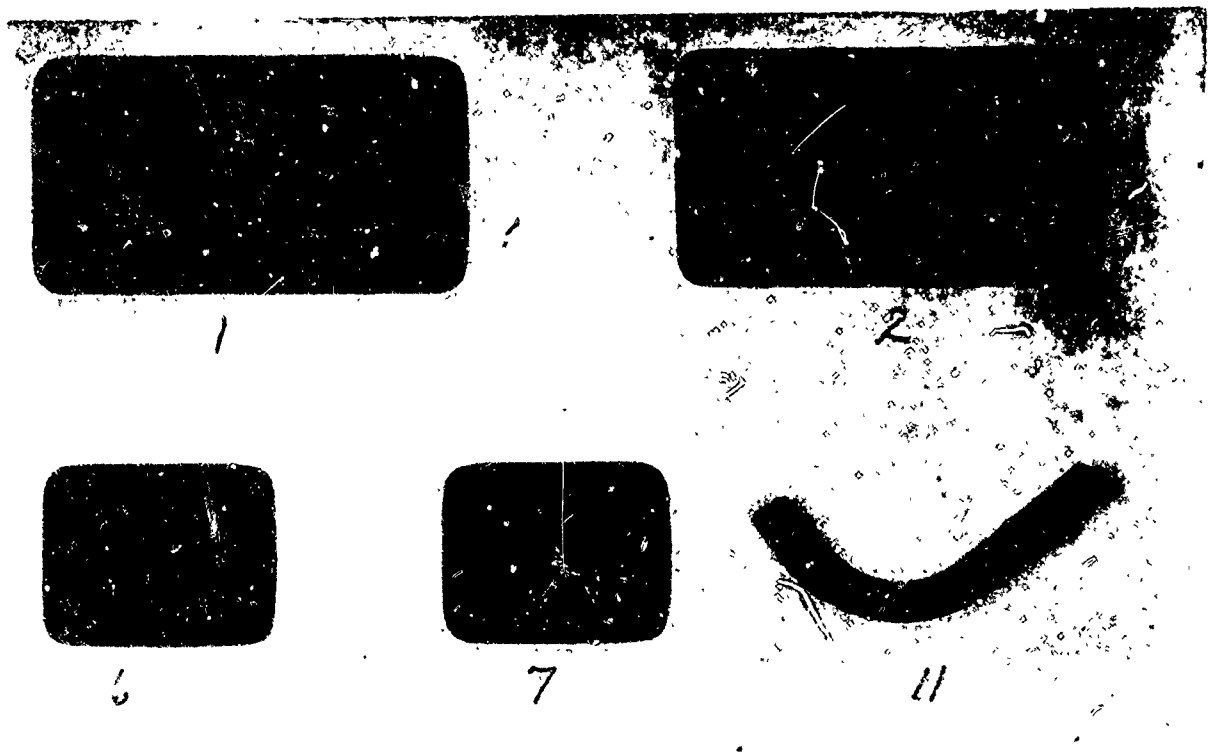

Before Testing

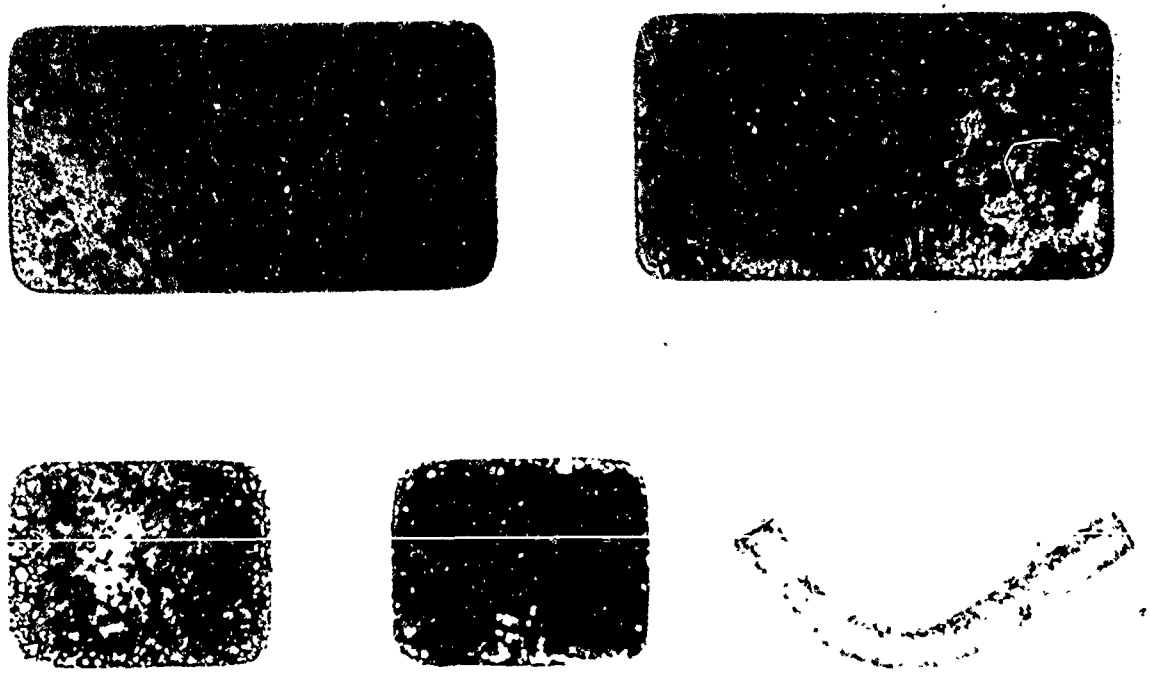

After Testing

Figure 14 – Silicide Type Coating on Columbium Alloy Specimens After Oxidation Testing for 30 Minutes at 2800°F and 30 Minutes at 2500°F.

Figure 15 – Scaly TAPCO Coating on a Columbium Leading Edge Assembly.

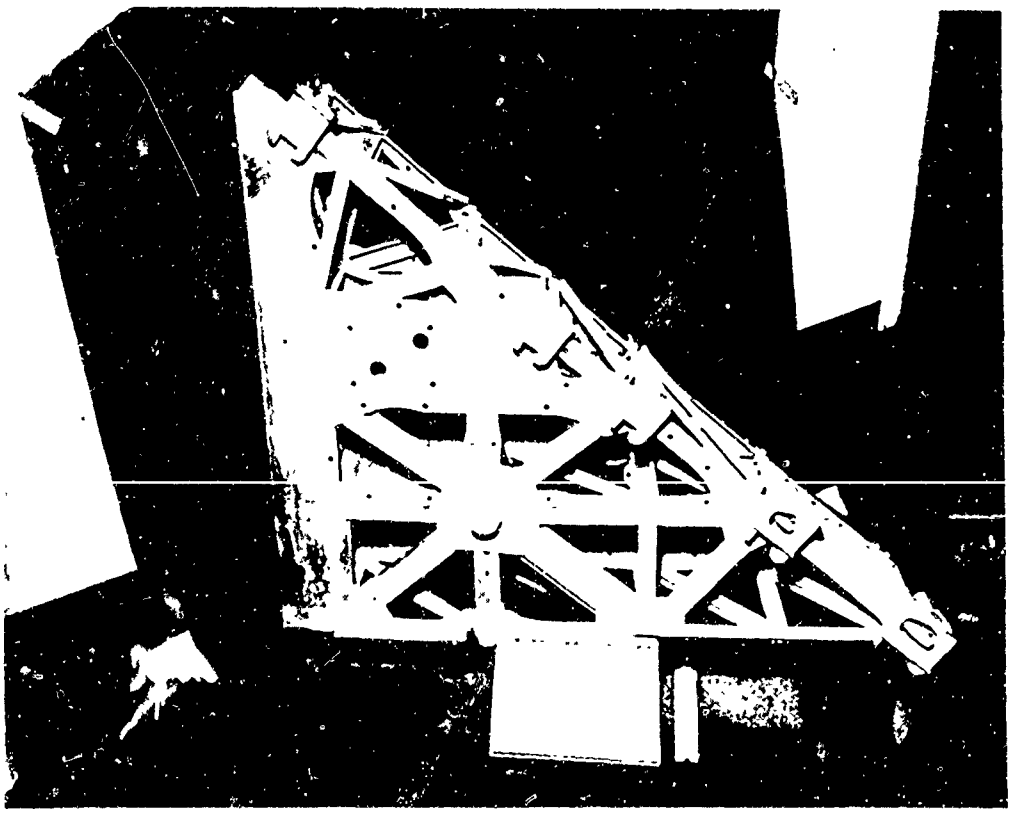

Figure 16 – Fin and One Panel Portions of the LB–2 Coated Fin-Rudder Structure.

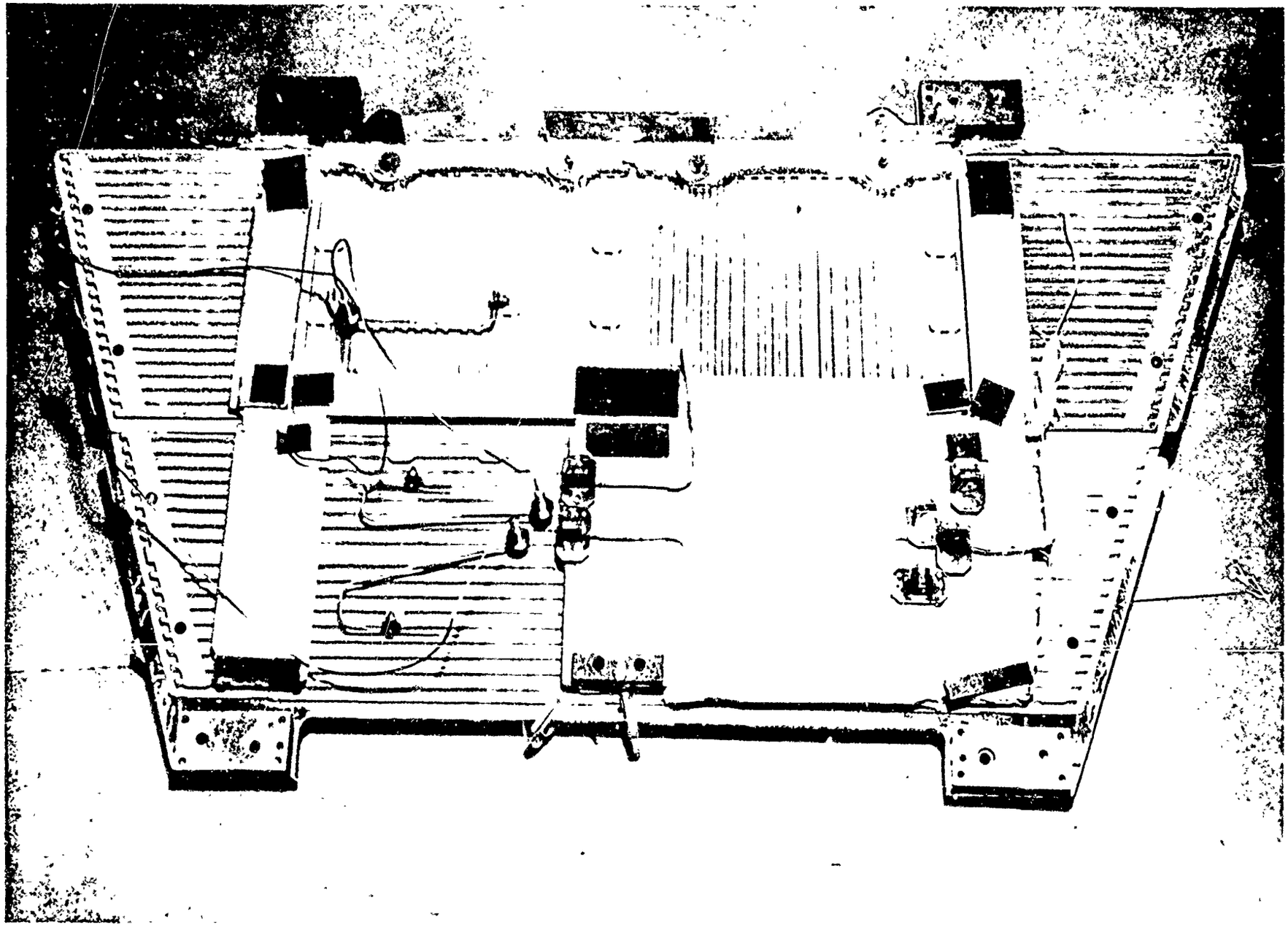

Figure 17 – LB–2 Coated Columbium Aft Lower Body Panels.

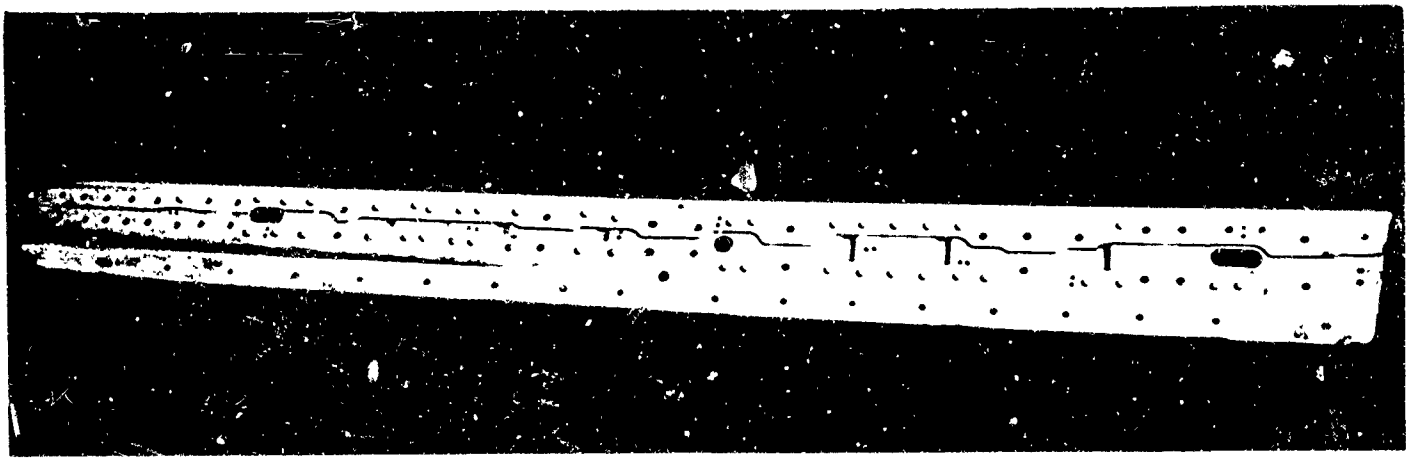

Figure 18 – LB–2 Coated Columbium Side Beam Assembly. This Test Unit has Been Exposed to 2500°F for One Hour in an Air Atmosphere. Mag approx. 0.2X

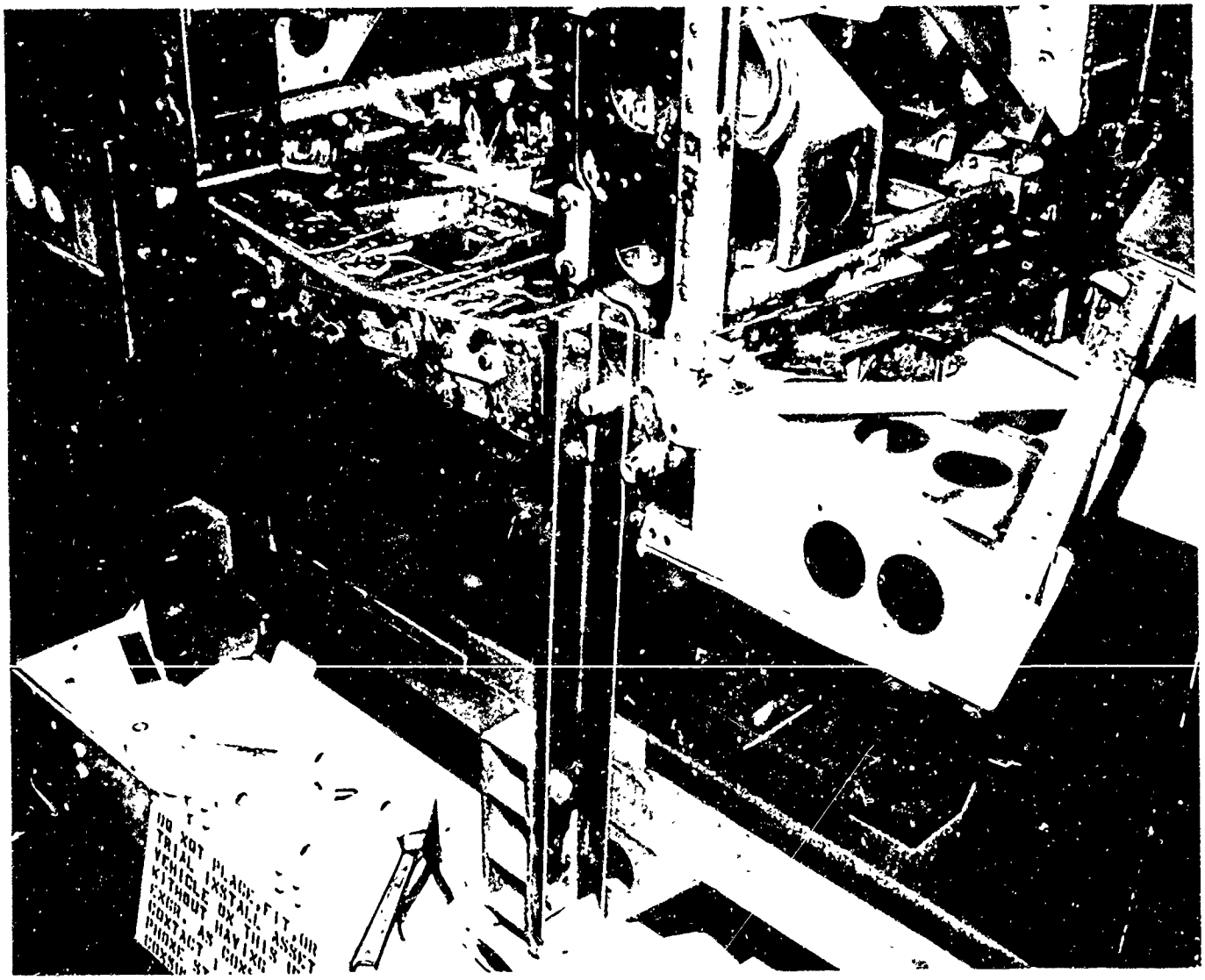

Figure 19 – Aft Beam and Truss Assembly After LB–2 Coating and Installation on the Vehicle.

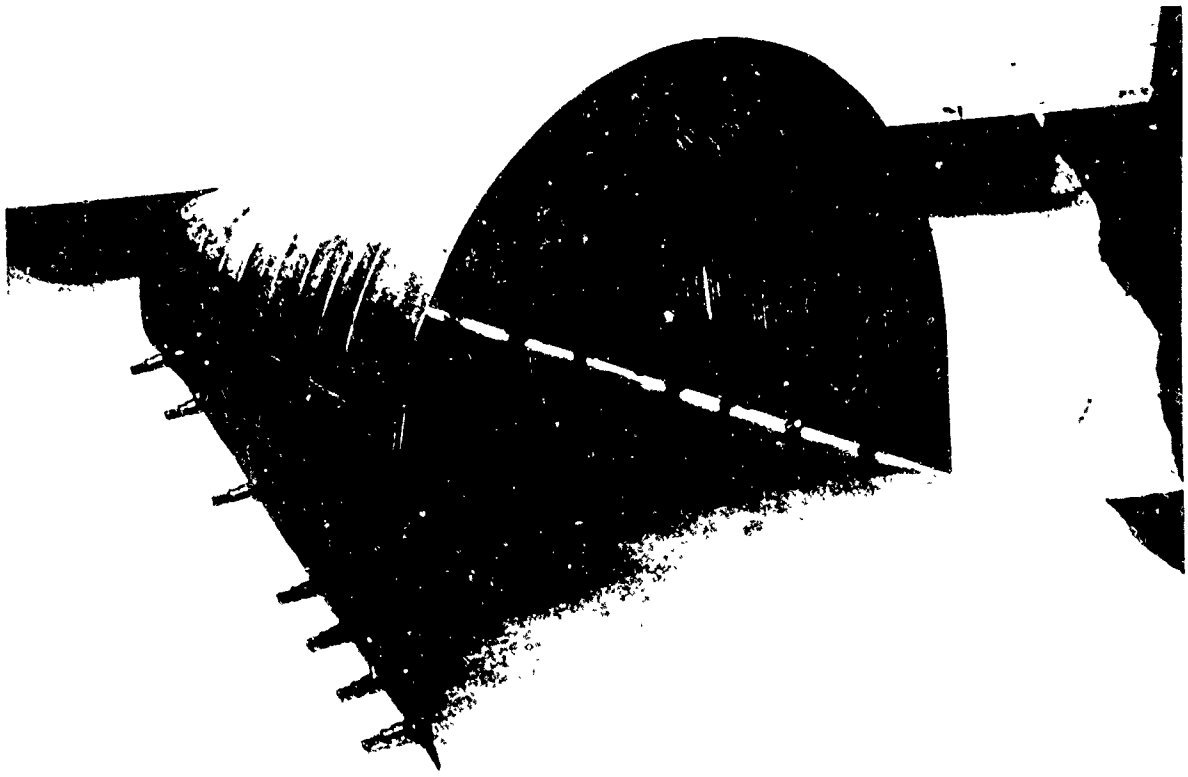

Figure 20 – D–14 Alloy Forward Upper Body Assembly in the Later Stages of Fabrication Before Coating, Showing Internal Details.

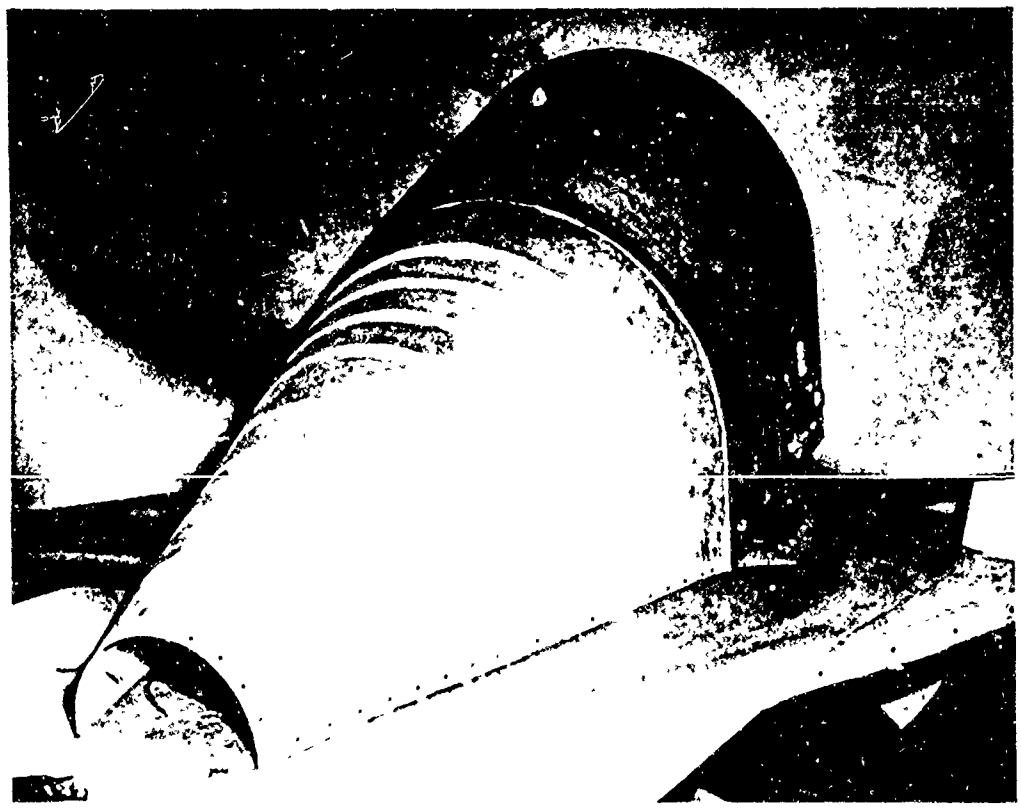

Figure 21 – Forward Upper Body Assembly After LB–2 Coating and Splice with the L–605 Aft Upper Body Assembly.

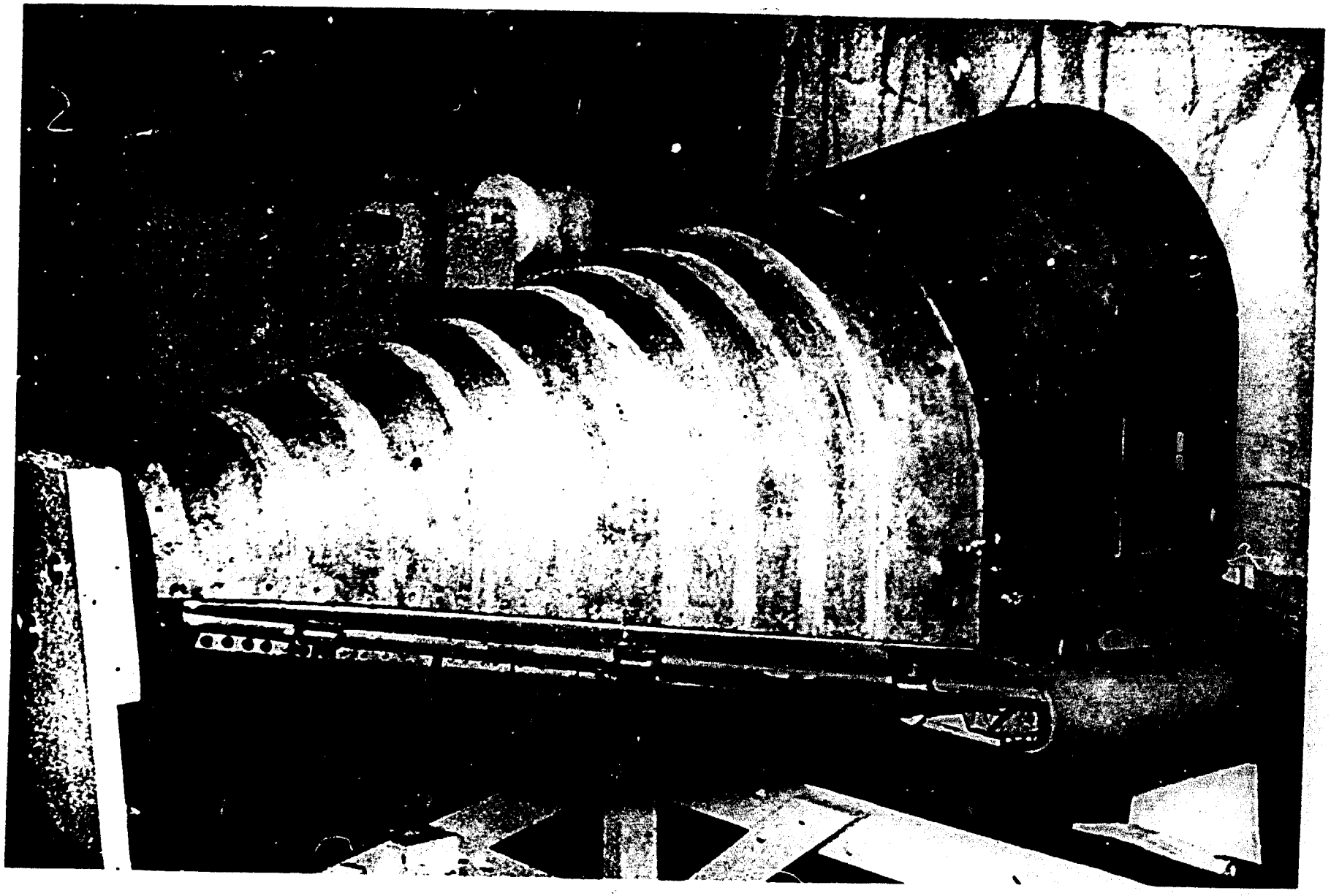

Figure 22 – Upper Body Assembly Installed on the Vehicle.

Figure 23 – Initial Upper Body Columbium Test Assembly After LB–2 Oxidation Testing for One Hour at 2500°F. Note Warping Due to Internal Oxidation.

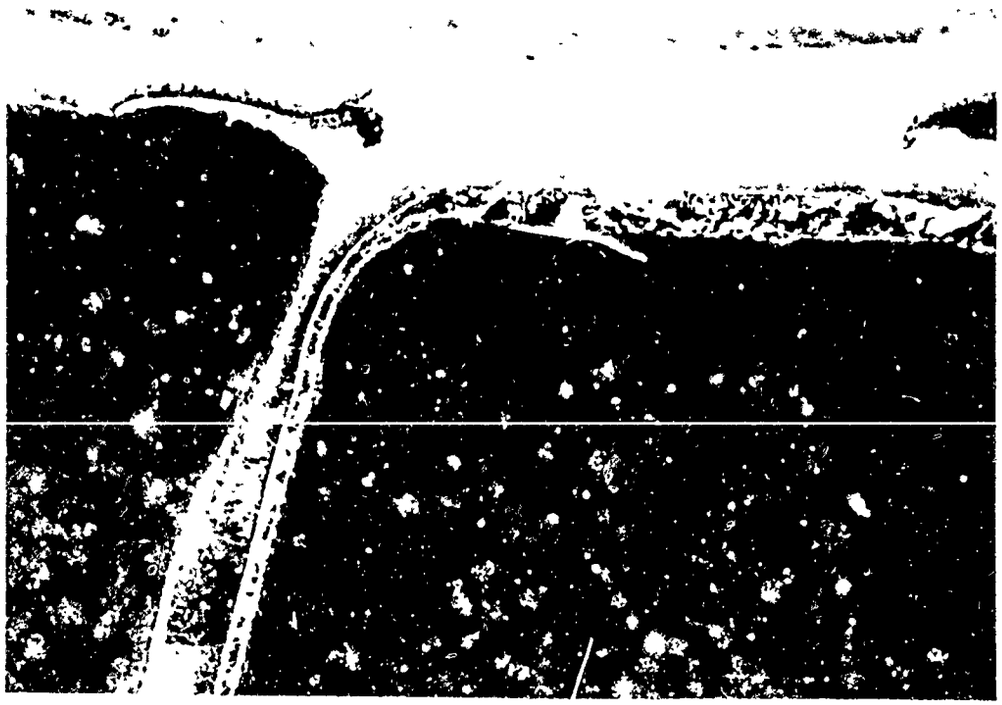

Figure 24 – Micrographic Section from Initial Upper Body Test Assembly in Area of Excessive Oxidation Between Skin and Corrugation.

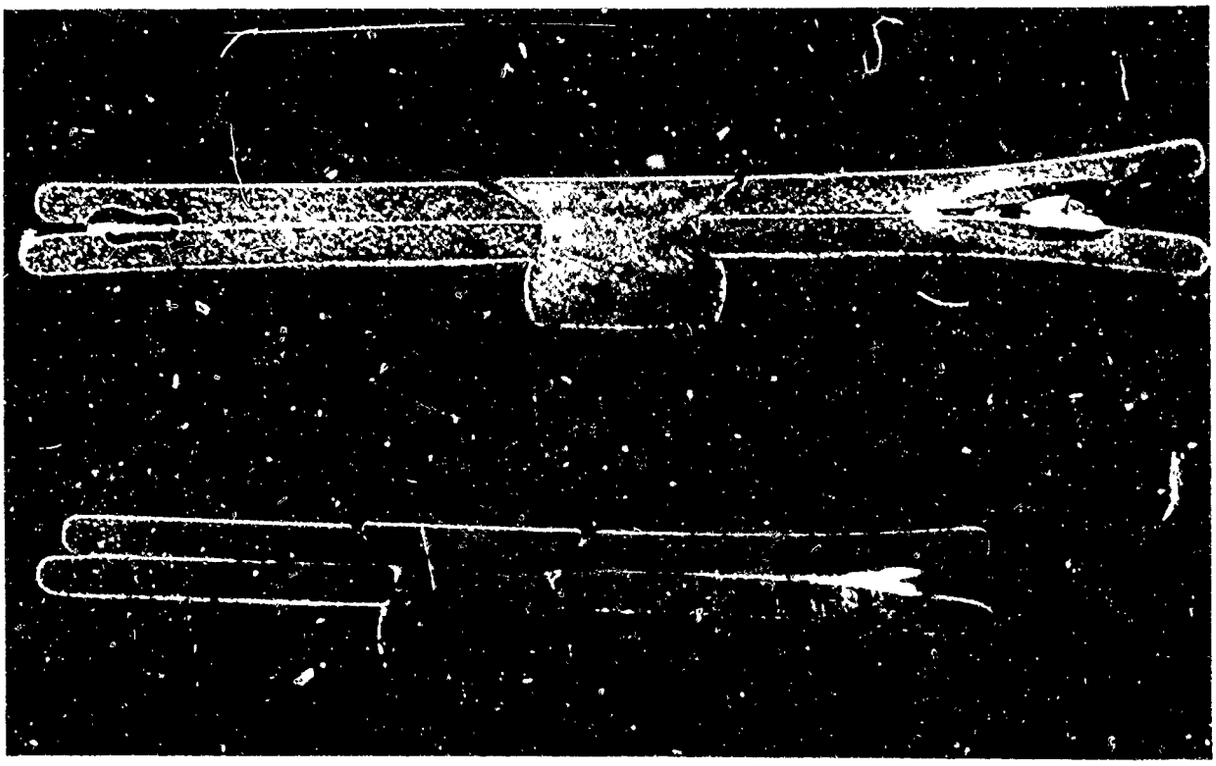

Figure 25 – Section Through Riveted Columbium Test Specimen Showing Warpage in a Faying Surface Due to Internal Oxidation.

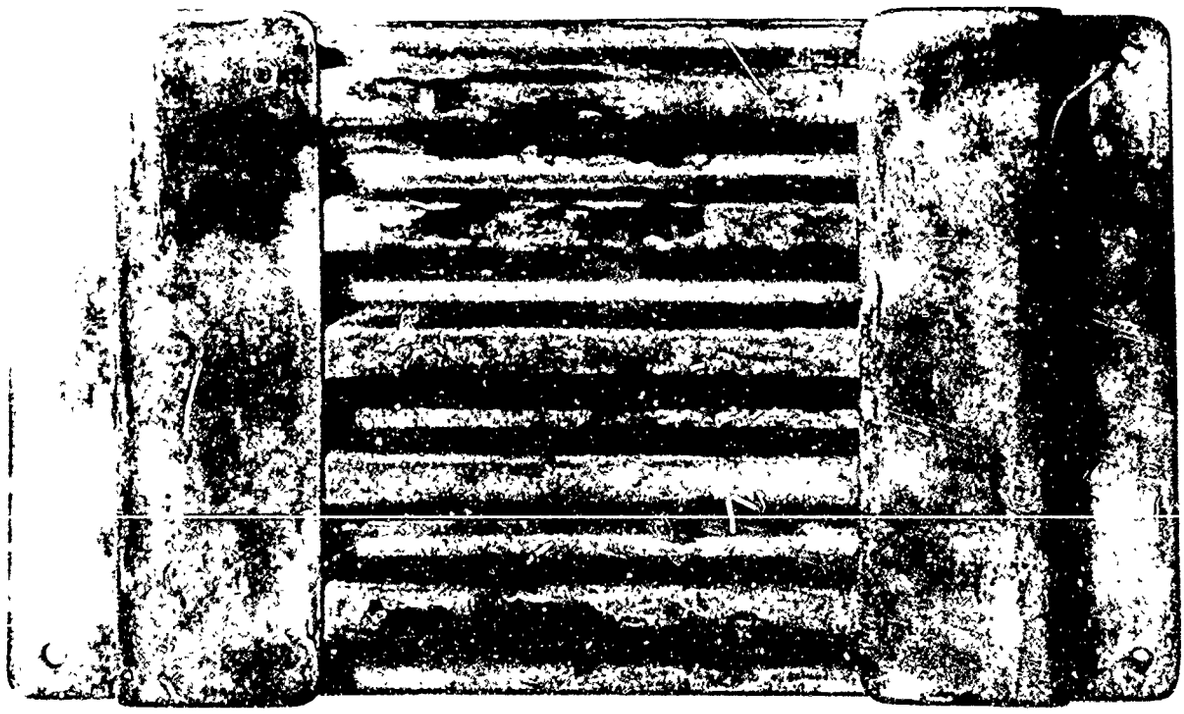

Figure 26 – Type of Resistance Welded Columbium Test Specimen of Single Faced Corrugated Design Used to Study Cold Slurry Coating Application Techniques.

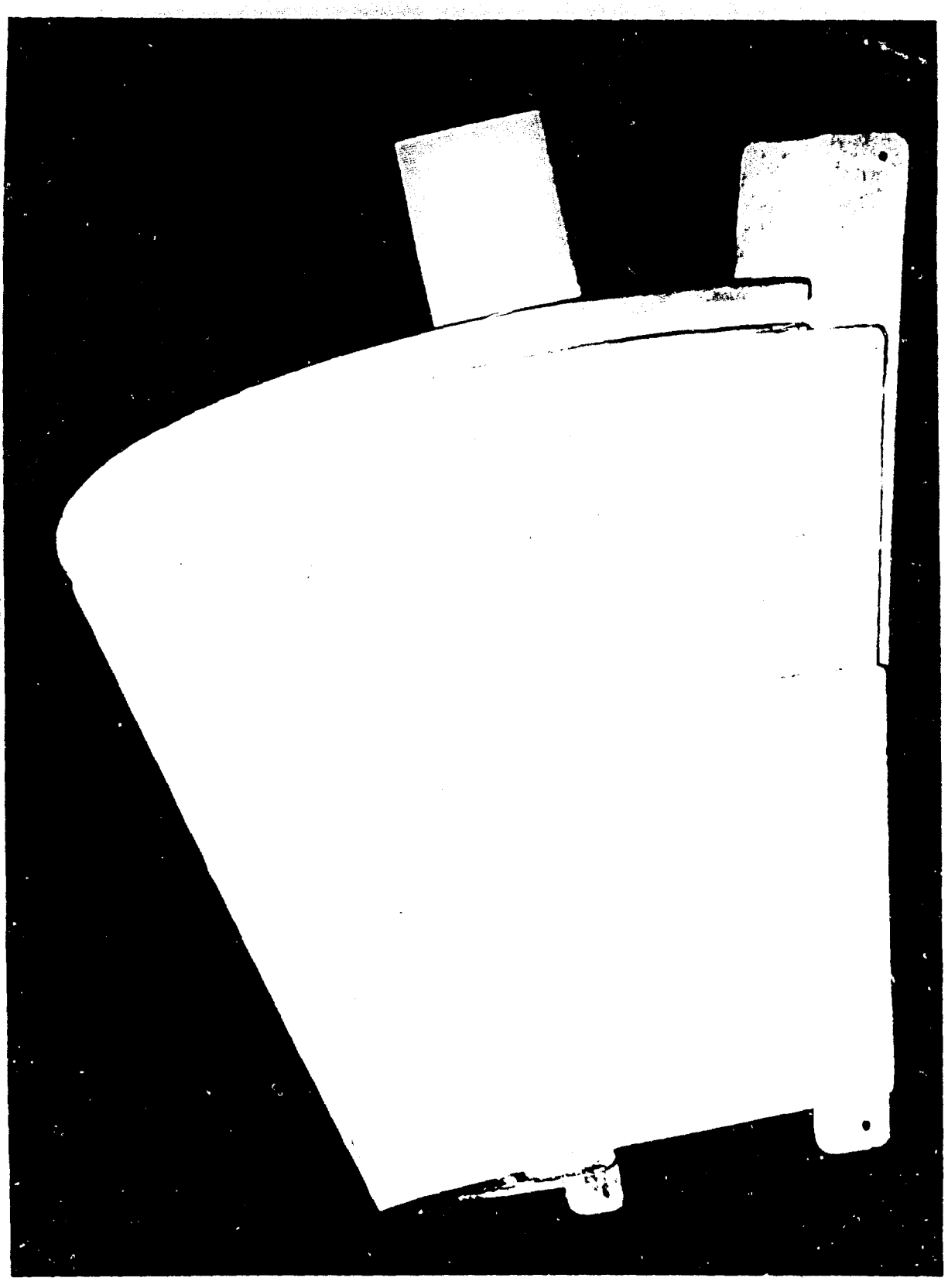

Figure 27 – LB–2 Coated Columbium Upper Body Test Assembly After Oxidation Testing for One Hour at 2500°F.

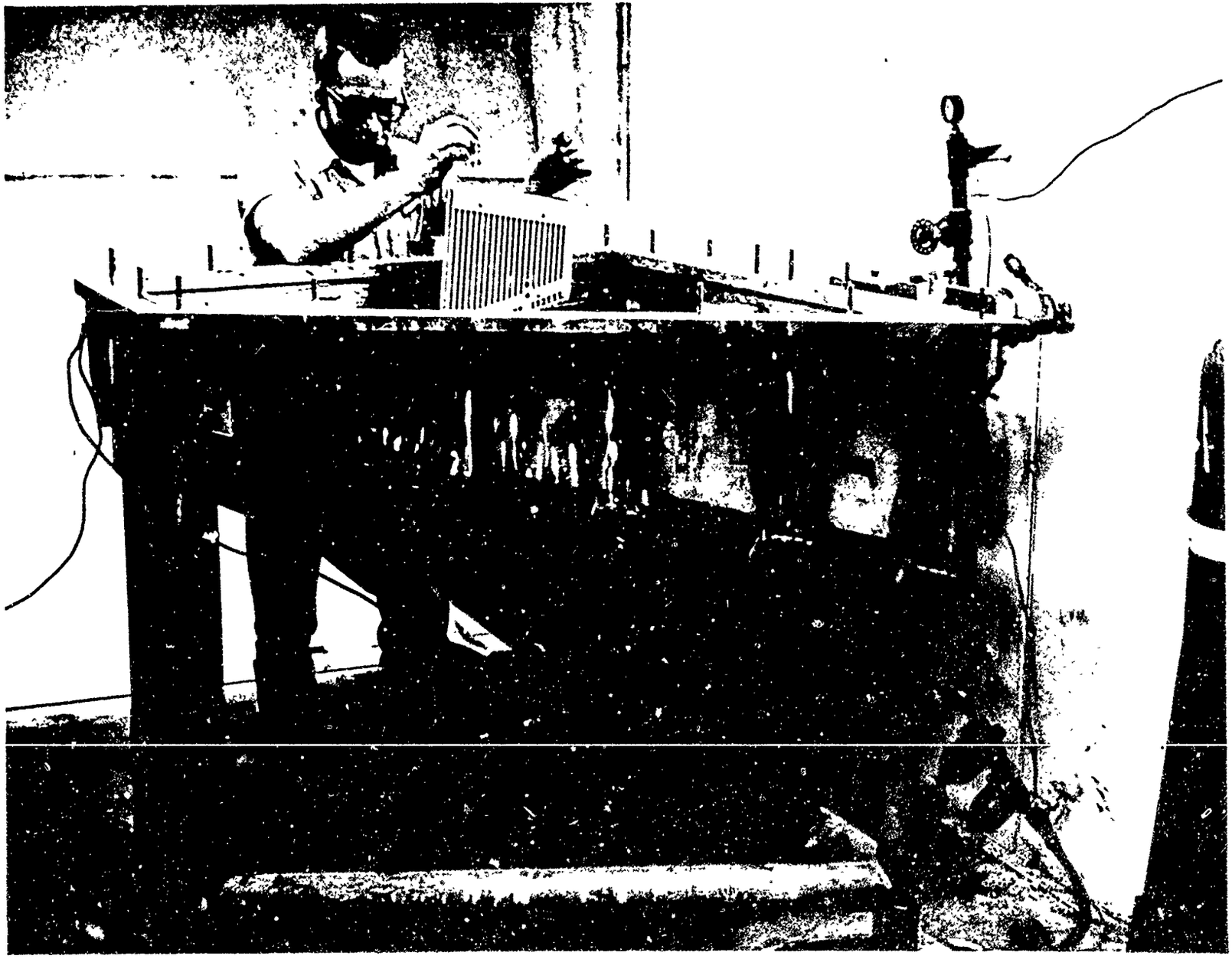

Figure 28 – Dip Tank Facility Used for the Coating of Production Columbium Hardware by the LB–2 Cold Slurry Process.

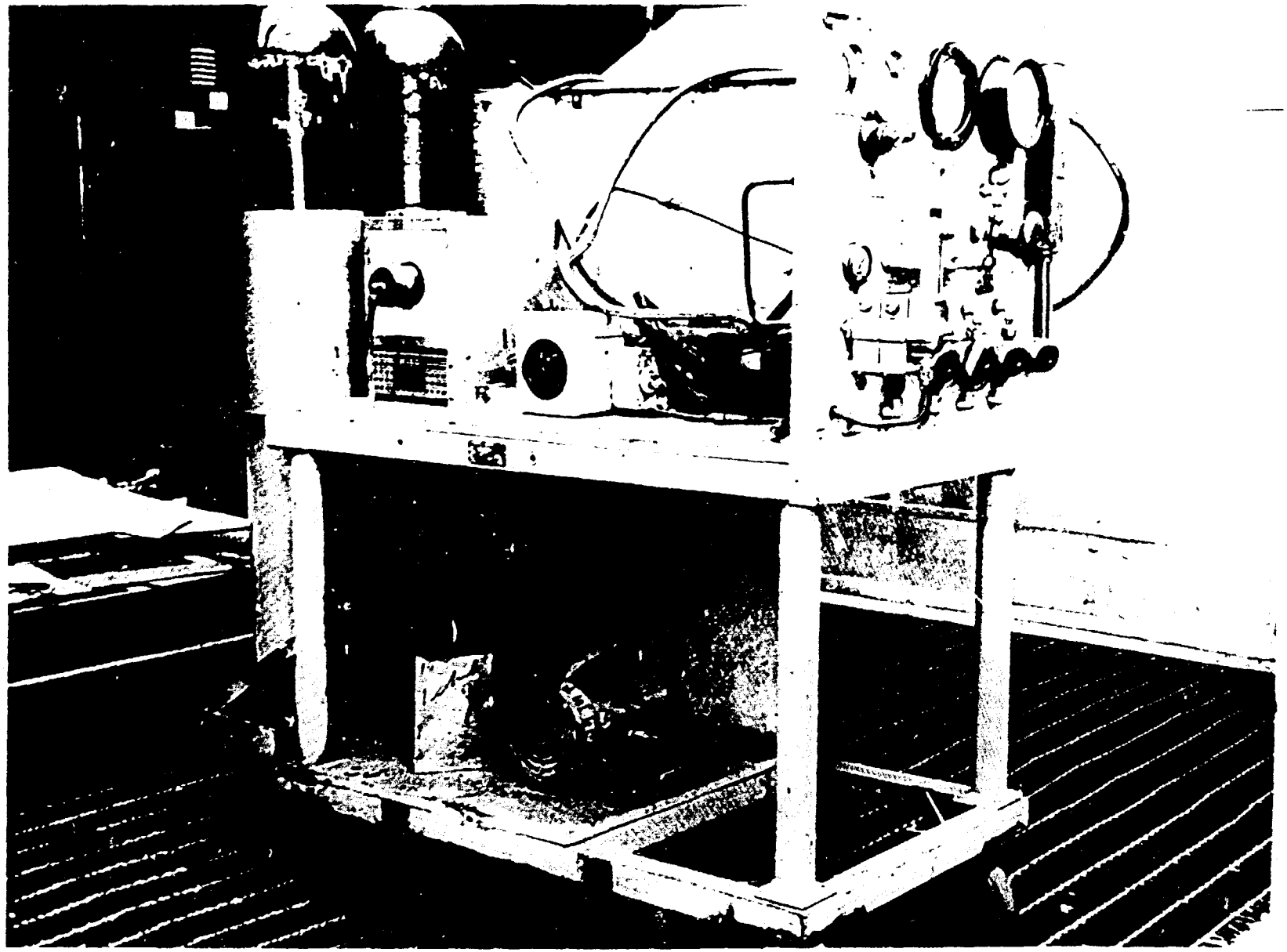

Figure 29 – Equipment Used for Atmosphere Purification and Control for the LB–2 Diffusion Cycle on Production Parts.

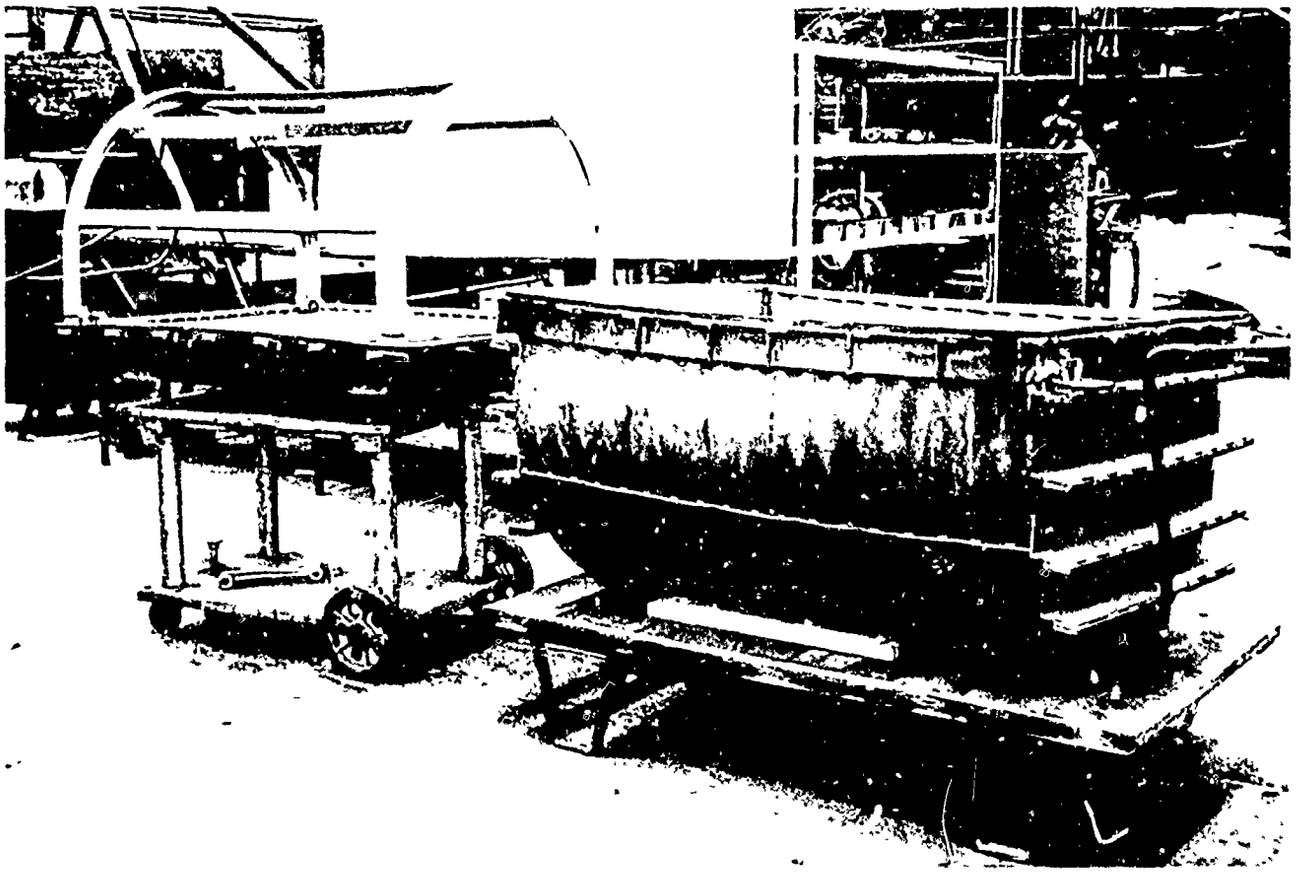

Figure 30 – One of the Retorts Used for the 1900°F LB–2 Diffusion Cycles.

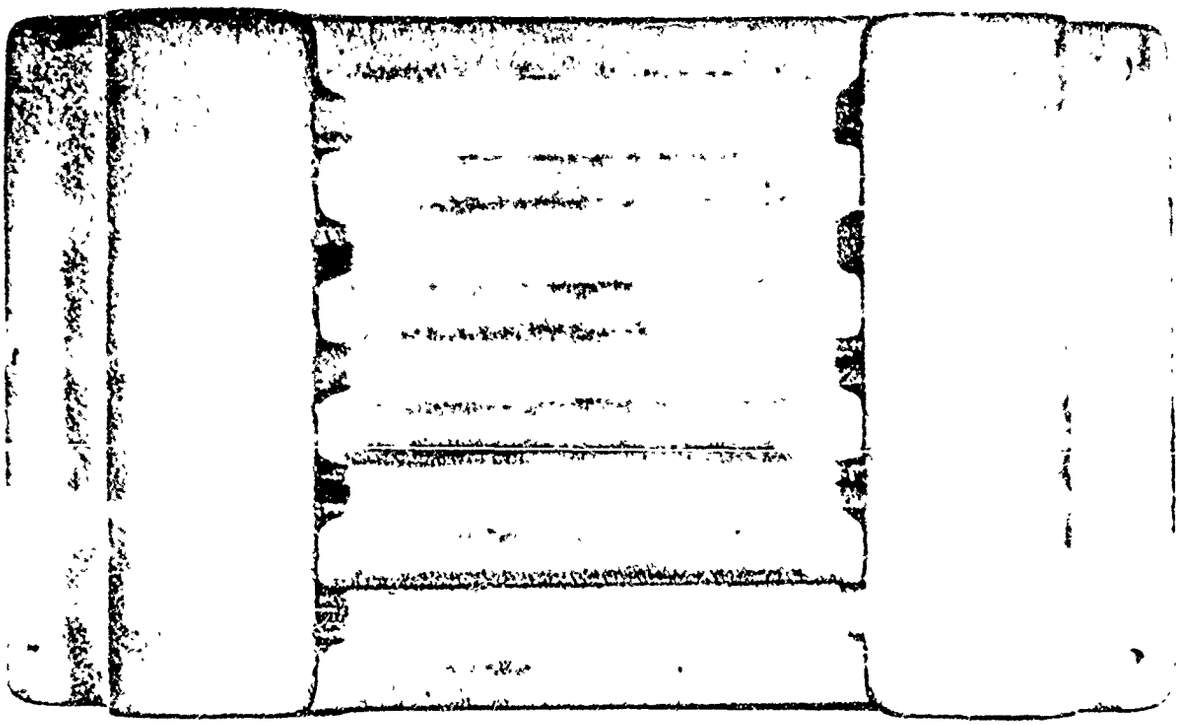

Figure 31 – LB–2 Coated Corrugated Test Specimen Diffused at 1700°F and Oxidation Tested for One Hour at 2500°F.

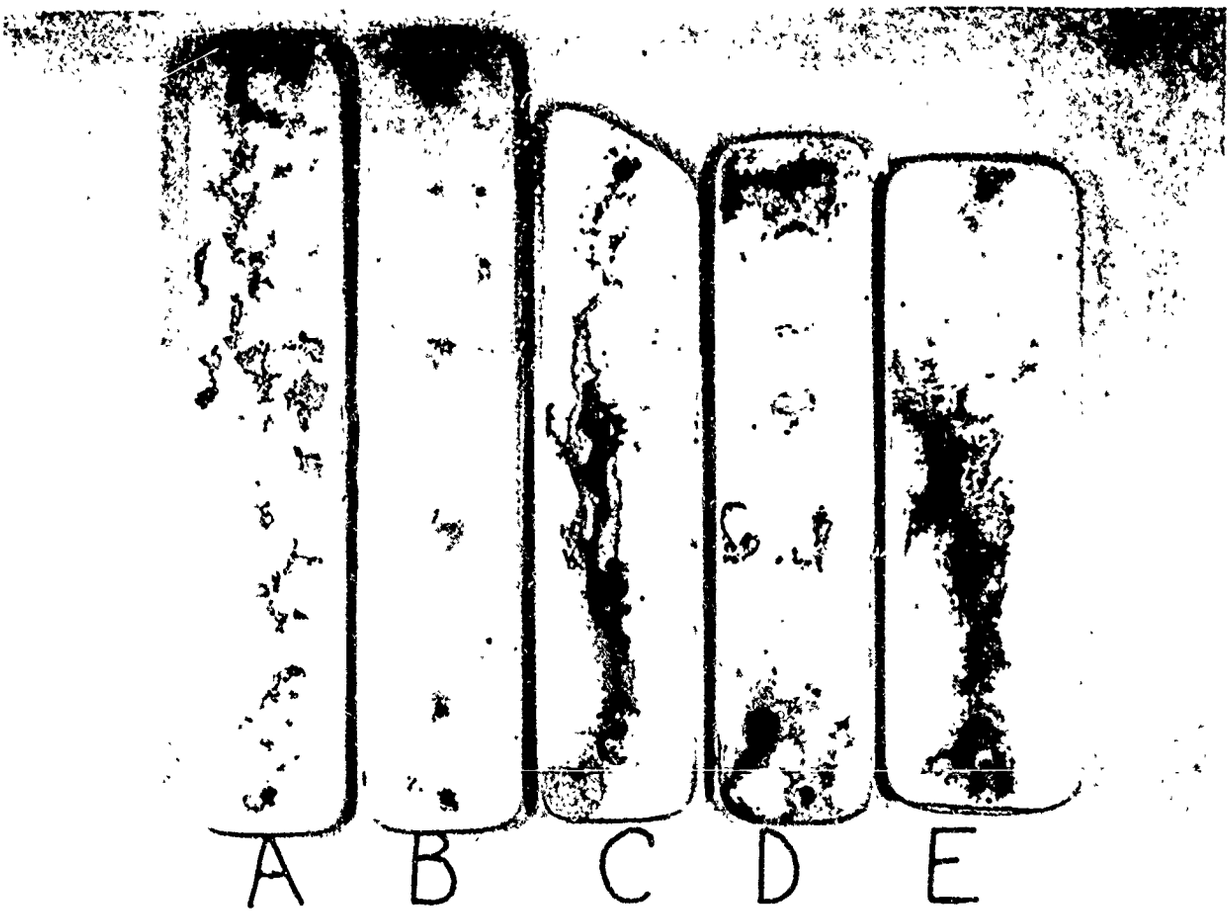

LB–2 Base and Over-Aged Top Coat Slurry

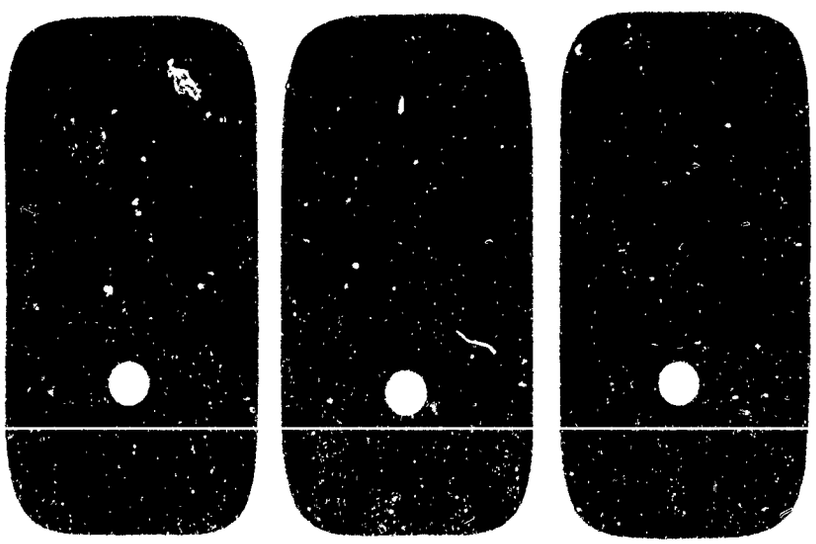

Double Application LB–2 Base Coat Slurry.

Figure 32 – Aging Effect of Top Coat Slurry in the LB–2 Process. Both Groups have Experienced a One Hour Oxidation Test at 2500°F.

HIGH TEMPERATURE OXIDATION RESISTANT SYSTEMS

H. W. LAVENDEL

Lockheed Missiles and Space Company

Palo Alto, California

FOREWORD

This report is a review of the research work, in progress at the Lockheed Missiles & Space Company Materials Sciences Laboratory, relating to high temperature behavior and oxidation mechanisms of refractory materials and systems. The purpose of these investigations is to evaluate and determine the potential which such materials and systems possess for applications in high temperature oxidizing environments.

The programs concerning the molybdenum disilicide and molybdenum disilicide coatings are sponsored by the LMSC General Research, while the work done on the oxidation of graphite and carbon has been carried out under U. S. Navy BUWEPS Contract NOw630050C.

CONTENTS

ILLUSTRATIONS

TABLES

Section 1

BEHAVIOR OF SILICIDE COATINGS IN HIGH TEMPERATURE-LOW PRESSURE ENVIRONMENT

W. L. Price and R. A. Perkins

1.1 INTRODUCTION

The use of silicide base coatings on refractory metals for re-entry applications requires that the coating must remain protective at high temperatures in air at reduced pressure. Previous work at LMSC has shown that disilicide coatings on molybdenum degrade when tested in air at pressures below 25 torr, as shown in Fig. 1. At reduced pressure the coatings fail to form a continuous protective surface glass, leading to localized attack of the substrate.

The general behavior and failure of molybdenum disilicide coatings on molybdenum, under these conditions, have been described in Lockheed's paper "Oxidation Protection of Structures for Hypersonic Re-Entry" presented at the Sixth Meeting of the Refractory Composites Working Group in Dayton, Ohio, June 16-19, 1962. In the following report, a testing program and its results are described for the last twelve months of work.

1.2 APPROACH

The investigative technique taken at LMSC has been to develop methods for testing coatings at low pressure, and to examine the behavior of representative coatings. More recently, a basic study of the mechanisms of protection and failure has been initiated.

In the future, work will be done on each of the silicides of Mo, W, Cb, and Ta, when applied as coatings to their respective metal substrates.

3120 °F – 760 TORR – 30 MIN
(1000 X)

2760 °F – 5 TORR – 30 MIN
(1000 X)

Fig. 1 Cross Section of Disil-II Coated Molybdenum After Tests in Air

1.3 EXPERIMENTAL EQUIPMENT AND PROCEDURE

The low pressure behavior of coated molybdenum rods is studied by using direct resistance heating of 0.1 in. diameter by 7 in. long specimens. The reaction vessel, shown in Fig. 2, is a water-cocled vacuum chamber 6 in. in diameter by 13 in. high having vertical water-cooled slip-fit electrodes. Specimen temperature was determined with a micro-optical pyrometer; calibration was obtained by taking brightness temperature readings from both the oxidized coating and an area of bare molybdenum. The brightness temperature versus true temperature for molybdenum was obtained by a melting point technique. The system pressure was measured with an absolute pressure meter (range 0.01 to 30 torr) and controlled by balancing an air or oxygen leak against the pumping speed of the pumping system.

The specimen was held at a fixed temperature and gas pressure for 30 minutes and then cooled. Visual and microscopic examination of tested specimens was used in determining the maximum temperature for which the coating prevented oxidation of the substrate.

The rate of oxygen consumption can also be used in determining the behavior of coatings tested in oxygen at low pressure. With this technique, the rate is measured every minute by recording the time required for the system pressure to drop to 90 percent of the test pressure, the pressure is restored between readings by introducing additional oxygen. A plot of consumption rate versus time qualitatively shows the oxidation behavior.

The major shortcoming of direct resistance heating is the temperature gradient along the test specimen, a gradient which precludes quantative study of the reaction between oxygen and the coatings. A 3400° F molybdenum-wound tube furnace is being constructed to permit low pressure testing of uniformly heated specimens, this furnace will also facilitate long-time tests.

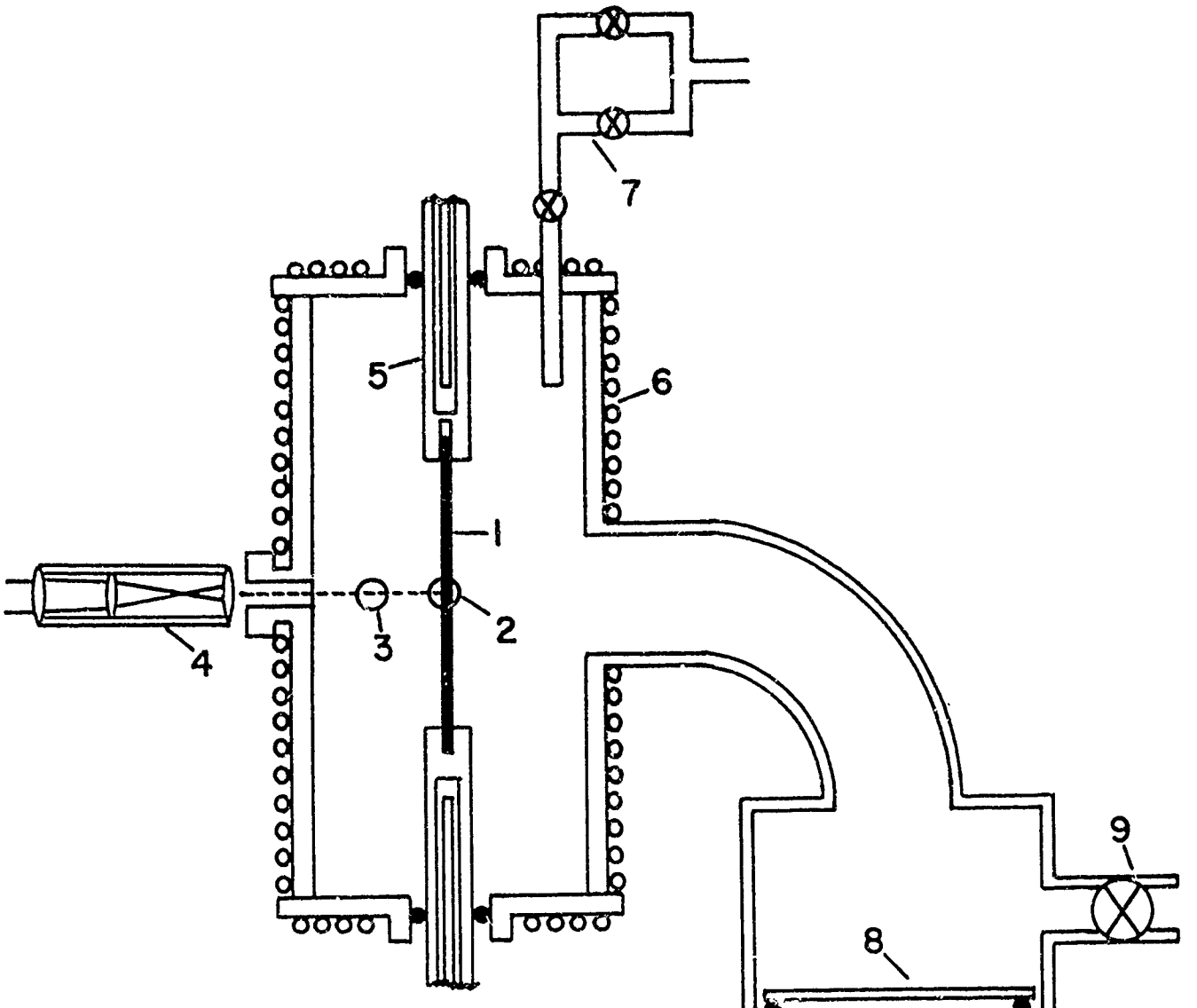

1 - SPECIMEN
2 - PRESSURE PORT
3 - TEMPERATURE PORT
4 - MEASURING TELESCOPE
5 - WATER-COOLED ELECTRODE
6 - COOLED REACTION CHAMBER
7 - GAS LEAK SYSTEM
8 - HIGH VACUUM VALVE
9 - ROUGHING LINE
10 - FORELINE
11 - DIFFUSION PUMP

Fig. 2 Schematic Diagram of Testing Apparatus

1.4 RESULTS

The results of the 30 minute life tests on four silicide base coatings – Durak-B (Chromizing Corp.), Disil II (Boeing Co.), PFR-6 (Pfaudler Co.), and a coating supplied by Chance Vought – are shown in Table 1 and Fig. 3. The curves represent the maximum temperature as a function of oxygen pressure, for a 30 minute test without attack of the substrate.

The micrographs in Fig. 4 illustrate the effect of oxygen pressure upon the behavior of the Durak-B coating.

Table 1

MAXIMUM TEMPERATURE FOR 30 MINUTE LIFE – °F

Coating	Thickness (mils)	760 mm air	21 mm O_2	10 mm O_2	5 mm O_2	1.05 mm O_2	0.21 mm O_2	0.1 mm OH
Durak-B	2.8	3170	3100	–	–	2975	2815	–
Disil II	1.5	3280	3240	–	3225	2975	2815	2700
PRF-6	2.6	3200	–	3200	3185	2850	2800	2775
Chance-Vought	3	3000	–	–	–	–	2950	–

The oxygen consumption data in Fig. 5 show the effect of temperature upon the oxidation behavior of Durak-B coated molybdenum rods. The initial rate of oxygen consumption is very high but drops in 2 to 3 minutes as the oxide layer forms. At 2575° F the coating is protective; at 2825 and 2900° F the coating continues to consume oxygen throughout the entire test and would eventually fail at these temperatures. The curves for 2950 and 3000° F reveal coating failures at 18 and 5 minutes, respectively.

The results show that generally silicide base coatings, with the exception of the Chance-Vought coating, do not have as high an operating temperature at reduced pressure as they have at one atmosphere pressure. This results from their inability to form a continuous protective surface glass. The coatings fail by localized attack at cracks and fissures.

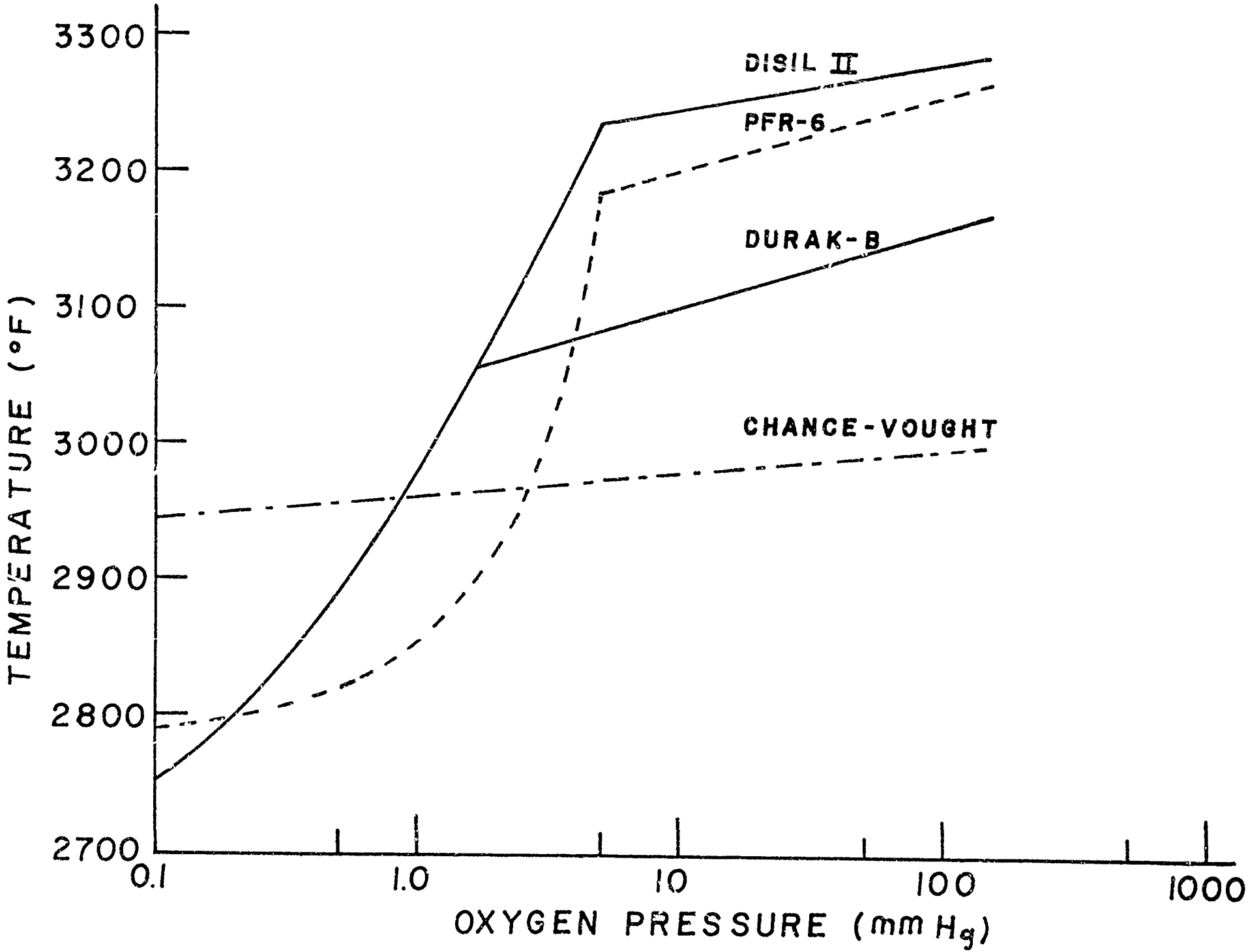

Fig. 3 Maximum Temperature for 30-Minute Life in Oxygen

DURAK-B IN OXYGEN

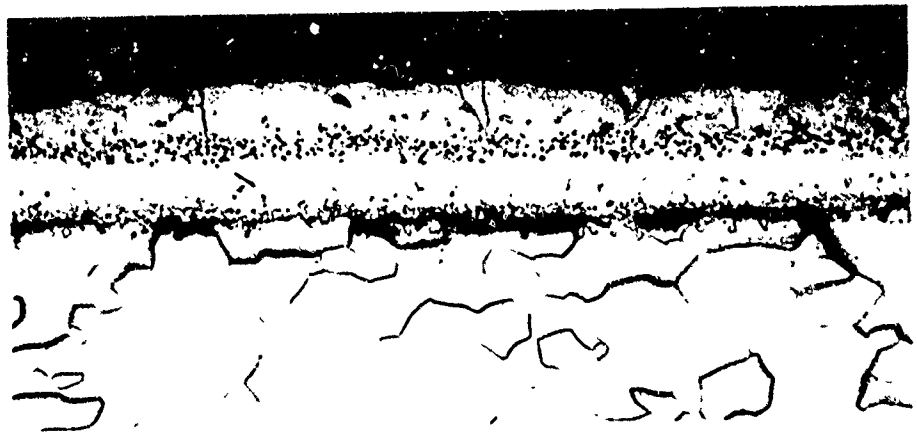

3050 °F – 21 TORR – 30 MIN
(150 X)

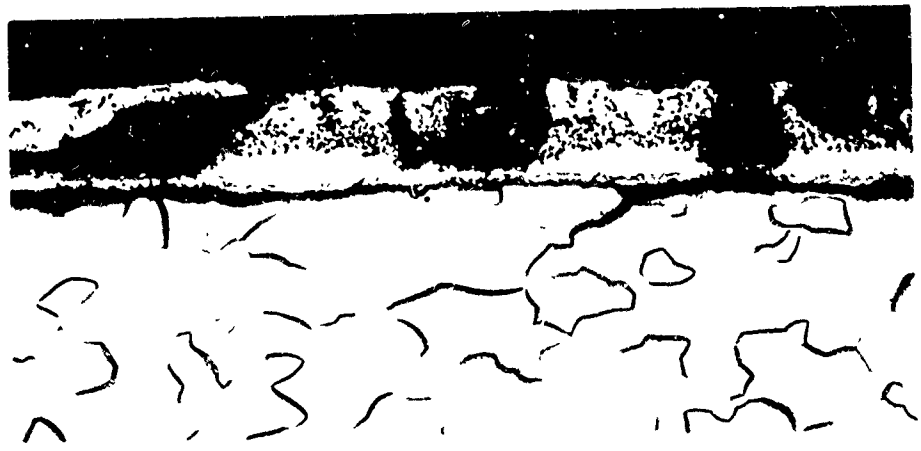

2960 °F – 1.05 TORR – 30 MIN
(150 X)

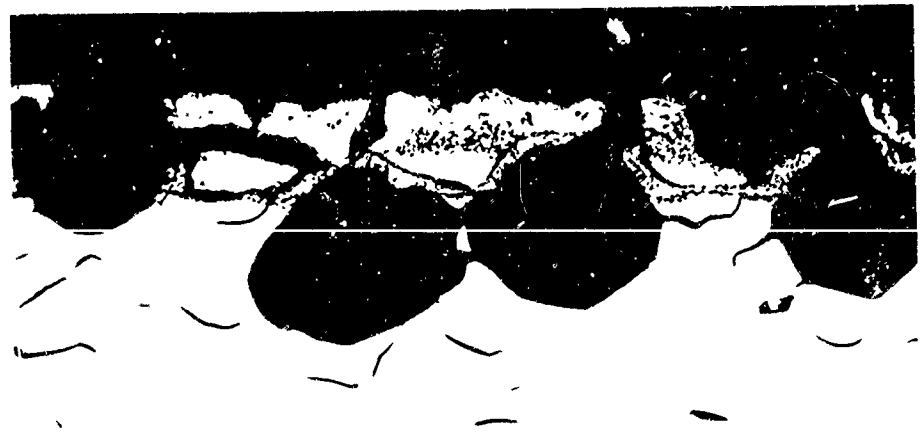

2960 °F – 0.21 TORR – 30 MIN
(150 X)

Fig. 4 Cross Section of Durak-B Coated Molybdenum After Tests in Oxygen

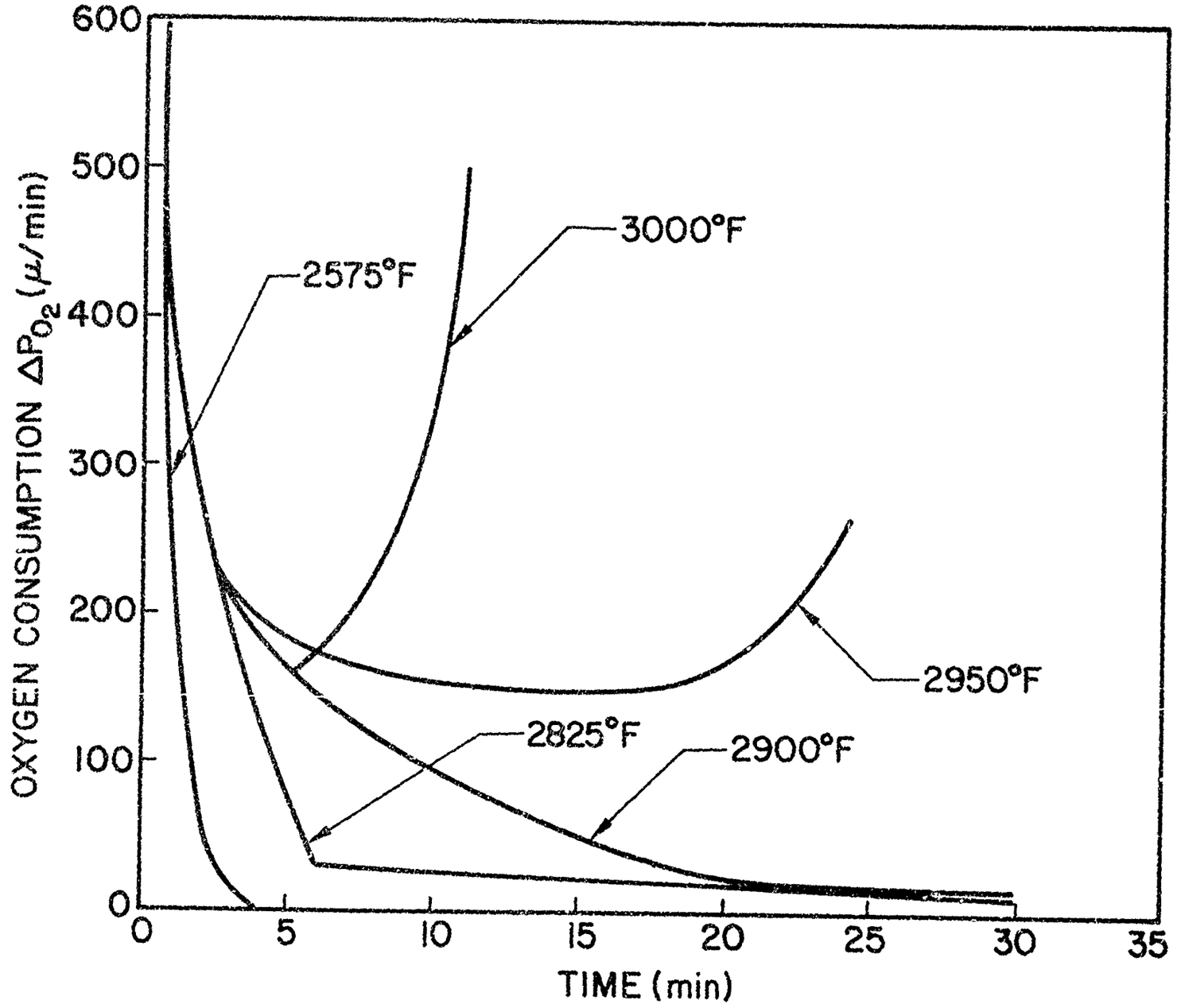

Fig. 5 Oxygen Consumption of Durak-B Coated Molybdenum in Oxygen at 1.05 Torr

1.5 CONCLUSIONS

The oxidation protection afforded by silicide coatings stems from their ability to form and maintain glassy surface layers, therefore, the formation, growth, continuity, and stability of the glass are the critical factors in coating behavior. The localized attack suffered by coated specimens indicates that the glass is not continuous. Glass continunity may be measured by recording the electrical conductivity between the surface and substrate of tested specimens. Figure 6 shows the effect of time at temperature upon the degree of glass continuity for a pure $MoSi_2$ coating tested at 3000° F in air at a pressure of 1 atmosphere. The data reveals that even after 15 minutes, the glass is still discontinuous, a condition confirmed by checking the electrical conductivity during oxidation at elevated temperature.

Microscopic examination of the surface of tested specimens will give additional information in glass thickness and continuity.

In tests at low pressure a gaseous oxidation product was produced; this product condensed on the cold walls as a filmy white deposit. X-ray diffraction revealed it to be amorphous, and spectrographic analysis showed the major constituent to be silicon. Thus, it has been shown that there is gaseous transport of silicon during oxidation at reduced pressure. Vapor pressure and thermodynamic consideration suggest the most probable mechanism to be the formation of SiO as postulated by Wagner.[1]

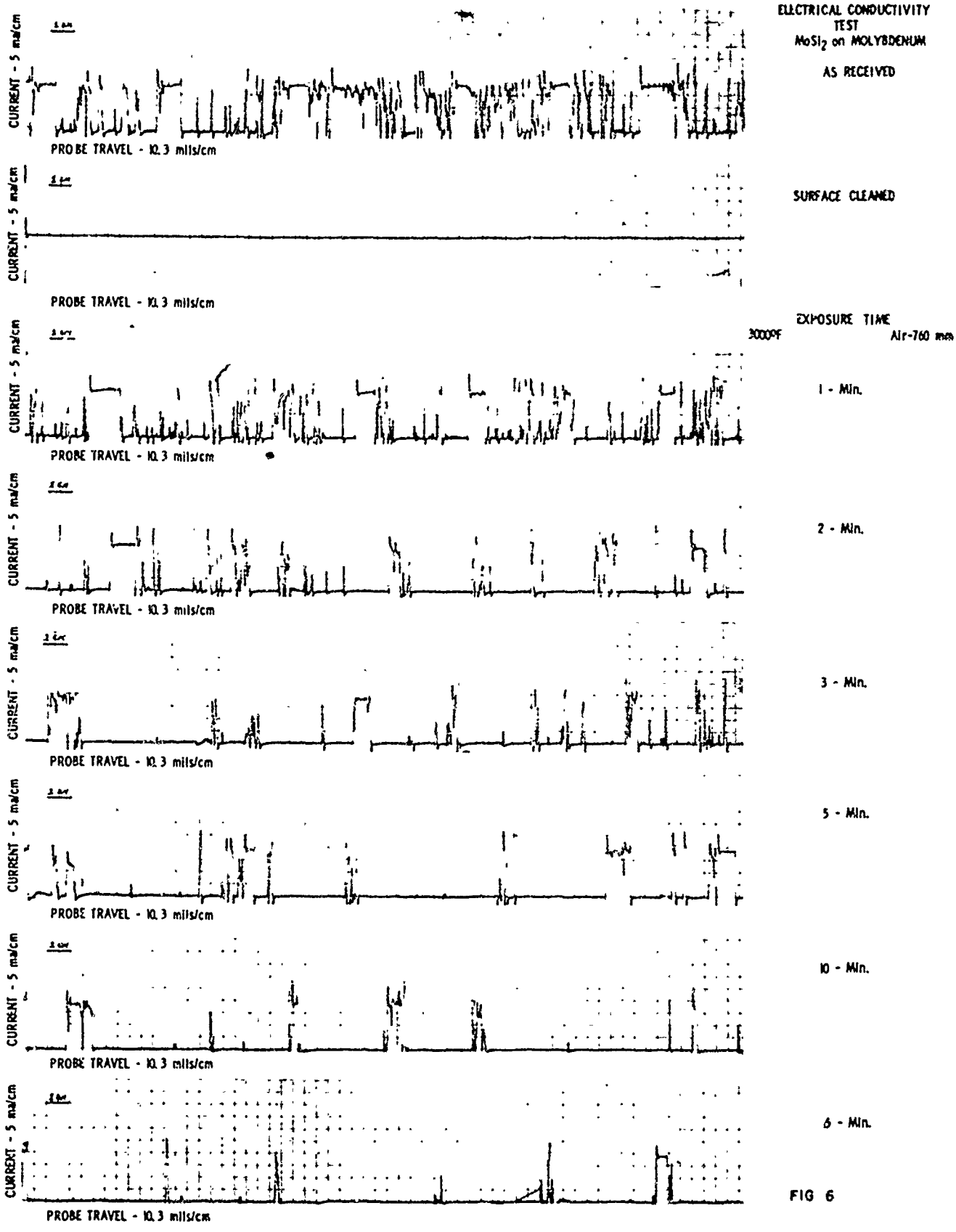

Fig. 6 Electrical Conductivity Profiles – $MoSi_2$ Coatings

Section 2

HIGH TEMPERATURE BEHAVIOR OF $MoSi_2$ IN VACUUM

George B. Cherniack and A. Grant Elliot

2.1 INTRODUCTION

Recent studies have shown that $MoSi_2$ coatings on molybdenum are nonprotective at high temperatures and low partial pressures of oxygen.[2] Other studies[3-8] mention the difficulty in fabricating dense $MoSi_2$ bodies and note that under certain conditions $MoSi_2$ appears to decompose below its melting point.[3,6,9]

A survey of the literature revealed little information that would adequately explain this behavior or define inherent limitations in the use of $MoSi_2$. Its behavior seemed to be related to disagreements in the reported data, and it was felt that a careful investigation of the high temperature properties of $MoSi_2$ was needed.

2.2 APPROACH

This investigation was initiated and conducted in the Materials Sciences Laboratory of Lockheed Missile & Space Company. It involved the heating of pure dense $MoSi_2$ in vacuum at high temperature and examining the resulting material by physical measurements, x-ray, and metallographic techniques.

2.3 EXPERIMENTAL EQUIPMENT AND PROCEDURE

Previous investigational variations in experimental conditions and material quality indicated that control of these variables might be the key to the understanding of the behavior of $MoSi_2$. Accordingly, experiments were designed with this objective in mind.

The $MoSi_2$ used in this work was high density material prepared by slip casting and sintering high purity powders.[6] Small samples were cut, ground, and cleaned and their density determined. These samples were heated in a cold-wall, tungsten-resistor vacuum furnace which was designed and built in this laboratory. The heat treatment consisted of bringing the samples up to temperatures ranging from 1750 to 2000° C and in holding them there for 1/4 and 2-1/2 hours.

By sighting on the sample through a small hole in the radiation shields, a Leeds and Northrup disappearing filament optical pyrometer was used to measure temperature. The pyrometer was calibrated by observing the melting points of various pure materials and correlating them to the pyrometer readings. After heating, the weight loss and density of the samples were measured. The samples were then broken up and sections submitted for metallography and x-ray analysis.

2.4 RESULTS

A preliminary investigation showed that sintered $MoSi_2$ reaches a maximum density at 1725° C. All the samples were heated at this temperature for 1 hour and gave an average density of 5.90 g/cc, about 95 percent of the theoretical density.

After this densification treatment, the samples were heated in vacuum for various times at different temperatures, and the results are recorded in Table 2.

The data show small weight losses and little change in density until 1900° C. At this temperature there is a large weight loss and a sudden drop in density. Figure 7, prepared from these data, shows the extent of this change.

2.5 CONCLUSIONS

2.5.1 Decomposition of $MoSi_2$

The microstructure of the original sintered untreated material consists of small, highly anisotropic grains and a large number of fine pores. Some of the pores appear

Table 2

PHYSICAL CHARACTERISTICS OF $MoSi_2$ HEATED AT VARIOUS TEMPERATURES IN VACUUM

Temperature (°C)	Time (hr)	Weight Loss (%)	Density (g/cc)	Appearance of Sample
1750	1/4	0.16	5.86	Discolored
1750	2-1/2	1.66	5.92	Discolored
1800	1/4	0.24	5.84	Discolored
1800	2-1/2	1.82	5.89	Slightly etched, cracks
1850	1/4	0.30	5.83	Slightly etched, cracks opening
1850	2-1/2	2.09	5.87	Etched, cracks opening
1875	1/4	0.55	5.83	Considerable etching
1875	2-1/2	2.75	5.88	Considerably etched, rough surface
1900	1/4	1.71	4.68	Slightly swollen, rough surface
1900	2-1/2	4.55	4.33	Swollen, rough surface
1925	1/4	3.51	4.57	Very swollen, blisters, rough surface
1925	2-1/2	5.92	4.31	Very swollen, large blister, rough surface
1950	1/4	6.35	4.89	Very swollen, large blisters, rough surface, shiny interface, porous interior
1950	2-1/2	9.79	4.91	
2000	1/4	–	–	Completely melted

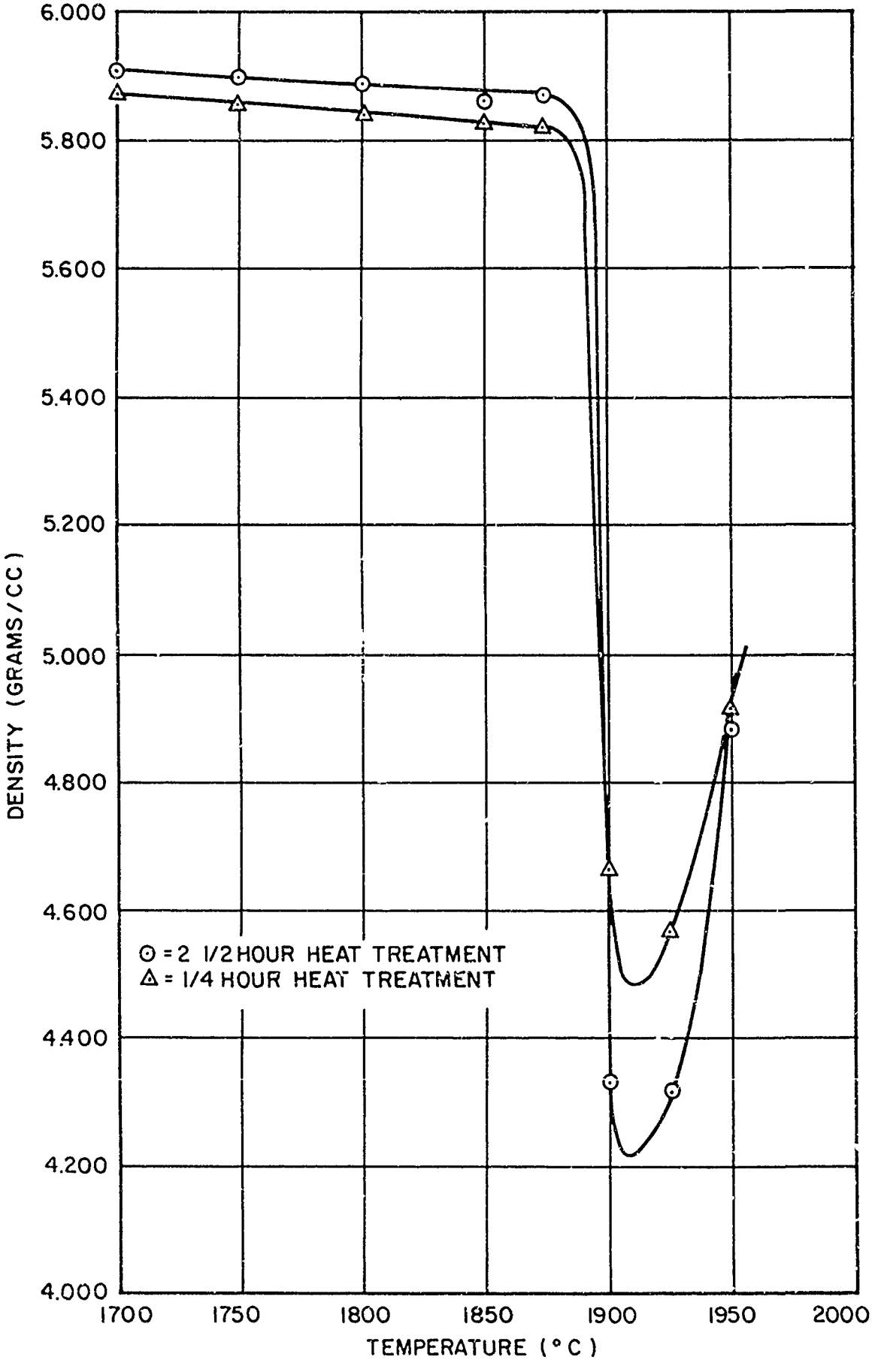

Fig. 7 Effect of Temperature and Time on Density of $MoSi_2$ in Vacuum

to be filled with a glassy material later identified as silica. A special etching treatment reveals also the existence of a small amount of another material which appears as very small grains evenly dispersed in the $MoSi_2$ matrix.

Heating of the samples at temperatures up to 1875° C causes the formation of a thickening porous coating as seen in Fig. 8. X-ray analysis reveals this coating to be Mo_5Si_3, a lower silicide of molybdenum. Another result of the heat treatment is the growth of the pores and the previously noted grains which are now always associated with the pores. These grains are the same as the coating material, since x-ray analysis of the interior material shows that the $MoSi_2$ now contains a detectable amount of Mo_5Si_3.

The decomposition of $MoSi_2$ is directly related to the loss of silicon. The work of Searcy and Thorp[10] shows that at high temperature the vapor pressure of silicon over $MoSi_2$ is significant,and the entire weight loss of the $MoSi_2$ is due to the vaporization of silicon. Therefore, it can be seen that the heating of $MoSi_2$ under dynamic conditions causes a loss of silicon with the subsequent formation and growth of a Mo_5Si_3 coating. In the interior, the Mo_5Si_3 grains also form due to the loss of silicon, but may be nucleated by a different mechanism. At lower temperature they are always associated with voids and form when silicon combines with absorbed or entrapped oxygen. This is confirmed by the presence of silica in the voids. Once formed, these Mo_5Si_3 grains grow by the loss of silicon due to outward diffusion.

2.5.2 The $MoSi_2 - Mo_5Si_3$ Eutectic

The graph of density versus temperature, Fig. 7, shows a sharp drop in density at about 1900° C. This sudden drop and the swollen appearance of the samples heated to 1900° C indicate a major change taking place. Metallographic examination of the sample heated for 1/4 hour, as shown in Fig. 9, shows that the interface between the coating and the $MoSi_2$ is no longer regular and appears to have been liquid. Longer heat treatment at 1900° C caused the appearance of large voids along the interface, as shown in Fig. 10. These heat treatments were accompanied by a burst in pressure as 1900° C was reached.

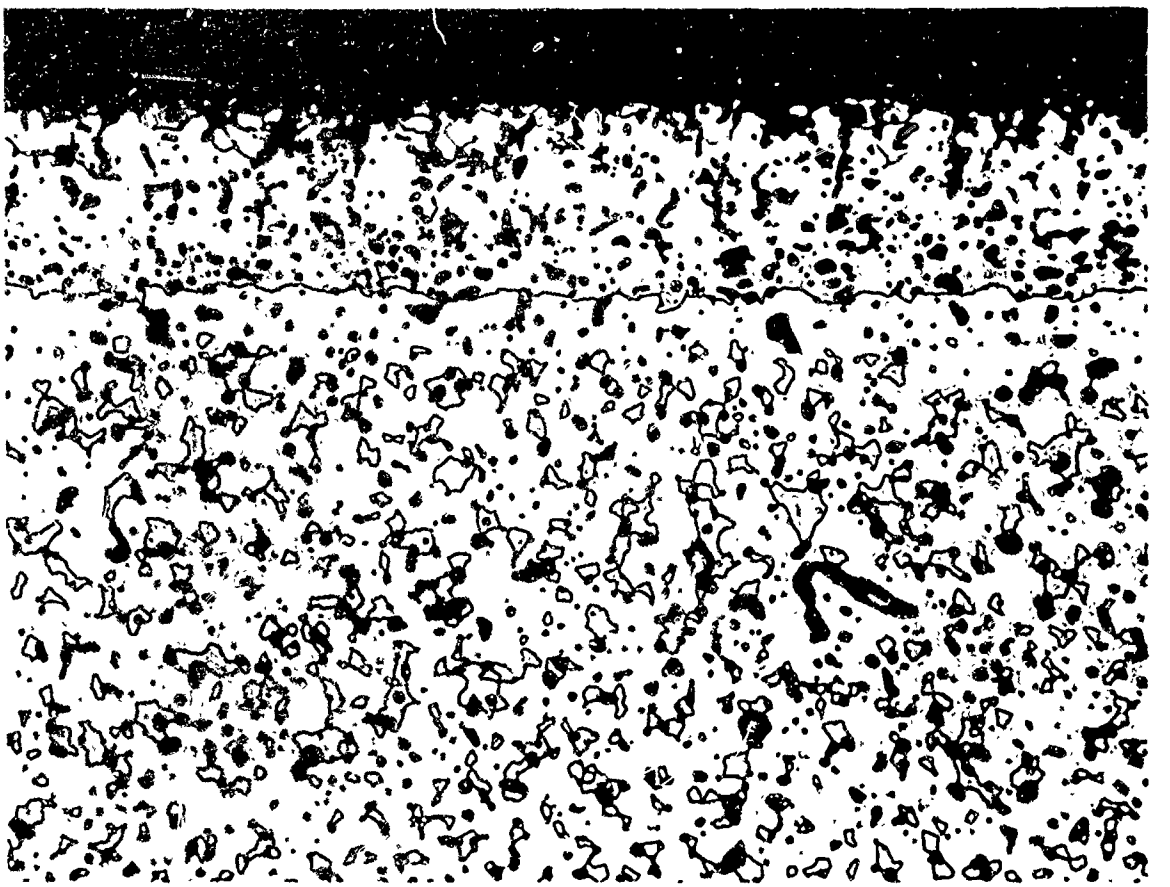

Fig. 8 Section of Surface Area of $MoSi_2$ Heated at 1875° C for 1/4 Hour. Electro-Etched in 0.5% CrO_3 500X

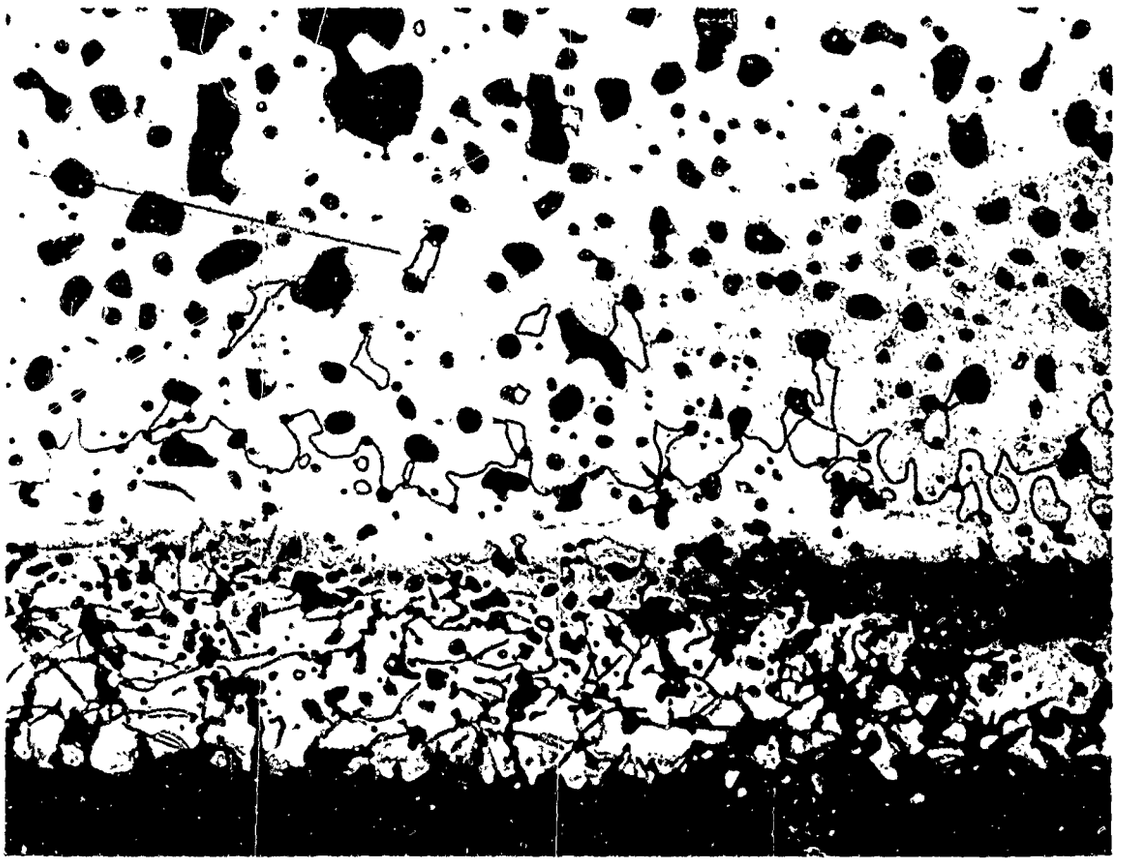

Fig. 9 Section of Surface Area of $MoSi_2$ Heated at 1900° C for 1/4 Hour. Electro-Etched in 0.5% CrO_3 500X

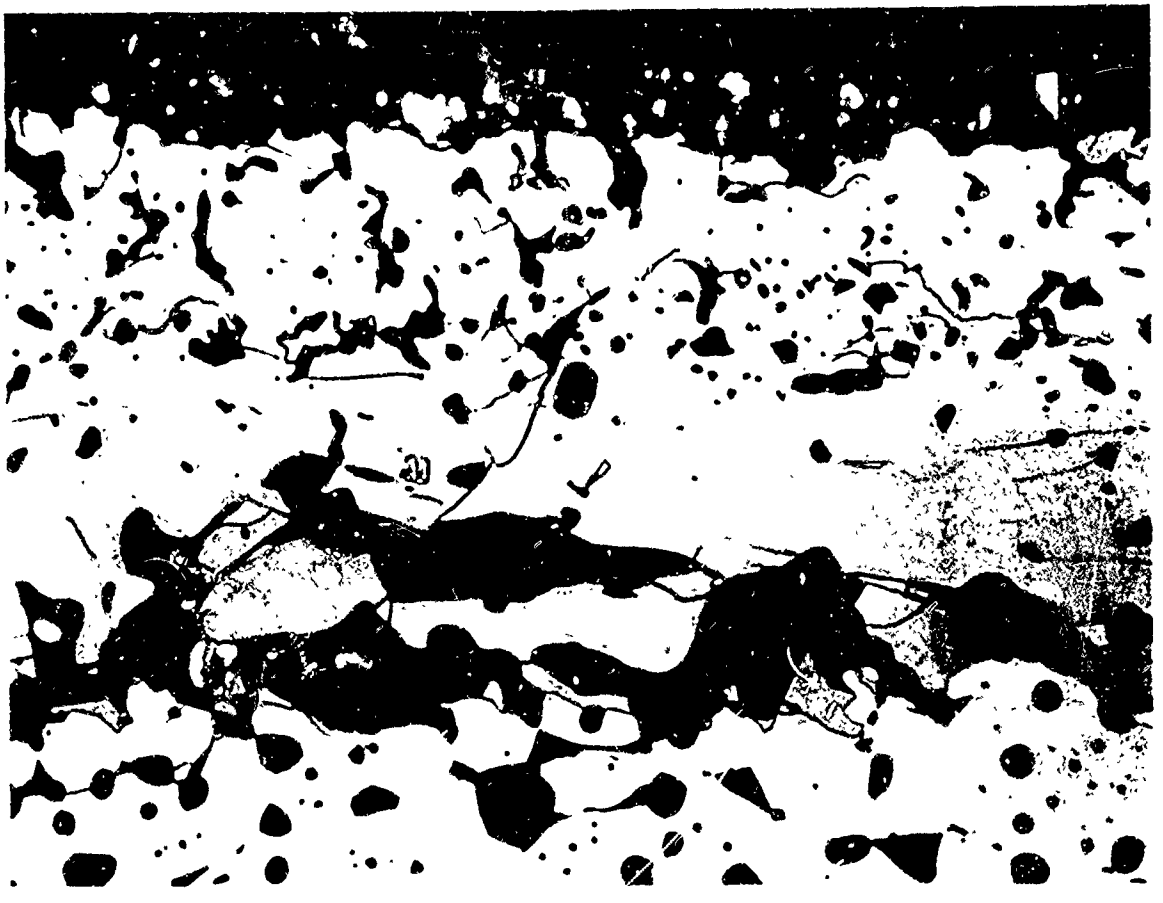

Fig. 10 Section of Surface Area of $MoSi_2$ Heated at 1900°C for 2-1/2 Hours. Electro-Etched in 0.5% CrO_3 500X

When the samples were heated above 1900° C, blisters appeared and the outer coating separated almost completely from the highly porous interior. The outer coating could easily be removed revealing a bright silvery inner coating that was clearly once liquid. X-ray analysis of the outer coating again showed it to be Mo_5Si_3 (with a trace of $MoSi_2$, probably due to some adherent inner material). These observations, indicating the formation of a liquid phase, confirm the existence of the eutectic between $MoSi_2$ and Mo_5Si_3 suggested by other investigators.[7,11] The first appearance of the liquid phases formation at 1900° C established the eutectic temperature. Examination of the interior of the samples heated over 1900° C showed the disappearance of the Mo_5Si_3 grains and the appearance of considerable amounts of eutectic in the grain boundaries, as shown in Fig. 11.

2.5.3 The Melting Point of $MoSi_2$

The melting point of $MoSi_2$ is particularly difficult to determine as it is masked by the formation of a liquid phase which can dissolve $MoSi_2$ at temperatures over 1900° C. Another complication is the continuing loss of silicon which changes the composition. These are probably the main reasons investigators have reported different melting points.

In order to accurately determine the melting point of $MoSi_2$, a series of samples were rapidly heated to temperatures above 1950° C at intervals of 10° C. The microstructures of these samples were examined under polarized light to determine which no longer contained unmelted grains of $MoSi_2$. By this method the melting point was found to be 1980° C.

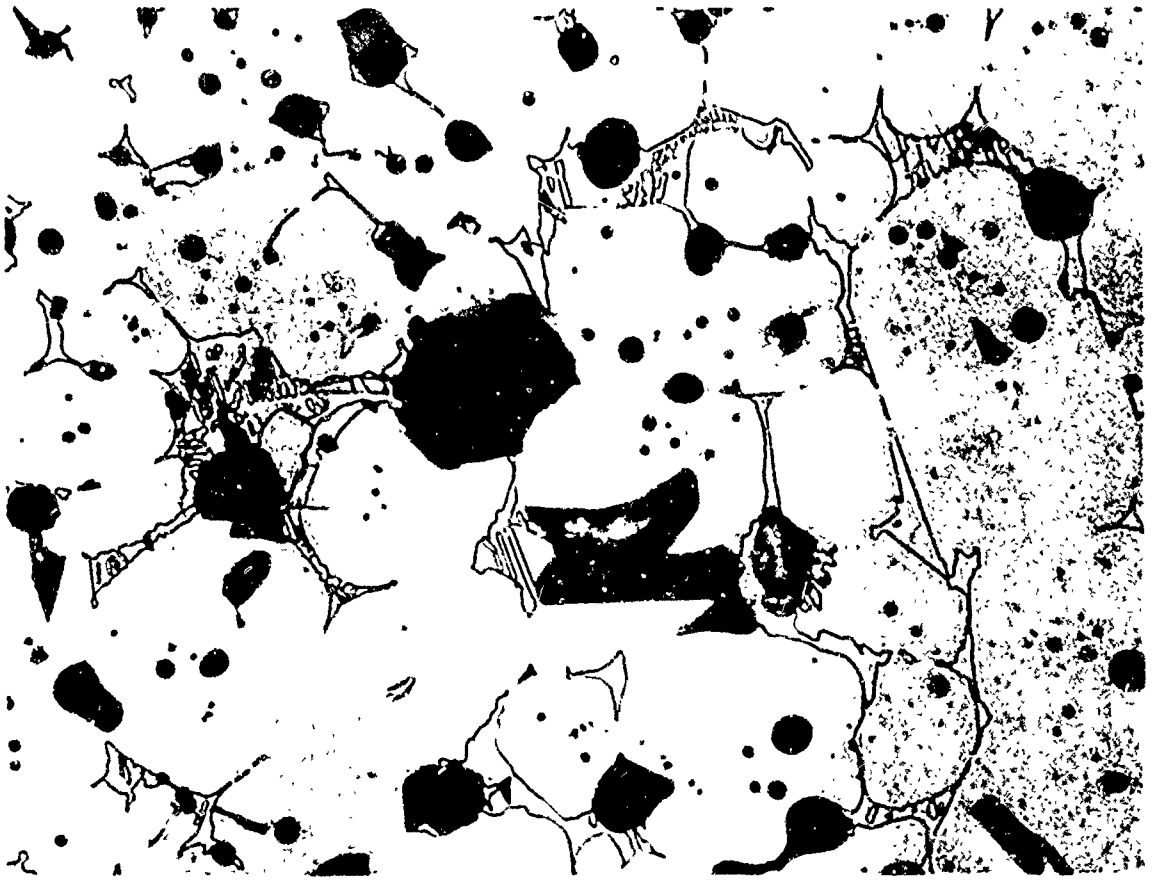

Fig. 11 Interior of $MoSi_2$ Heated at 1950° C for 1/4 Hour. Electro-Etched in 0.5% CrO_3 500X

Section 3

OXIDATION OF GRAPHITE AND VARIOUS TYPES OF CARBON

W. Bradshaw

3.1 INTRODUCTION

Pyrolytic graphites have been investigated as protective coatings for graphite and have shown merit in improvement of oxidation resistance of less dense graphites. However, such graphite coatings tend to fail by thermal shock or spalling.

Work done at LMSC indicates that glassy carbons with a low microporosity percentage are as oxidation resistant as pyrolytic graphite. Thus, oxidation protection depends primarily on producing an impervious, nonporous carbon surface. The rate of oxidation is independent of the degree of crystallization of the carbon or graphite.

3.2 APPROACH

The investigative technique chosen has been the study of the oxidation rates of various types of graphite and carbon in order accurately to predict their behavior in a hyperthermal environment. Factors evaluated included:

- Temperature – 500 to 3400° C
- Presure – 0.01 to 10 atmospheres air
- Gas-flow characteristics
- The nature of the carbon or graphite, including pore structure, degree of crystallization, and effect of impurity elements

3.3 EXPERIMENTAL EQUIPMENT AND PROCEDURE

Three test techniques were used to carry out these investigations. Thermal balance was recorded in the range from 500 to 1330° C with pressure from 0.01 to 5 atmospheres.

Rate was evaluated in terms of weight loss. A self-heated resistance furnace was used in the range from 400 to 3400° C with pressure from 0.1 to 10 atmospheres. Rate was evaluated in terms of surface recession as recorded by time-lapse photography. An arc-image furnace was used in the range to 3400° C with pressure from 0.1 to 10 atmospheres. Rate was evaluated in terms of surface recession as recorded by time-lapse photography.

As listed in Table 3, the carbonaceous materials evaluated vary in degree of crystallization, pore structure, and impurity content and were selected to represent a spectrum of the range of properties.

3.4 RESULTS

The oxidation of carbon or graphites generally falls into two categories:

(1) A low-temperature regime in which the rate is controlled by chemical reactivity – range 500 to ~1200° C
(2) A high-temperature regime in which the rate of reaction is controlled by bulk gas diffusion – range ~1200° C to sublimation temperature

It was found that in the chemically controlled regime the rate of reaction was dependent on the porosity of the sample or the degree of exposure of basal plane edges. This reaction rate was not a function of the degree of crystallization of the carbon or graphite. This can be seen in Table 4 by comparing the decreasing rate of oxidation as shown in Fig. 12 with other parameters. The microstructure, illustrating porosity and basal plane orientation, is shown for comparative purposes in Fig. 13.

Thus the rate of oxidation decreased as the porosity decreased (or the exposure of basal plane edges decreased). The most porous material had the least oxidation resistance. However, oxidation was independent of the degree of crystallization or rate of oxidation. The most oxidation resistant carbons were glassy carbon (the least graphitized) and pyrolytic graphite (the most oriented and the second most graphitized of these materials).

Table 3

COMPARISON OF VARIOUS TYPES OF CARBON AND GRAPHITE

Property	Type of Carbon or Graphite			
	Porous Carbon	AGOT Graphite	Glassy Carbon (C-201 Series)	Pyrolytic Graphite
Apparent Density (g/cc)	0.60	1.65	1.09	2.14
True Density (g/cc)	1.49	2.02	1.24	2.18
Porosity[a]				
Microporosity[b] (percent)	1.8	20	1.5	–
Intermediate porosity[c]	3.1	71.8	14.5	0.6
D_{50} (Microns)[d]	85	3.25	60.1[e]	100[f]
Total Volume (percent)	46.4	15.7	13.1[e]	2.02
Microstructure	Amorphous	Random, polycrystalline	Glassy	Oriented, crystalline
Lattice Spacing	3.76	3.37	3.86	3.45
Impurity Content	Fe, Ti present as catalyst	Relatively pure	Fe present as catalyst	High purity

(a) By mercury-intrusion porosimetry
(b) That portion of pores smaller than 1 micron in diameter but larger than 0.06 microns
(c) That portion of pores between 1 and 10 microns in size
(d) The diameter of the median (50 percent) pore volume
(e) Primarily cracks
(f) Surface convolutions, bubbles and depressions, which represent the surface of an unmachined sample

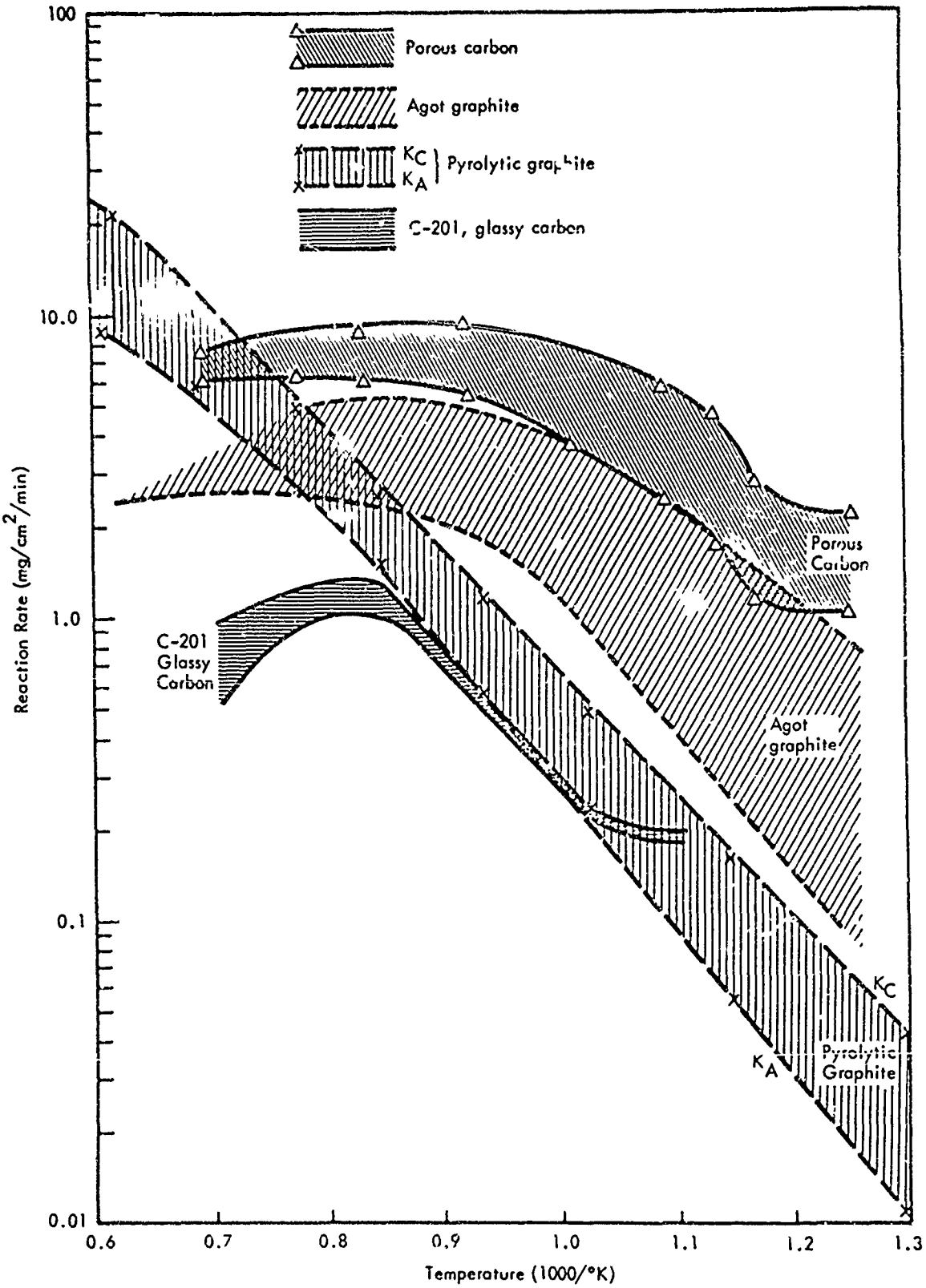

Fig. 12 Oxidation of Various Types of Graphite in One Atmosphere Air

Table 4

COMPARISON OF DIFFERENT GRADES OF GRAPHITIC MATERIAL

Property	Order of Intensity
Oxidation	Porous Char > AGOT > PG_{K_C} > PG_{K_A} ~ Glassy Carbon
Porosity or Exposure of Basal Plane Edges	Porous Char > AGOT > PG_{K_C} > Glassy Carbon ~ PG_{K_A}
Crystallization	AGOT > PG_{K_A} = PG_{K_C} > Porous Carbon > Glassy Carbon

It was found that small amounts of metallic impurities such as Fe or Ti apparently catalysed the oxidation rates in the temperature range at 500 to 600° C.

In the higher temperature range the observed oxidation rates fell off from those predicted by the reaction rate mechanism, as shown in Fig. 14. In the higher temperature range, rates observed became dependent on gas flow rates, indicating contr' by bulk-gas diffusion.

For pyrolytic graphite and graphite the point at which the high-temperature rate leveled off (i.e., became controlled by bulk gas diffusion) increased with flow rates, as shown in curves A, C, and D. If the low-temperature rate was high, as in AGOT graphite, the rate at which it leveled out was also higher.

In the noncrystalline carbons, porous, and glassy carbons, there was an actual decrease at higher temperatures, as shown in curves E and F. Because this material was highly disordered, it was surmized that an active site process somewhat like that proposed by Blyholder (Ref. 13) may have contributed here.

Bright Field M-3529 1000X
GLASSY CARBON
Bright Field M-876 1000X
PYROLYTIC GRAPHITE
Basal Plane Surface, As
Polarized Light M-906 1000X
PYROLYTIC GRAPHITE
Basal Plane Edges, As
Semitic Grade M-3501 500X
ATJ-S1 GRAPHITE

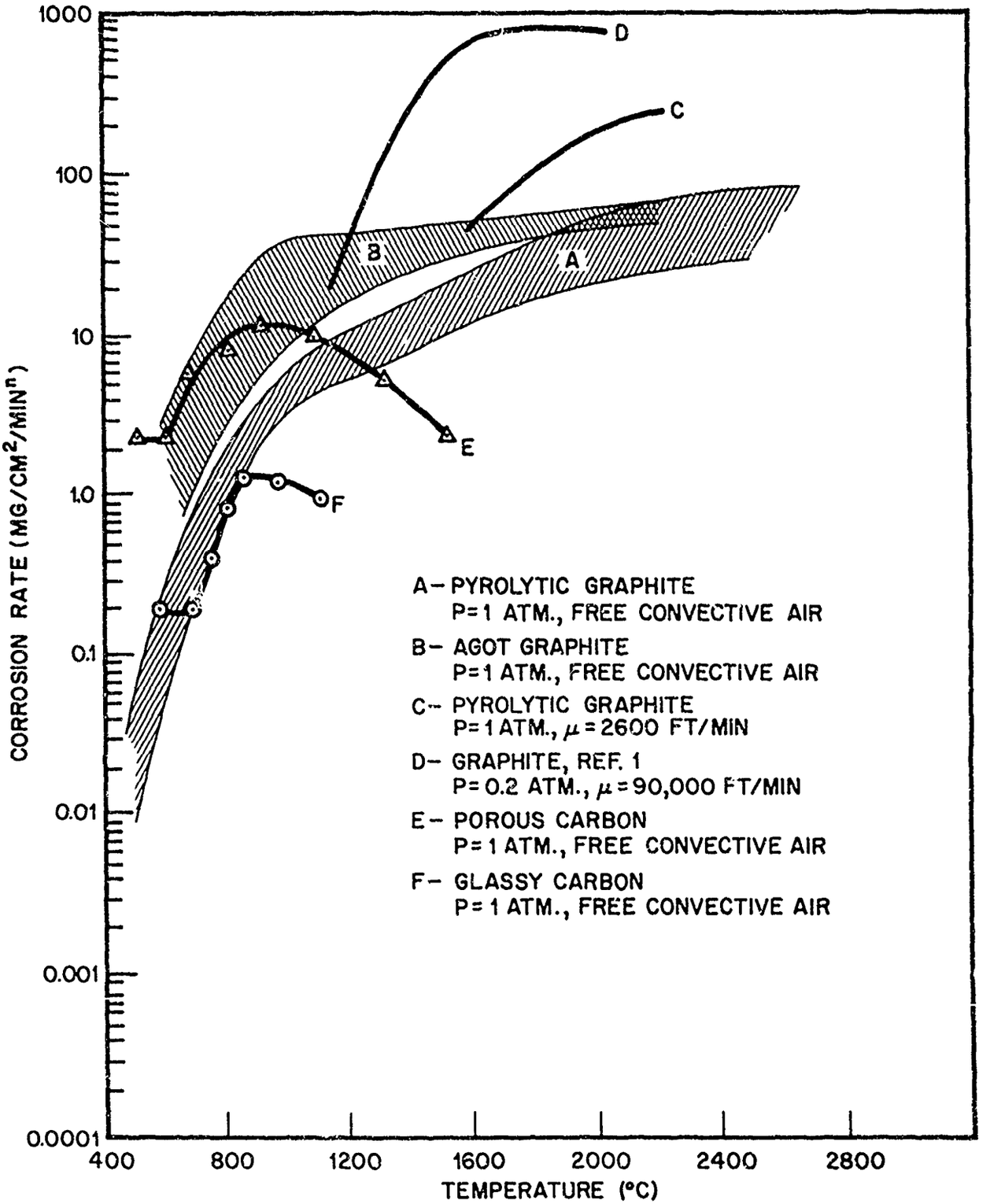

Fig. 14 Oxidation of Various Types of Graphite and Carbonaceous Materials in the Diffusion-Controlled Regime

3.5 CONCLUSIONS

To evaluate further the active-site diffusion controlled hypotheses, the following experiments are planned:

- Measurement of actual gas mass transfer conditions in our resistance-heated aparatus, and arc-image furnace
- Extension of work with poorly crystalline carbons to higher temperatures using the arc-image test facility
- Further investigation of the ratio of active to physical surface areas in the carbons tested

REFERENCES

1. C. Wagner, "Passivity During the Oxidation of Silicon at Elevated Temperatures," J. App. Physics, Vol. 29, 1295–7, 1958

2. R. A. Perkins, "Silicide Coating Degradation at Reduced Pressure," Sixth Meeting of the Refractory Composites Working Group, DMIC Report 175, September 24, 1962

3. "Refractory Molybdenum Silicides," Bulletin Cdb-6, Climax Molybdenum Company, January 1956

4. W. A. Maxwell, "Properties of Certain Intermetallics as Related to Elevated Temperature Applications: 1 – Molybdenum Disilicide," NASA Research Memorandum RM E9G01, October 1949

5. W. A. Maxwell, "Oxidation-Resistance Mechanism and Other Properties of Molybdenum Disilicide," NASA Research Memorandum RM E52A04, March 1952

6. J. W. Szymaszek, G. B. Cherniack, and R. F. R. Charvat, "Fabrication, Properties, and Uses of Molybdenum Disilicide," Metals Research Laboratories, Union Carbide Corporation, Niagara Falls, New York, February 1959

7. R. Kieffer, and E. C[illegible]wenka, "The Molybdenum-Silicon System," Z. Metallkunde, Vol. 43, (4), 101–105, 1952

8. R. A. Long, "Fabrication and Properties of Hot-Pressed Molybdenum Disilicide," NASA Research Memorandum RM E50F22, 1950

9. J. Berkowitz, "Stability of Ceramic Materials at Temperatures to 2000° C," WADD Technical Report 60-377, September 1960

10. A. W. Searcy and A. G. Tharp, "The Dissociation Pressures and the Heats of Formation of the Molybdenum Silicides," J. Phys. Chem. Vol. 64, 1539–1542, 1960

11. "Arc-Cast Molybdenum-Base Alloys," First and Second Annual Reports, Climax Molybdenum Company, 1950-1951

12. J. Nagle and R. R. Strickland-Constable, "Kinetics of Graphite Oxidation at Temperatures up to 20[illegible]°C, and at Pressures Approaching Atmospheric," Paper No. 120, Fifth Biennial Conference on Carbon, The American Carbon Committee, University Park, Pa., June 19–23, 1961

13. G. D. Blyholder, "Kinetics of Graphite Oxidation," University of Utah, Doctoral Dissertation Series, Publication No. 18,707, University Microfilms, Ann Arbor, Mich., 1956

PASSIVE THERMAL CONTROL COATINGS

J. E. GILLIGAN

M. E. SIBERT

T. A. GREENING

Lockheed Missiles and Space Company

Palo Alto, California

FOREWORD

This report reviews a part of the research work in progress in the field of passive thermal control of spacecraft at the Lockheed Missiles & Space Company Research Laboratory. The effort's purpose is to insure a reliable radiative surface, capable of maintaining the temperature of the vehicle's interior within the desired limits for long-term space missions.

The work described in this report was sponsored by U. S. Air Force Space Systems Division under Air Force Contracts AF 04(647)-787, and AF 04(695)-136.

CONTENTS

ILLUSTRATIONS

TABLES

Section 1
INTRODUCTION

The ultimate goal in the thermal design of any spacecraft is to assure that various components of the vehicle will operate within their respective allowable temperature ranges (as shown in Fig. 1) through all phases of the vehicle's mission. The problems associated with the thermal design of spacecraft are unique only insofar as the spacecraft environment is unique.

One of the major goals of the work reported in this paper is the practical attainment of four generic classes of materials which will insure reliable operation of a thermal control surface mosaic for one-year period. As originally described by Camack and Edwards (Ref. 1) these four classes are:

- Solar reflector – a surface which reflects the incident solar energy while emitting infrared energy
- Solar absorber – a surface which absorbs solar energy while emitting only a small percentage of the infrared energy
- Flat reflector – a surface which reflects the energy incident upon it throughout the spectral range from ultraviolet to far infrared
- Flat absorber – a surface which absorbs the energy incident upon it throughout the spectral range from ultraviolet to far infrared

Specific surfaces representative of the four basic surface classes are shown in Table 1.

Thermal-radiation characteristics comprise only one of a large number of important factors to be evaluated before choosing a material suitable for a specific application on spacecraft. From the point of view of passive thermal control, it is mandatory that materials be used which exhibit desirable α_s/ϵ ratios and values of emittance not

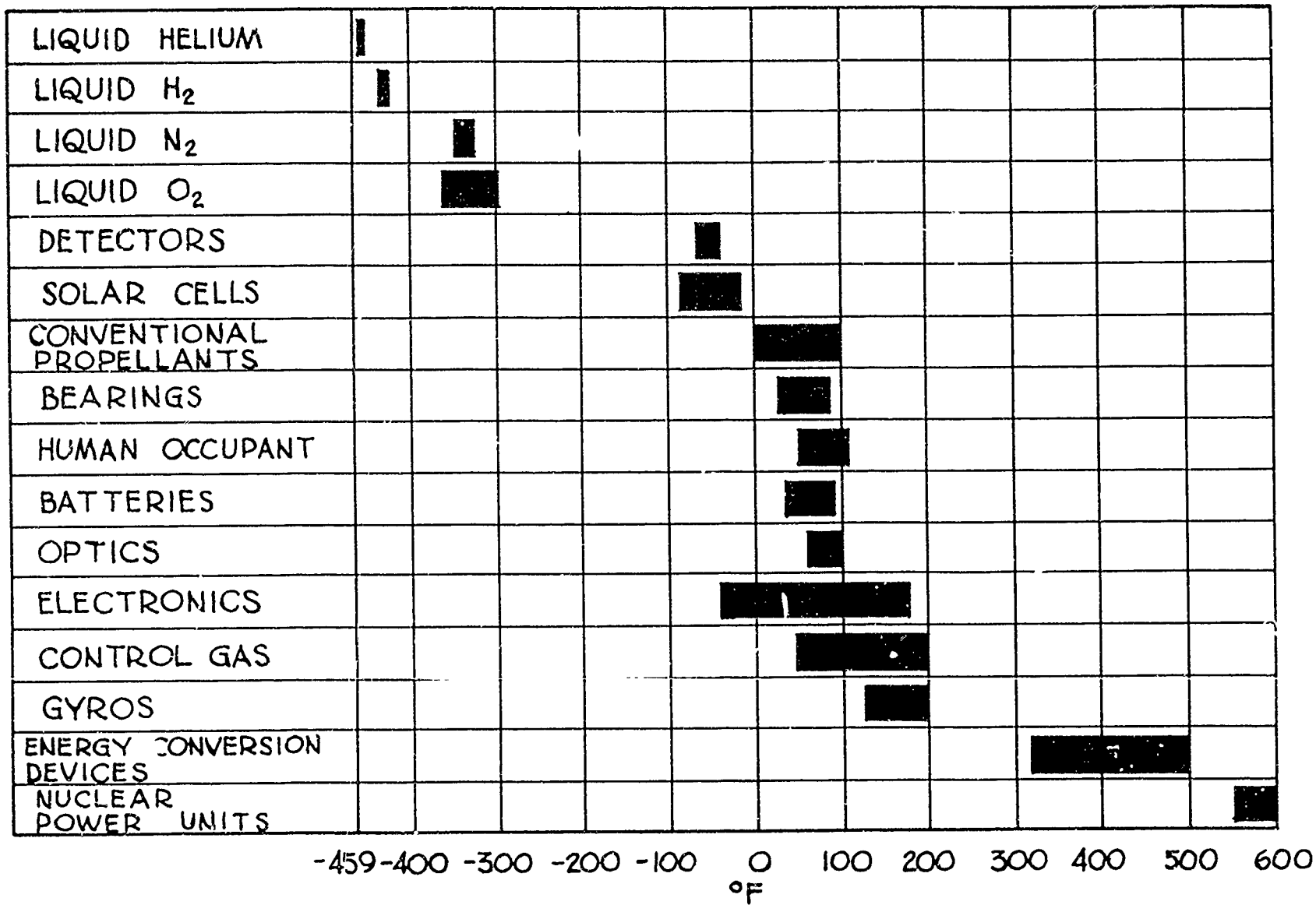

Fig. 1 Satellite Component Temperature Tolerances

Table 1

THERMAL CONTROL COATING TYPES

Type	Range			Example
	α	ϵ	α/ϵ	
Solar Reflector	0.1 - 0.3	0.8 - 0.9	0.1 - 0.4	White paint
Flat Reflector	0.1 - 0.3	0.1 - 0.3	1	Aluminum paints
Solar Absorber	0.2 - 0.5	0.03 - 0.3	2 - 15	Polished metal
Flat Absorber	0.8 - 0.9	0.8 - 0.9	1	Black paint

only initially, but also throughout the anticipated useful lifetime of the vehicle (Ref. 2). Therefore, materials must be found which are stable for a period of time in those environments characteristic of the particular mission profile. To outline the factors which influence choice of material, the environment is divided arbitrarily into two phases. (1) prelaunch environment, and (2) postlaunch environment, subdivided into the ascent, orbital, and re-entry phases. These phases must be examined separately, and the probable effect of each separate environment upon a material of interest must be considered.

In the prelaunch phase the thermal control surface is exposed not only to a number of handling and manufacturing processes, but also to the sometimes severe atmospheric environment (Ref. 4). Certain conditions which may influence the radiation parameters of materials are shown in Table 2. Postlaunch environment factors are outlined in Table 3, some changes of optical properties due to environment effects are shown in Table 4. A discussion of re-entry phase environments is beyond the scope of this paper.

Table 2

PRELAUNCH ENVIRONMENT

Sequence	Environmental Constituents and Parameters
Preparation of Raw Material	Contamination of Raw Coating Materials
Production of Thermal Control Surface	Coating Film Thickness
Exposure in Manufacturing Area	Surface Roughness
Transportation	Fingerprints
Captive Engine Test	Abrasion
Launch Site Environment	Natural Atmospheric Exposure
	Captive Test
	Fuel and Oxidizer Vapors

Table 3

POSTLAUNCH ENVIRONMENT

Possible Source of Damage to Thermal Control Surfaces	
Ascent	Space
Aerodynamic Heating*	Solar Electromagnetic Radiation*
Aerodynamic Shear Forces	Penetrating Radiation*
Aerodynamic Normal Forces	Planetary Atmospheres
Vibration and Shock	Vacuum
	Meteoroids
	Temperature Cycling

*Major sources of damage.

Table 4

ENVIRONMENT EFFECTS

Surface	Environment	Before	After	$\Delta\bar{T}$
Aluminum (Polished)	Fingerprints	$\epsilon = 0.08$	$\epsilon = 0.18$	-100°F
Gold Plate	Grease	$\epsilon = 0.05$ $\alpha_s/\epsilon = 6.0$	$\epsilon = 0.90$ $\alpha_s/\epsilon = 0.33$	-300°F
White Paint (Epoxy)	Ascent (750°F Peak)	$\alpha_s/\epsilon = 0.30$	$\alpha_s/\epsilon = 0.70$	+60°F
White Paint (Silicone)	Ascent (750°F Peak)	$\alpha_s/\epsilon = 0.37$	$\alpha_s/\epsilon = 0.41$	+10°F
White Paint (Sodium Silicate)	Ultraviolet (3 mos)	$\alpha_s/\epsilon = 0.20$	$\alpha_s/\epsilon = 0.30$	+20°F

Section 2

TYPES OF RADIATIVE COATINGS AND THEIR ENVIRONMENTAL RESPONSE

2.1 APPROACH

It was anticipated, and subsequently proven by experiment, that most thermal control coatings containing organic components were susceptible to alteration and damage by exposure to environmental conditions. Particularly destructive were the ascent heating, solar electromagnetic radiation, and penetrating nuclear radiation. In the following, LMSC work pertaining mainly to development, testing, and evaluation of purely inorganic optical coatings is discussed.

2.2 TYPES OF COATINGS

2.2.1 Silicate Coatings Systems

Solar Reflectors. Many present satellite designs require a solar-reflecting external surface, such as white paint, for proper thermal control (Ref. 5). When it was ascertained that epoxy-base white paints discolored rather badly during the ascent heating phase, an intensive effort was made to obtain a white paint with a suitable α_s/ϵ ratio which could successfully survive ascent.

The first paint vehicles to be evaluated were silicones. Since that time silicone base systems have been vastly improved and are being actively studied once again. Preliminary information indicates very promising overall stability. For longterm spacecraft use, these coatings were initially discarded because of inadequate resistance to ultraviolet radiation in vacuum. Phosphates seemed promising for use on aluminum substrates; however, due to extreme acidity, adhesion difficulties were encountered with magnesium and beryllium substrates.

As a compromise between pure ceramics and organic paints,work was undertaken on silicate coating systems. These silicate compositions are essentially inorganic paints based on aqueous alkali silicate vehicles (Ref. 6).

Both sodium and potassium silicates have been shown to be applicable as space-stable inorganic vehicles. Of a large variety of pigments studied, the refractory silicates generally possess the most stable optical character under ultraviolet irradiation. Of these, zircons and lithium-aluminum silicates have been evaluated in greatest detail, as shown in Table 5.

The silicate formulations are prepared by standard ball-milling procedures with water added to achieve a suitable application viscosity. Minimum particle size pigments are utilized to give minimum α_s values. Formulations are largely based on maximum pigment loading of the vehicle compatible with a final coherent coating. Coatings may be applied by spray, brush, or dip techniques. Individual coats must not exceed 2 to 3 mils; otherwise crazing or cracking will occur.

These coatings are stabilized by curing at 150 to 250° C. One hour at 100° C is usually adequate between coats, followed by 2 hours at 200° C for a final cure.

Flat Absorber Coatings. Flat absorbers have been formulated in a manner similar to solar reflector coatings, with black, oxidation-resistant pigments substituted for the white pigments. Preparation, application, and curing procedures are comparable in both cases.

Of particular interest as absorbers have been the spinel pigments based on oxides of Fe, Co, Ni and Mn. Such materials were prepared synthetically via solid state reactions of appropriate oxides, hydroxides, or carbonates. They were then ground, dispersed in alkali silicate vehicles, and utilized in the same manner as the solar reflectors.

On exposure to long-term simulated space environments, these spinel-based black solar absorbers show essentially no change. With regard to oxidation resistance, they also possess great superiority to carbon black-based absorbers. Some representative compositions of the spinel solar absorbers are given in Table 6.

2.2.2 Variable Systems

Continuously variable coating systems are composites of solar reflector and flat absorber coatings. Four systems have been studied in detail:

- Li-Al-silicate-Co_3O_4
- Li-Al-silicate-Fe_2O_3. NiO
- $ZrSiO_4$-Co_3O_4
- $ZrSiO_4$-Fe_2O_3° NiO

Representative compositions are given in Table 7. Compositions have been evaluated on Al-based substrates according to previously developed procedures. The compositions were cured at a maximum temperature of 200° C and evaluated both before and after exposure to a simulated space environment. Evaluation was primarily based on solar absorptance values. Emittance did not vary more than ± 0.02 for any given system studied.

2.2.3 Ceramics

Ceramics as a class show more promise for stability in the ascent and orbital phases than does the generic class of organic film-forming materials. Adhesion characteristics, abrasion and ultraviolet resistance, and high-temperature stability are generally superior for ceramics. Suitable application techniques represent a practical difficulty. Accordingly, porcelains, enamels, paste-type ceramics, and various silica deposition processes are being examined. Extensive investigation has been directed toward low firing-temperature ceramic coatings.

Table 5

SOLAR REFLECTOR COATINGS

Vehicle		Pigment		Pigment Vehicle Volume	Total Solids	Control		After Exposure 600 Sun Hours	
Type	w/o	Type	w/o	Ratio	percent	α_s	ϵ	α_s	ϵ
$Na_2O.SiO_2$	25.5	Li-Al-Silicate	43.1	4	54	0.10	0.85	0.14	0.86
$K_2O.SiO_2$	24.2	$ZrSiO_4$	50.4	4	57	0.12	0.86	0.18	0.86
$Na_2O.SiO_2$	19.2	$CaSiO_3$	39.0	4	59	0.14	0.84	0.19	0.85
$Na_2O.SiO_2$	36.8	Li-Al-Silicate	30.8	4	55	0.13	0.85	0.17	0.85

Table 6

FLAT ABSORBER COATINGS

Vehicle		Pigment		Pigment Vehicle Volume	Total Solids	Control		After Exposure 600 Sun Hours	
Type	w/o	Type	w/o	Ratio	percent	α_s	ϵ	α_s	ϵ
$Na_2O.SiO_2$	10.9	Co_3O_4	63.8	5.50	68.6	0.95	0.84	0.96	0.83
$Na_2O.SiO_2$	16.6	$Fe_2O_3.NiO$	61.2	2.75	68.5	0.82	0.85	0.83	0.86
$Na_2O.SiO_2$	21.8	Fe_3O_4	39.7	1.85	49.4	0.96	0.85	0.98	0.85
$Na_2O.SiO_2$	13.6	$Mn_2O_3.NiO$	68.2	4.75	74.0	0.94	0.83	0.94	0.83

Table 7

COATING FORMULATIONS

System	White wt	Black wt	Vehicle wt	P-V Volume Ratio	Solids w/o	Solids v/o	Black v/o	Black w/o
Li-Al-Silicate	190	0.3	114	4	53	33	0.05	0.12
Co_3O_4	190	1.5	114	4	53	33	0.25	0.62
Co_3O_4	190	6.1	114	4	53	33	1.00	2.50
$ZrSiO_4$	364	5.8	114	4	72	38	1	1.4
$Fe_2O_3 \cdot NiO$	345	29.0	114	4	73	38	5	6.8
$Fe_2O_3 \cdot NiO$	322	58.0	114	4	74	38	10	13.6

Fritted Enamels. True ceramic coatings such as frit enamels would probably yield materials with a high order of space stability. However, firing temperatures required are excessive for application to aluminum or magnesium alloys. Such coatings have been evaluated for limited use on more refractory substrates, as have been porcelain enamel frits based on ZrO_2 SiO_2, TiO_2, Sb_2O_3 and SnO_2 opacifiers.

Paste-type Ceramics. Commerically available cementitious type compounds, principally Sauereisen Cements (Ref. 7), have been investigated as self-curing coatings on satellite skins. Such compounds generally consist of a dispersion of silica, alumina, mullite, clay, talc or other oxide or silicate compounds in liquid sodium or potassium silicate or in an aqueous solution of a soluble phosphate. Coatings of such compounds have been applied to aluminum and magnesium substrates by trowelling, vibrating, splashing techniques, dipping and spraying. Extensive measurement of surface properties of as-prepared, modified, and baked surfaces has been made, and optical evaluation of such surfaces has been conducted.

Moderately acceptable results have been achieved with respect to adherance, thermal stability, irradiation characteristics, vacuum stability and reproducibility.

2.2.4 Plasma and Flame Spray Coatings

Offering more potential than most coatings for application to low-melting metals, plasma and flame-sprayed ceramics may be applied while maintaining the substrate at essentially room temperature (Ref. 8). In addition, the coating is cured as applied and is not so prone to thermal alteration, degradation, or other attendant changes in optical characteristics or stability.

A variety of such coatings prepared both in the LMSC laboratories and elsewhere has been evaluated for solar absorptance and spectral emittance properties. Such coatings include. ZrO_2, Al_2O_3, $ZrO_2.SiO_2$, TiC, TaC, ZrC, Cr_4C, TiN, Mo, Co, Ni, Al, plus many others. Attempts have also been made to plasma and flame-spray $Li_2O.Al_2O_3.nSiO_2$ and enamel frits.

2.2.5 Anodic Coatings

The employment of electrochemical conversion coatings for use as thermal control surfaces takes advantage of two radiation mechanisms (Refs. 9, 10, 11). Thin transparent coatings utilize the coating-metal interface as the reflecting interface, opaque films must rely on the reflectance of energy at the vacuum or air - coatings interface.

Opaque films, on the other hand, are comparatively thick with optical properties independent of the film thickness. This condition eliminates variations of optical properties due to film thickness. However, it does require that the anodic film be capable of reflecting the desired amount of solar energy.

2.2.6 Other Approaches

Chemical Coatings. An electroless copper surface subsequently oxidized, an electroless nickel surface also subsequently oxidized, and platinum black ($PtCl_2$) are some of the other coatings presently under study to produce a flat absorber. Such a flat-absorbing surface may be used as an external radiation heat shield for re-entry.

Stable Oxides of Metals. A recent development in thermal control has been the possible use of stable oxides as thermal control surfaces. Quite possibly, the stable oxide formed during prolonged high-temperature heating of stainless steel will produce a coating of high emittance ($\epsilon > 0.75$). The characteristics of stable oxides of such metals as beryllium, titanium, molybdenum, etc., are described in a NASA report (Ref. 4). Such a stable oxide coating may be adequate for many spacecraft materials, it would probably be cheaper than the use of an anodizing or chemical conversion process.

2.3 VARIATION WITH PHYSICAL PROPERTIES

Specification of composition and formulation of the coating do not, in themselves, insure achievement of expected, much less reproducible thermal radiative properties. Optical properties for any given formulation are a function both of the formulation itself and of the manner in which the coating is applied to the substrate.

In terms of the formulation, pigment particle size and pigment-binder ratio are of particular significance. Figure 2 illustrates the approximate effect of pigment particle size on solar absorptance before irradiation. It is seen that the absorptance value falls off fairly rapidly as the particle size of pigment approaches 1 micron. This particular curve reflects changes characteristic of a zircon-pigmented potassium silicate coating.

Similarly, the pigment content for any given coating strongly influences the absorptance and the absoptance-emittance ratio, a condition illustrated by data in Fig. 3. By increasing the pigment-binder ratio from about 3.5 to 5.5, a decrease of about 50 percent can be effected in both the absorptance and the absoptance-emittance ratios.

In determining the optical characteristics of final-coated specimens, the application technique used for substrate coatings is also important. Thicknesses of roughly 3 to 5 mils, required to effectively hide the metallic surface, are illustrated by the two

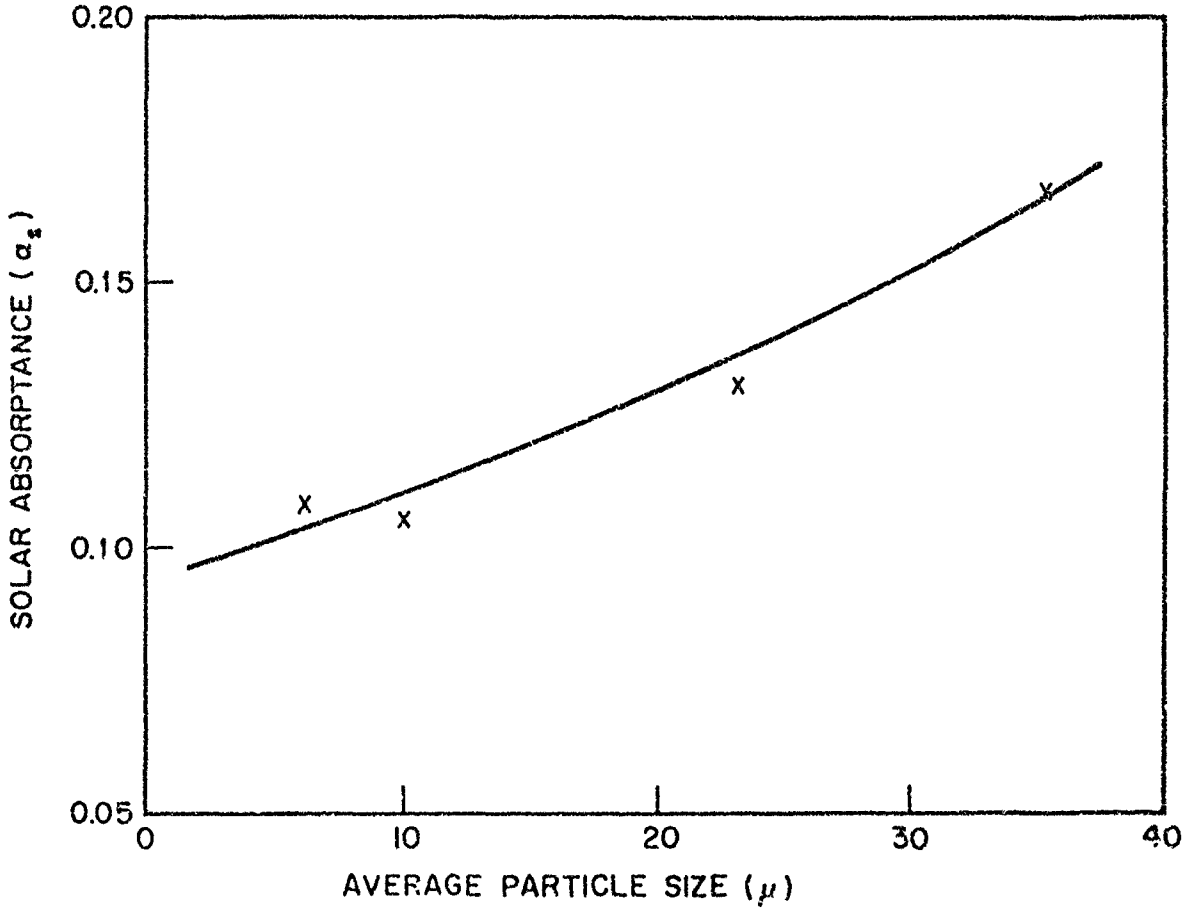

Fig. 2 Effect on Solar Absorptance Produced by Changes in Pigment Particle Size

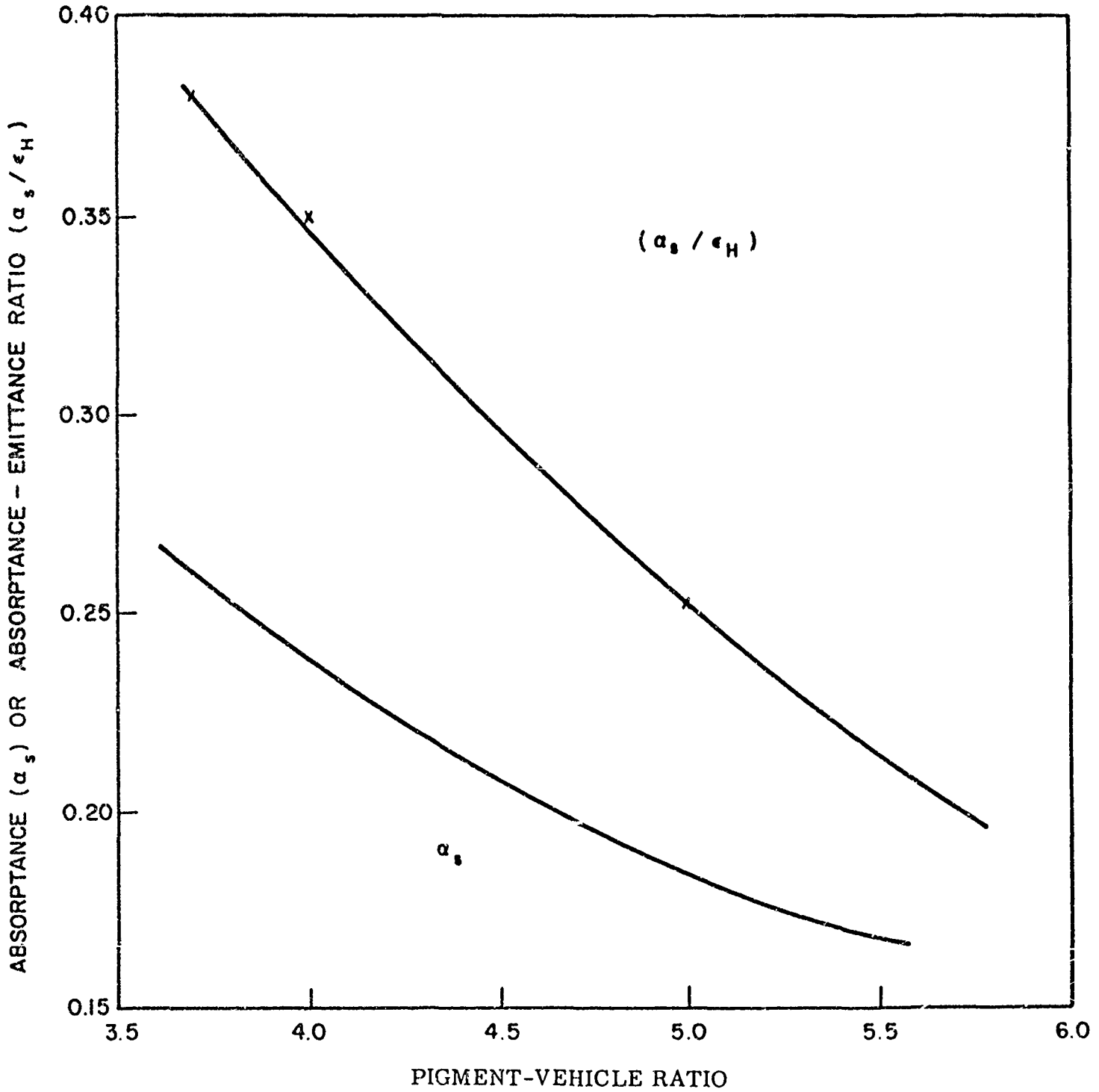

Fig. 3 Effects of Pigment-Vehicle Ratio on Absorptance and α/ϵ Ratio

curves in Fig. 4 showing both the absorptance and the absorptance-emittance ratios as a function of film thickness. Both values become essentially constant after about 5-mils' thickness is obtained.

It is also possible to alter significantly the α_s/ϵ ratio of most materials and particularly of metals by altering the roughness of the surface, as shown in Fig. 5 (Ref. 13).

Obviously then, surface polishing and controlled roughening can produce a specified α_s/ϵ ratio range characteristic of that material. It is equally obvious that carefully controlled fabrication and application techniques must be followed to insure attainment of optimum and reproducible surface properties, and that surfaces be maintained in their "as prepared" condition during the period between production and use.

2.4 OPTICAL EVALUATION OF COATINGS

In general, the solar absorptance and total hemispherical emittance are determined for each specimen before and after vacuum irradiation. Solar absorptance is determined by a measurement of the spectral reflectance from 0.25 to 1.8 microns, by use of a Cary double-beam spectrophotometer with an integrating sphere attachment (Ref. 2). With an alternate energy source, the wave-length range is expanded into the ultraviolet region to 0.2 microns. The absorptance values obtained are within 2 to 3 percent accuracy (Ref. 12).

Total normal emittance values are obtained by use of a Perkin-Elmer double-beam spectrophotometer in conjunction with 800° C Hohlraum. The actual quantity measured is the normal spectral reflectance. Total hemispherical emittance as a function of temperature is obtained by a weighted ordinate data-reduction process utilizing 100 points in the wave-length range of 2 to 25 microns. In general, these emittance values have an accuracy within 5 percent.

Complementary measurements of total hemispherical emittance as a function of temperature are made directly utilizing electrically heated samples in black walled

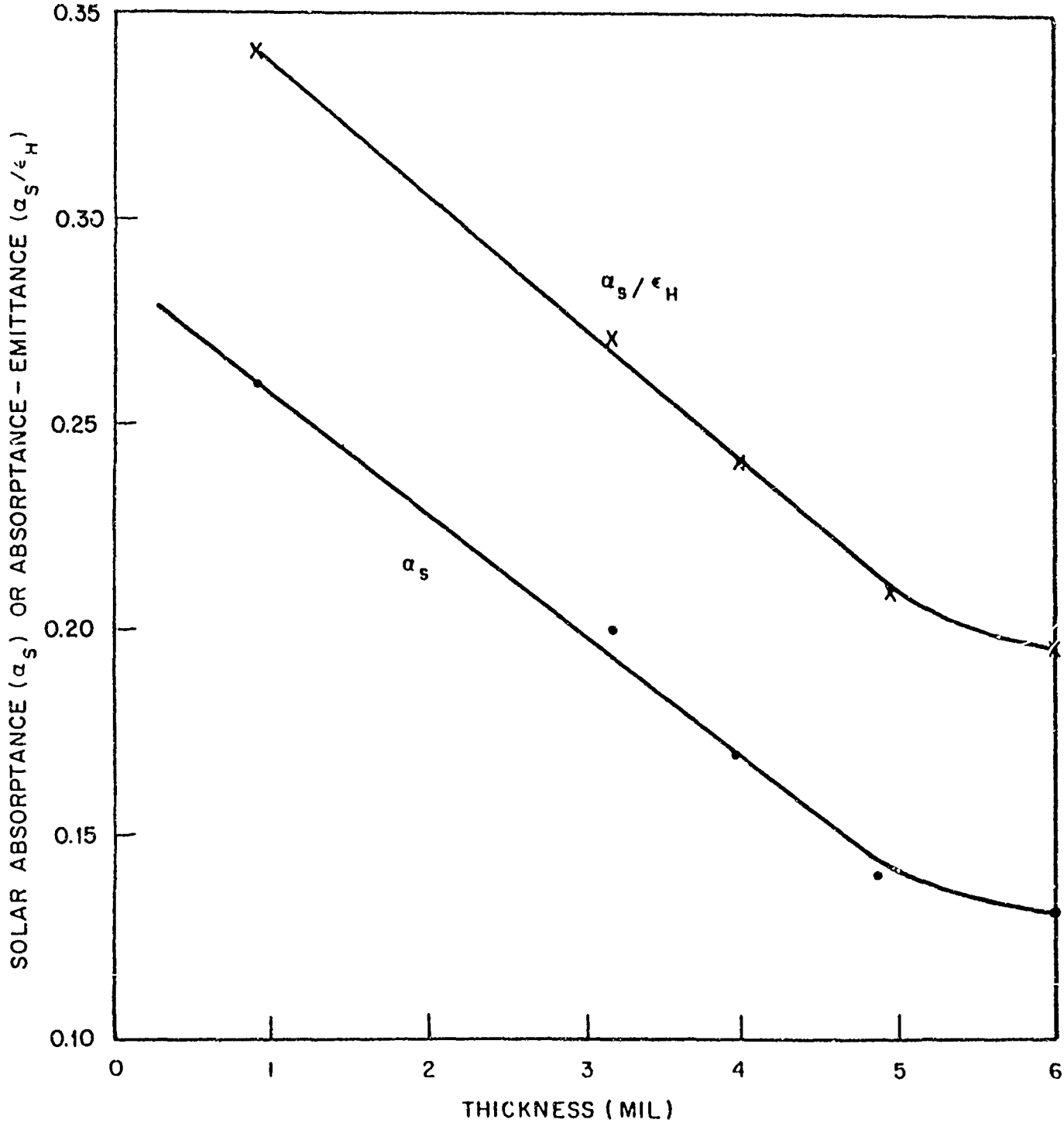

Fig. 4 Effect of Coating Thickness on Optical Properties

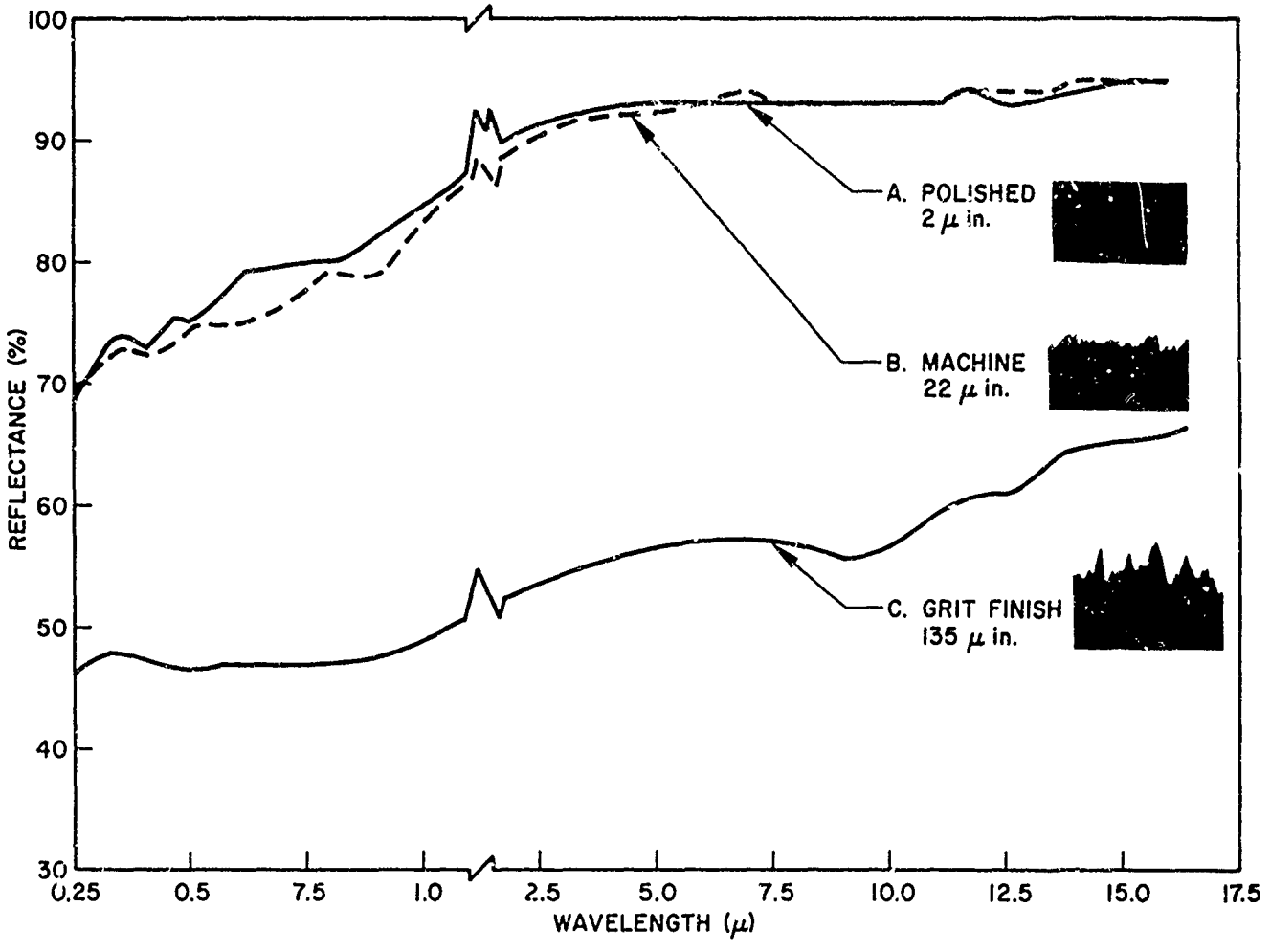

Fig. 5 Change in Optical Properties With Change in Surface Roughness

cryogenic chambers. Emittance is computed as the net power radiated by the surface material divided by the product of surface area, the Stefan-Boltzman constant, and the fourth power of the temperature. Accuracies of the order of 2 to 5 percent are easily attainable.

2.5 ULTRAVIOLET RADIATION

Ultraviolet radiation testing of coated specimens is carried out in a stainless steel vacuum chamber fitted with water-cooled, copper-block specimen holders. These holders are designed to accommodate 1 in. diameter specimens approximately 1/8 in. thick. The basic unit accommodates 6 specimens at 6X solar intensity and 1 specimen at 20X intensity. The vacuum system utilized consists of a 40-liter-per-second Vaclon pump in conjunction with a mechanical pump capable of producing a vacuum of 10^{-7} torr.

The ultraviolet source is an AH-6 high-pressure-mercury, argon-filled lamp. The lamp operates at 1,000 watts with an output of 65,000 lumens consisting of a continuous spectrum with superimposed lines. The spectral-energy curve for this lamp compares favorably with the known solar curve. Most of the wavelengths of less than 2,000 A are absorbed by the quartz tube, most of the infrared is absorbed by the water-cooling envelope around the lamp. As a screening operation, specimens are generally irradiated to 300 to 600 sun hours exposures. Final specimens may be irradiated 1,000 to 2,000 sun hours or more if changes are still evident.

A sun is defined as the intensity equivalent to that of the sun near the earth, but outside its atmosphere, at wavelengths less than 4,000 A. Thus, one sun-hour is the total incident energy (below 4,000 A) delivered by the sun or its equivalent over a period of one hour.

In order to illustrate the wide variety of optical data obtained for the series of coatings investigated, the percentage change in absorptance is shown in Fig. 6 as a

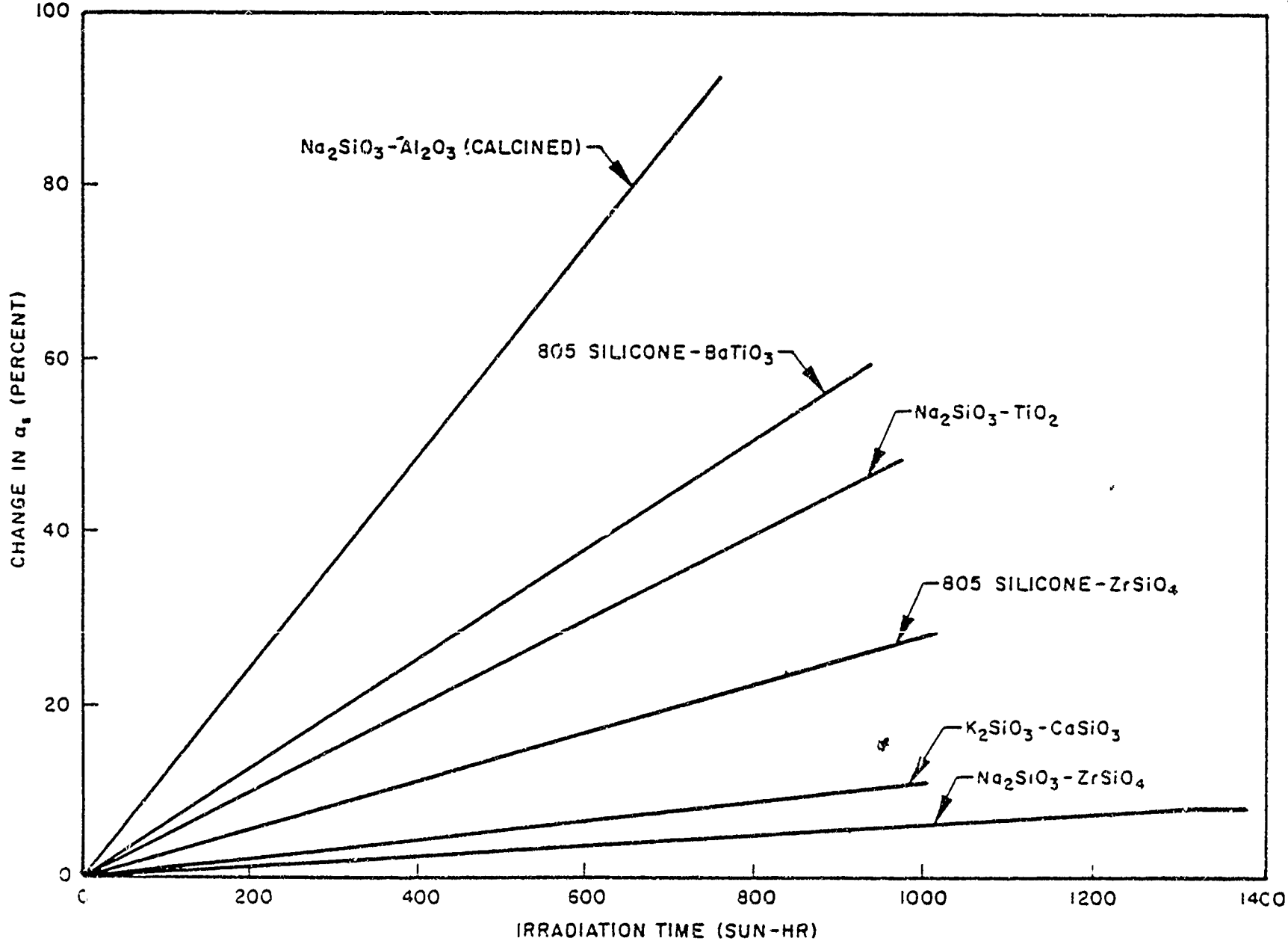

Fig. 6 Change in Solar Absorptance with Ultraviolet Irradiation for Six Coating Formulations (-325 Mesh Pigments)

function of irradiation time for six different coatings. Changes observed vary from as little as approximately 10 percent per thousand sun hours (certain all-silicate compositions) to greater than 100 percent per thousand sun hours (certain silicone and alumina-based compositions). Aluminas and titania pigments are particularly susceptible to ultraviolet radiation damage, illustrating why the present compositions were chosen for utilization as thermal-control surface materials.

Figures 7 and 8 show change of absorptance with ultraviolet exposure for a number of other coatings developed in the LMSC laboratories.

2.6 NUCLEAR RADIATION EFFECTS

LMSC has been conducting an extensive program to develop nuclear-radiation-hardened thermal-control materials. With the advent of spacecraft-borne nuclear reactors and the almost daily introduction of newer and more advanced nuclear spacecraft concepts, the demands upon state-of-the-art thermal control materials may greatly exceed their capabilities.

Before some of the more important results of this program are discussed, basic test concepts and exposure conditions should be explained. The majority of the samples, including both organic and inorganic materials as well as metals, were exposed in vacuo. Temperatures of the samples usually did not exceed 150° F. Several exposures were carried out at 77° K. To obtain comparative data, a number of samples were also irradiated in air. Pressures below 10^{-3} torr and liquid nitrogen (LN) surfaces within the vacuum chambers provided an adequate simulation of the net pressure effect of space. Nuclear damage was determined by comparison of pre- and post-test physical and thermal radiative properties.

Analyses of data from more than 1,000 samples of more than 150 different types of thermal control materials lead to the conclusions described below. These conclusions are based on total integrated exposures of roughly 10^{8}R(C) gamma radiation and 10^{15}n/cm^{2}, fast neutrons, respectively, and may be stated as follows:

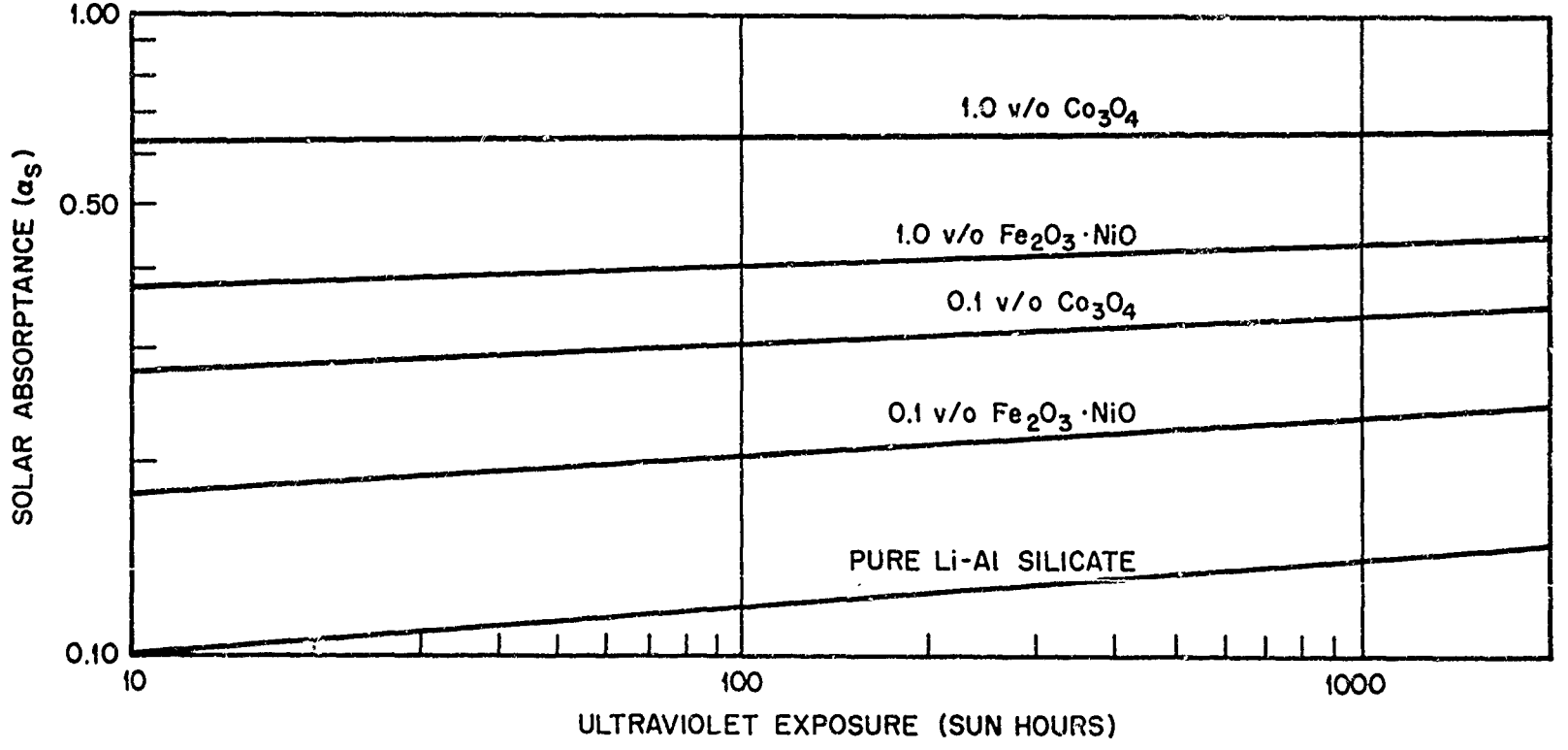

Fig. 7 Ultraviolet Exposure Effects on Li-Al Silicate Based Pigmented Compositions

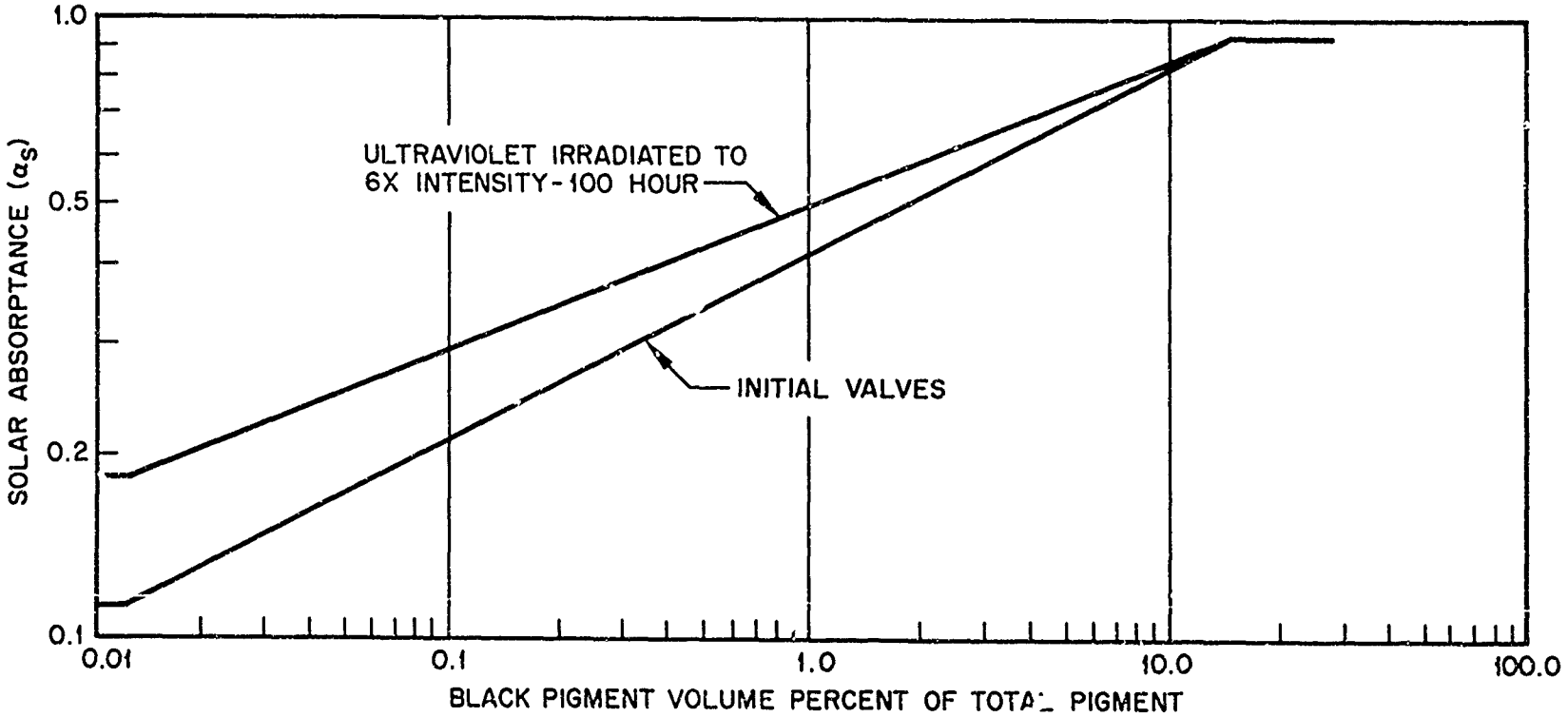

Fig. 8 Solar Absorptance Values for the $ZrSiO_4$ - Co_3O_4 System

- Organic-base materials degrade both mechanically and optically at exposures of approximately 3×10^{7}R(C) to 1×10^{8}R(C). In many materials the inception of detectable mechanical damage occurs prior to significant thermal radiative changes.
- With very rare exceptions inorganic materials incur only optical damage.
- Solar absorptance is the only thermal radiative property importantly affected. With several exceptions, emittance remains stable to within 5 percent of its initial value.
- Irradiations conducted in air produce effects which differ both in magnitude and manifestation from those in vacuo.
- Comparatively, vacuum irradiation at 77° K results in heavily increased damage to both organics and inorganics.

Pertinent to nuclear spacecraft vehicle design, these and other more detailed analyses have been tentatively phrased into the following conclusions:

(1) Inorganic materials are clearly superior to state-of-the-art organic materials.

(2) Radiation resistance is sharply increased by heat curing, room-temperature cured paint systems are clearly the least stable. (This conclusion applies to both inorganic and organic-base thermal control coating systems.)

(3) Solar reflectors (white paints) and flat reflectors pose the greatest problems, other classes being much less sensitive.

(4) Most importantly, for mission durations of 90 days up to several years, and where gamma radiation doses will exceed ten megarads, careful consideration must be given to the selection of thermal control materials.

Section 3

RESULTS

3.1 COMMERCIAL PAINTS

Many commercial paints display adequately superior adherence on aluminum, magnesium, and other metal surfaces. Vibration, thermal shock, and bending tests produced acceptable results as did salt-spray tests. Major problem areas were:

- Change of optical properties due to environmental effects notably in ascent heating
- Change of optical and physical properties with ultraviolet exposure

More specificly, the results of environmental tests indicate the superiority of various surface coating systems over others in individual environments. Generally, good overall stability can be realized by heat curing. Paints cured at room temperature inevitably suffer in the ascent heating tests and are less stable to ultraviolet radiation. Silicones, though initially displaying poor ultraviolet resistance, have been markedly improved and now rank very high on the list of flight-qualified paint surfaces. Presently available silicones require high-temperature cures, for this reason they are not extensively used. Acrylics, epoxies, and similar materials ordinarily are room-temperature cured. Again quite generally, acrylics are superior to epoxies, but inferior to silicones. The ultimate choice, as noted previously, is highly dependent upon vehicle mission parameters.

While a great deal is known about many paint systems, their basic thermal radiative properties, environmental resistance, and other applicable parameters have not been sufficiently tested to qualify them for general or even specific spacecraft appliations. This is not to say that the tests from which these data are obtained are unimportant; on the contrary, such tests are fundamental, and must be used when considering any candidate thermal control system. The point is that the evaluation of such a system

requires knowledge of a complex variety of test data and vehicle requirements, as well as value judgments of these criteria.

3.2 SILICATE-BASE PAINTS

Silicate-base paints present a matte-like, semi-porous appearance. Porosity is, however, of a discontinuous nature. The α_s/ϵ ratio may be varied for flat absorbers from about 0.95 to 1.15. Applicable spinel-type materials include Fe_3O_4, Fe_2O_3.NiO, Mn_3O_4, Mn_2O_3.NiO and Co_3O_4. Of a large number of white-coated solar reflectors evaluated under simulated space environmental conditions, the zircon and lithium aluminum silicate materials have shown the least change due to ultraviolet radiation effects. Tables 5 and 6 present data relating to the optical properties of several silicate based paint formulations.

Evaluation of these coatings under space environment conditions has shown them to be extremely stable. They have initial α_s values of 0.08 to 0.20, dependent on composition. Low α_s coatings may degrade 5 to 20 percent after 2000 sun hours of exposure, after which α_s becomes essentially constant. Initial emittance values are unaffected by ultraviolet, remaining constant at 0.82 to 0.87 for high-emittance coatings.

Physical testing of the silicate-based paints shows their adherence and coherence is excellent over aluminum substrates and Dow-17-coated magnesium-alloy substrates. In the case of aluminum-alloy substrates, adherence is somewhat less pronounced, as demonstrated through the use of thermal shock tests. Test panels heated to 100°C have been quenched in dry ice – isopropyl alcohol baths (approximately -70°C) – without damage to the applied coating. Silicate-based coated specimens have also survived severe vibration in tests up to 10,000 cycles per second.

Bend tests have also been made on coated panels using 3/4 in. to 1/2-in. mandrels. In general, coatings withstand this treatment using up to 180° bends. Some crazing is evident, but no actual exfoliation occurs.

Additionally, salt-spray tests have been run on representative zircon-silicate-coated magnesium panels. Such tests were carried out for 24 hours duration at 35° C, in a chamber containing 20 percent salt and 100 percent relative humidity. Coatings over bare magnesium exhibited moderate chalking and pitting. Those over Dow-17 surfaces exhibited only slight chalking, and a few evident pits could be traced to imperfections in the coating itself.

Major drawbacks associated with silicate paints concern the high temperature curing requirements, the high degree of skill and care necessary in their application, and the difficulties in prelaunch protection.

3.3 CERAMIC COATINGS

Ceramic-paste type products from the Sauereisen Cements Company have come under intensive investigation as self-curing thermal-control coatings. To produce smooth, consistent reproducible coatings yielding optically repeatable data, spraying was found to be the best application method. Some compounds required dispersion by ball-milling, others by intensive osterizer mixing, and others only by thinning with sodium silicate solution to the proper viscosity and solids per-unit-volume consistency. Trowelling on, vibrating, dipping, or dry applications produced inconsistencies in optical properties, introduced drying cracks, gave rippled surfaces, produced uneven coverage of the substrate, or promoted separation of the constituents.

Table 8 shows solar absorptance values obtained for those paste-type compounds which gave the greatest degree of reproducibility. Each of the products was dispersed to spraying consistency in sodium silicate solution. Compound number 1 is silica. Number 6 is mullite ($3Al_2O_3 . 2SiO_2$). Number 19 is silica dispersed with clay plus ponolith. Number 74 is alumina.

Table 8

SOLAR ABSORPTANCE OF SAUEREISEN COATINGS

Test	Sample	Varied Parameter	α_s
13116	Sauereisen No. 1	.035 in. thick	.35
13117	Sauereisen No. 1	.013 in. thick	.29
13118	Sauereisen No. 1	.004 in. thick smooth coating	.36
13119	Sauereisen No. 6	As received with specks	.44
13120	Sauereisen No. 6	Screened through 100 mesh, hot	.43
13121	Sauereisen No. 6	Screened through 100 mesh, cold	.46
13122	Sauereisen No. 19	.005 in. smooth coating, applied hot	.38
13123	Sauereisen No. 19	As received, not screened	.31
13124	Sauereisen No. 19	Cold slip over hot substrate	.38
13125	Sauereisen No. 19	Dried slowly	.39
13126	Sauereisen No. 74	Standard	.46
13127	Sauereisen No. 74	Standard	.45

Figure 9 illustrates change of solar absorptance and hemispherical emittance with change of surface treatment for four Sauereisen compounds. For each compound, C represents the optical values obtained for a coating of 0.010 in., while T and L represent values of the upper and lower surfaces of 0.125-in. thick samples cast in paraffin molds. The objective is to determine: (1) the probable effect of soluble salts and fine materials, which are carried to the surface during drying of the coating, on optical values, and (2) the role of surface roughness in variation of optical properties, the coatings being intermediate in roughness between the lower (smooth surface) and the upper surface of the cast sample. It can be seen that α_s of the coatings are intermediate between those values of the top and bottom of the cast sample. This result reflects the response of absorptance to surface roughness. The declining emittance values for the coatings, as compared with the top and bottom surfaces of the cast sample, show the effect that the fine and soluble salts have in altering the emitting surface.

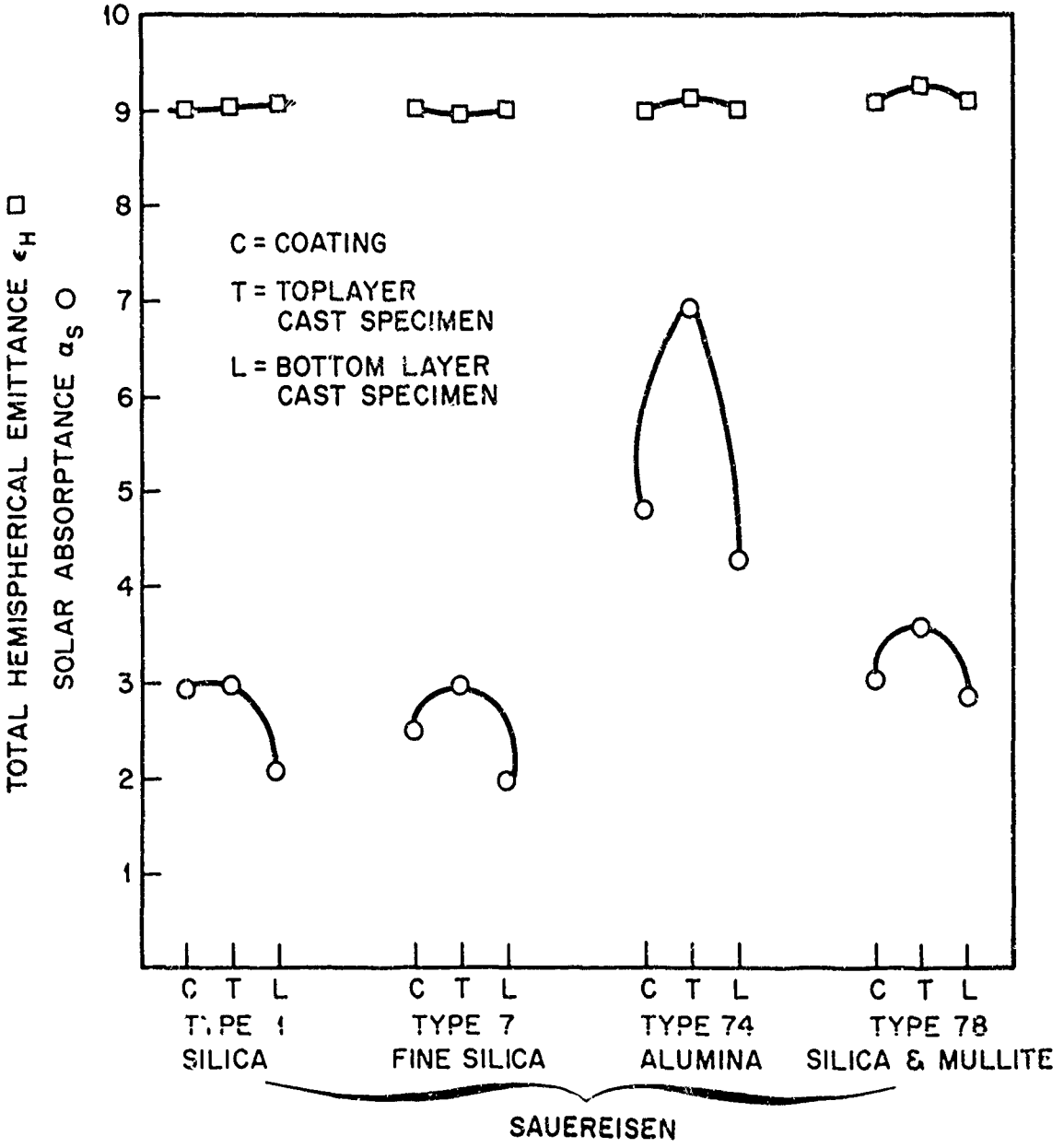

Fig. 9 Change of Optical Properties With Surface Alteration

3.4 PLASMA COATINGS

Table 9 shows the optical measurements for some plasma-sprayed materials both before and after nuclear irradiation. Fast neutron (>2.9mev) flux were approximately 8.7×10^{14} n/cm^2.

In general, absorptance values of the test sample increased as a result of irradiation. To the eye, the change is a discernable darkening of the coating. Emittance values also tended to increase in some materials and to decrease in others.

Table 9

PLASMA-SPRAYED COATINGS – OPTICAL MEASUREMENTS

Material	Composition	Optical Properties		
		α_s	ϵ_{HS}	
Zirconia	ZrO_2	.434	.741	Plasmadyne
Zirconia	ZrO_2	.323	.719	
Alumina	Al_2O_3	.156	.724	
Molybdenum	Mo	.634		
Titanium Carbide	TiC	.867	.747	
Titanium Nitride	TiN	.801	.612	
Alumina	Al_2O_3	.255	.710	
Tantalum Carbide	TaC	.816		
Lith-Alum-Silicate	$Li/Al/SiO_3$	.512	.837	$Li_2O.Al_2O_3$-$8SiO_2$
Zirconia	ZrO_2	.349	.705	Zirconium Corp.
Zirconium-Carbide	ZrC	.809	.627	
Chromium Carbide	CrC	.783	.543	
Nickel Chromium	NiCr	.400	.248	
Tantalum Beryllium	$TaBe_{12}$	.492	.238	
Zircon	$ZrSiO_4$	.46	.81	
Spinel	$MgO.Al_2O_3$	.42	.75	
Wallastonite	$CaO.SiO_2$	.64	.85	

α_s – Cary Solar Absorptance

ϵ_{HS} – Hohlraum Spectral Emittance

Figure 10 shows variations of spectral emittance for plasma sprayed molybdenum disillicate for coarse (44μ to 74μ) and for fine (<44μ) materials as compared with a sintered body.

Figure 11 shows the change of normal spectral reflectance for plasma-sprayed lithium aluminum silicate, as compared with data for a paint coating of the same product dispersed in sodium silicate. The lower values for surface reflectance of the plasma product are partly attributable to the increase in surface roughness of such a sample as compared with the smoother paint surfaces. Also, finer particle pigment sizes in the paints (1 micron vs. 44 microns) promote lower α_s values.

Flame-sprayed coating employing oxy-acetylene flames and powders are very subject to variation in optical properties with a change of oxygen-to-acetylene ratios. Any partial burning of the acetylene results in co-deposition of carbon, sharply increasing values of α_s. Oxy-hydrogen flame sources promote greater reproducibility of optical properties with essential elimination of surface darkening of light coatings. There remains, however, the problem of stability of all but oxide materials in flame-spray environments. Even oxide vary in properties, due to changes in the relative amount of the different oxide forms present, which are to some extent a function of the amount of free oxygen in the flame.

Rokide coatings, which are achieved by employing pre-sintered ceramic rods in a flame-spray process, do offer some stability and reproducibility of optical properties. The chief difficulties involve differences in thermal expansion of the coatings and the substrate, differences resulting in failure during ascent or re-entry; this problem is common to all plasma or flame sprayed coatings, however, and perhaps to all coatings of whatever design.

Careful surface preparation by vacuum grit blasting, followed by an application of a nickel-chromium-boron interstrate, often promotes improved bonding and resistance to thermal stresses in plasma and flame sprayed coatings.

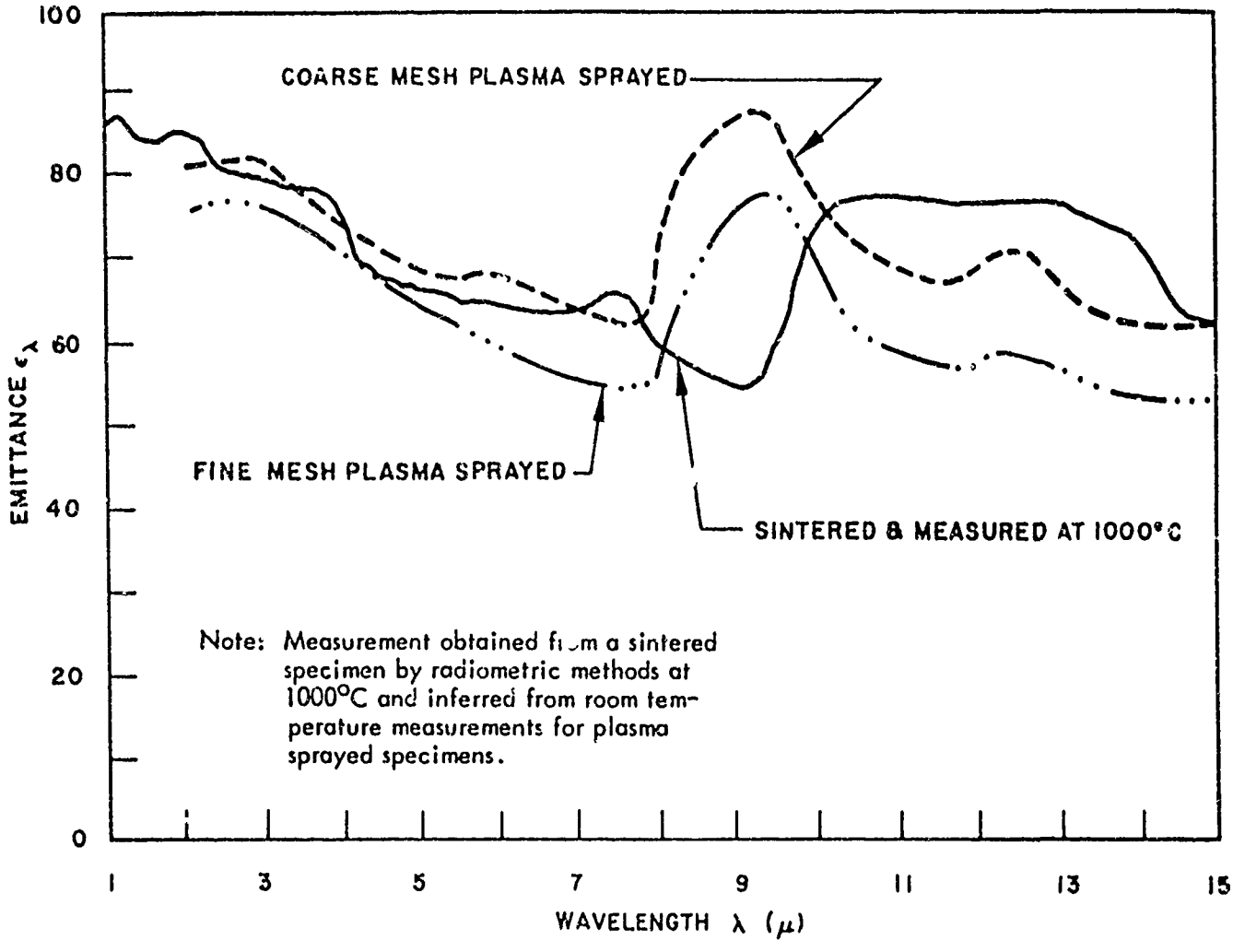

Fig. 10 Spectral Emittance for Molybdenum Disilicide

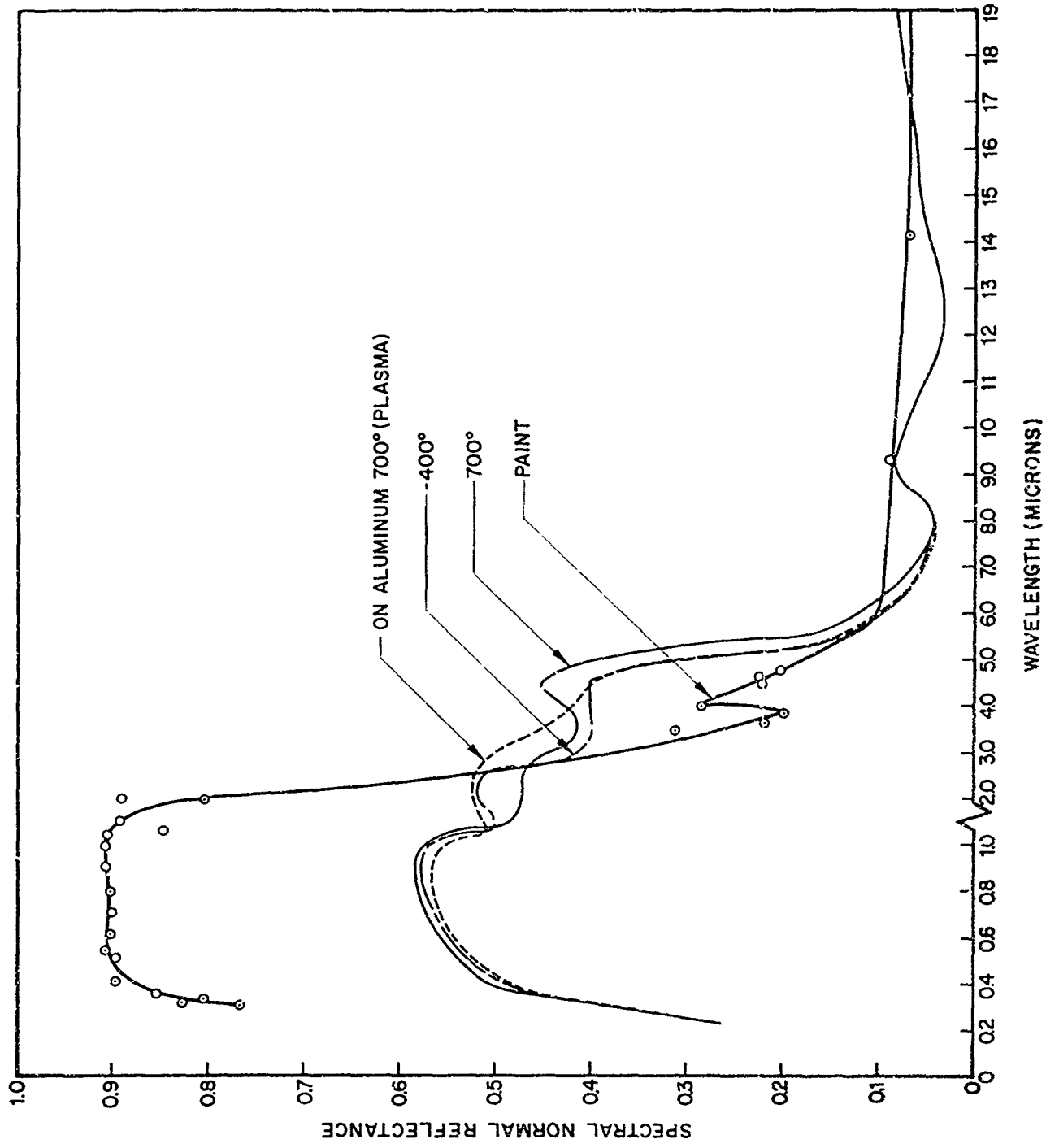

Fig. 11 Normal Reflectance of Plasma-Sprayed Lithium Aluminum Silicate and of Lithium Aluminum Silicate Paint Pigment Dispersed in Sodium Silicate

Table 10 presents solar absorptance data for plasma-sprayed lithium aluminum silicate ($Li_2O.Al_2O_3.8SiO_2$) which alters during spraying to $Li_2O.Al_2O_3.2SiO_2 + 6SiO_2$. It can be seen that lower values of α are obtained for all coatings with lower power inputs. Premixed samples of 33 and 50 percent Al_2O_3 were also plasma-sprayed, reflecting an increase in α_s for such compositions.

Table 10

SOLAR ABSORPTANCE OF LITHIUM ALUMINUM SILICATE COATINGS

Test	Sample	Weight Ratio	Percent Ratio	Plasma Current	αs
13114	Lithafrax + Al_2O_3	(1-0)	(100-0)	650 amps	.30
13115	Lithafrax + Al_2O_3	(1-0)	(100-0)	300 amps	.22
13112	Lithafrax + Al_2O_3	(2-1)	(67-33)	600 amps	.38
13113	Lithafrax + Al_2O_3	(2-1)	(67-33)	300 amps	.25
13108	Lithafrax + Al_2O_3	(1-1)	(50-50)	600 amps	.35
13111	Lithafrax + Al_2O_3	(1-1)	(50-50)	300 amps	.26

3.5 ANODIC COATINGS

Many studies of anodic coatings have been accomplished at LMSC and elsewhere. Basically, these studies have sought to develop solar reflector and flat absorber coatings, with some special attention to solar absorbers. Anodized aluminum typifies the solar reflector work. It has been found that the optical properties are indeed characteristic of solar reflectors but are extremely sensitive to film thickness. Optical-interference effects also arise due to the thinness of the oxide deposition, mainly in the near infrared. Though the developments have been successful in producing very low α_s/ϵ surfaces, the practicality of anodic solar reflector coatings leaves much to be desired. Black coatings, however, have been much more successful. Black chromium and black nickel exemplify the latter types, yielding very high values of solar absorptance ($\geq$0.85) and moderate-to-high values of emittance (0.6 - 0.8). Little demand has been shown for the solar absorber class (Taber coatings). Its

development consequently has not kept pace with those of the other classes. These coatings are generally prepared as very finely divided metal oxides in anodic or electrophoretic baths. Nickel oxide coatings on suitable substrates have exhibited α_s/ϵ ratios of approximately 15 and above.

3.6 OTHER COATINGS

Chemical coating approaches to thermal surface control have not only been spectacularly successful in development but also have been placed in production in several instances. A process for the deposition of platinum black (finely divided metallic coating) on beryllium, for example, renders a surface with a solar absorptance of 0.90 to 0.93 and an emittance of 0.87 to 0.89. This process is being extended to a number of other basis materials including copper, aluminum, and titanium. The major problem has been adhesion, optical properties being excellent. Electroless nickel chromium and copper deposited on various basis metals show results analogous to platinum black, i.e., excellent optical properties and adherence dependent upon basis metal. Palladium black has been another successful development. In general, these coatings possess α_s/ϵ ratios slightly less than one, with solar absorptances of 0.9 or better. With some reservations, at least one of these electroless coatings can be successfully applied to any common spacecraft vehicle substrate.

3.7 ADHESIVE-BACKED TAPES AND FOILS

Efforts to develop these types of materials have been generally successful. Of particular note are the adhesive-backed aluminum foil tapes, many of which are now routinely used. These are simply thin aluminum foils (0.001-0.005 in.) with pressure-sensitive adhesives on one side. The best tapes incorporate silicone adhesives and can withstand peak ascent heating temperatures in excess of 750° F. Their thermal radiative properties are essentially those of rolled aluminum. Many of these tapes are supplied with a protective film however, which, if not removed, will have a drastic effect on the tapes' thermal radiative properties. Even those tapes which do not have protective films should be thoroughly cleaned, since a certain amount of adhesive transfer in the rolls is inevitable.

Only a limited amount of work has been done to obtain solar reflector tapes. Basic work has achieved encouraging excellent stability to simulated solar ultraviolet and ascent heating, as demonstrated in the laboratory. Beyond the fact that they are silicone-based, a fuller description of these tapes would be premature at the present time.

3.8 STABLE OXIDES OF METALS

The generation of a stable oxide on a basis metal by heating the latter in an oxidizing atmosphere is, at best, only of marginal value due to the many attendant problems. Certain exceptions – specifically in the formation of (black) oxide films on high-temperature, high-emittance surfaces – can be made. Current interest remains with white coatings, however, although development has been unsuccessful for a variety of reasons. Some coatings are hygroscopic (e.g., MgO); others have little or no adherence on thermal shock stability (e.g., TiO_2); still others (e.g., Al_2O_3) can not be formed in sufficient thicknesses at reasonable basis metal temperature to obtain opaque coatings. In the last analysis, the generation of solar reflector surfaces by direct oxidation of the basis metal appears to be a fruitless approach. Even the black coatings, such as those produced by oxidation of stainless steels and inconels at temperatures approaching 2000° F, may not withstand close scrutiny in view of the many competing processes, comparative performance characteristics, and economic factors involved.

Section 4
CONCLUSIONS

Work at LMSC, as well as that of other organizations engaged in this type of investigative activity, has clearly shown that spacecraft thermal-control surfaces reliable for periods of 90 days to a year or more will necessitate much more research and development. It can be concluded that many major parameters remain to be determined. Some of these are:

- Effects of solar ultraviolet exposures equivalent to several years in space
- Simulation of the space environment and its combined effects
- Effects of nuclear radiation corresponding to periods of 90 days to several years
- Combined effects of nuclear radiation and conventional space environments
- Development of room temperature curing paint systems with suitable thermal properties and with predictable and reliable behavior in the total spacecraft environment

Development of a unique class of coating material systems for passive temperature control surfaces has been described. Certain alkali silicate-based all-inorganic coating systems offer considerable promise for current long-term applications in this area of space technology. The major objective of this program has been the development of coating systems with stable α/ϵ values of less than 0.30 after 2,000 to 6,000 sun-hour exposures under space environmental conditions with lesser emphasis in systems with α/ϵ values of up to 1.20.

Preliminary work indicated that coatings containing organic materials could not meet these requirements. In addition, a number of conventional pigment materials were

found to be unsuited to the space environment. Vehicle-pigment systems based on alkali-metal silicates pigments with refractory materials were found to exhibit promise for the current solar reflector applications. Coating systems have been applied exhibiting α/ϵ values of less than 0.20 and showing less than a 50 percent change after 2,000 sun hours of irradiation. At this point the α/ϵ value becomes essentially constant. Higher α/ϵ values are obtained by use of spinel-oxide pigments, partially or wholly replacing the white pigment.

These coating systems have the advantage of application by standard spray techniques analogous to procedures for conventional organic paints. These coatings may be stabilized by low-temperature curing cycles of the order of 100 to 200°C. This class of coatings also has thermal stability to at least 500°C, excellent resistance to thermal shock from 100 to -70°C, and a remarkable degree of flexibility and ductility. Thus, these coatings systems demonstrate considerable promise for application to thermal-control surface problems.

Further study of semi-organic paint vehicles has been continued in the hope of obtaining coating systems which have higher resistance to all aspects of the spacecraft environment.

It has become increasingly obvious that there are major problems of manufacturing and quality control, handling techniques, and surface protection for thermal control surfaces, problems intensified in the case of large satellites such as the Agena vehicle. In general, it is mandatory that thermal control surfaces be treated as the optical surfaces they actually are, if reliable spacecraft operation is to be insured. It has been stated that the state of cleanliness of a surface is all-important in determining the surface emittance, in most research laboratories a standard method for cleaning metallic surfaces is the successive application of acetone, ethyl alcohol, and ethyl ether. However, procedures satisfactory in the laboratory often are not applicable to a production situation.

A large amount of environmental testing has been performed, and much more is proposed, both in scope and in depth. Present indications are that the elements of the spacecraft environment most harmful to thermal control surfaces are ascent heating, ultraviolet radiation, nuclear reactor radiation (where applicable), penetrating space radiation, and, for some materials, extreme high-vacuum conditions. For the special case of surfaces entering a planetary atmosphere, the entry environment would be most severe.

It is possible to alter significantly the α_s/ϵ ratio of metals by altering the roughness of the surface. If this could be done in a controlled fashion, variations within a range of the α_s/ϵ ratio characteristic of a particular metal or alloy could be specified. The potentialities of sandblasting, vapor blasting, and vapor honing for this application are worth serious investigation.

In addition to a study of the effects of roughening procedures, several methods of obtaining very smooth surfaces have been explored. It is conceivable that one outgrowth of this work will be tables of maximum allowable rms profile-roughness values for each alloy of interest which will insure various desired maximum emittances. Such tables would have a direct application in interior radiation "heat shield" manufacturing.

Section 5
REFERENCES

1. W. G. Camack and D. H. Edwards, "Effects of Surface Thermal-Radiation Characteristics on the Temperature Control Problem on Satellites," First Symposium on Surface Effects on Spacecraft Materials, ed. F. J. Clauss, Wiley, New York, 1960
2. R. E. Gaumer and L. A. McKellar, "Thermal Radiative Control Surfaces for Spacecraft," LMSD 704014, March 1961
3. "Space Materials Handbook," ed. C. G. Goetzel and J. B. Singletary, Air Force Contract AF 04(647)-673, LMSC, 1962
4. "Satellite Environment," NASA, Washington, D.C., September 15, 1959
5. L. Whitby, "Design of Paint Coatings for Spacecraft," LMSD 703026, June 1960
6. M. E. Sibert, "Organic Surface Coatings for Space Applications," LMSC 3-77-61-12, August 1961
7. Sauereisen Cement Company, "Sauereisen Engineers Production Manual," Pittsburgh, Pa.
8. S. C. Poulsen, "The Arc Plasma Jet," Machinery, October 1961
9. A. E. Hultquist, "Electrolytic Conversion Coatings for Temperature Control Surfaces," LMSC 2-84-62-2, June 1962
10. M. Schenk, Ematal Electrochemical Corp., New York, U.S. Patents: 2,213,371; 2,260,278; 2,262,967
11. M. Schenk, "Werkstoffe - Aluminum und Seine Anodische Oxydation," A. Franke Ag. Verlag, Bern, Switzerland, 1948

12. C. Show, J. Berry, and T. Lee, "Spectral and Total Emissivity Apparatus and Measurements of Opaque Solids," LMSD 48488, March 1959

13. E. R. Streed, "Experimental Determinations of the Thermal Radiation Properties of Temperature Control Surfaces for Spacecraft," Spacecraft Thermodynamics Symposium, Holden-Day, Inc., San Francisco, 1962

INDEX INFORMATION SHEET

RTD-TDR-63-4131. SUMMARY OF THE SEVENTH REFRACTORY COMPOSITES WORKING GROUP MEETING. November 1963. Unclassified. Air Force Materials Laboratory, Wright-Patterson Air Force Base, Ohio. L. N. Hjelm, Lt. D. R. James, Capt. C. S. Lee. P 7381. T 738103. In DDC.

This report is a compilation of 49 papers describing most of the information discussed at the Seventh Refractory Composites Working Group Meeting held at the Lockheed Missiles and Space Company, Palo Alto, California, on 12-14 March 1963. The representatives of approximately 40 organizations presented informal discussions of their current activities in fields of development, evaluation, and application of inorganic refractory composites for use in high-temperature environments.